technische universität
dortmund

MAX PLANCK INSTITUTE
OF MOLECULAR PHYSIOLOGY

Development and Evaluation of Small Molecule- and Bifunctional Modulators Targeting the Ribonuclease L for RNA Degradation

Dissertation

For the achievement of the academic degree of

Doctor in Natural Sciences

(Dr. rer. nat.)

Submitted to

The Faculty of Chemistry and Chemical Biology

Technical University Dortmund

by

Jimin Hwang, M. Eng.

Born at 02.11.1993 in Masan, South Korea

Dortmund 2023

The work presented in this dissertation was performed during the period from July 2019 to January 2023 under the supervision of Dr. Peng Wu at Chemical Genomics Centre from Max Planck Institute of Molecular Physiology and Faculty of Chemistry and Chemical Biology at the Technical University Dortmund.

1st Examiner: Prof. Dr. Dr. h.c. Herbert Waldmann

2nd Examiner: Prof. Dr. Hannes Mutschler

Results presented in this dissertation contributed to the following publications:

J. Hwang, L. Borgelt, P. Wu* "Multicomponent Petasis Reaction for the Synthesis of Functionalized 2-Aminothiophenes and Thienodiazepines" *ACS Comb. Sci.* 22, 495–499 (2020)

J. Hwang[#], X. Qiu[#], L. Borgelt, N. Haacke, L. Kanis, S. Petroulia, R. Gasper, D. Schiller, P. Lampe, S. Sievers, J. Imig, P. Wu* "Synthesis and evaluation of RNase L-binding 2-aminothiophenes as anticancer agents" *Bioorg. Med. Chem.* 58, 116653 (2022)

J. Hwang[#], N. Haacke[#], L. Borgelt, X. Qiu, R. Gasper, P. Wu* "Rational design and evaluation of 2-((pyrrol-2-yl)methylene)thiophen-4-ones as RNase L inhibitors" [Manuscript submitted]

Related methods and results can also be found in the following publications:

L. Borgelt[#], F. Li[#], P. Hommen[#], P. Lampe[#], J. Hwang, G. L. Goebel, S. Sievers, P. Wu* "Trisubstituted Pyrrolinones as Small-Molecule Inhibitors Disrupting the Protein–RNA Interaction of LIN28 and Let-7" *ACS Med. Chem. Lett.* 12(6), 893–898 (2021)

L. Borgelt[#], N. Haacke[#], P. Lampe[#], X. Qiu, R. Gasper, D. Schiller, J. Hwang, S. Sievers, P. Wu* "Small-molecule screening of ribonuclease L binders for RNA degradation" *Biomed. Pharmacother.* 154, 113589 (2022)

Acknowledgments

The past four years which I feel were very short but also quite long during my PhD study and were so precious time to let me learn a lot not only in my scientific life but also in my social life. I would like to show my great appreciation to all the people who were around during my journey for PhD study. Each one of you made all of this possible.

I would like to thank Prof. Dr. Herbert Waldmann for taking the responsibility of the first examiner of my dissertation. This work was possible because you instituted and headed the Chemical Genomic Centre (CGC) with providing great scientific input.

I also thank Prof. Dr. Hannes Mutschler for taking over the second examiner position of my PhD dissertation.

Moreover, I would like to thank Dr. Peng Wu for giving me the opportunity to work on this interesting topic in such a nice environment. Your patient teaching and supervision to a person who was not from this field are very much appreciated. Thank you for all the constructive discussions and scientific input which greatly benefitted this work and made it into what it is today. I learned a lot from you and the group, which will be very helpful for the rest of my scientific career.

Next, I would like to thank all the people who helped me to start and work in this field. First of all, I would like to give much appreciation to the most senior student in the CGC III, Pascal Hommen. The great introduction into everything I should have encountered over the time of my PhD as well as endless help for everything around the scientific matters including experiments, discussions, and administrative works are so much appreciated and are one of the most necessary parts to let me finish this work. I would like to thank Jen-Yao Chang, Mao Jiang, and Dr. Fubao Huang who always kindly share me great chemistry knowledge and their time for fruitful discussions. I would also like to thank Lydia Borgelt, Neele Haacke, and Xiaqiu Qiu for kindly providing the biological effort to this project and teaching me the biological experiments.

I am also grateful to HRMS and NMR team for providing nice and helpful facilities in MPI.

Thanks to Pascal Hommen, Dr. Rachel O'Dea, Jen-Yao Chang, Aylin Binici, Dr. Tzu-Chen Lin for proofreading my dissertation and giving grateful corrections and comments.

I want to give a special and big thanks to Dr. Lucia Sironi and Christa Hornemann. I really appreciate your constant support and encouragement during the entirety of my PhD. I am sorry

Table of contents

Abstract

Ribonucleases are one of the critical regulatory enzymes in cells while mediating RNA-involved metabolism. Ribonucleases are becoming promising therapeutic targets due to the importance of RNA in many disease mechanisms. In particular, ribonuclease L (RNase L) has attracted great attention as a regulatory enzyme implicated in innate immune responses against viral infections. Viruses infect most organisms including humans to replicate and some cause severe damage to the host system. The importance of host immune system in preventing viral spreading was clearly demonstrated throughout the Covid-19 pandemic. RNase L plays a vital role in the antiviral response by degrading viral and host RNAs, which positively correlates to the prevention of viral propagation as well as the promotion of alternative antiviral pathways. However, viruses have evolved different mechanisms to escape from the antiviral responses through the 2', 5'-oligoadenylate synthetase (OAS)–RNase L pathway, such as suppressing RNase L activation. Therefore, restoring and recruiting the RNase L and associated antiviral pathway by using small molecule-based strategies are one of the promising therapeutic approaches to preserve innate immune responses. Although a few small molecule-based RNase L modulators have been reported, the scarcity of potency and selectivity of reported modulators highly requires a thorough optimization and discovery of new scaffolds as well as development of new approaches.

In this study, we pursued our efforts in acquiring potent small-molecule modulators of RNase L using two different strategies. In the first approach, an approach based on small molecule-ligand pursued improved potency of ligands. The second approach was to develop new bifunctional molecules which could help mediating the challenging protein target's activity. In the small molecule-ligand approach, we assessed whether scaffold-based design, structure-activity relationship (SAR) study, and rational design for a new scaffold could facilitate the generation of a more potent modulator. Although the scaffold-based design yielded two scaffolds with improved chemical features under the development of a straightforward synthetic route, none of the obtained compounds induced RNase L activity change. The SAR approach yielded compounds which revealed improved binding to RNase L than previously reported compounds and showed RNase L-mediated cellular downstream effects. The rational design based on cocrystal structure between RNase L and ATP-mimetic sunitinib led to a promising fusion scaffold of RNase L modulators, 2-((pyrrol-2-yl)methylene)thiophen-4-one, and compounds which exhibited 30-fold improved inhibitory effect than sunitinib in *in vitro* biochemical evaluation and a potent inhibitory effect in the cell.

In our second approach, bifunctional molecule-based approaches were performed with the aim to achieve new interesting strategies to modulate RNase L activity by using three types of bifunctional molecules. The three bifunctional molecules consist of a homobifunctional molecule to recruit a monomeric RNase L to another monomer to dimerize and thus activate RNase L, a heterobivalent molecule targeting two different sites in a protomer of RNase L, and the PROTAC molecule to degrade an RNase L-inhibiting protein. The homobifunctional molecule improved the potency of the activator. However, the low sensitivity of biochemical in-house evaluations required more potent ligands and an orthogonal validation method. Although a heterobivalent molecule was successfully synthesized, it lost both activation and inhibition effects. Lastly, PROTAC molecules have been synthesized to target the 2',5'-oligoadenylate (2-5A) degrader protein. The effect of the PROTAC molecules on the 2-5A level will be evaluated in a future study.

We focused on multiple approaches to modulate the challenging but promising target RNase L. A potent binder and inhibitor were discovered but no activator could be obtained through the small molecule-based strategy. The bifunctional molecule strategy posed a novel concept for RNase L-activating probes with improved potency. However, more generations of bifunctional molecules are required, specifically with more potent activator ligands to generate high efficacy tool compounds. This study will contribute to the development of new chemical entities for a potent RNase L modulator and thus for an innate immunity modulator.
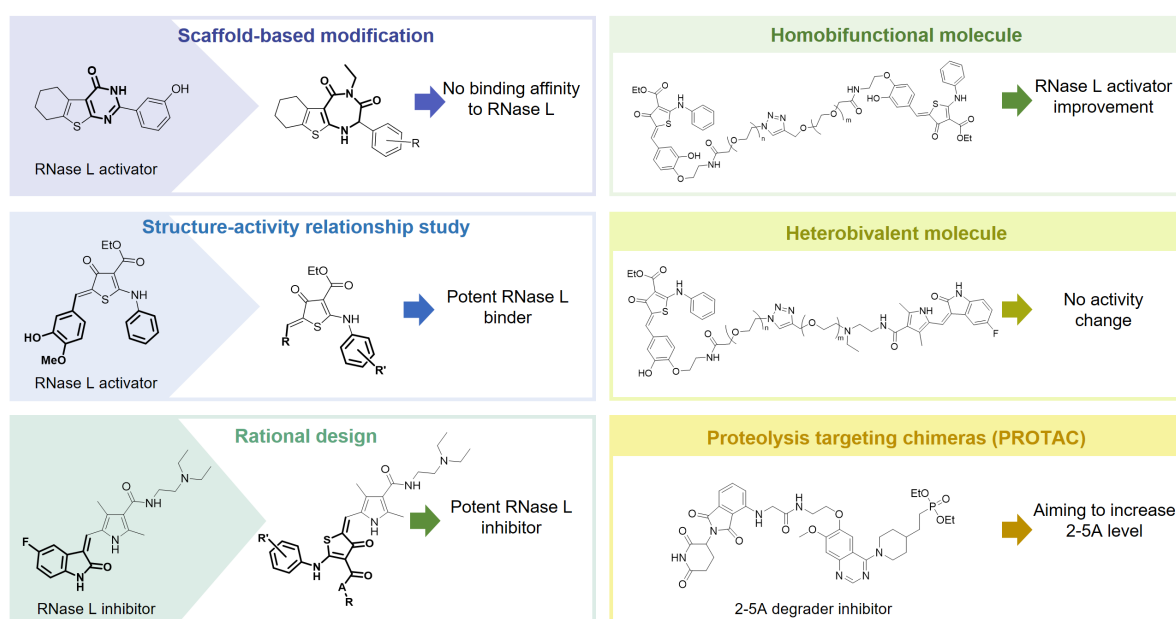
Figure 1. Summary of strategies for modulating RNase L activity.

Kurzzusammenfassung

Ribonukleasen sind eines der wichtigsten regulatorischen Enzyme in Zellen, die den RNA-Stoffwechsel regulieren. Aufgrund der Bedeutung von RNA bei vielen Krankheiten sind Ribonukleasen zu vielversprechenden therapeutischen Zielen geworden. Insbesondere die Ribonuklease L (RNase L) ist als regulatorisches Enzym der angeborenen Immunantwort in den Fokus gerückt. Viren infizieren die meisten Organismen, um sich zu vermehren, und können dabei schwere Schäden im Wirtssystem verursachen. Die Bedeutung des körpereigenen Abwehrsystems bei der Verhinderung viraler Infektionen wurde während der Covid-19-Pandemie deutlich hervorgehoben. RNase L baut sowohl interne als auch fremde RNA ab und spielt eine wichtige Rolle bei der Virenabwehr. Viren haben jedoch verschiedene Antworten entwickelt, um den antiviralen Abwehrreaktionen über den 2',5'-Oligoadenylat-Synthetase (OAS)-RNase L-Weg zu entgehen. Daher ist die Wiederherstellung der RNase L Aktivität und die damit verbundene Virusabwehr mit Hilfe von Ansätzen, basierend auf niedermolekularen Strukturen, ein vielversprechender Weg, die angeborene Immunantworten zu erhalten. Obwohl einige wenige RNase-L-Modulatoren bekannt sind, erfordert deren niedrige Affinität und Selektivität eine gründliche Optimierung. Zusätzlich bedarf es der Entdeckung neuer Grundstrukturen sowie einer Neuentwicklung von bisherigen Ansätzen.

In dieser Arbeit haben wir die Gewinnung potenter niedermolekularer Modulatoren von RNase L durch zwei Strategien verfolgt. Im ersten Ansatz wurde eine Liganden-basierte strukturelle Optimierung verfolgt. Der zweite Ansatz bestand darin, neue bifunktionelle Moleküle zu entwickeln, die dieses anspruchsvollen Proteintarget selektiv aktivieren können. Bei der Optimierung des Liganden-Konzepts wurde geprüft, ob ein scaffold-basierter Entwurf, eine SAR-Studie (Struktur-Wirkungsbeziehung) und ein rationaler Entwurf einer neuen Grundstruktur die Entwicklung eines optimierten Aktivators ermöglichen könnten. Obwohl das scaffold-basierte Design zwei Grundstrukturen mit verbesserten chemischen Eigenschaften in Kombination mit einem unkomplizierten Syntheseweg ergab, führte keine Verbindung zu einer Veränderung der RNase-L-Aktivität. Der SAR-Ansatz erzeugte Verbindungen, die eine bessere Bindung an RNase L aufwiesen und zusätzlich RNase L-vermittelte zelluläre Downstream-Effekte verursachten. Das rationale Design auf Basis der Kristallstruktur von RNase L und dem ATP-Mimetikum Sunitinib führte zu einer vielversprechenden Fusion aus dem RNase-L-Modulator, 2-((Pyrrol-2-yl)methylen)thiophen-4-on, und einer Verbindung, die bei der biochemischen *in vitro*-Bewertung eine 30-fach bessere Hemmwirkung als Sunitinib und eine starke Hemmwirkung in der Zelle zeigte.

In unserem zweiten Ansatz wurden drei Typen von bifunktionellen Molekülen verwendet, um die RNase-L-Aktivität gezielt zu erhöhen. Zuerst wurde ein homobifunktionelles Molekül entwickelt, das eine monomere RNase L mit einem zweiten Monomer zusammenführen soll, um RNase L zu aktivieren. Als Zweites wurde ein heterobivalentes Molekül mit demselben Ziel entwickelt, welches aber an zwei verschiedenen Stellen des gleichen RNase L Monomers bindet. Die dritte Strategie besteht aus einem PROTAC-Molekül, das ein RNase L-hemmendes Protein abbaut. Das homobifunktionelle Molekül verbesserte die Wirksamkeit des Aktivators. Aufgrund geringer Empfindlichkeit der biochemischen Evaluierung sind potentere Liganden und eine orthogonale Validierungsmethode erforderlich. Obwohl ein heterobivalentes Molekül erfolgreich synthetisiert wurde, verlor es sowohl die Aktivierungs- als auch die Hemmwirkung. Schließlich wurden PROTAC-Moleküle synthetisiert, die auf das 2-5A-Abbauprotein abzielen. Die Wirkung auf den 2-5A-Spiegel soll in einer zukünftigen Studie untersucht werden.

Wir haben uns auf mehrere Ansätze konzentriert, um das vielversprechende Protein RNase L zu modulieren. Es wurden ein potenter Binder und ein Inhibitor entdeckt, aber es konnte kein Aktivator basierend auf niedermolekularen Strukturen gefunden werden. Die Strategie der bifunktionellen Moleküle stellt ein neues Konzept für RNase L aktivierende Sonden mit verbesserter Wirksamkeit dar. Es sind jedoch weitere Generationen bifunktioneller Moleküle erforderlich, um hochwirksame Modulatoren zu entwickeln. Diese Studie wird zur Entwicklung neuer chemischer Substanzen für einen wirksamen RNase-L-Modulator und damit für einen Modulator der angeborenen Immunität beitragen.
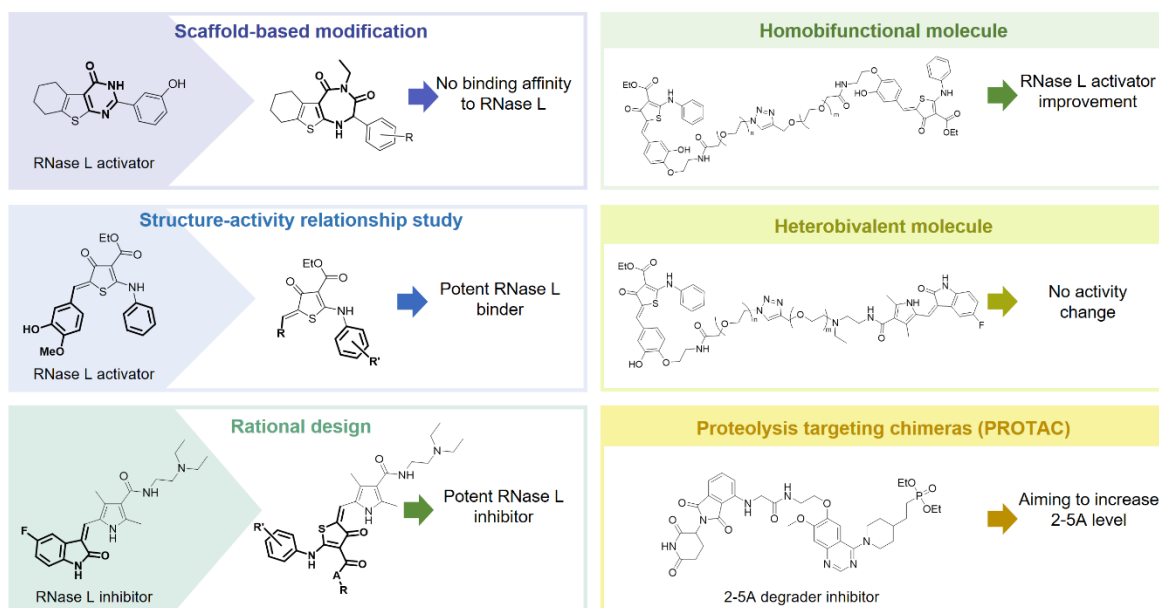
Figure 1. Übersicht der Strategien zur Modulierung der RNase L Aktivität.

1. Introduction

1.1 Interferon (IFN)-induced antiviral state

Viruses exist in all living environments and infect a variety of organisms, such as bacteria, plants, and animals, for their replication. It is known to date that more than 220 different viruses are characterized to infect humans.[1] Viral infection is a danger to life as it is capable of causing severe damage to cells such as inducing protein production shutoff, signaling arrest, and ultimately cell death.[2] Viruses continuously evolve to adapt to changing environments to ensure replication. Due to not having own metabolism, viruses evolve at a much faster rate than other organisms. This in turn makes the development of drugs to treat each type and variant of a virus particularly challenging. Therefore, it became extremely important to understand and control the universal antiviral responses to suppress viral infection/replication and avoid critical damage to the host by aiding and employing the internal antiviral host system.

One of the first innate immune responses upon the infection of cells by viruses is the production of cytokines. These cytokines are released to propagate the defense by binding to receptors on other cells and inducing an antiviral response in other cells. One of the critical families of these cytokines is interferon (IFN). Interferon was first discovered in 1950 as a key factor of antiviral innate immunity.[3-4] IFNs are classified into three subclasses depending on the respective signal-transferring receptors at the cell membrane. These receptors bind different interferon types in a highly specific manner. Type I IFNs include many homologs such as IFNα, IFNβ, IFNω, and IFNε and are expressed in response to viral infections and recognized by the IFNα receptor complex. Type II IFNs bind to the IFNγ receptor. Type II IFNs regulate immune responses against the broader target over viral infected cells, such as mitogenic or antigenic stimulation. So far the only known type II IFN is IFNγ. Lastly, type III IFNs are the most recently discovered. They behave similarly to type I IFNs but do so in a less severe way while serving as the first line of defense to the organism. Type III IFNs are recognized by the receptor complex of IL-28Rα and IL-10Rβ and include IFNλ. Type I IFNs are the most well-understood IFN family.[5] The antiviral response induced by type I IFNs occurs through several pathways. In addition to activation of classical Janus kinase (JAK)-signal transducer and activator of transcription (STAT) signaling, Type I IFNs induce the transcription of numerous genes known as IFN-stimulated genes (ISGs). ISGs elicit direct and indirect antiviral responses in several pathways. As a direct response, IFN-inducible proteins, such as RNA-dependent protein kinase (PKR), RNA-specific adenosine deaminase (ADAR), Mx protein GTPase, 2', 5'-oligoadenylate

synthetase (OAS), and ribonuclease L (RNase L), are expressed (Figure 2).

Upon type I IFNs binding, PKR regulates protein synthesis in response to environmental stimulation such as double-stranded RNA (dsRNA) and polyanionic molecules. The translation initiation factor eIF2α is phosphorylated by activated PKR, which leads to the inhibition of translation and thus synthesis of new viral elements.[6] Mx proteins are a family of GTPases and are associated with viral proteins. The mechanism by which Mx proteins affect viral action alters depending on the type of Mx protein and virus. ADAR generates posttranscriptional RNA modification, specifically the deamination of adenosine to inosine. This sequence modification can destabilize the RNA molecule and effect the function of the translated protein.[7] Among the diverse antiviral pathways induced by IFNs, RNase L in combination with OAS plays a vital enzymatic role in antiviral innate immunity through the direct regulation of viral replication and the indirect another pathway promoter.[8] One of the main antiviral responses through the OAS/RNase L system is accomplished by the degradation of viral and cellular RNA in cells. This leads to the inhibition of viral replication and eventually to host cell apoptosis eliminating infected cells entirely.
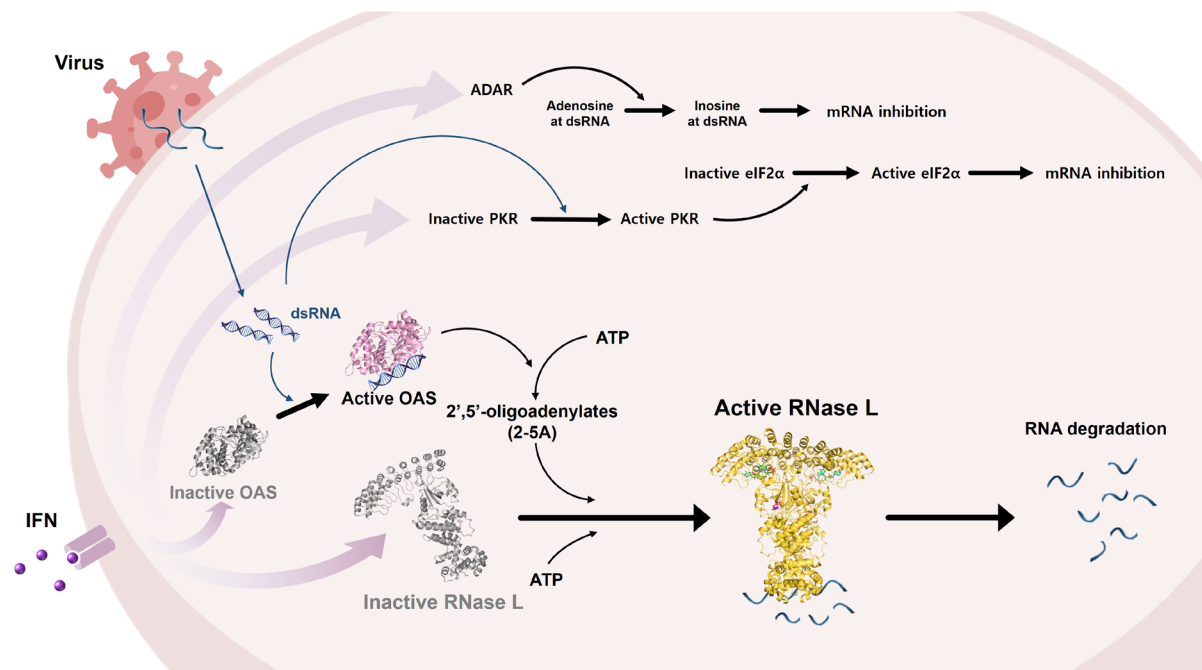
Figure 2. IFN-mediated antiviral pathway.[9] 2'-5' oligoadenylate synthetase (OAS), ribonuclease L (RNase L), adenosine deaminase acting on RNA (ADAR), protein kinase (PKR), eukaryotic translation initiation factor 2 subunit 1 (eIF2α).

Most antiviral pathways mainly inhibit one type of viral action. However, the OAS/RNase L

pathway is a major antiviral defense system as it not only suppresses viral action like other pathways but critically it also shuts off viral replication and this happens in a non-specific manner. The OAS/RNase L pathway is therefore a fascinating target to discover drug candidates showing a wide range of antiviral activities against different viral pathogens.

The efforts to mediate proteins produced in response to interferon stimulation have been carried out. The investigation has been performed into the mediation by small molecules owing to their advantageous characteristics as drug candidates. Small molecules following the "Rule of Five" guidelines in medicinal chemistry have a low molecular mass of 500 Da or less, which makes them more cell-permeable.[10] Furthermore, small molecules can be produced by organic synthesis, leading to facile accessibility and allowing the modulation of the chemical structure to change and improve the molecular activity. Of particular interest are non-natural small molecules which possess fewer targets in cells and are more resistant to cellular enzymes. A few adenosine derivatives were identified as ADAR inhibitors. For example, the editing activity of ADAR is inhibited by 8-azaadenosine at 1 and 2 µM in TPC1 and Cal64 cells, respectively.[11] PKR loses the phosphorylation activity with single-digit micromolar sunitinib.[12] However, these molecules are either natural product analogs or different target ligands, which results in off-target issues. Similarly, even though a few studies identified small molecule-modulators of RNase L, the potency, selectivity, and characterizations are required to be improved. A detailed explanation of RNase L ligands will be described in chapter 1.6.2.

1.2 OAS/RNase L pathway inhibiting viral replication

Decades of effort have been carried out to investigate how RNA is degraded in virus-infected cells. The relation between OAS and RNase L was clearly elucidated upon the discovery of the atypical oligonucleotide, 2',5'-oligoadenylate (2-5A).[13-14] The existence of IFN-inducible ribonuclease and dsRNA-dependency of the ribonuclease was first claimed in 1976 by Lengyel and coworkers. Kerr and coworkers characterized that OAS is the dsRNA-dependent protein and synthesizes the 2-5A.[15-17] The structure of 2-5A was characterized and RNase L was unveiled as a 2-5A-dependent endoribonuclease.[18]

In order for the OAS/RNase L antiviral response to take place, proteins must first undergo activation. This occurs via a cascade.[9, 19-21] IFN binding to the receptor at the cell membrane, results in OAS being expressed in an inactive form. OAS is then activated by dsRNA which is produced in cells from viral pathogens. Active OAS catalyzes the synthesis of 2-5A, from ATP.

Latent endoribonuclease, RNase L, is ubiquitous in most mammalian cells to be ready for activation in case of viral infection. The synthesis of RNase L can also be induced by IFN in mice cells or minorly in human cells. The secondary messenger, 2-5A, binds to the inactive monomeric form of RNase L and causes RNase L to form stable homodimers, which yields RNase L endoribonuclease catalytic activity. The active RNase L cleaves single-stranded RNA (ssRNA) in cells and consequently blocks viral replication and further infection.[22-23]

OAS is the viral pathogen recognition receptor protein.[24] As aforementioned, dsRNA from different origins including viruses, is a natural activator of OAS and several studies have reported how viral RNA activates OAS.[18, 20] Upon dsRNA binding, OAS generates a stable secondary structure with dsRNA resulting in an activating conformational change at the active site of OAS through ATP binding. There are three forms of OAS, OAS1, OAS2, and OAS3 with different sizes and different numbers of OAS domain repeats.[25] They require different states for activation by dsRNA. OAS1 and OAS2 form a tetramer and a dimer, respectively, to show enzymatic activity whereas OAS3 stays as a monomer. Followed by OAS activation, 2-5A synthesis is accomplished as the adenosine monophosphate of a donor ATP is transferred to another acceptor ATP. A 2',5'-phosphodiester bond is then formed to give 2-5A. The different OAS forms synthesize different lengths of 2-5A.[4, 26] OAS1, OAS2, and OAS3 synthesize trimeric, tetrameric, and dimeric 2-5A, respectively.

When 2-5A and ATP bind, inactive monomeric RNase L dimerizes to the active form.[27] A specific stable dimeric configuration is required to give RNase L a ribonuclease catalytic function against ssRNA, which enables the dimer to associate with the ssRNA and causes degradation.[22-23] RNase L can mediate the IFN-inducible antiviral state in multiple ways as either the last stage effector or a promoter inducing other IFN-induced innate immunity pathways. RNase L not only directly degrades viral RNA and blocks viral replication, but also inhibits protein synthesis through the cleavage of ribosomal RNA (rRNA). Furthermore, the small RNA cleavage products by RNase L induce the amplification of the expression of the IFNβ gene.[8] RNase L plays an important role in the IFN-induced innate immunity in multiple critical pathways. The RNase L pathway is a strong defense mechanism against viral infection. However, some viruses have evolved to evade destruction by this pathway through modulation of RNase L activity.

1.3 Viral antagonist of OAS/RNase L pathway

Multiple pathways have been implemented for the virus to adapt and inhibit OAS/RNase L defense mechanisms (Figure 3).[28] Viruses can encode proteins which bind dsRNA, inhibiting OAS-dsRNA interactions. Blocking the dsRNA binding to OAS results in the inhibition of OAS activation and thus restraining the synthesis of 2-5A and ultimately preventing RNase L catalytic activity. This virulent adaptation is seen in vaccinia virus, influenza A virus, and the reovirus. When cells are infected by the vaccinia virus, dsRNA binding proteins E3L are expressed.[29-32] Another example of this is seen in uring influenza A virus infection, the viral protein NS1, which possesses an N-terminal RNA-binding domain, inhibits dsRNA binding to OAS.[33-35] Lastly, the reovirus suppresses activation of OAS through dsRNA-binding σ3 protein which is structurally outer capsid protein.[36-38]
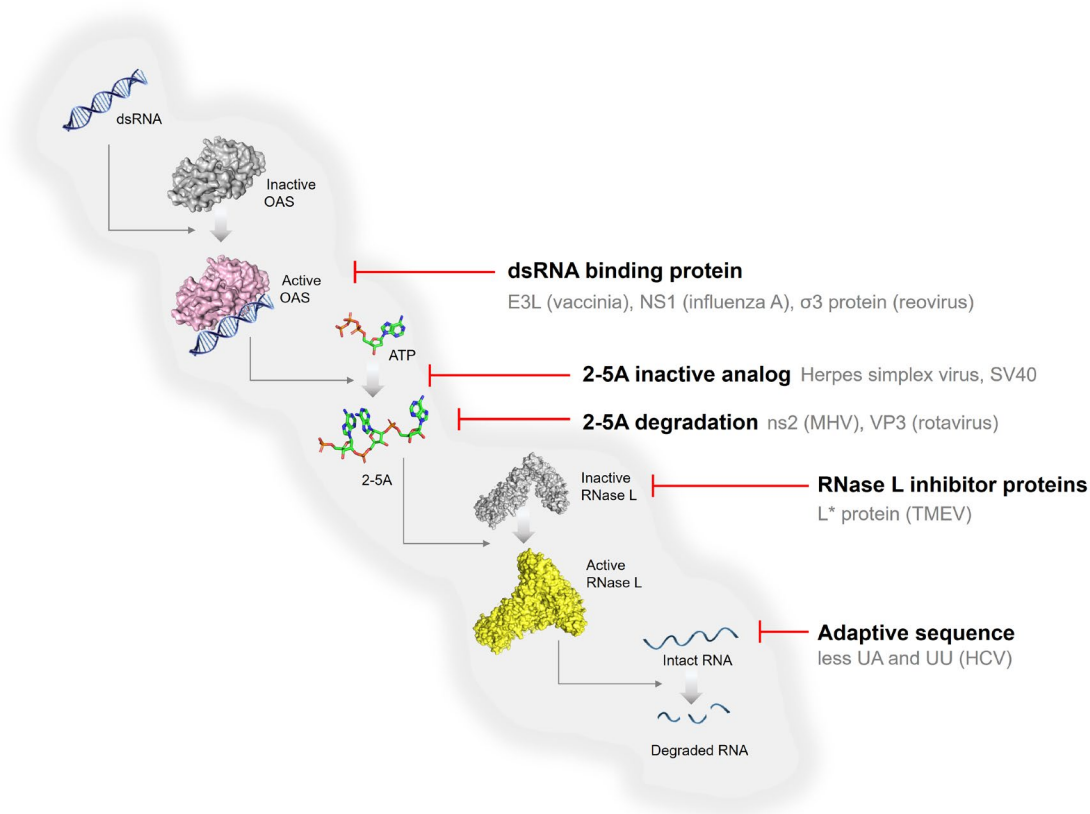
Figure 3. Viral antagonizing OAS/RNase L antiviral state.

In addition to dsRNA binding proteins, some virus induces the expression of 2',5'-phosphodiesterase (PDE) to degrade to 2-5A, which blocks RNase L activation.[39-40] In the case of mouse hepatitis virus (MHV), the accessory protein ns2 inhibits host gene expression and innate immune response by prompting host mRNA degradation through 2',5'-

phosphodiesterase activity.[41] Rotavirus VP3 protein has a similar sequence at the C-terminal so that it is considered as a potential 2',5'-PDE.[40] Additionally, some host cellular 2',5'-PDEs exist to control the 2-5A level in cells and inhibit continuous activation of RNase L. Several studies suggested the possibility that some viruses recruit host 2',5'-PDE, such as PDE12 and ectonucleotide pyrophosphatase/phosphodiesterase 1 (ENPP1), to prevent RNase L activation.[42]

RNase L inhibitor (RLI) protein is another mechanism for viruses to suppress RNase L activation. This is a cellular protein which can directly bind to and thus inhibit RNase L activity. Some viruses can increase the expression of RLI which binds to RNase L and inhibit enzymatic activity.[43] RLI was first discovered in 1995 as a protein that specifically inhibits RNase L without inducing the degradation of 2-5A.[44] RLI is not regulated by interferon but by dsRNA. For an example of RLI, ATP-binding cassette sub-family E member 1 (ABCE1) is a protein induced by encephalomyocarditis virus (EMCV). This forms a heterodimer with monomeric RNase L to prevent RNase L homodimerization.[45] Theiler's murine encephalomyelitis virus (TMEV) L* protein binds the ankyrin repeats 1 and 2 of RNase L and inhibits 2-5A binding to RNase L.[46]

Another mechanism to counteract OAS/RNase L pathway is to synthesize 2-5A analogs which have low RNase L activation ability. Herpes simplex virus type 1 and 2 promote the synthesis of 2-5A analogs which has a weaker activation ability than the common trimer 2-5A.[46-48] Similarly, simian virus 40 (SV40) also uses the 2-5A derivatives to inhibit activation of RNase L.[49] Another way to escape from RNase L is that hepatitis C virus (HCV) variants reduce the UA and UU dinucleotides, which is the favored sequence of RNase L, on its messenger RNA (mRNA).[50] RNA of poliovirus has a phylogenetically conserved region that competitively binds to the RNase domain and inhibits RNase L, which is observed similarly in other group C enteroviruses, called competitive inhibitor RNA (ciRNA).[51-52]

In summary, viruses have a number of ways to avoid innate immunity destruction, of which a number culminate in the reduction of RNase L activity. In many cases, viruses use multiple pathways to suppress OAS/RNase L system. Therefore, understanding the role of RNase L in the antiviral response and how the activity can be modulated is a fascinating topic for the development of therapeutic drug candidates to control the innate immune system against viral infections.

1.4 Structure of RNase L
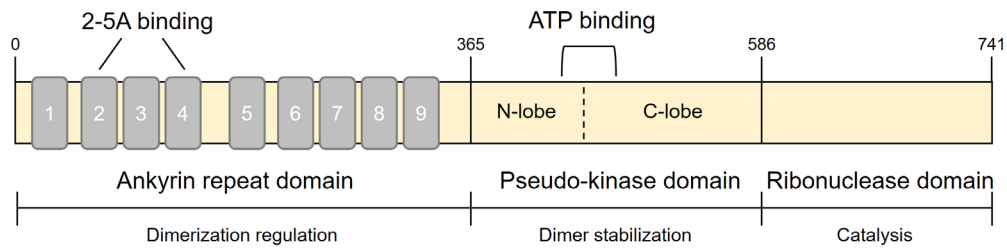
Figure 4. RNase L amino acid sequences with three domains.[9, 21]

Understanding how to modulate RNase L activity is largely facilitated by the knowledge of RNase L structure. RNase L was first partially purified in 1978 by Lengyel and Revel and later optimized by Lengyel and Silverman group.[53-56] The cloning of RNase L was first performed by Silverman and coworkers in 1993.[57] Human RNase L contains 741 amino acids and is constituted of three domains, an ankyrin repeat (AKR) domain, a pseudo-kinase (PK) domain, and a ribonuclease (RNase) domain from N to C terminal (Figure 4).[9, 22-23, 58] While AKR domain contributes to dimerization with binding of specific activator 2-5A, the PK domain stabilizes the dimer through ATP binding. Target RNA binds to the RNase domain and is degraded by the catalytic activity of RNase L.
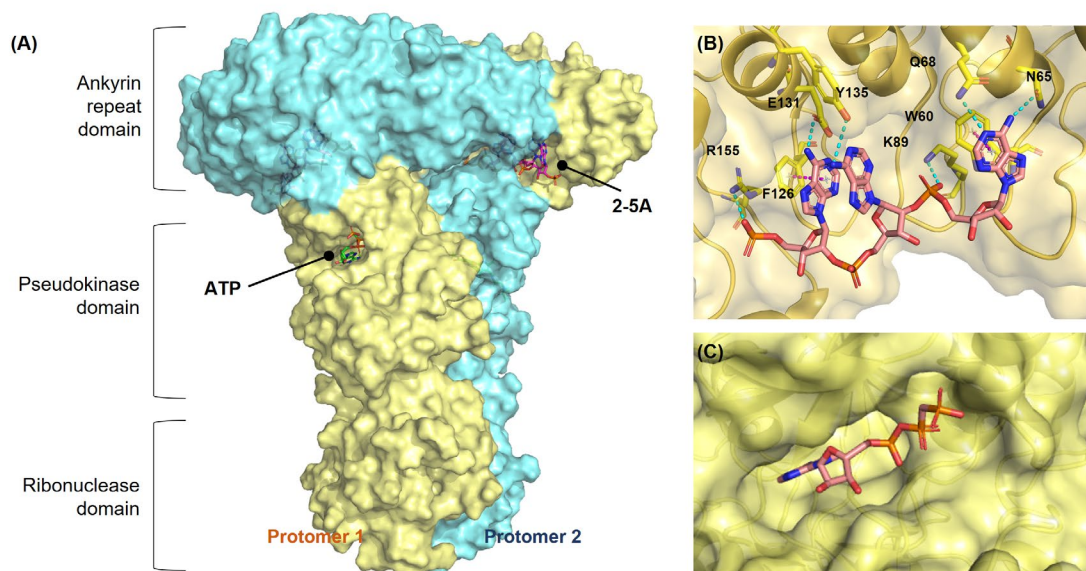
Figure 5. (A) RNase L dimeric structure and (B) interaction of 2-5A at AKR domain and (C) ATP at PK domain.[22-23]

AKR domain of RNase L was the first part to be unveiled to contain nine ankyrin repeats, eight complete, and one partial AKR by crystallography in 2004.[59] AKRs commonly function as a domain to induce protein-protein interactions. Similarly, the AKR domain in RNase L plays a role as a regulatory domain to mediate interactions between RNase L monomers. The atypical event of RNase L AKR domain is that intermolecular binding is regulated by an additional molecule, 2-5A. The 2-5A binds to ankyrin repeats 2 and 4 while the binding event induces a conformation change of RNase L. Once 2-5A binds, the RNase domain, which was initially repressed by internal interactions at the monomer state, is released through the induced conformational change from suppression of the AKR domain and hence allows dimerization and subsequent RNA binding.[26] Consequently, the removal of the AKR domain resulted in continuously active RNase L even without environmental stimulation.

Direct binding interactions between the AKR domain and 2-5A occur through hydrogen bonds between surrounding residues and both adenine and phosphates as well as π-π interaction between adenines and aromatic amino acids (Figure 5). The amino acid residues contributing to interactions are Trp60, Asn65, Gln68, and Lys89 in AKR 2 and Phe126, Glu131, and Arg155 in AKR 4.[59] Moreover, other ankyrin repeats, such as AKR 1, AKR 7, AKR 8, and AKR 9, are also essential for 2-5A binding, which has been proven through truncations or mutations of AKRs.[57, 60] For example, RNase L with Lys to Asn mutations in AKR 7 and 8 loses the 2-5A affinity and thus RNase activity. Therefore, it is believed that almost the entire AKR domain through intramolecular secondary bonds and conformational maintenance is directly or indirectly involved in the 2-5A binding. The 2-5A in RNase L dimer interacts with both RNase L protomers like a molecular bridge.[22-23]

The role of the PK domain in RNase L has not been clearly identified, but research has been conducted on enzyme stabilization through the binding of adenosines. The PK domain of RNase L shows the closest homology with RNA-dependent protein kinase (PKR) while the PK and RNase domain of RNase L have homology with endoplasmic reticulum (ER) transmembrane sensor protein, inositol-requiring enzyme 1 (IRE1).[6, 61] IRE1 is a kinase and endoribonuclease while the N-terminal stress response domain of IRE1 is located in ER and the kinase and RNase domain is located in cytoplasm. IRE1 also has an N-terminal regulatory domain to stimulate the dimerization of IRE1. The regulatory ligand for dimerization of RNase L and IRE1 is different as IRE1 dimerization is stimulated by the binding of an unfolded protein instead of 2-5A. In contrast with IRE1 and PKR, the PK domain in RNase L lacks critical residues for an active kinase so that RNase L does not show catalytic kinase function, which is

the reason it is called as 'pseudo' kinase domain.

The crystal structure of full length-RNase L in the presence of 2-5A and ATP analogs was reported in 2014, which greatly advanced the understating of the PK and RNase domain.[22-23] PK domain of RNase L contains canonical five antiparallel β sheets and two α helices at the N-lobe. The αA helix connects AKR and PK domains while contributing to interaction with 2-5A when RNase L is dimerized. C-lobe shows a noncanonical configuration which explains the loss of kinase activity of RNase L. C-lobe consists of three antiparallel β, a two-strand β sheet, and seven α helices. Especially, the C-lobe of RNase L is featured with a noncanonical β9-αF loop where the activation segment of prototype protein kinase is usually located, which leads to a nonstandard position of αG helix and thereby loss of protein kinase substrate recognition position. Additionally, uncommon Gly502 instead of Asp502 in RNase L also resulted in a different configuration of the PK domain of RNase L than other kinases, which also relates to the loss of kinase activity in RNase L. Nevertheless, the PK domain is a necessary domain for interactions of dimeric RNase L. It contributes to stable dimeric conformation upon ATP binding by parallel back-to-back interaction between two PK domains and cross-interaction between the AKR domain of one protomer and the PK domain of the other protomer.

The RNase domain contains nine α helices and a disordered sequence of 19 amino acids. A gap space is formed between two RNase domains in the center of α4 helix when dimerized. This cleft becomes the active site of the RNase domain. Residues surrounding the solvent-exposed area are disparate from IRE1 whereas the catalytic residues show high similarity with IRE1, which explains the difference in RNA substrates.

Substrates of RNase L are ss RNA and include RNase L-favored U-rich sequences, mainly after UU and UA dinucleotides. While rRNA is known as a major target of RNase L, mRNAs are also actively degraded by RNase L. Especially, ribosomal protein mRNAs, such as RRL7 and RPS12, were the main target of RNase L among mRNAs of which level is regulated by RNase L.[62] Another mapping study by transcriptome-wide profiling described mRNAs possessing AUUUA/UAUAU motif are the main target of RNase L.[63] In this study, they also showed that transcripts regulated by miRNA are often affected by RNase L, which suggests the possibility of antiproliferative effects through RNase L. Recent studies unveiled the viral RNA targets of RNase L.[64-65] In short, U-rich sequences were favored by RNase L-mediated cleavage while PB1, PB2, and PA segments were mainly cleavage site on and influenza viral RNA.

1.5 The role of RNase L in antiviral state and other diseases

It is clear that RNase L is a critical component in antiviral innate immunity. The cells in which RNase L activity is inhibited yielded an increase in virus production. For example, the expression of truncated RNase L in SVT2 cells which lost enzymatic activity revealed a 100-fold increased level of EMCV virus.[66] In addition, the MEF cells from RNase L knockout (RNase L$^{-/-}$) mice showed up to a 5-fold difference in EMCV level in the presence of IFNα. Furthermore, EMCV-infected RNase L$^{-/-}$ mice showed up to 40% lower survival than EMCV-infected wild-type mice.[67]

Besides viral and cellular RNA degradation inhibiting viral protein synthesis, RNase L contributes to several other signaling pathways to promote an antiviral response.[68] RNase L leads to IFN-β production via cleavage products. The RNA cleavage products bind to pathogen recognition receptors to activate the signaling pathway of IFN-β production.[8, 69]

The apoptotic activity of RNase L is another critical mechanism against the virus by rapid elimination of infected cells. It is considered that apoptosis by RNase L is induced by more than one mechanism. The overexpression of RNase L led to an increased sensitivity of cells to the apoptosis inducer staurosporine. Additionally, rRNA cleavage by RNase L resulted in the activation of the pro-apoptotic JNK pathway.[70] Apoptosis through cascade activation is also suggested to be related to RNase L.[71] Other mechanisms for RNase L to be engaged in INF-induced innate immunity are to prevent infected cell proliferation and to activate NLR family pyrin domain (NLRP)-inflammasome.[72]

Beside viral infections, OAS/RNase L system is mediated in chronic fatigue syndrome, in which 2-5A is produced as dimers which fail to bind or activate RNase L.[19] It has been reported that the onset of type I diabetes in both biobreeding (BB) rats and streptozotocin (STZ)-treated mice is IFNα and IFNγ-dependent.[73-74] Indeed, deficiency of RNase L in mice showed a significant delay of diabetes onset induced by polyinosinic:polycytidylic acid (poly I:C), a type of dsRNA, and streptozotocin.[75] The elevated expression of RNase L and mRNA in colorectal adenocarcinomas suggests the involvement of RNase L in early events of colorectal carcinogenesis.[76] Moreover, it has been found that RNase L is also involved in bacterial infection, protecting the central nervous system against viral-induced demyelination, or tumor suppression.[19]

Mediating RNase L activity not only affects virus infection-related disease but also other immune response-related diseases. Therefore, a ligand which can control the RNase L activity

will be the basis of promising therapeutics to treat various RNase L-related diseases as well as viral infections. RNase L activation originates from dimerization which is induced by 2-5A binding to the AKR domain. The oligonucleotide-based study to elucidate the RNase L activation mechanism and interaction between ligand and RNase L has been conducted over decades.

1.6 RNase L ligands

1.6.1 Oligonucleotides

The RNase L natural activator 2-5A was first characterized as a protein synthesis inhibitor in 1978.[18] In the same year, it was first suggested that RNase L is a 2-5A-dependent ribonuclease by Maroney and coworkers.[17] The direct target of 2-5A was defined by using 2-5A-binding assay with wild type and RNase L$^{-/-}$ mice.[67] Extracts from organs were incubated with ^{32}P- and Br-labeled 2-5A and further crosslinked with protein by UV irradiation. While the wild type showed the presence of RNase L, extracts from RNase L$^{-/-}$ mice did not detect any 2-5A binding protein.

It remains that the only characterized role of 2-5A is the natural ligand of RNase L to activate its enzymatic activity. 2-5A is a nucleotide oligomer which possesses a 2',5'-phosphodiester bond linkage instead of common 3',5'-phosphodiester bonds from RNA or DNA. The orientation of the molecule made by the 2',5'-phosphodiester bond is one of the factors that likely makes 2-5A a specific ligand to RNase L than other oligoadenylates. Among different lengths of 2-5A (p_x5'A(2'p5'A)$_n$; x=1–3; n>2), the most naturally abundant species of 2-5A in cells is the trimeric triphosphate form, ppp5'A2'p5'A2'p5'A, which activates RNase L most efficiently (Figure 6A). The trimeric triphosphate 2-5A has single-digit nanomolar IC$_{50}$ according to *in vitro* assay.[27] 2-5A is necessary to form an active dimeric RNase L and give a catalytic activity. Therefore, excessive 2-5A analog studies have been conducted to analyze the origin of specific interactions and to mediate RNase L activity.
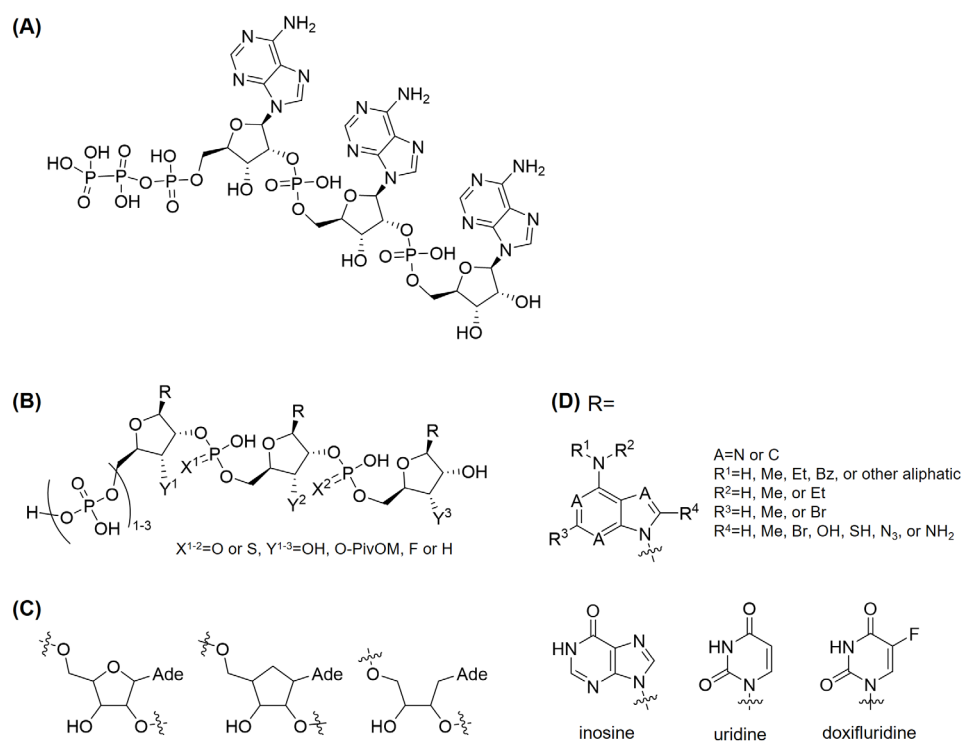
Figure 6. The chemical structure of (A) trimeric triphosphate 2-5A and (B) analogs with (C) ribose derivatives and (D) adenine derivatives.

2-5A analogs which consist of a different number of adenosine than trimer showed reduced or no activity to dimerize RNase L.[27] Indeed, 2-5A analog of which the phosphoryl group was removed showed drastically reduced capability of RNase L dimerization while the monomeric form of the phosphoryl group showed a comparable ability with triphosphate 2-5A to convert RNase L monomer to dimer.[27, 58]

Detailed modifications on each moiety of 2-5A have been performed to investigate the importance of each part (Figure 6B–D). Firstly, several modifications to the ribose ring have been implemented. The 3'-hydroxy group of each ribose ring was reduced to hydrogen to show which hydroxy substituent is critical for effective activation of RNase L.[77-78] In summary, the reduction to cordycepin, 3'-deoxyadnosine, for all adenosine residues for trimer and tetramer 2-5A retained the activity of RNase L with reduced potency. A following study revealed that the cordycepin at the second 5'-ended adenosine has the most influence on RNase L activation in comparison to other positions while ppp5'A2'p5'(3'dA)2'p5'A showed 500-1000 fold decreased potency.[79] However, the activation potency stayed comparable when the hydroxy group was substituted with fluoride, which indicates 3'-hydroxy contributes through a

hydrogen bond towards RNase L binding.[80] Furthermore, the substitution of one ribose unit with an acyclic nucleoside also retained the structure of the original 2-5A as well as the RNase L activation ability (Figure 6C).[81] A replacement of all ribofuranose oxygen to methylene resulted in a major reduction of activation ability.[82]

Moreover, phosphoryl linkage showed that each phosphoryl linkage groups contribute to the binding to RNase L. The phosphoryl group is substituted with phosphorothioate to study the role of phosphoryl internucleotide linkages in trimer 2-5A.[83-85] The monophosphorothioate drastically reduces the potency of RNase L activation and the diphosphorothiate derivatives completely lost the activation even though all derivatives show binding to RNase L. The effects of methylene group insertion in the linkage between adenosine were determined through the synthesis of 2'-phosphonate-modified trimers and tetramers.[86]

In addition, a number of studies have been performed in an effort to understand the binding mode of adenine moieties (Figure 6D). A methyl-, hydroxy-, thiol-, bromide-, amino-, or azido-group is added to the 2- or 8-position of adenine. The potency is notably varied depending on the type and position of modification. For instance, the addition of 8-methyl, 8-bromide, 2-methyl, or 2-bromide groups retained the activation ability on a single modification of a specific position while addition to a critical adenine position or all adenines gave reduction or loss of potency.[87-91] The addition of an 8-hydroxy group did not change the RNase L activation ability while 8-thiol group reduced the potency drastically.[92-94] Interestingly, the insertion of 8-azido group at one certain adenosine increased the RNase L activation potency.[95] Additionally, nitrogen atoms at adenine were methylated to elucidate the critical atom position of adenine for RNase L binding and activation.[96-97] The exchange of adenine to inosine, uridine, doxifluridine, or tubercidin showed how many adenines are necessary and which position of adenine is critical for activation.[98-101] In addition, a report from Kitade group showed the possible binding mode of each 2-5A analog in schematics and explained why the activity is retained or reduced.[101]

Several significant researches have shown how 2-5A binds and activates RNase L. This information is critical to understanding the specificity and mechanism of this activation however this natural 2-5A ligand does not appear to be a feasible therapeutic tool. Even though 2-5A shows a low nanomolar IC_{50} to activate RNase L *in vitro*, 2-5A is challenging to use as a treatment. 2-5A cannot penetrate the cell membrane by itself because 2-5A is an oligonucleotide with a large molecular mass and several charges in the phosphate backbone.

Additionally, 2-5A is unstable in cells due to dephosphorylation and degradation by 2'-phosphodiesterase and 5'-phosphatase, hence resulting in a cellular half-life of only a few minutes.[39] Nonetheless, 2-5A was used to recruit RNase L with the help of carrier systems in the form of bifunctional molecules, such as ribonuclease-targeting chimera (RIBOTAC) and in conjugates as 2-5A-linked peptide nucleic acid (PNA).[102-103] Development of alternative small, not so easily degraded RNase L ligands could facilitate the modulation of RNase L activity in cells as such small molecule-ligands are currently being explored.

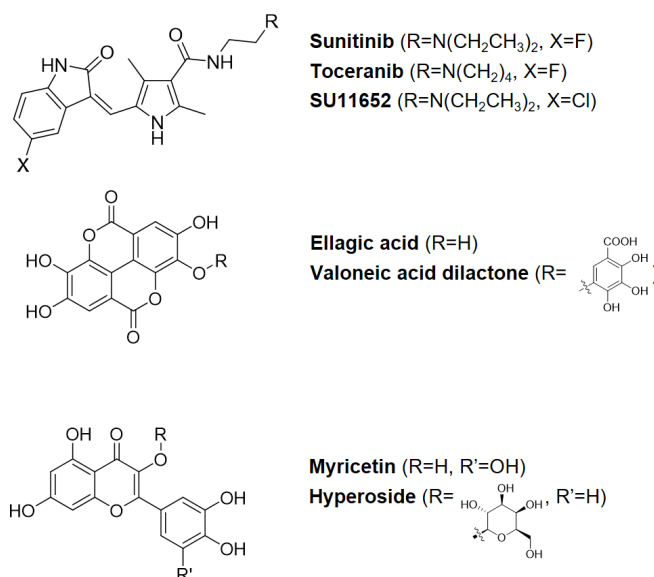## 1.6.2 Small molecule-ligands
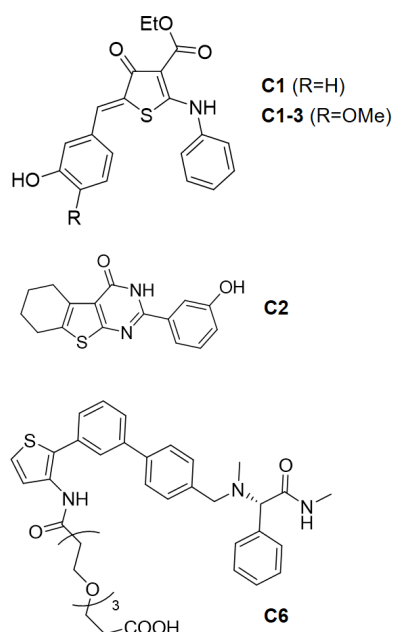
Figure 7. Reported small molecule-(A) activators and (B) inhibitors of RNase L.

The first screening campaign to attain RNase L small molecule-activators was reported in 2007 by Silverman and coworkers (Figure 7A). Two activator scaffolds, thiophenone **C1** and thienopyrimidine **C2**, revealed 26 and 22 μM IC_{50} at Förster resonance energy transfer (FRET)-based *in vitro* RNA cleavage assay described in Figure 10.[104] Although a thiophenone derivative, **C1-3**, was identified as an improved potent small molecule-activator by a preliminary structure-activity relationship (SAR) study for RIBOTAC design, the potency still has a limitation since normalized fluorescent recovery, indicating RNase activity, showed only

48% after the treatment of 130 μM **C1-3** in FRET assay.[105] In addition, the most recent study reported a new thiophene-based scaffold **C6** to have ~60% RNA cleavage at 1 μM in FRET-based assay by using DNA-encoded library screening in 2022.[106] Compound **C6** is the most potent RNase L small molecule-activator by today. However, the potency was drastically reduced to around 45% fluorescent recovery at 50 μM when carboxylic group is protected to t-butyl carboxylate.

For inhibitors, sunitinib, an ATP-competitive inhibitor of kinases, such as vascular endothelial growth factor receptor (VEGF-R), platelet-derived growth factor receptor (PDGF-R), and IRE1, is reported as a potent inhibitor of both RNase L and PKR with IC_{50} values of 1.4 and 0.3 μM, respectively (Figure 7B).[12] The inhibition of RNase L against sunitinib was observed in both *in vitro* assay and cellular assay in Hey1b cells while the binding event was monitored by surface plasmon resonance. The following study revealed the first cocrystal structure of RNase L with small molecule-ligand, resolving that the origin of strong binding is the halogen bond between fluoride and Cys435.[107] Additionally, sunitinib derivative SU11652 with chloride instead of fluoride was reported with slightly improved potency IC_{50} of 7.6 μM for SU11652 and 33 μM for sunitinib. Polyphenolic natural products, ellagic acid and valoneic acid dilactone, were reported as allosteric RNase L inhibitors.[108] The most recent study for RNase L small molecule-inhibitors discovered through a fragment-based screening, giving polyphenolic myricetin and hyperoside with IC_{50} of 364 μM and 1.6 μM respectively in *in vitro* FRET assay.[109] However, the critical drawback for all of the reported small molecule-inhibitors of RNase L is that they are multi-targeting molecules. Sunitinib is an FDA-approved drug for the treatment of cancers while targeting multiple receptor tyrosine kinases (RTKs) in the nano-molar range; vascular endothelial growth factor receptor 2 (VEGFR2, Flk-1) and platelet-derived growth factor receptor β (PDGFRβ) with K_i values of 9 nM and 8 nM, respectively.[110-112] Polyphenolic natural products including ellagic acid and myricetin show multi-target bioactivity.[113-114]

Considering the limited potency of RNase L-targeting molecules and the associated application potential of reported molecules, RNase L modulators with improved potency and selectivity are highly sought after.

2. Objective

Modulating RNase L activity is not only important in the context of viral infection but also in various immune-related diseases. RNase L has a unique binding pocket to regulate the RNase activity as a result it has been challenging to obtain a sensitive and selective ligand. This was proven by the limited number of RNase L small molecule-modulators which have been reported to this day. In this study, we aimed to efficiently modulate RNase L activity by using two different branches.

In one branch, we aimed to identify modulators using ligand binding-based methods. In this branch, we aimed to investigate whether improved modulators of RNase L could be identified by using either the high throughput screening (HTS) campaign or the modification of reported small molecules. However, our HTS campaign effort did not lead to obtaining a small molecule-modulator against challenging target RNase L. Therefore, we focus on optimizing reported small molecules. The first approach is the chemistry-oriented scaffold-based design. For this purpose, the modified core scaffold of reported activators is designed, which is based on physicochemical properties and shared chemical features of reported ligands. The next approach is a structure-activity relationship (SAR) study. A preliminary SAR study with six 2-aminothiophene derivatives to identify a linker attachment position in a previous study resulted in a compound that demonstrated improved potency to activate RNase L. On this basis, an excessive SAR study is carried out. The third approach to search for a potent small molecule-ligand is a rational design strategy based on the reported crystal structure.

In the second branch, we aim to identify improved modulators of RNase L activity by investigating various bifunctional molecule approaches. Here, we assess if RNase L activity could be modulated by bifunctional molecule-promoting RNaseL dimerization or a heterobivalent molecule targeting two different RNase L domains. Additionally, the PROTAC molecule is designed to degrade a protein, which inhibits RNase L activation, and hence restores RNase L activity.
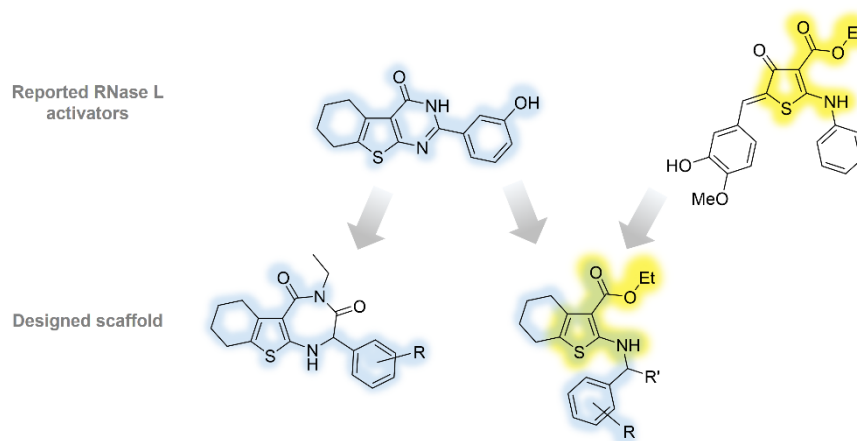
3. Result and discussion

3.1 Small molecule-ligand-based approach

3.1.1 Scaffold-based design

3.1.1.1 Objective of design

This work was published at ACS combinatorial science in 2020.[115] FRET assay was performed by Lydia Borgelt.


Figure 8. Designed strategy of scaffold-based design from two reported RNase L activators.

The first approach to improve the potency of RNase L modulators initiated from chemistry-oriented scaffold-based design. This approach is based on the chemical structure of reported ligands. One approach was from thienopyrimidine which is one of the scaffolds published as an RNase L activator from the only successful HTS campaign to obtain an RNase L small molecule-activator (Figure 8).[104] Two main bottlenecks of this scaffold are the limited potency as a small molecule-ligand and the rigid chemical structure originating from the high amount of sp^2-hybridized carbons. The thienopyrimidines showed poor solubility in both organic and aqueous solvents because the scaffold reveals a conjugated structure between three aromatic rings which give a highly flat 2-dimensional structure and enables strong π-π stacking between respective molecules. Another drawback is the weak potency to activate RNase L (22 μM) possibly due to its 2-dimensional structure limiting efficient binding to a 3-dimensional binding pocket (Figure 8). The thiophenone appears repeatedly in RNase L activators so that thiophene core scaffold should be conserved in future interactions to find a suitable high affinity-activator (Figure 7). Therefore, our synthetic effort was focused on the substitution of a 2-dimensional pyrimidine to a 3-dimensional diazepine ring. Once thienopyrimidine is replaced by

21

thienodiazepine, the core functionalities, such as 3-carbonyl and 2-amino moieties, correlate with the original scaffold but with increased 3-dimensionality and H-donors and -acceptors. Moreover, the thienodiazepine core scaffold is well-studied in toxicology or pharmacology as found within the list of scaffolds of FDA-approved drugs. For example, olanzapine is a thienodiazepine-containing FDA-approved drug as an antipsychotic drug to treat schizophrenia and bipolar disorder.[116] Another thienodiazepine-containing JQ1 is a potent inhibitor of bromodomain and extra-terminal motif protein families to treat inflammation and cancer.[117]

Another approach in scaffold-based design was to synthesize a fused chemical structure combing two reported scaffolds of RNase L activators. The shared chemical feature of two scaffolds is 3-carbonyl-2-aminothiophene. We designed a combinatorial scaffold that possesses the key structure of both thienopyrimidine and 2-aminothiophenone, noted as the fused scaffold below. The synthetic route to synthesize thienodiazepine and fused scaffold was designed according to the combination of two multicomponent reactions (MCRs), Gewald and Petasis borono-Mannich (Petasis) reaction (Figure 9). Gewald reaction is the typical reaction to yield aminothiophene.[118-119] A reaction to functionalize the primary amine at 2-position of thiophene was required to synthesize two designed structures. Petasis reaction was applied to give multifunctionalized amine as Petasis reaction is a facile amine-functionalizing reaction while enabling the introduction of a variety of functional groups in mild reaction conditions.[120-121]
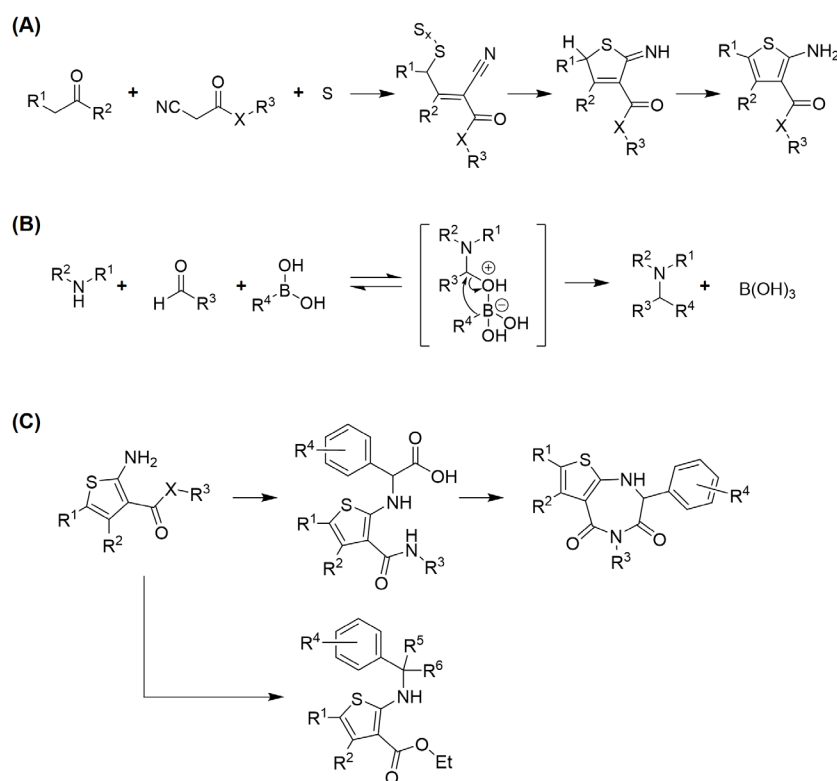
Figure 9. The mechanism of (A) Gewald reaction and (B) Petasis reaction. (C) Synthetic route to obtain thienodiazepines and fused scaffold.

Gewald reaction is a straightforward MCR synthesizing aminothiophene from components of ketone, α-cyanoester, and sulfur (Figure 9A). Thiophenone ring forms from intramolecular cyclization. Petasis reaction is another MCR of an amine, an aldehyde, and a boronic acid to synthesize multi-substituted amines via the *in situ* formation of a tetraboronate intermediate (Figure 9B). Even though a wide range of carbonyl components and boronic acids have been successfully carried out in Petasis reactions, the number of amine substrate types shows scarcity. Most amine substrates are limited to secondary non-aromatic amines, as shown in recent studies in peptide modification and DNA-encoded library synthesis.[122-123] The primary aromatic amine substrate which is required in the design of this study is considered as less reactive substrate in Petasis reactions although a few reported anilines, such as pyridine-2-amines, and naphthalene-2-amines, were applied to the reaction with the help of catalysis, increased temperature, or microwave irradiation. As the Gewald products give the challenging amine substrates in Petasis reaction, we first started reaction condition screening to identify an optimized reaction condition for this atypical amine substrate in Petasis reaction.

3.1.1.2 Synthetic route optimization

Gewald product to give 2-aminothiophene **2** and **3** was synthesized as amine substrate for Petasis reaction from cyclohexanone, sulfur, respective cyanate substrates, 2-cyano-*N*-ethylacetamide or ethyl 2-cyanoacetate. In our design, Gewald products were employed as amine substrates while glyoxylic acid was used as an aldehyde component introducing carboxylic acid for the later intramolecular cyclization to afford thienodizaepines. Phenyl boronic acids to provide an aromatic ring that mimics the initial RNase L activator structure were used for the initial screening of Petasis reaction conditions. The reaction solvent, temperature, reaction time, and reagent adding order were varied. Molecular sieves were added to all reaction conditions to remove generated water molecules throughout the reaction. The screened reaction conditions are summarized in Table 1.

Table 1. Reaction condition screening to optimize Petasis reaction
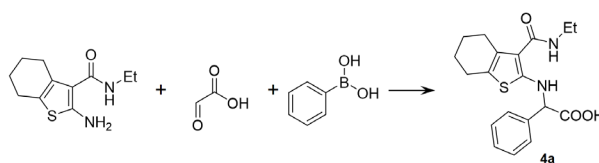
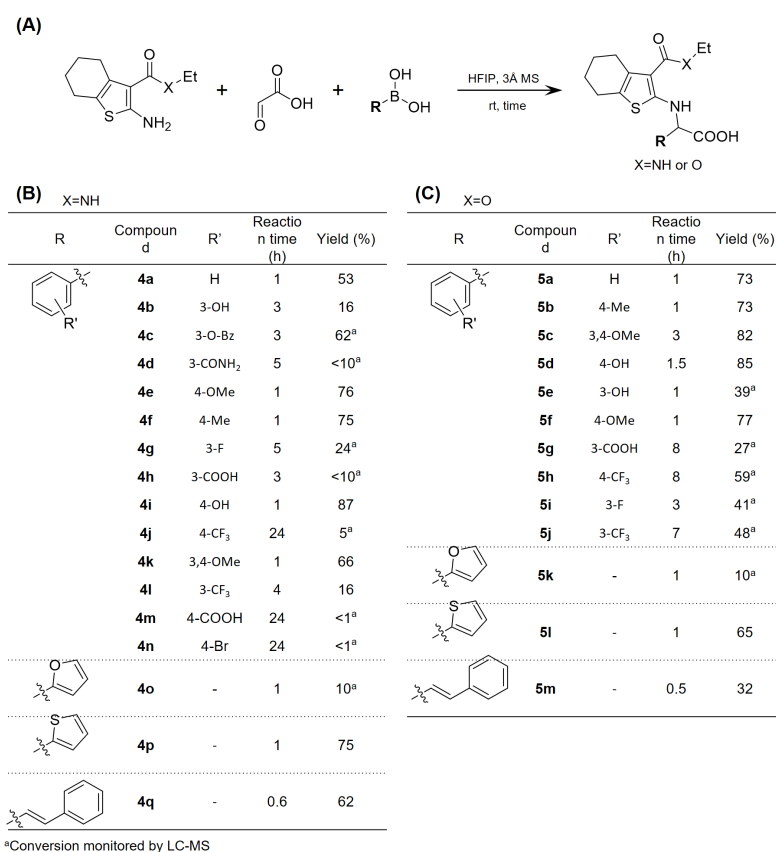| Entry	Solvent	Reagent addition	Max. conversion time (h)[a]	Max. conversion rate (%)[a]
1	DCM	Seq.[b]	24	24
2	HFIP	Seq.[b]	1	37
3	DCM/HFIP (1:1 v/v)	Seq.[b]	6	24
4	THF	Seq.[b]	24	3
5	ACN	Seq.[b]	6	14
6	EtOH	Seq.[b]	12	8
7	MeOH	Seq.[b]	24	0
8	DMF	Seq.[b]	24	0
9	Toluene	Seq.[b]	24	6
10	DCM	Simul.[c]	1	48
11	HFIP	Simul.[c]	1	63

[a]conversion measured by LC-MS. [b]Seq.: sequential addition of reagents with preactivation of an amine substrate and an aldehyde for 10 min, [c]Simul.: simultaneous addition of reagents without preactivation.

The most influencing factor was the type of solvent. In short, DCM, HFIP, and ACN showed better conversion than the other solvents. Among all the tested solvents, HFIP showed higher conversion than the others. However, the mixture of the best two solvents, DCM and HFIP, did not result in an improved conversion. The reaction was monitored for more than 20 h for all conditions and major increase of conversion for all the conditions showed within 6 h. Conversion after 1 h in DCM was distinctly higher and only a minor improvement in conversion was observed over a longer reaction time. In case of HFIP as a solvent, 1 h reaction time showed the best conversion 37% than a longer reaction time (Figure S1). For all the reaction conditions, the elevated temperature did not improve the conversion. The final variation was to add reagents sequentially or simultaneously. Surprisingly, the simultaneous addition of reagents showed up to 2-fold higher conversion than the sequential addition of boronic acid after 10 min incubation of amine and ketone components. This result might be either due to potential byproduct formation between amine and aldehyde or because Petasis reaction happens through the formation of tetraboronate intermediate instead of sequential imine intermediate formation and then Petasis product. The best condition showing 63%

conversion was the reaction in HFIP for 1 h reaction at room temperature with the simultaneous addition of reagents, which was selected in further derivatives synthesis. Acceleration in HFIP condition is caused due to stabilization of ionic transition states and iminium moiety in the boronate intermediate. The converted product was successfully isolated by facile titration with ACN and H_2O with 53% yield of compound **4a**. Polar Petasis product was collected as precipitate and byproducts stayed at the supernatant.

3.1.1.3 Synthesis of a fused scaffold from Petasis reaction

Two series of derivatives were obtained from a sequential Gewald-Petasis reaction (Scheme 1). One series is 3-carboxyamide-2-aminothiophenes for amine components and glyoxylic acid as aldehyde components introducing carboxylic acid to the product for further cyclization to diazepine. The other series was carried out with 3-ethylester-2-aminothiophenes as amine components to synthesize the fused scaffold combining two activator scaffolds.

(B) X=NH

R	Compound	R'	Reaction time (h)	Yield (%)
(phenyl, R')	4a	H	1	53
	4b	3-OH	3	16
	4c	3-O-Bz	3	62[a]
	4d	3-CONH$_2$	5	<10[a]
	4e	4-OMe	1	76
	4f	4-Me	1	75
	4g	3-F	5	24[a]
	4h	3-COOH	3	<10[a]
	4i	4-OH	1	87
	4j	4-CF$_3$	24	5[a]
	4k	3,4-OMe	1	66
	4l	3-CF$_3$	4	16
	4m	4-COOH	24	<1[a]
	4n	4-Br	24	<1[a]
(furan)	4o	-	1	10[a]
(thiophene)	4p	-	1	75
(styryl)	4q	-	0.6	62

(C) X=O

R	Compound	R'	Reaction time (h)	Yield (%)
(phenyl, R')	5a	H	1	73
	5b	4-Me	1	73
	5c	3,4-OMe	3	82
	5d	4-OH	1.5	85
	5e	3-OH	1	39[a]
	5f	4-OMe	1	77
	5g	3-COOH	8	27[a]
	5h	4-CF$_3$	8	59[a]
	5i	3-F	3	41[a]
	5j	3-CF$_3$	7	48[a]
(furan)	5k	-	1	10[a]
(thiophene)	5l	-	1	65
(styryl)	5m	-	0.5	32

[a]Conversion monitored by LC-MS

Scheme 1. Synthesis of two series of 2-aminothiophenes from Gewald-Petasis sequential reaction. (A) Synthetic route of Petasis reaction from Gewald product. Series of (B) 3-carboxiamide-2-aminothiophenes to synthesize thienodiazepine and (C) 3-ethylester-2-aminothiophenes as a fused scaffold.
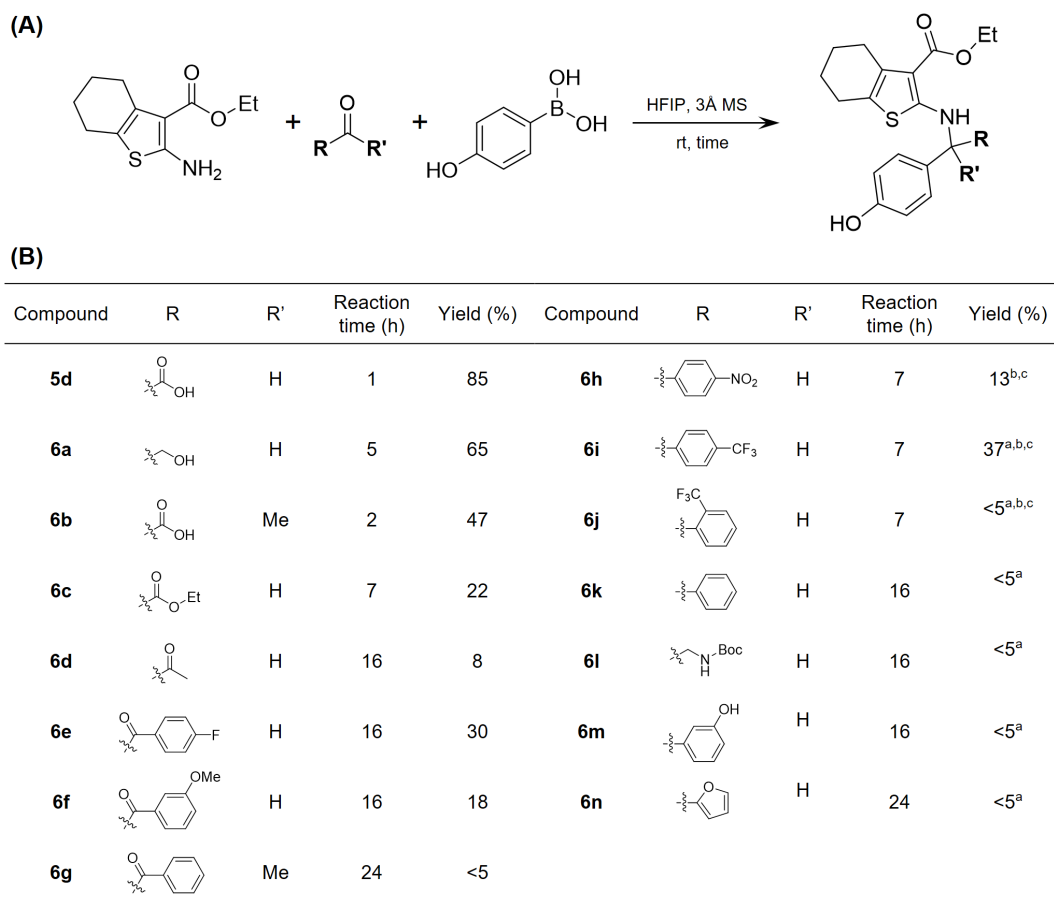
To introduce different moieties on the phenyl ring, various substituents on the boronic acids were applied to the reaction. Phenyl rings with electron-donating groups, methyl, methoxy, benzyl, and hydroxy group, were introduced while normally showing higher yield than compounds with phenyl rings with electron-withdrawing groups, trifluoromethyl, fluoro, bromo, carboxamide, and carboxylic acid. Heterocyclic aromatic rings as well as vinylic aromatic ring were tested to broaden the scope of the reaction (Scheme 1B). For the second series of 3-carboxyamide-2-aminothiophenes, selected reagents were tested and compounds showing more than 50% were isolated (Scheme 1C). Similar to the first series of 3-ethylester-2-aminothiophenes, electron-donating substituents at the aromatic moiety resulted in higher yields.

The initial two series were synthesized with glyoxylic acid as aldehyde components to introduce carboxylic acid. The next series was accomplished by changing the aldehyde component to another carbonyl group by using different aldehydes or ketones (Scheme 2). This series will only be employed in the fused RNase L activator scaffold route, therefore 3-ethylester-2-aminothiophene as exclusively used as one of the starting materials. 4-Hydroxyboronic acid was kept since an RNase L activator, thienopyrimidine, has a hydroxy group and 4-hydroxyboronic acid showed a much higher yield than 3-hydroxyboronic acid (Scheme 2A). The scope included aldehydes conjugated with different carbonyl moieties, carboxylic acids, ethyl esters, and methyl ketones. Isolation methods were altered according to the products because the polarity of products varied dependent on functional groups at R and R' positions.

The conversion was generally proportional with the electronegativity of functional groups at R position in case of the aldehyde components where R' is a proton. The product **5d** with a carboxylic acid at R position showed a higher yield than other carbonyl groups with reduced electronegativities, such as ethyl carboxylate **6c** and methyl ketone **6d**. When the carbonyl group at R position was substituted to the phenyl ring, **6k**, only a trace amount of conversion was observed by LC-MS. However, electron-withdrawing groups at the para-position of phenyl rings such as **6h** and **6i** improved the conversion. The strong electron-withdrawing groups at the α position of aldehydes accelerated the reaction while making aldehydes a stronger electrophile. Additionally, ketones were applied instead of aldehydes. Only ketones with strong electron-withdrawing groups, such as carboxylic acid **6b**, allowed major conversion, which indicates a strong driving force by electronegativity is required to overcome the steric hindrance of ketone.

(A)

(B)

Compound	R	R'	Reaction time (h)	Yield (%)	Compound	R	R'	Reaction time (h)	Yield (%)
5d	(COOH)	H	1	85	**6h**	(4-NO₂-phenyl)	H	7	13[b,c]
6a	(CH₂OH)	H	5	65	**6i**	(4-CF₃-phenyl)	H	7	37[a,b,c]
6b	(COOH)	Me	2	47	**6j**	(2-CF₃-phenyl)	H	7	<5[a,b,c]
6c	(CO-O-Et)	H	7	22	**6k**	(phenyl)	H	16	<5[a]
6d	(acetyl)	H	16	8	**6l**	(NH-Boc)	H	16	<5[a]
6e	(4-F-benzoyl)	H	16	30	**6m**	(3-OH-phenyl)	H	16	<5[a]
6f	(3-OMe-benzoyl)	H	16	18	**6n**	(furanyl)	H	24	<5[a]
6g	(benzoyl)	Me	24	<5					

[a]Conversion monitored by LC-MS; [b]HFIP/DCM (1:1 v/v) as the solvent; [c]reflux

Scheme 2. Combinatorial scaffold to mimic two RNase L small molecule-activator scaffolds with different aldehyde components employed in Petasis reaction. (A) Synthetic scheme and (B) variation of different aldehyde or ketone components used in this compound series.

3.1.1.4 Intramolecular cyclization for thienodiazepines

Lastly, a Petasis product series with 3-carboxamide-2-aminothiophenes and *N*-methylenecarboxylic acid was cyclized to obtain diazepine by using amide coupling (Scheme 3). A reaction condition for amide coupling was also screened because the carboxamide is less basic than the amine. A range of amide coupling reagents was tested. Among DCC, EDC, HATU, and COMU, EDC showed the best conversion to yield the intramolecular cyclization product. The reaction concentration affected to conversion between intramolecular and intermolecular cyclized products. While intramolecularly cyclized products were obtained to give diazepine with a reaction concentration lower than 5 mM, a higher concentration yielded intermolecularly dimerized products. For example, DCC with ~30 mM starting material concentration showed 67% conversion to a dimer product. Selected derivatives were cyclized to give thienodiazepines. In total, 8 derivatives were obtained under the same reaction

conditions and isolated by flash chromatography with good yields.
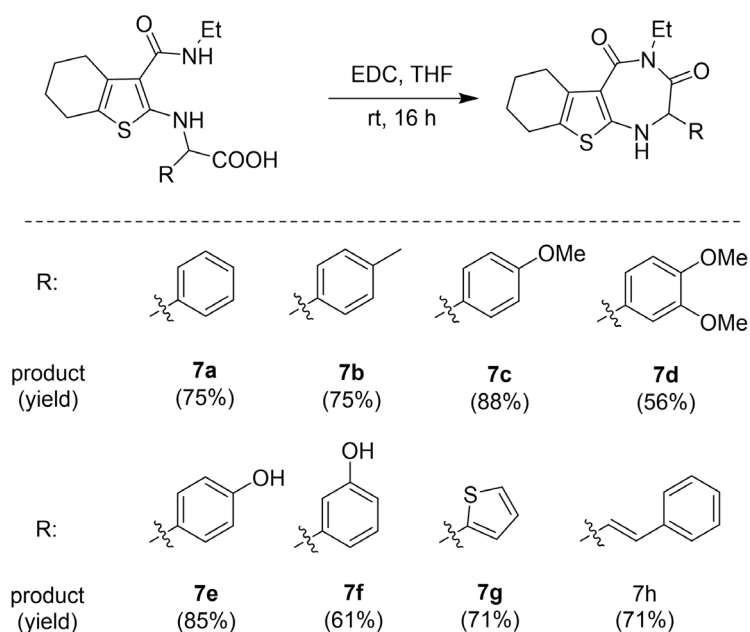
Scheme 3. Intramolecular cyclization from 3-carboxamide-2-aminothiophene Petasis product to yield thienodiazepines with different aromatic moieties.

Additionally, one more derivative of thienodiazepine was obtained to give thienodiazepine without *N*-ethyl group to introduce an additional H-donor (Scheme 4). The Gewald product **8** with a primary amide in the 3-position was obtained from 3-cyanoacetamide. Interestingly, Petasis reaction was selectively reactive at the aromatic primary amine position to give **9** while 3-carboxamide was not reactive under the established Petasis reaction condition. This reaction selectivity is derived from the low nucleophilicity of the amide group which requires strong catalytic conditions in reported Petasis reactions. Lastly, **10** was obtained with an additional H-donor by established intramolecular cyclization conditions with extended scope of reaction and products.
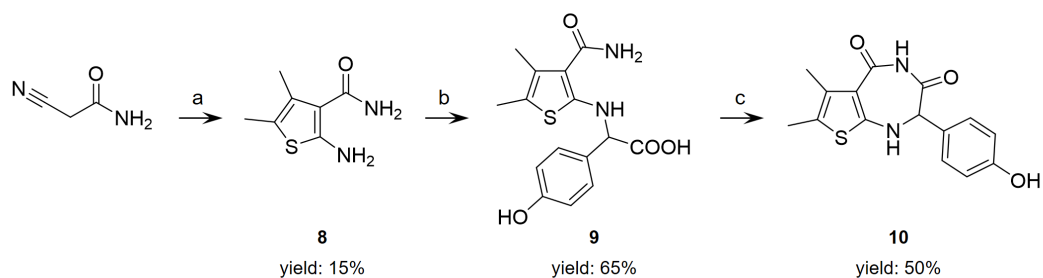
Scheme 4. Synthesis of a derivative of thienodiazepine. **a**. Ethyl methyl ketone, sulfur, TEA, EtOH, rt, o.n.; **b**. Glyoxylic acid, 4-hydroxyphenyl boronic acid, 3Å MS, HFIP, rt, 1 h; **c**. EDC, THF, rt, 3 h.

3.1.1.5 Biological evaluation

All derivatives were evaluated by FRET-based RNA cleavage assay. FRET-based RNA cleavage assay is a fluorescent-based turn-on assay to monitor the RNase activity of RNase L. The 33-mer RNA probe was labeled with a fluorophore and a quencher and designed to arrange the fluorophore and quencher in close proximity (Figure 10). The fluorescence is quenched by energy transfer to a quencher while the RNA structure is intact. Once the probe is degraded, the RNA structure is destroyed so that the distance between the fluorophore and quencher becomes far enough to recover the fluorescence signal. In this study, an established RNA sequence with FAM as fluorophore and black hole quencher 1 as a quencher was used.[104-105, 108] Under optimized conditions, the assay showed a reported range of fluorescent recovery by activating RNase L with 2-5A.
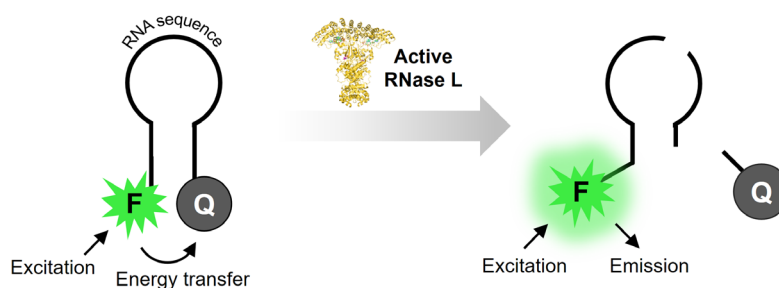
Figure 10. Schematic for FRET-based RNA cleavage assay.

All series of compounds, fused compounds combining two RNase L activator structures and thienodiazepines, were investigated in FRET-based RNA cleavage assay to evaluate their capability to activate RNase L. The fluorescent recovery was normalized with data from 100 nM 2-5A intensity. However, none of the designed fused scaffolds and thienodiazepines showed significant activation of RNase L at 130 µM (Figure 11). The compound **4q** showed 7% fluorescent recovery being the highest among the synthesized compounds. However, while considering the negative control with DMSO induced up to 5% fluorescent recovery, the fluorescent recovery induced by synthesized compounds including **4q** was not significant enough to continue further evaluation of compounds from scaffold-based design.
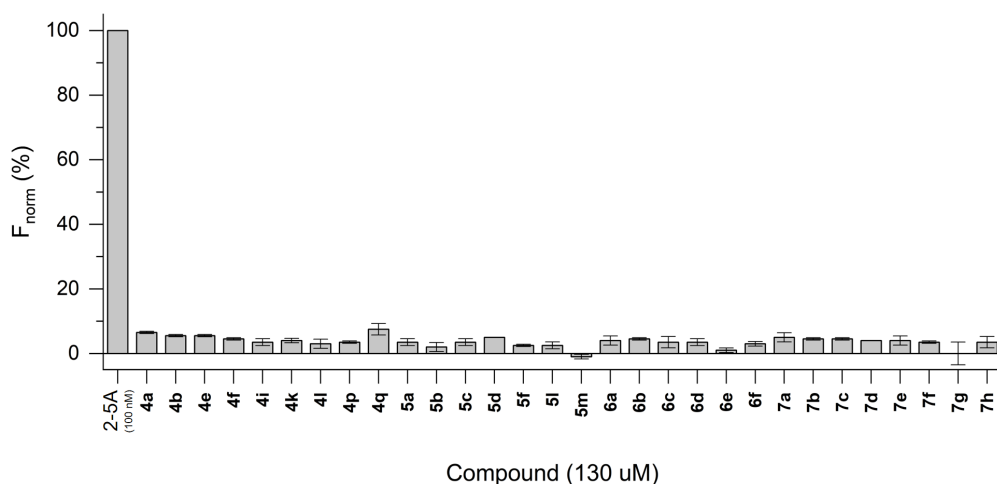
Figure 11. FRET-based RNA cleavage assay showing fluorescent recovery upon RNA degradation. The fluorescent recovery was normalized with the result of 100 nM 2-5A.

3.1.1.6 Summary

In summary, two scaffolds were devised from a scaffold-based design. One is to replace thienopyrimidine with thienodiazepine in order to improve the 3-dimensional conformation of the scaffold as well as solubility. The other scaffold is a fused scaffold, 2-amino-3-ethylester-*N*-methylenephenyl-thiophene, which is a fusion structure of two reported RNase L activators. The synthetic route was optimized to synthesize two scaffolds by using combinatorial multicomponent reactions, Gewald and Petsis reaction, followed by intramolecular cyclization. The optimized reaction showed broad scope for a range of all different components used. However, none of the derivatives showed significant activation ability in the FRET-based RNA cleavage assay. The possible drawback for the thienodiazepine series is that the highly sp^2-hybridized structure from thienopyrimidine might be required to mimic the nucleotide and bind to the 2-5A-binding pocket. In case of a fused structure, the reduction of aromatic rings affected binding affinity and 5-benzylidene ring which is replaced with cyclohexyl moiety could be necessary for binding to RNase L. Even though the scaffold-based design did not lead to obtain an RNase L activator with improved potency, the synthetic effort to obtain a novel scaffold in facile reaction conditions was noteworthy.

3.1.2 Structure-activity relationship (SAR) study of thiopheneone

*This work was published at Bioorganic medicinal chemistry in 2022.[124] The compounds **20a**–**20l** were provided by Laurin Kanis. SB1301 was provided by Pascal Hommen. FRET-, gel-based RNA cleavage, and thermal shift binding assay were performed by Lydia Borgelt and Neele Haacke. Cellular antiproliferation assays were performed by Xiaqiu Qiu and Stavroula Petroulia. Apoptosis assay was performed by Xiaqiu Qiu, Damian Schiller, and Stavroula Petroulia.*

3.1.2.1 Background

The second approach to achieve a potent RNase L modulator was based on a structure-activity relationship (SAR) study. SAR study is a medicinal chemistry approach to elucidate a relationship between the chemical structure of a compound and the respective biological activity and hence pursuing to obtain the improved potency of ligands. An excessive variation on each moiety of a chemical structure is required in a SAR study to properly identify a relation between chemical structure and biological activity. For the SAR study, 2-aminothiophenone-3-carboxylates (ATPCs) were selected because the preliminary SAR study which gave five derivatives altering the 5-benzylidene moiety improved the potency and th hence excessive SAR study was required. ATPC structure was retained as the core structure; two phenyl rings are varied for extensive SAR because ATPC moiety is one of the shared features of reported RNase L small molecule-activators.

3.1.2.2 Chemical synthesis

ATPC was synthesized from ethyl 4-chloroacetoacetate and isothiocyanates with different aromatic moieties by the reported synthetic method.[125] Following Knoevenagel condensation with aldehydes introduced 5-benzylidene to give final products (Scheme 5A). In the first series, different aldehyde components were used for exclusive diversification of *N*-phenyl functionalities while ATPC obtained from phenyl isothiocyanate was preserved. The straightforward reactions gave 13 derivatives with a different substitution pattern on the 5-benzylidene moiety (Scheme 5B). This series included the reported RNase L activators, **C1** and **C1-3**, as well as the less reactive compound **C1-4**. The substituents at 5-benzylidene included electron-donating groups, such as hydroxy and methoxy, as well as electron-withdrawing groups, such as carboxylic acid, trifluoromethyl, cyanide, and halogen atoms at different positions. Furthermore, different heterocycles were applied instead of a phenyl ring (Scheme 5C). Commercially available aldehydes with a 5-membered ring, such as furane, thiophene, pyrrole, and 6-membered piperidine were utilized. Especially, pyrrole often revealed as a key

moiety for drugs and our initial cellular antiproliferation assay showed that pyrrole-containing **16c** is one of the most potent compounds.[126-127] Therefore, extended synthetic efforts to verify the 2-pyrrole moiety were performed to introduce 4-ethylester-2-pyrrole and 3-pyrrole. Additionally, a few bicyclic aromatic rings containing pyrrole were designed to mimic the purine moiety of nucleotides. As RNase L activators are hypothesized to bind to dimerization-regulatory nucleotide-binding pocket, an adenine-mimetic indole and azaindole can improve the binding. While indole was introduced to obtain **16g**, azaindole-aldehydes have been synthesized to introduce a purine-like azaindole compartment (Scheme 6). A total of 4 derivatives of azaindole-aldehyde were synthesized with different nitrogen positions on the pyridine moiety of azaindole. The nitrogen of azaindole was protected with phenyl sulfonamide. The aldehyde was introduced at 2-position selectively while directed by sulfonamide under the strong basic condition to deprotonate the aromatic proton. The purine-aldehydes were obtained after deprotecting phenyl sulfonamide under basic conditions. The 4-,5-,6-, and 7-azaindoles were introduced to ATPC structure to provide **17a–17d**. In total, eleven derivatives with heteroaromatic rings were obtained.
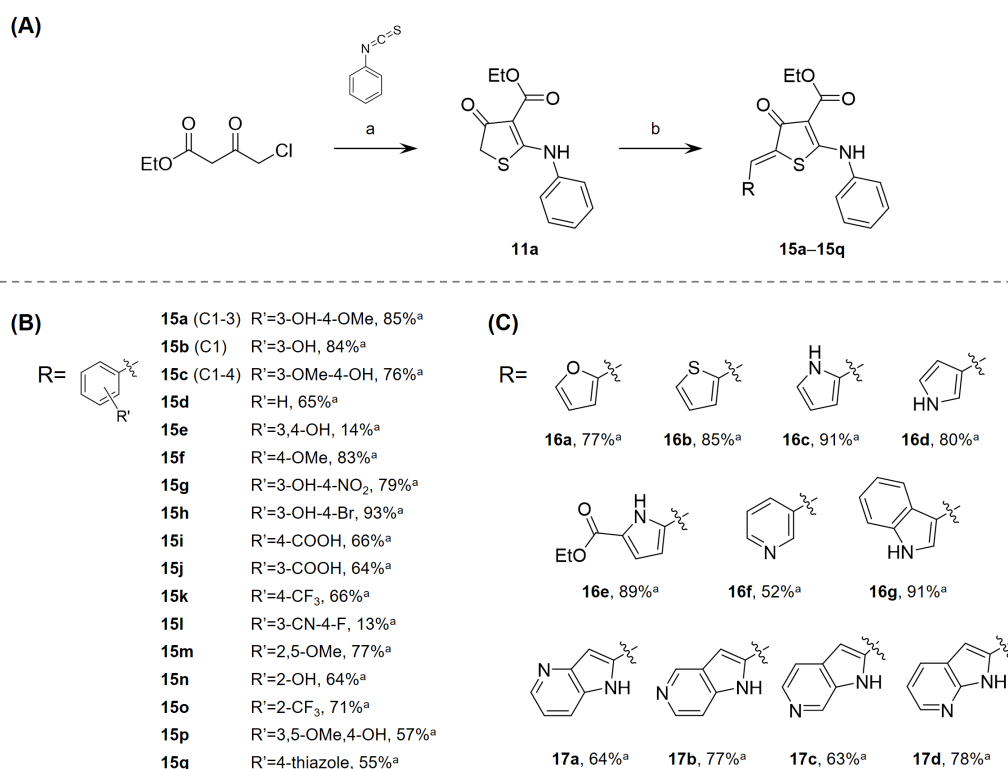
Scheme 5. (A) Synthesis route of ATPCs and derivatives (B) **15a–15q** with phenyl moiety, (C) **16a–16g** and **17a–17d** with heteroaromatic rings. **a**. NaH, dioxane, rt, 2 h; **b**. piperidine, EtOH, reflux, 4–6 h. [a]isolated yield.

32
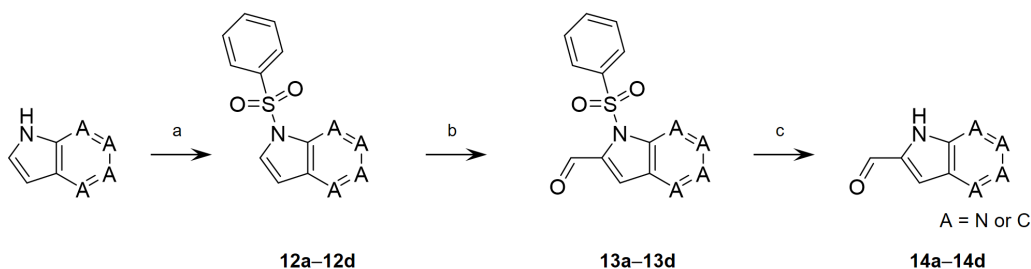
Scheme 6. Synthesis to obtain purine-aldehydes **14a–14d**. **a**. Benzensulfonyl chloride, NaH, THF, rt, 2 h; **b**. LDA, DMF, THF, -78 °C, 1 h, -10 °C, 1 h; **c**. KOH, H$_2$O, MeOH, rt, 30 min–2 h.

Additionally, ATPCs with non-aromatic rings were obtained in the form of cyclohexylmethylene **19** or cyclic ketone **18a–18e** (Scheme 7). This set of compounds showed that the scope of the reaction was able to cover ketones as the carbonyl components instead of aldehydes. The ring size and components of cyclic ketones were varied to give five different ATPCs with aliphatic cycles.
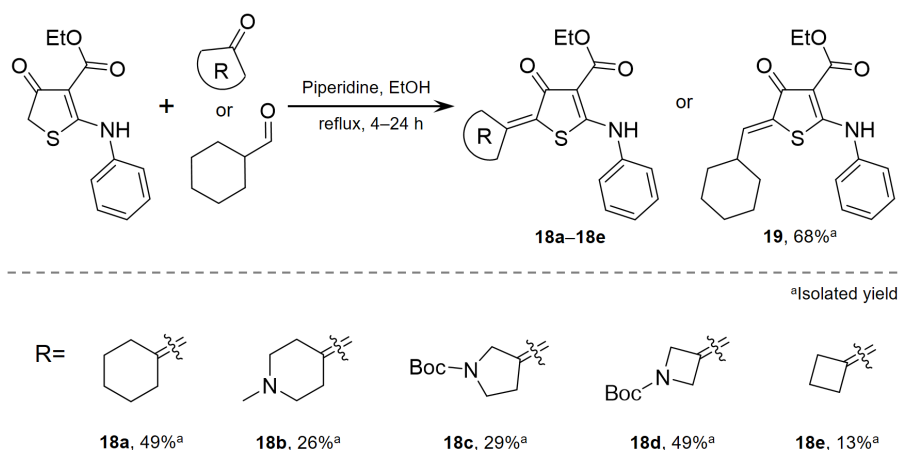
Scheme 7. Synthesis of ATPCs **18a–18e** and **19** using cyclic aliphatic aldehydes.

The last series of ATPCs were synthesized by using different isothiocyanates. For the aldehyde components, pyrrole aldehyde was selected due to the potent inhibitory effect of **16c** in the initial cellular antiproliferation assay (Scheme 8). Electron withdrawing groups and electron donating groups as well as halogen atoms were introduced to *N*-phenyl ring to give 13 derivatives.
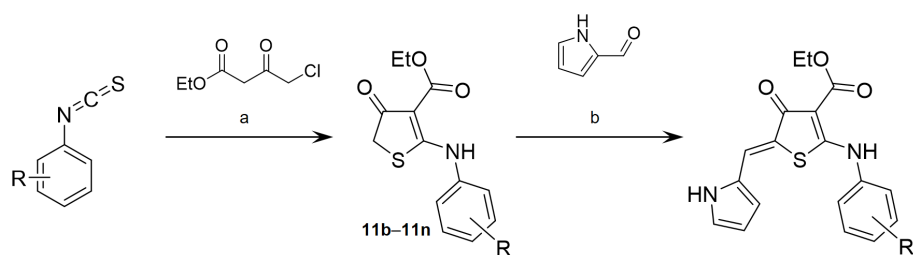
Compound	R	Yield (%)	Compound	R	Yield (%)
20a	4-OMe	79	20h	4-CF$_3$	71
20b	3-OMe	78	20i	3-CF$_3$	68
20c	3,4-OMe	70	20j	4-NO$_2$	84
20d	4-Br	84	20k	3-NO$_2$	82
20e	2-Br	81	20l	4-Me	44
20f	4-F	77	20m	4-Et	64
20g	3-F	76			

Scheme 8. Synthesis of ATPCs **20a–20m** using 1*H*-pyrrole-2-carbaldehyde. **a**. NaH, 1,4-dioxane, 40 °C, 1 h; **b**. piperidine, EtOH, reflux, 2 h.

3.1.2.3 *In vitro* biological evaluation

In total 46 ATPC derivatives were obtained and further evaluated as RNase L modulators *in vitro* biochemical RNA cleavage assays. In this study, the FRET-based RNA cleavage assay used 12-mer structured RNA labeled with Alexa647 and IBQ. Autofluorescence of compounds at the range of FAM emission interfered with the assay. Therefore, the fluorescent label was replaced with Alexa647 which shows the emission in a further range of wavelength. The fluorescent recovery was measured and normalized with the value of 2 nM 2-5A as 100% and DMSO as 0%. The result showed that none of the compounds induced significant RNA cleavage in the FRET assay (Figure 12A). However, it is noteworthy that selected ATPCs, **15h** of 6%, **17d** of 8%, and **17a** of 6%, revealed more potent fluorescent recovery than reported activator **C1** and **C1-3**, 3% and 1% respectively. However, the weak potency of ATPCs and low sensitivity of the assay against reported small molecule-activators could not lead to a clear conclusion of the SAR study.
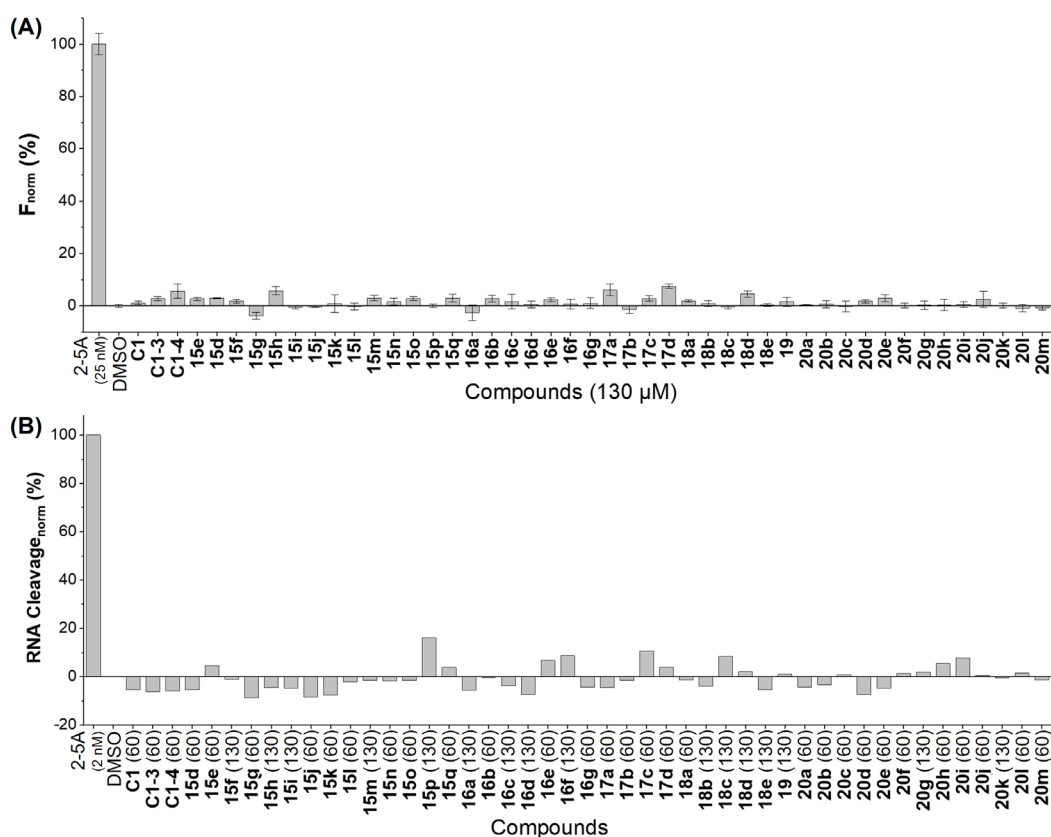
Figure 12. Biochemical assay to evaluate RNase L activity by ATPCs. (A) FRET-based assay at 130 μM ATPCs and (B) gel-based RNA cleavage assay at 60 or 130 μM ATPCs.

Gel-based RNA cleavage assay was designed as an orthogonal RNase L activity assay based on gel electrophoresis. One side of 32-mer RNA probe is labeled with fluorophore Cy3. The RNA sequence has one UU sequence which can easily be cleaved by RNase L. Cleaved and uncleaved RNA is separated by gel electrophoresis to give two bands. The compounds were incubated with RNA at two concentrations: 60 μM or 130 μM. The intensity of the band was quantified and normalized with the full cleavage by 2 nM 2-5A and DMSO (Figure 12B). Although a few compounds showed notable cleavage bands, such as 16% for 130 μM **15p** and 11% for 60 μM **17c**, the result did not correspond with results from the FRET-based RNA cleavage assay. Moreover, the cleavage induced by ATPCs was not significant in comparison with 2-5A.

The biophysical assay by using nano differential scanning fluorimetry (nanoDSF) was performed to monitor the binding event between proteins and ligands. NanoDSF is a thermal shift assay which shows the stability of proteins by measuring the denaturing process of proteins. This process can be influenced by ligand-binding events. In this assay, the intrinsic

tryptophan and tyrosine fluorescence were measured. The temperature of the chamber containing the respective protein with or without compounds was elevated from 20 to 60 °C and the change of the fluorescent signal at 330 and 350 nm was measured. The first derivative was calculated and fitted with a Gaussian plot to determine melting temperature when the first derivative is at the lowest peak. All the compound derivatives including the reported modulator and 2-5A were measured in nanoDSF and the thermal shift value change was shown in Figure 13.
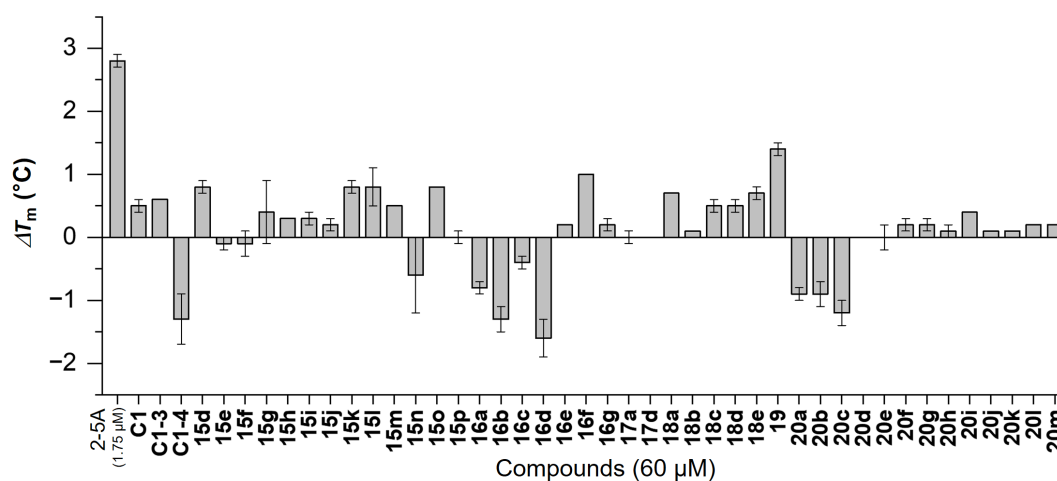
Figure 13. Thermal shift ΔT_m (°C) induced by ATPC compounds (60 μM) or 2-5A (1.75 μM) binding to RNase L.

While the thermal shift induced by 2-5A was observed to be 2.8 °C, the reported small molecule-activator of RNase L induced minor change of T_m, 0.5 and 0.6 °C, respectively, at 60 μM (Figure 13 and Table 2). The majority of ATPC derivatives did not induce thermal shifts as strong as 2-5A upon binding to RNase L. However, a few compounds, such as **15e**, **15g**, **15l**, **15o**, **16f**, **18a**, **18d**, and **19**, showed more than 0.5 °C shift, which is relevant since the reported activator showed a weaker effect. Especially, ATPC **19** with cyclohexylmethylene and **15l** with 5-(3-cyano-4-fluoro)benzylidene, , showed an enhanced affinity with ΔT_m values of 1.4 °C and 1 °C, respectively. The result indicated a promising binding of the new ligands to RNase L.

Table 2. Thermal shift values ΔT_m (°C) induced by selected compounds binding to RNase L

Index	Compound (60 μM)	ΔT_m (°C)
1	2-5A (1.75 μM)	2.8 ± 0.1
2	**15a (C1)**	0.5 ± 0.1
3	**15b (C1-3)**	0.6 ± 0.0
4	**15c (C1-4)**	-1.3 ± 0.4
5	**15d**	0.8 ± 0.1
6	**15k**	0.8 ± 0.1
7	**15l**	0.8 ± 0.3
8	**15m**	0.5 ± 0.0
9	**15o**	0.8 ± 0.0
10	**16f**	1.0 ± 0.0
11	**18a**	0.7 ± 0.0
12	**18c**	0.5 ± 0.1
13	**18d**	0.7 ± 0.1
14	**18e**	0.5 ± 0.1
15	**19**	1.4 ± 0.1

3.1.2.4 Antiproliferation effect evaluation in cellular assays

Even though the RNase L activity change was not induced significantly by ATPCs in *in vitro* biochemical assays, the biophysical assay indicated improved binding of ligands to RNase L. Therefore, we designed a cell-based assay to monitor the effect of compounds in cells. Once RNase L is activated in cancer cells, RNase L induces antiproliferation and apoptotic death of cancer cells. Thus, we evaluated the antiproliferation effects of ATPC compounds as anticancer agents by monitoring cancer cell growth, migration, and colony formation. First of all, cell growth inhibition was monitored by 3-(4,5-dimethylthiazol-2-yl)-2,5-diphenyltetrazolium bromide (MTT) cell viability assay. MTT assay is a colorimetric assay using MTT. MTT is reduced to formazan by NAD(P)H-dependent oxidoreductases while the color changes from yellow to purple. This chemical reduction only occurs in alive cells, which makes the assay represent cell number and growth.

In our evaluation, JAR cells were initially used to monitor cell growth inhibition. Surprisingly, a few ATPCs showed a potent antiproliferation effect against JAR cells at 10 μM (Table 3). Especially, **15k**, **15l**, **15n**, **15p**, **16e**, **16g**, **17d**, **18d**, **19**, **20e**, and **20k** showed higher proliferation inhibition than SB1301, a known LIN28 small molecule-inhibitor which suppress cancer cell growth. Additionally, it is noteworthy that part of the compounds, **15k**, **15l**, **18d**,

and **19**, showed strong antiproliferation effects, these results corresponded with the results observed in the thermal shift change upon binding to RNase L. This result suggested a correlation between RNase L binding and the observed antiproliferation effect.

Table 3. Antiproliferation activity monitoring with cell growth inhibition of compounds at 10 μM against different human cancer cell lines.

Index	Compound	Growth inhibition rate (%)			
		JAR	K562	A549	MCF7
1	**15a (C1)**	51.9 ± 5.3	-[a]	30.62 ± 1.5	24.13 ± 3.5
2	**15b (C1-3)**	NA[b]	NA[b]	11.03 ± 3.7	NA[b]
3	**15c (C1-4)**	49.7 ± 4.3	-[a]	24.17 ± 1.5	23.23 ± 2.5
4	**15d**	20.3 ± 5.6	42.9 ± 4.12	29.6 ± 3.0	23.6 ± 1.5
5	**15e**	48.7 ± 4.6	-[a]	30.7 ± 2.6	38.1 ± 2.6
6	**15f**	32.9 ± 6.6	9.6 ± 1.95	17.5 ± 4.1	14.7 ± 1.9
7	**15g**	51.2 ± 4.5	-[a]	-[a]	41.5 ± 3.2
8	**15h**	39.8 ± 7.8	22.0 ± 3.1	13.6 ± 2.3	16.4 ± 1.1
9	**15i**	16.8 ± 3.3	27.5 ± 2.1	11.6 ± 4.1	< 10
10	**15j**	50.6 ± 3.7	-[a]	< 10	< 10
11	**15k**	68.7 ± 2.8	-[a]	-[a]	41.3 ± 3.4
12	**15l**	99.9 ± 0.3	-[a]	-[a]	-[a]
13	**15m**	38.1 ± 3.5	30.7 ± 7.7	< 10	< 10
14	**15n**	89.4 ± 5.0	-[a]	-[a]	-[a]
15	**15o**	29.0 ± 12.5	19.7 ± 1.4	< 10	< 10
16	**15p**	57.5 ± 5.6	-[a]	19.2 ± 2.1	12.9 ± 2.8
17	**16a**	NA[b]	NA[b]	NA[b]	NA[b]
18	**16b**	NA[b]	NA[b]	NA[b]	NA[b]
19	**16c**	49.2 ± 8.0	16.2 ± 3.8	23.5 ± 5.1	18.3 ± 3.0
20	**16d**	19.5 ± 6.2	18.9 ± 2.0	< 10	< 10
21	**16e**	60.1 ± 4.6	18.6 ± 3.4	< 10	NA[b]
22	**16f**	32.1 ± 8.7	< 10	< 10	< 10
23	**16g**	57.6 ± 5.2	NA[b]	19.8 ± 1.5	25.0 ± 4.5
24	**17a**	54.3 ± 4.9	-[a]	16.7 ± 0.2	18.2 ± 1.2
25	**17b**	26.3 ± 8.3	22.8 ± 3.6	17.1 ± 1.5	18.2 ± 1.6
26	**17c**	< 10	NA[b]	NA[b]	NA[b]
27	**17d**	74.8 ± 3.1	-[a]	-[a]	42.2 ± 2.9
28	**18a**	15.5 ± 4.4	18.7 ± 2.9	NA[b]	NA[b]
29	**18b**	< 10[c]	NA[b]	< 10	< 10
30	**18c**	-[a]	-[a]	-[a]	29.6 ± 0.8
31	**18d**	70.2 ± 5.3	-[a]	-[a]	40.4 ± 1.6

32	**18e**	-[a]	-[a]	-[a]	33.8 ± 1.9
33	**19**	95.2 ± 4.5	-[a]	-[a]	45.3 ± 2.8
34	**20a**	27.6 ± 7.0	NA[b]	< 10	< 10
35	**20b**	NA[b]	NA[b]	NA[b]	NA[b]
36	**20c**	47.9 ± 5.8	NA[b]	NA[b]	NA[b]
37	**20d**	41.5 ± 5.6	17.0 ± 0.6	< 10	< 10
38	**20e**	62.7 ± 10.2	20.5 ± 4.4	-[a]	29.4 ± 2.6
39	**20f**	61.5 ± 4.7	NA[b]	< 10	< 10
40	**20g**	45.4 ± 6.2	-[a]	< 10	< 10
41	**20h**	38.5 ± 4.3	NA[b]	30.1 ± 3.2	19.1 ± 2.4
42	**20i**	52.9 ± 6.5	-[a]	22.8 ± 3.2	22.9 ± 3.3
43	**20j**	54.9 ± 9.0	NA[b]	NA[b]	NA[b]
44	**20k**	57.4 ± 12.5	-[a]	-[a]	27.4 ± 0.9
45	**20l**	< 10	NA[b]	20.9 ± 1.3	< 10
46	**20m**	< 10	NA[b]	17.5 ± 1.6	NA[b]
47	SB1301	53.5 ± 2.3	-[a]	-[a]	-[a]

[a]-: not tested, [b]NA: not active, no inhibition observed at 10 μM.

Table 4. Dose-dependent antiproliferation activity of compounds against different human cancer cell lines.

Index	Compound	IC$_{50}$ (μM)			
		JAR	K562	A549	MCF7
1	**15a (C1)**	16.97 ± 2.1	38.71 ± 1.6	-[a]	-[a]
2	**15b (C1-3)**	NA[b]	NA[b]	-[a]	NA[b]
3	**15c (C1-4)**	8.88 ± 1.9	10.39 ± 2.4	> 100	> 100
4	**15e**	6.1 ± 0.9	5.2 ± 0.7	> 100	25.2
5	**15j**	12.7 ± 2.3	12.7 ± 0.9	19.1 ± 0.8	-[a]
6	**15k**	11.7 ± 1.2	16.2 ± 3.2	-[a]	-[a]
7	**15q**	5.9 ± 0.4	7.0 ± 1.0	9.8 ± 0.9	13.7
8	**15l**	1.5 ± 0.1	1.6 ± 0.3	8.0 ± 0.8	5.2 ± 2.0
9	**15n**	8.0 ± 1.6	8.8 ± 2.4	16.9 ± 2.1	15.1 ± 2.4
10	**15p**	17.4 ± 2.7	31.7 ± 2.3	19.2 ± 2.1	-[a]
11	**16c**	9.5 ± 4.4	71.0	> 100	48.0
12	**16e**	10.6 ± 2.6	46.8	> 100	30.5
13	**16g**	14.1 ± 1.6	> 100	-[a]	-[a]
14	**17a**	14.4 ± 3.3	> 100	-[a]	-[a]
15	**17d**	9.6 ± 0.9	6.6 ± 0.7	13.6 ± 0.4	-[a]
16	**18c**	23.2 ± 1.5	10.7 ± 1.0	35.8 ± 2.9	-[a]
17	**18d**	8.4 ± 2.2	4.5 ± 0.9	17.0 ± 0.5	18.1
18	**18e**	37.0 ± 2.8	11.6 ± 1.0	47.0 ± 2.0	-[a]

19	**19**	3.7 ± 0.8	5.9 ± 1.1	18.0 ± 0.8	6.4
20	**20d**	27.0 ± 3.7	$-^a$	$-^a$	$-^a$
21	**20e**	8.9 ± 3.1	36.3	43.2 ± 1.7	27.1
22	**20f**	15.9 ± 5.7	> 100	$-^a$	$-^a$
23	**20g**	22.6 ± 3.6	> 100	$-^a$	$-^a$
24	**20h**	46.8 ± 3.3	$-^a$	$-^a$	$-^a$
25	**20i**	19.7 ± 2.8	> 100	$-^a$	$-^a$
26	**20j**	15.6 ± 1.1	> 100	$-^a$	$-^a$
27	**20k**	10.1 ± 2.9	7.2 ± 0.5	23.9 ± 3.8	20.7
28	SB1301	9.3 ± 0.8	16.5 ± 1.3	>100	$-^a$

^{a}-: not tested, ^{b}NA: not active, no inhibition observed at 10 µM.

The selected compounds, characterized with higher inhibition than 50%, were also tested in single-dose against other human cancer cell lines, K562, A549, and MCF-7, and also underwent dose-dependent response evaluation (Table 3 and Table 4). The results showed that the selected compounds exerted comparable antiproliferation effects against K562 and slightly reduced effects against A549 and MCF7 cells. Collectively, Compounds **15l** (IC$_{50}$: 1.5 µM) with a 3-cyano-4-fluorobenzylidene moiety and **19** (IC$_{50}$: 3.7 µM) with a cyclohexylmethylene moiety were the most potent inhibitors against JAR cells (Table 4). Especially, compound **15l** showed all single-digit IC$_{50}$ values of growth inhibition against all four cancer cells (Figure 14). The IC$_{50}$ values of compound **15l** were 1.6 µM against K562 cell, 8.0 µM against A546 cell, and 5.2 µM against MCF7 cell. The general antiproliferation effect against different types of cancer cell lines implies that the compounds influenced the general system of human cells, which correlates to the RNase L pathway in the immune response against cancer. Additionally, compounds **15l** and **19** revealed an antiproliferation effect in a time-dependent manner at 10 µM (Figure 15A–B). Notably, compound **15l** showed a strong antiproliferation effect from 3 h incubation at 10 µM.
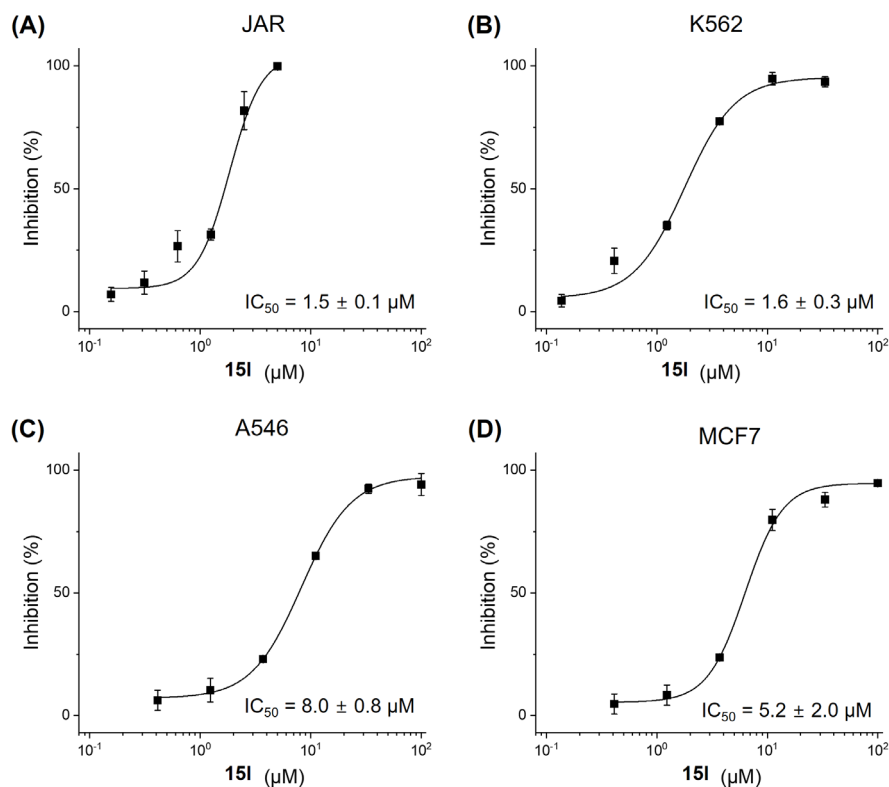
Figure 14. Antiproliferation activity of the most active ATPCs **15l** and **19**. Dose-dependent response and IC$_{50}$ values of **15l** against the four different human cancer cell lines, (A) JAR, (B) K562, (C) A549, and (D) MCF7. Time-dependent antiproliferation effect of compound (E) **15l** and (F) **19** against JAR cell at 10 µM.
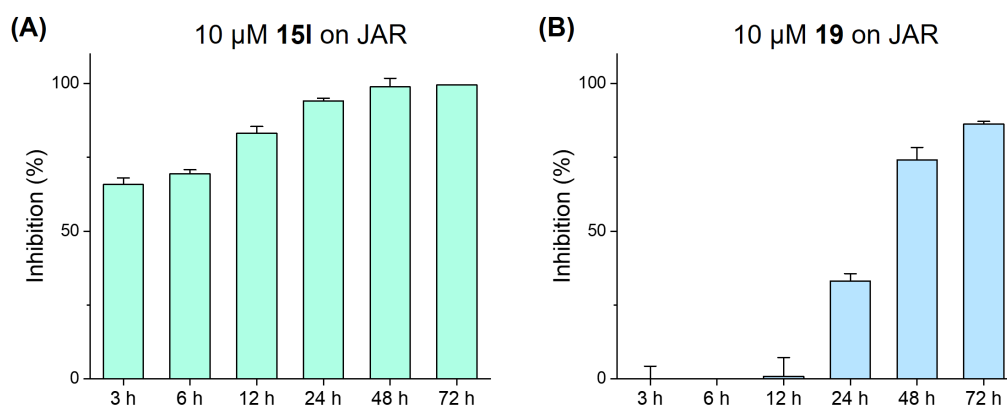
Figure 15. Time-dependent antiproliferation effect of compound (A) **15l** and (B) **19** against JAR cell at 10 µM.

In addition to growth inhibition measurement, cell migration and colony formation assays were performed to monitor the antiproliferation effect of compounds **15l** and **19** (Figure 17). For cell migration assay, the middle region of the cell colony was removed by mechanical scratch to

form a wound. The width of the wound was measured after a defined time of incubation in the presence or absence of compounds. For both compounds **15l** and **19**, wound healing was inhibited in a concentration-dependent and time-dependent manner (Figure 16A–D). For instance, the wound closure was suppressed 85% and 42% in the presence of compounds **15l** and **19**, respectively, after 72 h incubation at a concentration of 5 µM. The complementary result was observed at the cell colony formation assay. The inhibition was exhibited clearly at a lower concentration than in the cell migration experiment. When JAR cells were exposed to 600 nM and 5 µM of **15l** and **19**, respectively, for 72 h, cell colony formation was completely inhibited (Figure 16E–F). The proliferation inhibition through compounds **15l** and **19** was observed in cell migration and cell colony formation experiments.
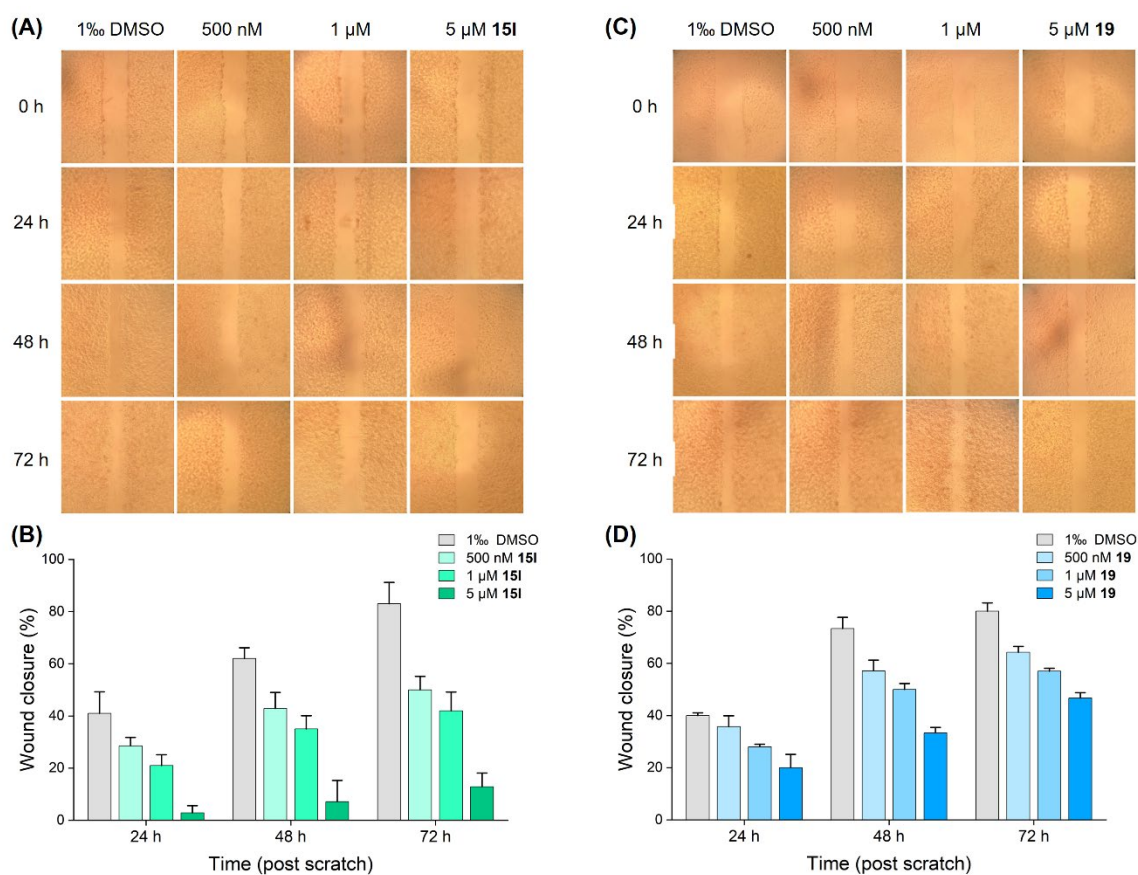
Figure 16. Antiproliferation effect measured through cell migration assay. The migration was measured by monitoring wound healing on JAR cells after incubation with compounds (A) **15l** and (C) **19**. (B), (D) The quantification of wound closure in cell migration assay shown in (A) and (C), respectively.
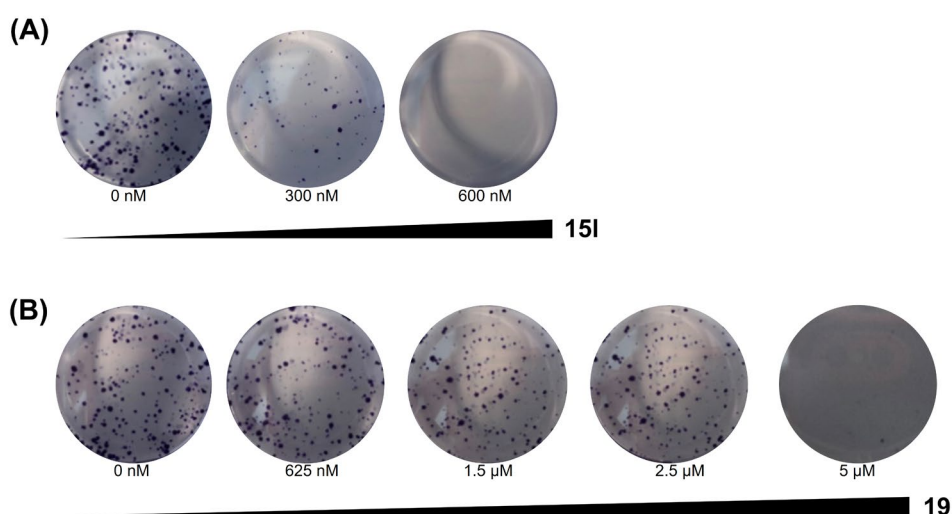
Figure 17. Antiproliferation measured by colony formation assay. Cell colony formation inhibition in dose-dependent response after 72 h incubation with (A) **15l** and (B) **19**, respectively.

3.1.2.5 Apoptotic assays

To evaluate the correlation between the antiproliferation effect and RNase L binding, we performed apoptosis assays. Once RNase L is activated in cells, RNase L induces apoptotic death of cells. Two types of apoptosis assays were performed. One is poly(ADP-ribose) polymerase (PARP) cleavage assay, and the other is flow cytometry-assisted apoptosis assay determined by the ratio of two dyes propidium iodide (PI) and annexin V-FITC. Surprisingly, both **15l** and **19** were inducing apoptotic death of the cells in PARP cleavage assay, indicated by an increased ratio of cleaved PARP/GAPDH (Figure 18A). Compound **15l** exhibited dose-dependent apoptosis, which showed more than 2-fold increase in PARP cleavage at 5 µM and 10 µM than the negative control. Compound **15l** was also further tested in flow cytometry assisted-apoptosis assay (Figure 19). In this assay, propidium iodide was used to detect dead cells and annexin V-FITC to visualize the cells with apoptotic death. The compound **15l** was inducing 50% of apoptosis at 5 µM and 61% of apoptosis at 10 µM. Both apoptosis assays exhibited that **15l** induced apoptotic death in cancer cells. This result introduces a new angle that the RNase L binding monitored in biophysical assay and evaluation of RNase L-activation in cells causing apoptosis of cancer cells which inhibit cell growth needs to be evaluated in parallel.
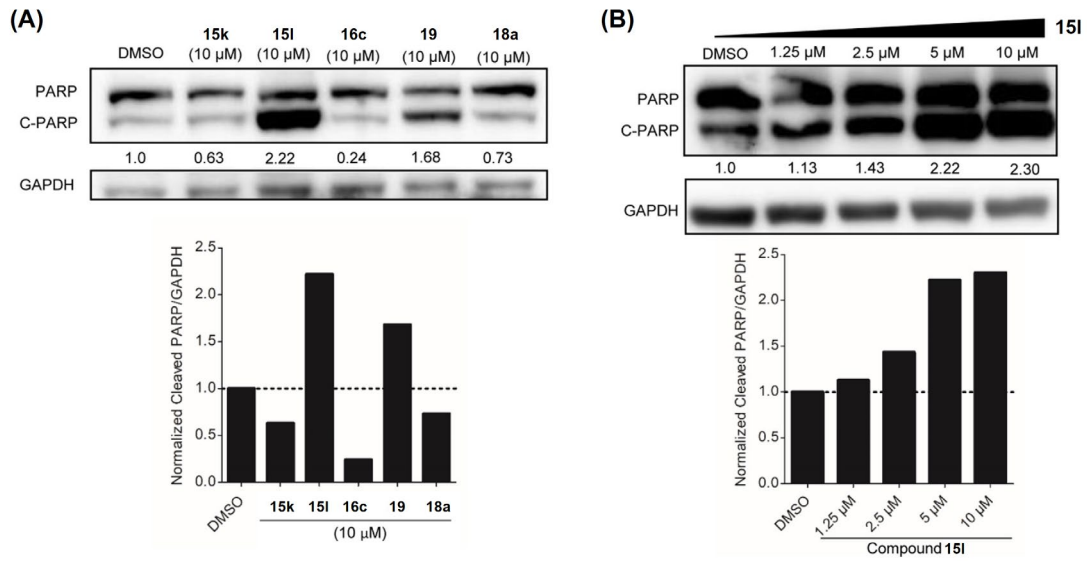
Figure 18. Apoptosis assay by selected ATPC compounds in JAR cells. (A) The protein levels of PARP and cleaved PARP and quantification of ratio. (B) Dose-dependent PARP cleavage by compound **15l**
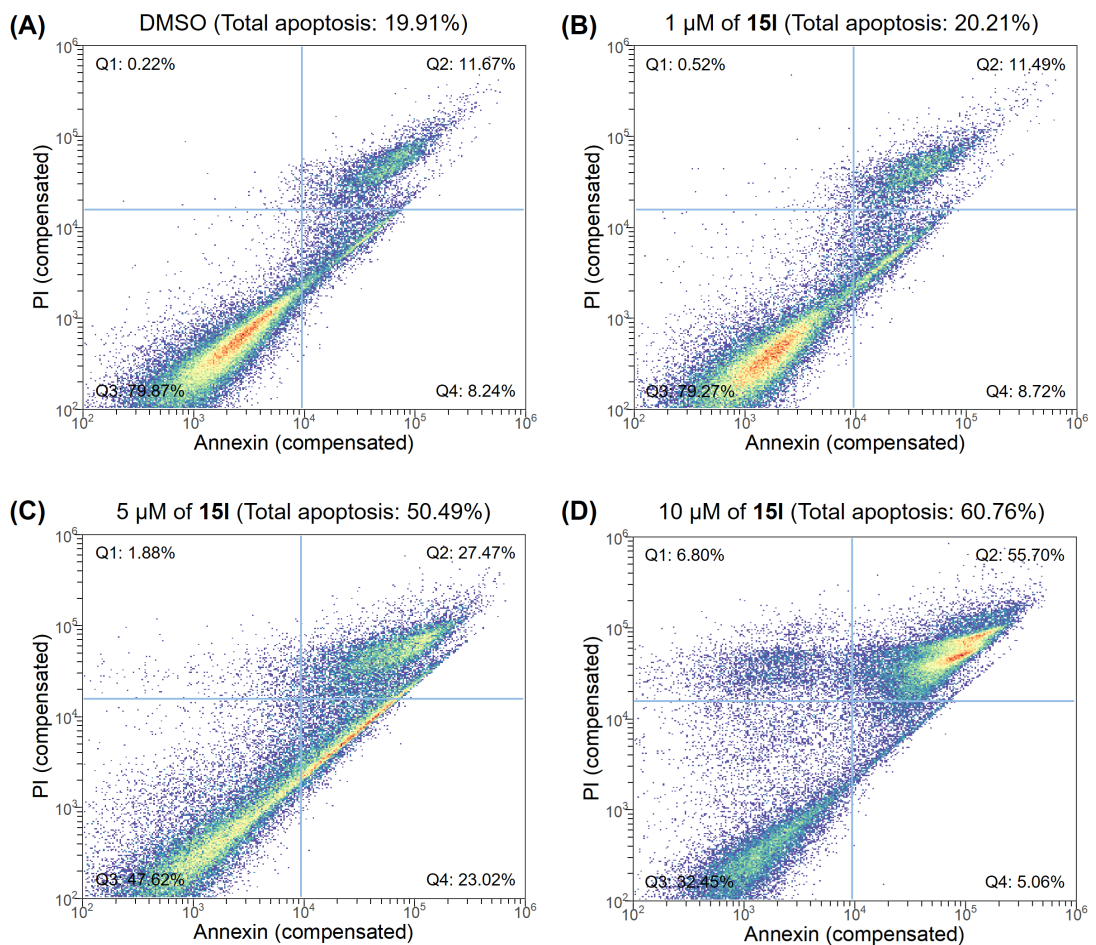
Figure 19. Compounds **15l** induced apoptosis in JAR cells, measured by the ratio between propidium

44

iodide (PI) and Annexin V-FITC in flow cytometry. Q1: necrotic; Q2: late apoptotic; Q3: viable; Q4: early apoptotic. Q2 + Q4: total apoptosis.

The cellular antiproliferation assays commonly indicated that a few ATPCs including **15l** and **19** revealed promising antiproliferation effects against four different cancer cell lines. Furthermore, compounds **15l** and **19** induced apoptosis of cancer cells in a dose-dependent and time-dependent manner. Interestingly, the compounds **15l** and **19** showed potent binding to RNase L in biophysical assay and had promising antiproliferation effects demonstrating the expected phenotype in cancer cells in which RNase L is activated. Therefore, it is noteworthy to mention that antiproliferation activity and apoptosis-inducing effects might be induced as RNase L-mediated downstream effects.

3.1.2.6 Summary

In summary, the SAR study of ATPC scaffold for RNase L activators was initially designed to identify more potent RNase L small molecule-activators. We have obtained 46 derivatives of ATPC. Selected ATPCs including **15l** and **19** showed improved binding to RNase L in comparison with the reported RNase L activators **C1** and **C1-3**, which was monitored by a thermal shift assay. Considering the role of RNase L as tumor suppressor and RNase L activation-mediated apoptosis, a further evaluation for the antiproliferation activity of the synthesized ATPCs against four human cancer cell lines was proceeded and apoptosis-inducing activity of selected compounds was investigated. We identified that ATPCs, such as compounds **15l** and **19**, showed potent antiproliferation activity with single-digit micromolar IC_{50} values in our in-house screening against four human cancer cell lines. The further evaluations for compounds **15l** and **19** represented dose-dependent apoptosis-inducing activity and inhibition of cell migration and colony formation against cancer cells. The correlation between biophysical assay and antiproliferation with apoptosis-inducing effect implied that **15l** and **19** potentially caused RNase L-involved downstream effects in cells. However, further phenotypic and mechanistic studies need to be performed. For example, cellular rRNA cleavage assay can show the activation of RNase L in cells. Additionally, the knockout of RNase L in cancer cells can confirm whether the observed cellular result was induced by RNase L-related pathways.

3.1.3 Rational design from ATP-competitive sunitinib

FRET and gel-based RNA cleavage assays were performed by Neele Haacke. BLI binding assay and cellular rRNA cleavage assay were performed by Lydia Borgelt.

3.1.3.1 Objective of rational design

The third approach in the small molecule-based approach is to attain a new scaffold of RNase L modulator according to rational design. Even though none of the reported activators has been investigated through a mechanistic study including crystallography and point mutation, two RNase L small molecule-inhibitors, sunitinib and myricetin, were characterized through crystallography showing the mode of action of RNase L inhibition. However, both ATP-mimetics sunitinib as well as polyphenolic natural products myricetin interact with multiple targets in cell biology as described in chapter 1.6.2. Therefore, the discovery of a new ligand with improved potency and selectivity is highly required. The crystallography allowed the rational design of a new ligand with an improved chemical scaffold so the ligand achieves better binding to the protein. Both inhibitor molecules bind to the ATP-binding pocket at the PK domain of RNase L while disrupting ATP analogs binding, which results in less stable dimerization of RNase L and hence loss of enzymatic activity. Although ATP-binding pockets have not attracted attention as an activation regulatory part at the beginning of RNase L discovery, recent studies have proved that the stabilization of RNase L dimeric configuration by the PK domain is important for RNase L enzymatic activation. Furthermore, RNase L homolog protein, IRE1, studies showed that the ATP-binding part can be a critical factor to dimerize and activate the protein.[131] The crystallography study of sunitinib in RNase L demonstrated that sunitinib binds to the ATP-binding pocket while affecting the arrangement of α helix linkage between the ankyrin repeat domain and the pseudokinase domain, which destabilized the dimeric conformation of RNase L. This fact led to an intriguing starting point to study an ATP-competitive ligand because a small molecule-activator of IRE1, an RNase L homolog, is developed by targeting the ATP-binding pocket and mediating the α-helix. Therefore, affecting the secondary structure of surrounding residues at ATP-binding pocket with different binding modes of small molecules might enable mediating the activity of RNase L as it was possible with IRE1.
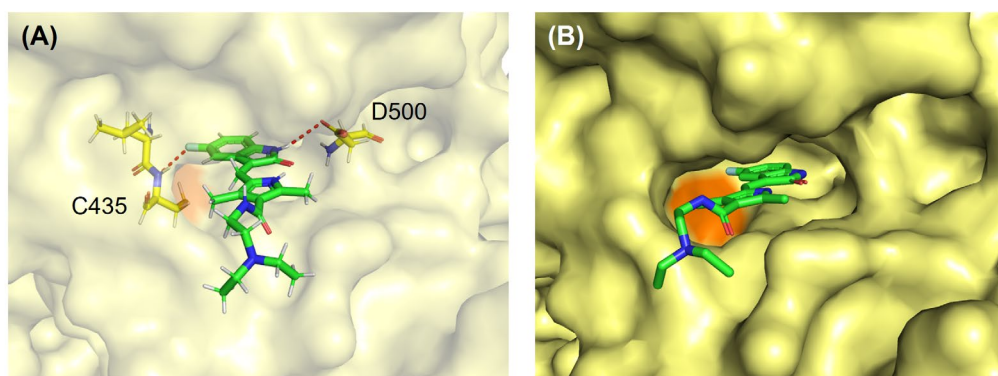
Figure 20. Crystal structure of RNase L with Sunitinib at ATP-binding pocket and (A) the interactions between sunitinib and RNAse L (PDB code: 6M11). (B) Unoccupied region when sunitinib binds to the ATP-binding pocket.

3.1.3.2 Rational design of new scaffold

The rational design of the new scaffold as RNase L modulators was based on the structural characterization of a complex between RNase L and sunitinib. Sunitinib is an ATP-competitive ligand, mimicking the chemical structure of ATP while the 1*H*-pyrrole-3-carboxamide moiety of sunitinib resembles the ribose and phosphate tale, and the oxindole moiety mimics adenine. The co-crystal structure of sunitinib and RNase L suggested drawbacks of the binding mode of sunitinib (Figure 20). The binding of sunitinib to the ATP-binding pocket of RNase L relied on only two interactions, a hydrogen bond and a halogen bond between 6-fluoro-2-oxindole and RNase L Cys435 (Figure 20A). Moreover, the 3-dimensional conformation of sunitinib revealed low complementary orientation since the orange part of the pocket was not occupied (Figure 20B). The 1*H*-pyrrole-3-carboxamide moiety attended neither in interactions nor 3-dimensionally fitting in the pocket due to the orientation of pyrrole and oxindole moieties. Given these binding features, alternative adenine mimetics, instead of oxindole, a small molecule-building block was investigated to conjugate with the ribose-mimetic moiety, 1*H*-pyrrole-3-carboxamide. Interestingly, 2-aminothiophenone-3-carboxylate (ATPC) moiety from RNase L activator showed structure similarity with oxindole. Oxindole has a 5-membered heterocyclic ketone conjugated with a phenyl ring while the ATPC moiety also consists of a 5-membered heterocyclic ketone and is conjugated with a phenyl ring through the 2-amino compartment. Additionally, the 3-carbonyl group together with *N*-phenyl moiety enables to provide higher complementarity, which mimics an acyclic form of adenine-mimetic pyrimidone. Additionally, the conjugation in *N*-phenyl ATPC can give more potent three-

dimensional conformation and flexibility than oxindole, which might contribute to better binding to the ATP binding pocket. Therefore, a conjugated structure between ATPC and 1*H*-pyrrole-3-carboxamide moiety, 2-((pyrrol-2-yl)methylene)thiophen-4-one scaffold, was designed (Figure 21).
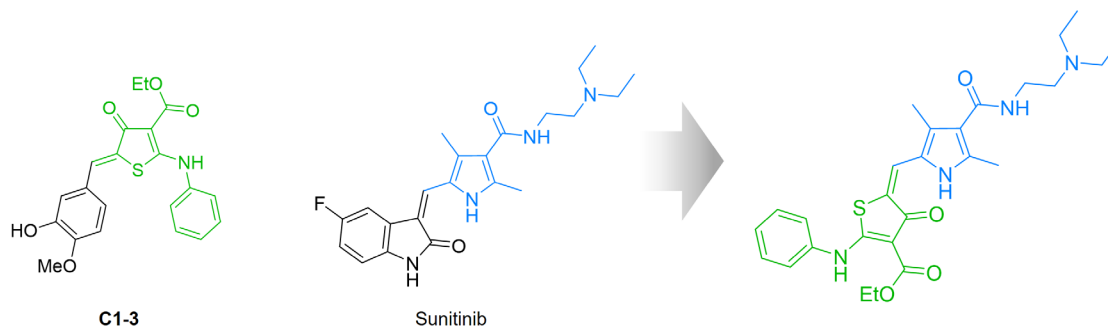
Figure 21. Conceptual design of new scaffold 2-((pyrrol-2-yl)methylene)thiophen-4-one scaffold.

A molecular docking study has been first carried out to verify the potency of a newly designed scaffold. Molecular docking enables the prediction of the binding mode of the ligand into defined pockets of a protein by computational calculation of interactions and conformational complementation. The designed scaffold is a nucleotide mimetic which is able to bind both of ATP-binding pocket and the 2-5A-binding pocket. Thus, the docking study of 2-((pyrrol-2-yl)methylene)thiophen-4-ones has been performed in both of the ATP-binding pocket in the PK domain and the 2-5A-binding pocket in the AKK domain. Firstly, the two designed molecules with different functionality surprisingly exhibited a promising 3-dimensional complementary at the ATP-binding pocket (Figure 22A–B). Even though the two molecules contain different terminal functional groups, representing the same arrangement of molecules in the pocket, which implied that the binding mode mainly originated from the core scaffold of the molecule. For both molecules, the *N*-phenyl ATPC moiety was located inside of the pocket while substituting oxindole to ATPC with yielding higher occupancy of the pocket. Meanwhile, the docking of the designed molecule at the 2-5A-binding pocket showed an interesting result. The arrangement between a molecule of the designed scaffold and 2-5A revealed high similarity, indicating the possibility of merging these two molecules into one to make a more potent binder (Figure 22D). Two 5-membered rings, pyrrole and thiophenone, were replacing the original location of ribose while *N*-phenyl ring and triethylamine moiety were substituting adenine and the phosphoryl tail of 2-5A respectively. The docking study proved that the designed scaffold is a promising ligand of RNase L with an optimal design of mimicking each

moiety of nucleotide or ATP.
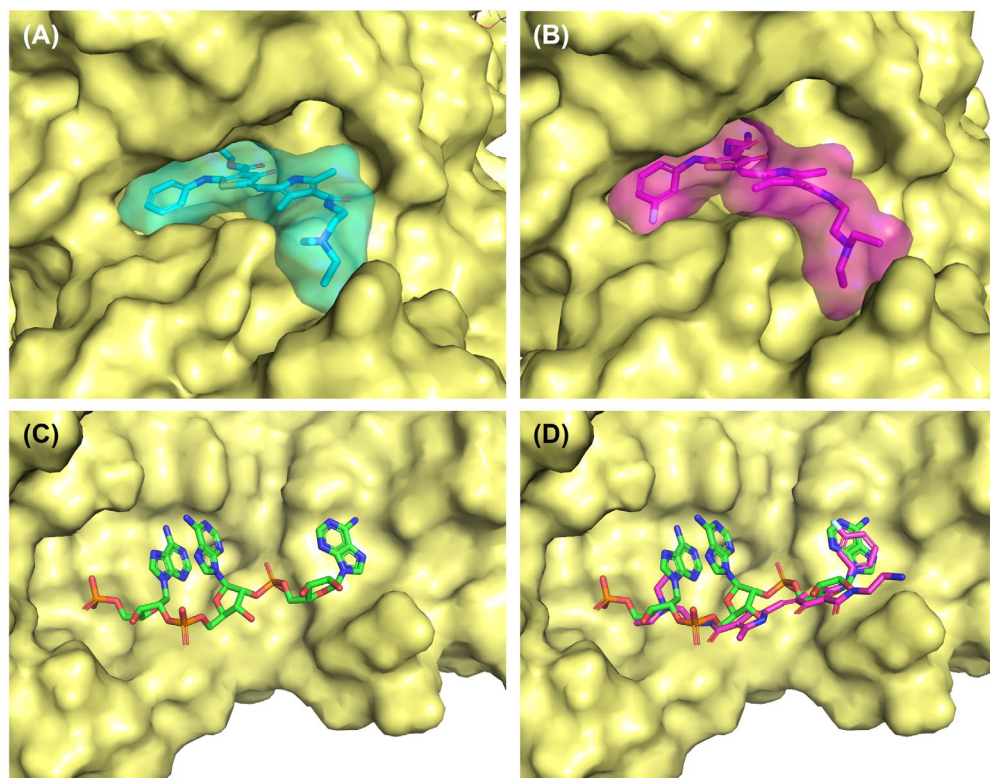
Figure 22. Molecular docking of (A) **29a** and (B) **32a** to ATP-binding pocket of RNase L (PDB code: 4OAV) and (C) crystal structure of RNase L with 2-5A at AKR domain (PDB code: 1WDY). (D) Superimposed image of 2-5A (green) and docking of **32a** (pink) to the 2-5A-binding pocket.

3.1.3.3 Chemical synthesis and biological evaluation

Extensive structural variations have been performed on 2-((pyrrol-2-yl)methylene)thiophen-4-ones. The structure of 1*H*-pyrrole-3-carboxamide was retained because the adenine mimetic feature of 1*H*-pyrrole-3-carboxamide has been proved in several studies as well as our molecular docking study. Three parts in the chemical structure of *N*-phenyl ATPC have been diversified. Firstly, several functional groups at the *N*-phenyl ring were introduced. Secondly, 3-ehtylcarboxylate was substituted with 3-carboxamide for two main reasons. The carboxamide formation makes the facile functionalization by coupling carboxylic acid and different amine substances. Furthermore, carboxamide is more stable in cells whereas carboxylate esters are easily degraded by esterases in the human liver, plasma, and erythrocytes and lose the activity of the original compounds. Lastly, thiophenone was replaced with furanone. Due to the different electronegativity and atomic size-related ring conformation, the heterocycle reveals different interactions of small molecule-ligands. The synthetic route to

obtain 2-((pyrrol-2-yl)methylene)thiophen-4-one and described derivatives were designed.

The 2-aminothiophen-4-one moiety was synthesized as described in previous chapter 3.1.2 whereas one new thiophenone and two new furanones including **11o–11q** were newly synthesized from isothiocyanates or isocyanates functionalized with different substituents as summarized at Scheme 9. The 3-carboxylate was further reduced to carboxylic acid under a basic condition to obtain ten derivatives in total. In the reduction, a longer reaction time than described in experimental methods resulted in complete cleavage of the carboxylate. Therefore, the reaction should stop as soon as the carboxylate is converted to carboxylic acid, which was able to be observed in the reaction by a color change from a white opaque solution to a yellow transparent solution. Following 3-carboxamide was formed by amide coupling between 3-carboxylic acid and amines to give a series of 2-aminothiopheone-3-carboxamides (Scheme 9).

Cpd	A	R	Yield (%)		Cpd	A	R	Yield (%)
11a	S	H	52		21a	S	H	62
11h	S	3-F	55		21b	S	3-F	75
11o	S	3-Cl	75		21c	S	3-Cl	85
11c	S	3-OMe	57		21d	S	3-OMe	56
11j	S	$3-CF_3$	69		21e	S	$3-CF_3$	80
11l	S	$3-NO_2$	69		21f	S	$3-NO_2$	51
11g	S	4-F	65		21g	S	4-F	76
11p	O	H	44		21h	O	H	54
11q	O	3-F	70		21i	O	3-F	84

Cpd	A	R	R'	Yield (%)	Cpd	A	R	R'	Yield (%)
23a	S	H	CONHMe	49	24b	S	3-F	CONH-Et-NH-Boc	26
23b	S	3-F	CONHMe	44	24c	S	3-Cl	CONH-Et-NH-Boc	21
23c	S	3-Cl	CONHMe	17	24d	S	3-OMe	CONH-Et-NH-Boc	35
23d	S	3-OMe	CONHMe	46	25	S	3-F	CONHBz	48
23e	S	$3-CF_3$	CONHMe	57	26	O	H	CONHMe	51
23f	S	$3-NO_2$	CONHMe	23	27a	O	H	CONH-Et-NH-Boc	62
23g	S	4-F	CONHMe	25	27b	O	3-F	CONH-Et-NH-Boc	48
24a	S	H	CONH-Et-NH-Boc	42					

Scheme 9. Synthesis to obtain 2-aminothiophen-4-one-3-carboxylate (ATPC) or 2-aminothiophen-4-one-3-carboxamide. **a**. Ethyl 4-chloroacetoacetate, NaH, 1,4-dioxane, 40 °C, 1 h; **b**. KOH, H_2O, EtOH, 95 °C; **c**. R'NH$_2$, PyBOP, DIPEA, DMF, RT o.n.

In this study, two series of 2-((pyrrol-2-yl)methylene)thiophen-4-one scaffolds were

subsequently synthesized. The first series contains ethyl 2-aminothiophenone-3-carboxylates or 2-amino-*N*-methyl-thiophenone-3-carboxamides with different substituents at the *N*-phenyl moiety (Table 5). Another series is either to introduce different 3-carboxamide or to exchange thiophenone to furanone (Table 6). The adenine mimetic 1*H*-pyrrole-3-carboxamide moiety was synthesized by straightforward amide coupling between 5-formyl-2,4-dimethylpyrrole-3-carboxylic acid and *N,N*-diethylethylenediamine to give **28** (Scheme 10). The first series 2-((pyrrol-2-yl)methylene)thiophen-4-ones were obtained by conjugation of thiophenones and **28** through Knoevenagel condensation yielding 20 derivatives (Scheme 10 and Table 5). The second series of compounds were synthesized from **28** and 2-aminothiophenone-3-carboxamides with different functionality at *N*-methyl moiety with 14 derivatives (Scheme 10 and Table 6).
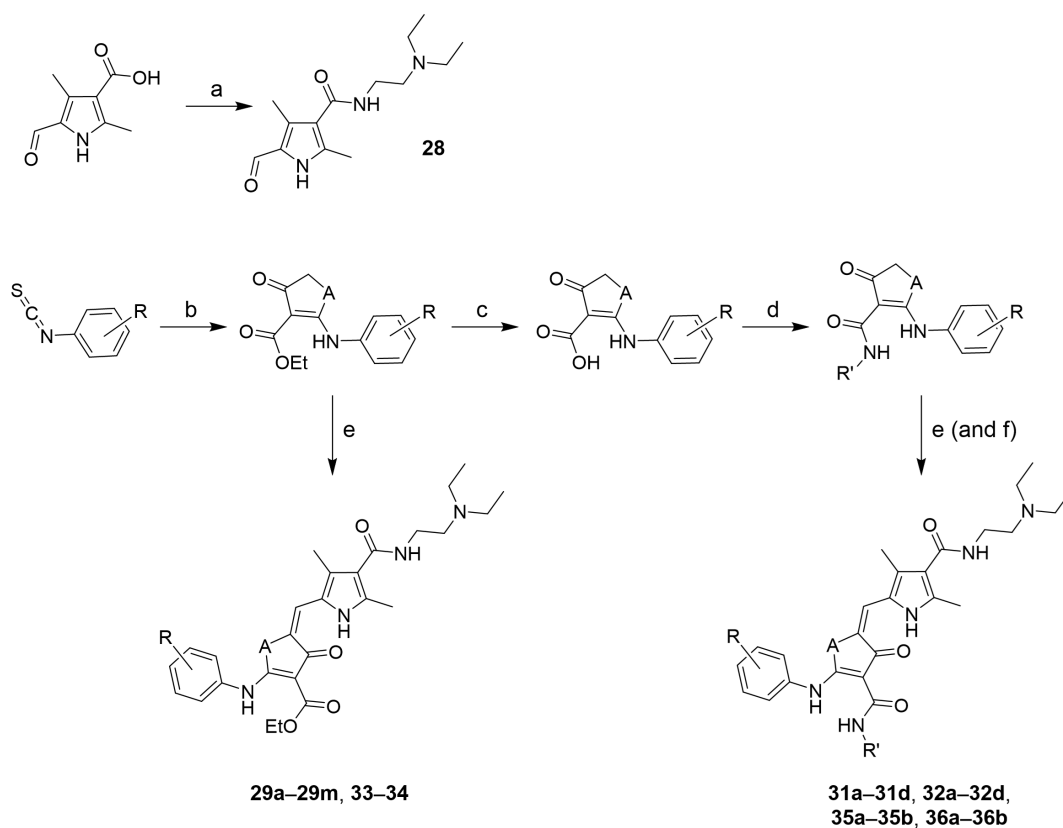
Scheme 10. Synthesis of 2-((pyrrol-2-yl)methylene)thiophen-4-one scaffold. **a**. N,N-diethylethylenediamine, EDC, HOBt, TEA, DMF, o.n.; **b**. ethyl 4-chloroacetoacetate, NaH, 1,4-dioxane, 40°C, 1 h; **c**. KOH, H₂O, EtOH, 95°C; **d**. R'NH₂, PyBOP, DIPEA, DMF, rt, 1 h; **e**. **28**, piperidine, EtOH, reflux, 2 h; **f**. TFA, DCM, rt, 1 h.

The first series of 2-((pyrrol-2-yl)methylene)thiophen-4-ones with substituents on the *N*-

phenyl ring with either a 3-ethylester or a 3-methylamide were mostly obtained in good yields above 80%, although a few derivatives substituted with a strong electron-withdrawing group, such as **30d**–**30g**, were obtained with reduced yields ranging between 30% and 70%. The Knoevenagel reaction to synthesize 2-((pyrrol-2-yl)methylene)thiophen-4-ones was more robust in yield with reduced reaction time than previously discussed in chapter 3.1.2 because pyrrole aldehyde is a stronger electrophile than phenyl aldehyde. Due to the formation of a double bond, a mixture of E- and Z-configuration was obtained while one isomer was dominant. The E- or Z-configuration of the dominant isomer was determined by monitoring the presence of the nuclear Overhauser effect (NOE) between protons from the methyl group of pyrrole and protons from *N*-phenyl ring. The absence of NOE demonstrated that the E-configuration of compounds was majorly obtained. The E-configuration is possibly favored due to a stronger hydrogen bond and closer distance between pyrrole and oxygen of thiophenone than sulfur. This feature was also observed in sunitinib which mainly gives the Z-configuration due to hydrogen bond formation between pyrrole and oxygen of oxindole.

The obtained first series of compounds were evaluated in *in vitro* FRET-based RNA cleavage assay to monitor RNase L inhibitory activity. In this study, 12-mer RNA was applied instead of the previous 33-mer RNA due to the higher sensitivity of the assay. All compounds were initially tested at a single concentration of 130 µM to evaluate the potency of the synthesized scaffold and derivatives as RNase L inhibitors. Most of 2-((pyrrol-2-yl)methylene)thiophen-4-ones revealed comparable or improved inhibitory effects against RNase L in comparison to sunitinib. Indicating that 2-((pyrrol-2-yl)methylene)thiophen-4-one is a promising scaffold to be investigated for RNase L inhibitors (Table 5 and Figure 23). Even though the substituents variation did not lead to a dramatic change in the inhibition effect, **30b** exhibited 99% inhibition rate of RNase L activity. Therefore, the *N*-(3-methoxyphenyl) group or 3-carboxamide moiety was retained in the synthesis of the next series. Furthermore, considering the presence of a halogen atom in 5-fluoro-2-oxindole of sunitinib provided a halogen bond which was a critical interaction for binding with RNase L residue, two more *N*-phenyl substituents, 3-fluoride and 3-chloride, were also synthesized.

Table 5. A series of design and synthesized 2-((pyrrol-2-yl)methylene)thiophen-4-ones scaffold as RNase L inhibitors
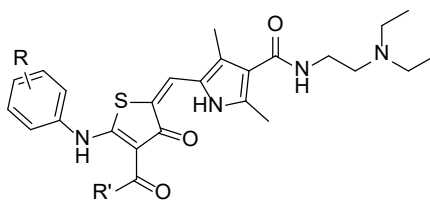
Index	Name	R	R'	Yield (%)	Inhibition rate (%)[a]
1	Sunitinib	-	-	-	83 ± 10
2	**29a**	H	-OEt	85	78 ± 8
3	**29b**	4-F	-OEt	99	80 ± 5
4	**29c**	3-F	-OEt	93	76 ± 8
5	**29d**	4-CF$_3$	-OEt	92	90 ± 3
6	**29e**	4-OMe	-OEt	93	70 ± 7
7	**29f**	3-OMe	-OEt	89	78 ± 1
8	**29g**	4-Br	-OEt	77	90 ± 4
9	**29h**	2-Br	-OEt	82	85 ± 6
10	**29i**	4-NO$_2$	-OEt	77	67 ± 3
11	**29j**	3-NO$_2$	-OEt	99	76 ± 4
12	**29k**	4-Me	-OEt	97	83 ± 9
13	**29l**	3,4-OMe	-OEt	93	79 ± 5
14	**29m**	4-Et	-OEt	97	83 ± 11
15	**30a**	H	-NHMe	87	59 ± 22
16	**30b**	3-OMe	-NHMe	94	99 ± 3
17	**30c**	3-F	-NHMe	90	58 ± 12
18	**30d**	4-F	-NHMe	65	< 5
19	**30e**	3-Cl	-NHMe	61	88 ± 4[b]
20	**30f**	3-CF$_3$	-NHMe	82	97 ± 1[b]
21	**30g**	3-NO$_2$	-NHMe	31	60 ± 3[b]

[a]Determined in FRET assay at a single concentration of 250 µM; [b]Determined in FRET assay at a single concentration of 130 µM.

The second series of 2-((pyrrol-2-yl)methylene)thiophen-4-ones were obtained by either differentiating 3-carboxamide function groups or replacing the thiophenone with a furanone to further study the structure-activity relationship (Table 6). The evaluation of compounds with a variation on the 3-carboxamide group revealed that the introduction of an additional amine, such as an ethylenediamine on **32a**, **32c**, and **32d**, led to 100 % inhibition against RNase L at 130 µM concentration. However, the replacement of the thiophenone with furanone slightly reduced the inhibitory potency at single-dose evaluation. Selected compounds that showed the best inhibition rates, such as **32a**, **32b**, **32c**, **32d**, and **36b**, were further evaluated in dose-dependent biochemical assays.

Table 6. Structure-activity relationship (SAR) study of 2-((pyrrol-2-yl)methylene)thiophen-4-ones
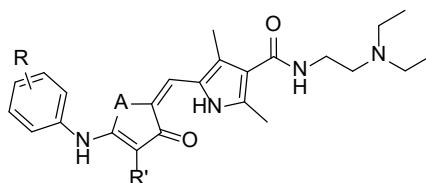
Index	Name	A	R	R'	Yield (%)	Inhibition rate (%)[a]
22	**31a**	S	3-F	CONH-Et-NH-Boc	58	100 ± 2
23	**31b**	S	H	CONH-Et-NH-Boc	56	75 ± 7
24	**31c**	S	3-Cl	CONH-Et-NH-Boc	57	96 ± 1[c]
25	**31d**	S	3-OMe	CONH-Et-NH-Boc	75	49 ± 1[b,c]
26	**32a**	S	3-F	CONH-Et-NH$_2$	quant.	102 ± 2
27	**32b**	S	H	CONH-Et-NH$_2$	quant.	101 ± 5
28	**32c**	S	3-Cl	CONH-Et-NH$_2$	quant.	101 ± 0[c]
29	**32d**	S	3-OMe	CONH-Et-NH$_2$	quant.	101 ± 0[c]
30	**33**	S	3-F	CONHBz	89	99 ± 0[c]
31	**34**	O	H	CONHMe	50	71 ± 16
32	**35a**	O	H	CONH-Et-NH-Boc	35	41 ± 37
33	**35b**	O	3-F	CONH-Et-NH-Boc	15	67 ± 21
34	**36a**	O	H	CONH-Et-NH$_2$	quant.	93 ± 9
35	**36b**	O	3-F	CONH-Et-NH$_2$	quant.	97 ± 8

[a]Determined by FRET assay at 250 µM; [b]Determined by FRET assay at 130 µM.

The dose-dependent response of selected compounds was tested in FRET assay (Figure 23B). The selected thiophenones with *N*-ethyleneamine-3-carboxamide represented much improved inhibition potency than sunitinib. The IC$_{50}$ values were determined as 15.9 µM for **32a**, 27.9 µM for **32b**, 12.4 µM for **32c**, 12.1 µM for **32d** whereas sunitinib showed more than 300 µM of IC$_{50}$ in this assay. The furanone with an *N*-ethyleneamine-3-carboxamide moiety revealed less potency while showing IC$_{50}$ value of 77.0 µM for **36a** and 41.9 µM for **36b**. Although the type of substituents at the *N*-phenyl ring did not induce a significant change in the inhibitory effect, the presence of a substituent in the 3-position of *N*-phenyl ring resulted in a higher inhibition effect. The halogen atoms or methoxy group at the *N*-phenyl ring might not be involved in secondary interactions but provide complementary conformation in the binding pocket. An orthogonal assay to evaluate 2-((pyrrol-2-yl)methylene)thiophen-4-ones including **32a**, **32c**, and **32d** was further performed in a gel-based RNA cleavage assay in a single dose (Figure 24).
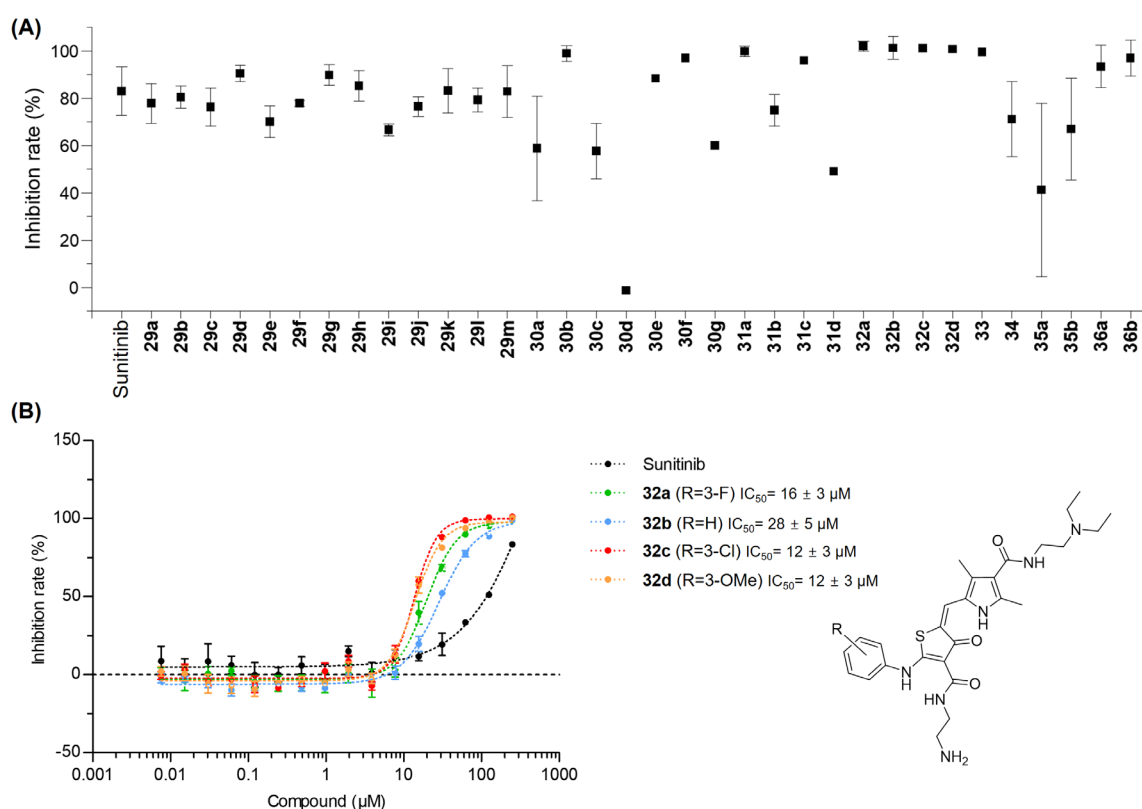
Figure 23. Evaluation of RNase L inhibition by 2-((pyrrol-2-yl)methylene)thiophen-4-ones in *in vitro* assays. (A) FRET assay tested with a single concentration of 130 µM compounds except for 60 µM **30g** and **31d**; (B) Dose-dependent inhibition of sunitinib and selected thiophen-4-ones against RNase L.

55
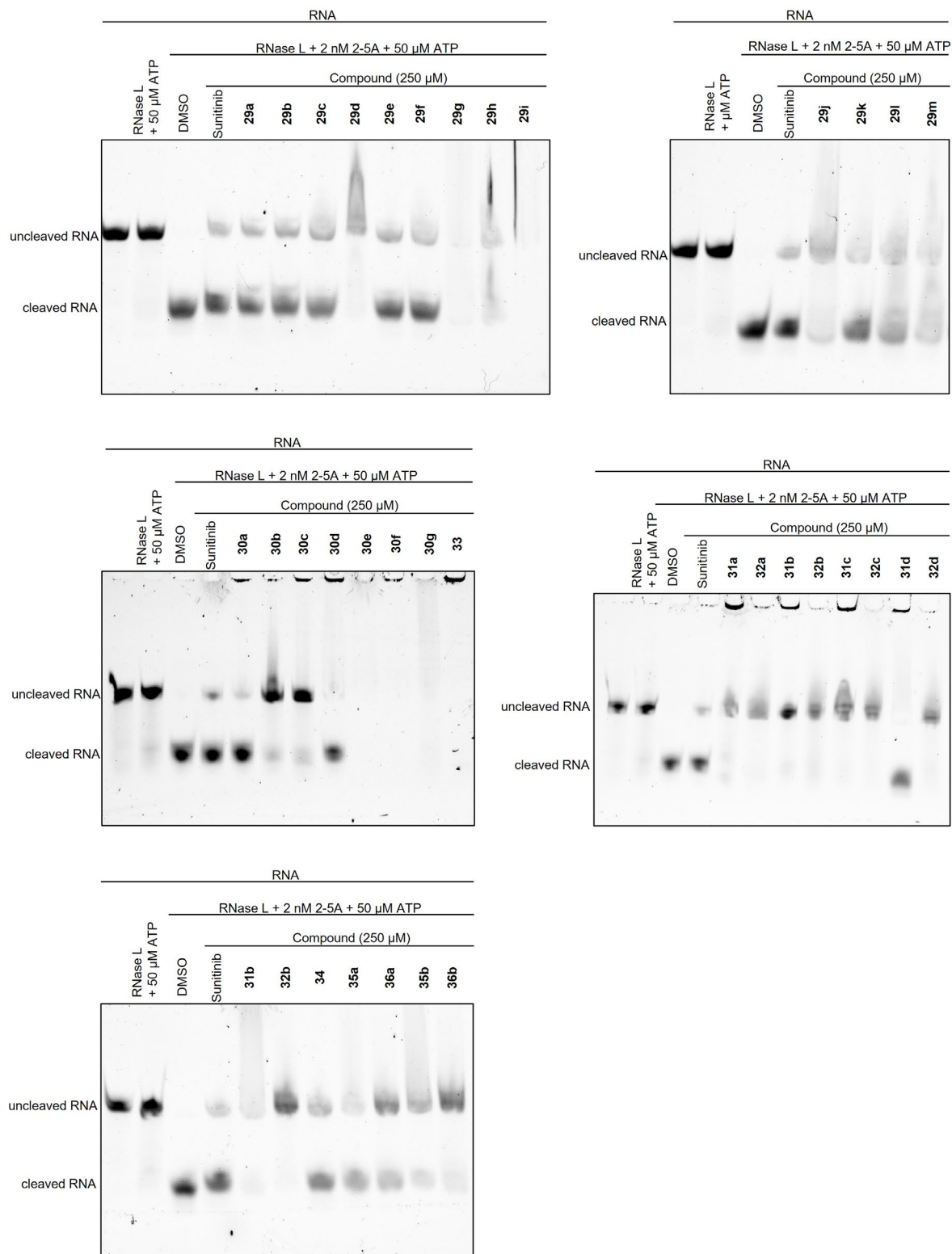
Figure 24. Evaluation of RNase L inhibition by 2-((pyrrol-2-yl)methylene)thiophen-4-ones in *in vitro* gel-based RNA cleavage assays at a single concentration of 250 µM compounds.

In this assay, sunitinib showed incomplete inhibition of RNase L at 250 μM, which is observed as the appearance of cleaved RNA in the respective band (Figure 24). However, all three compounds, **32a**, **32c**, and **32d**, exhibited almost full inhibitory effect at 250 μM although RNase L activation should be complete in the presence of 2 nM 2-5A and 50 μM ATP. Generally, the gel-based RNA cleavage evaluation indicated the same result with the FRET assay. However, a few compounds which were evaluated as potent RNase L inhibitors in the FRET assay did not show the corresponding result in the orthogonal assay. For example, **33** inhibited 99% of RNase L activity in the FRET assay at the concentration of 130 μM (Table 6). However, the band in the orthogonal gel-based assay did not appear with **33**. This result can be explained by the low solubility of **33** interacted with RNA probe and induced aggregation of RNA, which was observed through fluorescent signal remaining in the gel pockets. The compounds **32a**, **32c**, and **32d** which were evaluated as potent RNase L inhibitors in both FRET- and gel-based biochemical assays were further evaluated in a dose-dependent manner in the gel-based assay (Figure 25 and Figure S2). The three compounds revealed dose-dependent inhibition in the gel-based RNA cleavage assay and are further evaluated in the biophysical assay.
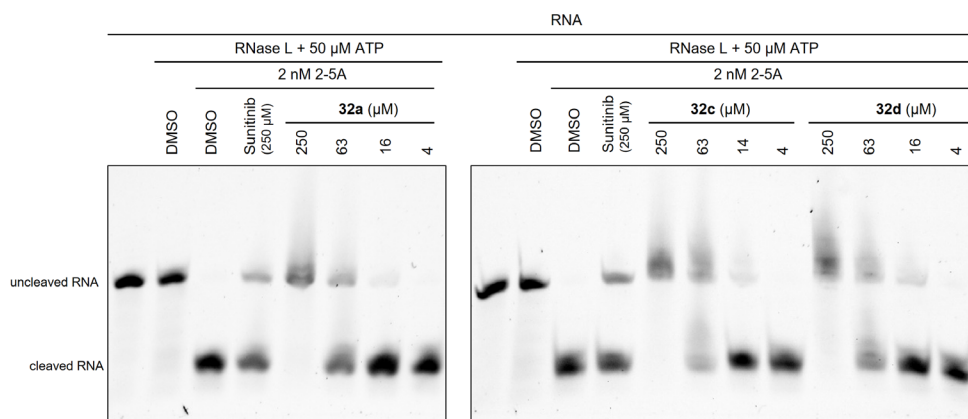
Figure 25. Dose-dependent response of selected 2-((pyrrol-2-yl)methylene)thiophen-4-ones inhibiting RNase L activity in *in vitro* gel-based RNA cleavage assays.

The direct binding event was evaluated by using biolayer interferometry (BLI). The full-length RNase L was biotinylated and immobilized at the surface of the biosensor. A range of concentrations of selected compounds was measured in the mobile phase within the chamber and induced wave interference was measured to monitor the binding event. Firstly, sunitinib indicated weak binding to RNase L with a weak intensity of wave interference (Figure 26A). On the contrary, the compounds **32a**, **32c**, and **32d** induced stronger wavelength shifts upon binding (Figure 26B–D). The improved inhibitory activities of compounds **32a**, **32c**, and **32d**

in comparison with that of sunitinib shown in previous *in vitro* assays were reconfirmed by the BLI data, in which all three thiophenones showed significantly higher binding affinity towards RNase L than sunitinib (Figure 26).
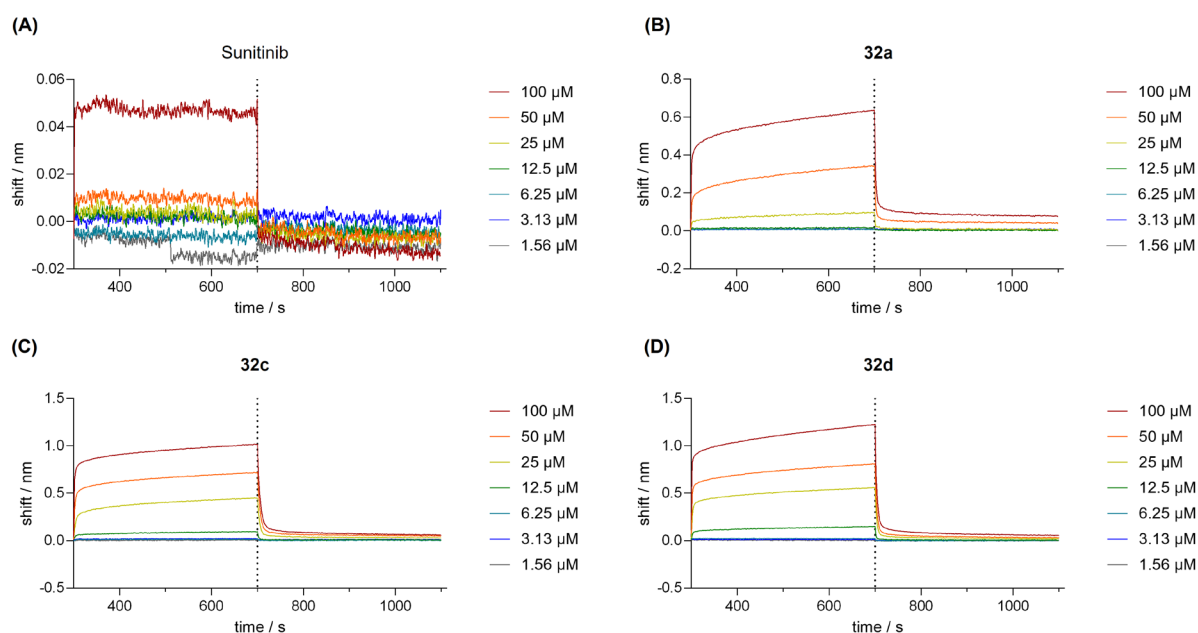
Figure 26. Binding between RNase L and (A) sunitinib, (B) **32a**, (C) **32c**, and (D) **32d** measured in the biolayer interferometry.

3.1.3.4 Molecular docking for mechanistic study

Following these results, a molecular docking analysis was performed to study the binding mechanism contributing to the improved inhibitory effect. The complex of sunitinib binding to the ATP-binding pocket of RNase L displayed an unoccupied region shown as the orange-colored back pocket in Figure 27A. Two compounds **29a,** which is a simple structure of the designed scaffold, and **32a,** which is one of the most potent inhibitors, were tested in docking by using the ATP-binding pocket of RNase L crystal structure (PDB code: 4OAV). Docking of two 2-((pyrrol-2-yl)methylene)thiophen-4-ones to the ATP-binding pocket of RNase L not only revealed similar improved shape complementarity in the pocket but also formed similar interactions with side chains of key residues (Figure 27A–B). The two carbonyl oxygens from ATPC moiety formed hydrogen bonds with Lys392 while protonated triethylamine tail from 1*H*-pyrrole-3-carboxamide interacted with Gln489. Especially, the interactions between **29a** and **32a** revealed close similarity, which described that the major interactions are driven from the core scaffold. The result confirmed a successful design of a new scaffold, 2-((pyrrol-2-yl)methylene)thiophen-4-ones. Additionally, the origin of improved potency of **32a** than other

compounds was determined as strong hydrogen bond formation between protonated ethyleneamine moiety and Glu404.

Furthermore, molecular docking of **32a** at the 2-5A-binding pocket has been performed. As abovementioned, 2-((pyrrol-2-yl)methylene)thiophen-4-ones showed close similarity in the arrangement of 2-5A at 2-5A-binding pocket (Figure 22D and Figure 27C). Additionally, protonated ethyleneamine at 3-position of thiophenone formed a hydrogen bond with Glu57. Protonated triethylamine tail formed cation-π interaction with Tyr124 while 3-fluorophenyl ring formed π-π interaction with Trp60. Introducing an additional ethyleneamino moiety in **32a** facilitated the formation of necessary interactions with surrounding residues and strengthened the binding of the molecule in both pockets. In summary, the molecular docking study proposed that the improved shape complementary of the designed compounds resulted in higher occupancy of the pocket and the formation of stronger interactions between compounds and RNase L residues. This resulted in the more potent binding between small molecules and RNase L. Consequently, stronger binding led to more potent inhibitory activities of the obtained 2-((pyrrol-2-yl)methylene)thiophen-4-ones inhibitors.
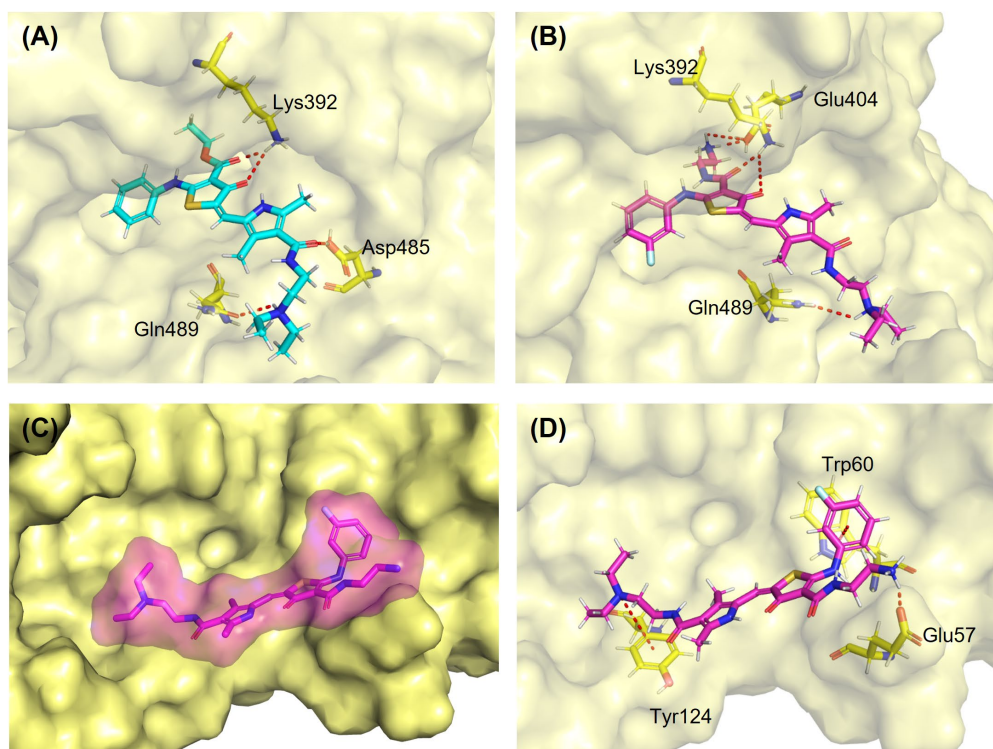
Figure 27. Ligand interaction of docking of (A) **29a** and (B) **32a** at ATP-binding pocket (PDB code: 4OAV). (C) Molecular docking of **32a** at 2-5A-binding pocket (PDB code: 1WDY) and (D) its ligand interaction.

3.1.3.5 Cellular evaluation

Lastly, the potency of **32a** to inhibit RNase L activity in cells was evaluated by monitoring the degradation of rRNA. Because rRNA is known as the target of RNase L, rRNA degradation determined RNase L activity in cells from previous studies.[16] In this assay, HeLa cells were transfected with poly I:C to induce the synthesis of 2-5 and thus activation of RNase L, followed by compound treatment. In comparison with intact cells in the third lane of Figure 28, transfected cells showed clear cleaved RNA bands for both 28S and 18S rRNA (Figure 28, 2nd lane). Surprisingly, cells treated with 10 μM **32a** showed complete disappearance of the cleaved rRNA band, which indicated extensive inhibition of RNA degradation by **32a**. Furthermore, when cells were treated with 2 μM **32a**, the degradation inhibition showed a similar range with 10 μM of sunitinib. Treatment with 2 μM **32a** showed more than 50% inhibition of RNase L activity in cells. The cellular RNA cleavage assay demonstrated that compound **32a** revealed efficient inhibition of RNase L in HeLa cell.
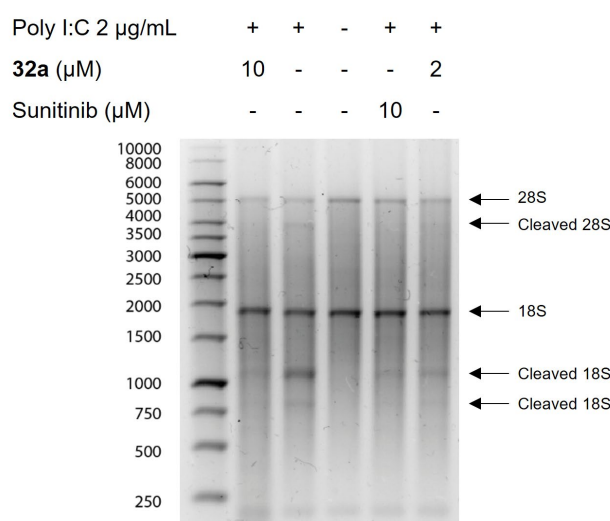
Figure 28. rRNA degradation induced by poly I:C transfection and inhibited by compound treatment in HeLa cell.

3.1.3.6 Summary

In this study, we applied a structure-based rational design approach for the development of new RNase L modulators according to the reported crystallography study of sunitinib. The conjugation of 1*H*-pyrrole-3-carboxamide and 2-aminothiophenone yielded a combinatorial scaffold 2-((pyrrol-2-yl)methylene)thiophen-4-one. The established synthetic route provided 34 derivatives with different functionalities on the *N*-phenyl ring, 3-carbobyl moiety, or by

replacing the thiophenone ring. The following *in vitro* evaluations of obtained compounds indicated that the designed scaffold displayed a potent inhibitory effect against RNase L. Further SAR study of 2-((pyrrol-2-yl)methylene)thiophen-4-one indicated that the introduction of an ethyleneamino moiety at the 3-carboxamide position led to improved RNase L inhibitory activity. The compounds **32a**, **32c**, and **32d** exhibited ~30-fold improved inhibitory effect in comparison with that of sunitinib. The binding event was monitored in BLI and the preliminary mechanism of inhibition on RNase L activity was evaluated by using a molecular docking study. The improved inhibitory effect of selected thiophenones could be attributed to the formation of additional molecular interactions with key residues surrounding the ATP-binding pocket, as well as the three-dimensional complementarity between the ligand and the ATP-binding pocket. Additionally, cell-based rRNA degradation assay indicated that **32a** inhibited RNA degradation efficiently in single-digit micromolar concentration in HeLa cells. We successfully obtained the promising RNase L inhibitor with improved potency than sunitinib while providing a series of new chemical tools to modulate the RNase L activity. These compounds can be further evaluated in RNase L-related immune diseases. However, the designed ligands did not lead to the activation of RNase L. The docking study suggested that the compounds might bind 2-5A binding pocket, which implies a potential of the 2-((pyrrol-2-yl)methylene)thiophen-4-one as RNase L activator. An extensive structure optimization based on crystallography can lead to the discovery of a new RNase L activator with promising potency. For example, based on molecular docking, *N*-phenyl ring can be replaced with *N*-purine to improve the interaction with Trp60. Additionally, another purine moiety can be introduced to one of the methyl groups of pyrrole to mimic the structure of 2-5A.

3.2 Bifunctional molecule-based approach

A bifunctional molecule consists of two molecular entities, often connected through a linker. The two entities can have the same or different structures. Bifunctional molecules chemically induce the proximity of two targets while binding to the target proteins simultaneously and thus induce the formation of a ternary complex.[132-133] Different types of bifunctional molecules have been developed in chemical biology such as molecular glue, bivalent kinase inhibitor, proteolysis targeting chimera (PROTAC), ribonuclease targeting chimera (RIBOTAC), and deubiquitinase targeting chimeras (DUBTAC). Molecular glue was implemented to help the induction and stabilization of protein-protein interactions.[133] Bivalent kinase inhibitor is a molecule conjugating two ligands that target two different binding sites within the same protein in order to bind both pockets to efficiently modulate the kinase activity.[134] Targeting chimeras are the strategy to recruit a specific type of protein to induce the desired change to an entity, mostly selective degradation, within the cellular environment. PROTAC recruits E3 ligase which induces ubiquitination and therefore proteasomal degradation of a target protein. RIBOTAC degrades target RNA by chemically induced proximity between target RNA and RNase.[103, 106] DUBTAC uses deubiquitinase to prevent ubiquitination and degradation of target protein, which results in higher stability of target protein.[135]

The bifunctional molecule is an intriguing concept for challenging targets of which activity is difficult to modulate only by ligand binding. For example, protein-protein interactions are one of the challenging targets due to their large and complex surface and interface, which was overcome by bifunctional molecules.[136-137] Other challenging biological phenomena were modulated by bifunctional molecules and a few bifunctional molecules are under clinical trial.[138] RNase L shows a characteristic which reveals in the targets of the bifunctional molecule. For example, RNase L requires interactions between protein monomers for activation and possesses multiple binding pockets. Therefore, a completely new approach for RNase L, a design of bifunctional molecule, can lead to the development of a breakthrough to activate RNase L despite the limited potency of small molecule-ligands. In this study, homodimerizer, heterobivalent molecule, and PROTAC strategies were investigated to modulate RNase L activity.

3.2.1 Homobifunctional molecules

Biochemical RNA cleavage assays were performed by Neele Haacke.

3.2.1.1 Design of homobifunctional molecule

First of all, the concept of molecular glues to induce and stabilize protein-protein interactions inspired the design to apply this concept to the dimerization of two RNase L monomers through the synthesis of a homobifunctional molecule approach. Therefore, recruiting one protomer close to another protomer by a bifunctional molecule is capable to increase the possibility of dimerization (Figure 29A). These chemical inducers of homodimerization by homobifunctional molecules were attempted *in vitro* in other homodimeric systems.[133] For example, two methotrexates were conjugated to induce the dimerization of dihydrofolate reductase.[139] Similarly, we designed a homobifunctional molecule in which two identical ligands were connected with a linker. For the selection of small molecule-ligands, six small molecule-ligands were reported to bind and modulate RNase L activity. In this homodimer formation approach, a small molecule-activator is a suitable choice because RNase L requires an activator to dimerize and show enzymatic activity. The homobifunctional molecule increases the potency of the activator by increasing binding events between monomers. Thiophenone **C1-3** was selected as the ligand to be homodimerized because **C1-3** was the most active RNase L small molecule-activator when the concept was designed. Furthermore, **C1-3** was implemented in a bifunctional molecule in the form of RIBOTAC, which helps to design the chemical synthesis of bifunctional molecules. In the linker design, azide and alkyne-tagged PEG linkers were selected in this synthetic route to bring a certain flexibility and facile click chemistry to link two ligands.

(A)   **(B)**
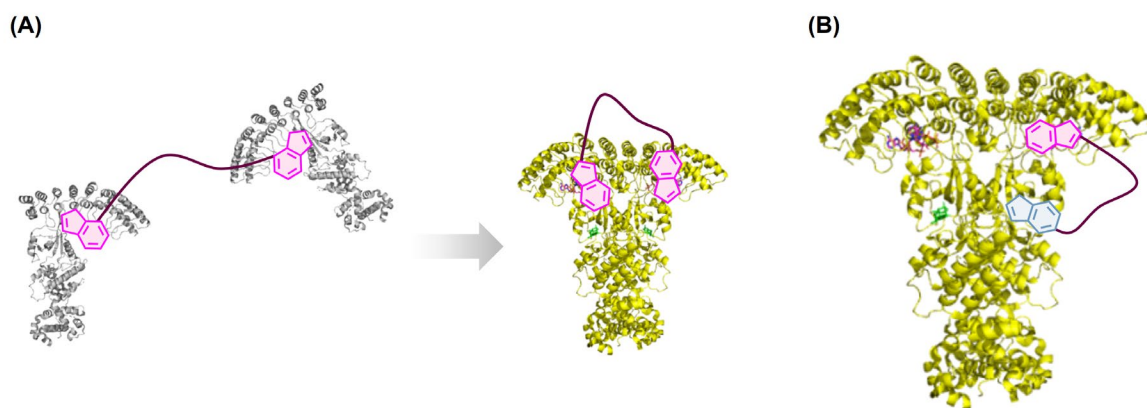
Figure 29. Schematics showing the concept of (A) homobifunctional molecule to recruit one RNase L

monomer to another RNase L monomer. (B) heterobivalent molecule targeting both the 2-5A-binding pocket at the AKR domain and the ATP-binding pocket at the PK domain.

3.2.1.2 Chemical synthesis

Firstly, PEG linker was designed to be connected with the ligand through a carboxylic acid, as well as click chemistry moiety, azide or alkyne (Scheme 11A). As a ligand attachment moiety, we selected amide coupling, therefore PEG linker was functionalized by carboxylic acid, and the ligand was functionalized with an amine according to a previously reported bifunctional molecule study.[105] In order to introduce azide tag for click chemistry, two strategies were introduced. One is to halogenate one end of the PEG linker and then substitute halogen for azide. Another method is to tosylate the hydroxy group at one end of PEG linker and then substitute it with azide. For a rather short PEG linker, nucleophilic substitution by using halogenated PEG was applied since a monochlorinated PEG linker was commercially available. The chloride or bromide was substituted for azide by the reaction between aliphatic halogen and sodium azide in an aqueous solution.

Three lengths of PEG linker with azide tag were synthesized to give **37a**, **37b**, and **37c** with isolated yields of 38–73%. A Carboxylic acid moiety was then introduced by using bromoacetic acid via nucleophilic substitution with sodium hydride as a base. The use of NaI improved the conversion due to the halogen atom substitution from the solubility difference between iodide and bromine salt. Three PEG linkers functionalized with azide and carboxylic acid at each end were obtained to give **40a**, **40b**, and **40c** with good yields of 84–96%. For a rather longer PEG linker, another azide introduction route was carried out because the initial trial to synthesize chlorinated PEG linker gave a low yield. Due to the low conversion and high solubility of chlorinated products, a reduced amount of crude dissolved in the organic phase at the aqueous washing step. Tosylation of the hydroxy group is another common way for nucleophilic substitution as O-tosyl is a good leaving group. Therefore, the tosyl group was introduced to one end of PEG, giving **38** with a good yield of 82%. Following azide group introduction with sodium azide in DMF also gave the product **39** with an excellent yield of 99% under reduced reaction time in comparison to that from chlorinated PEG. In the following step, carboxylic acid was then introduced to the unsubstituted side of the PEG linker by using the same method to yield **40d** with 79% yield.

The second step was designed to functionalize the thiophenone ligand with an amine to couple the carboxylic acid-functionalized linkers (Scheme 11B). Linker attachment position is one of the critical factors to design a bifunctional molecule because the linker attachment can interfere with the ligand binding to the target. Because thiophenone **C1-3** was used in a previous bifunctional molecule study to recruit RNase L, the linker attachment position was already defined as the para position of 5-benzylidene.[105] In the previous study, oxygen at the para position was necessary to induce a moderate range of RNase L activation. Therefore, we introduced nitrogen to the benzylidene moiety. Boc-protected ethyleneamine was introduced to p-hydroxy group of 3,4-dihydroxyphenylacetaldehyde by using 2-(Boc-amino)ethyl bromide in the presence of potassium carbonate in DMF to give **42** in 46% yield. Nucleophilic substitution of 2-(Boc-amino)ethyl bromide occurred at the para position selectively by using potassium carbonate. The functionalized aldehyde component was then conjugated with the thiophenone component by Knoevenagal condensation, resulting in **43** with 88% yield. Subsequent Boc-deprotection yielded **44** for further amide coupling with azide or alkyne-tagged linkers.

(A)

37a (n=0), 70%[a]
37b (n=1), 38%[a]
37c (n=2), 73%[a]

40a (n+1=1), 84%[a]
40b (n+1=2), 96%[a]
40c (n+1=3), 91%[a]

38 (n=5), 82%[a]

39 (n=5), 99%[a]

40d (n+1=6), 79%[a]

(B)

42, 46%[a]

11a

43, 88%[a]

44, quant.[a]

A=N₃ or O-propargyl

45a (A=N₃, n=1), 87%[a] **45b** (A=N₃, n=2), 70%[a],
45c (A=N₃, n=3), 69%[a] **45d** (A=N₃, n=6), 95%[a]
46 (A=-O-propargyl, m=0), 48%[a]

65
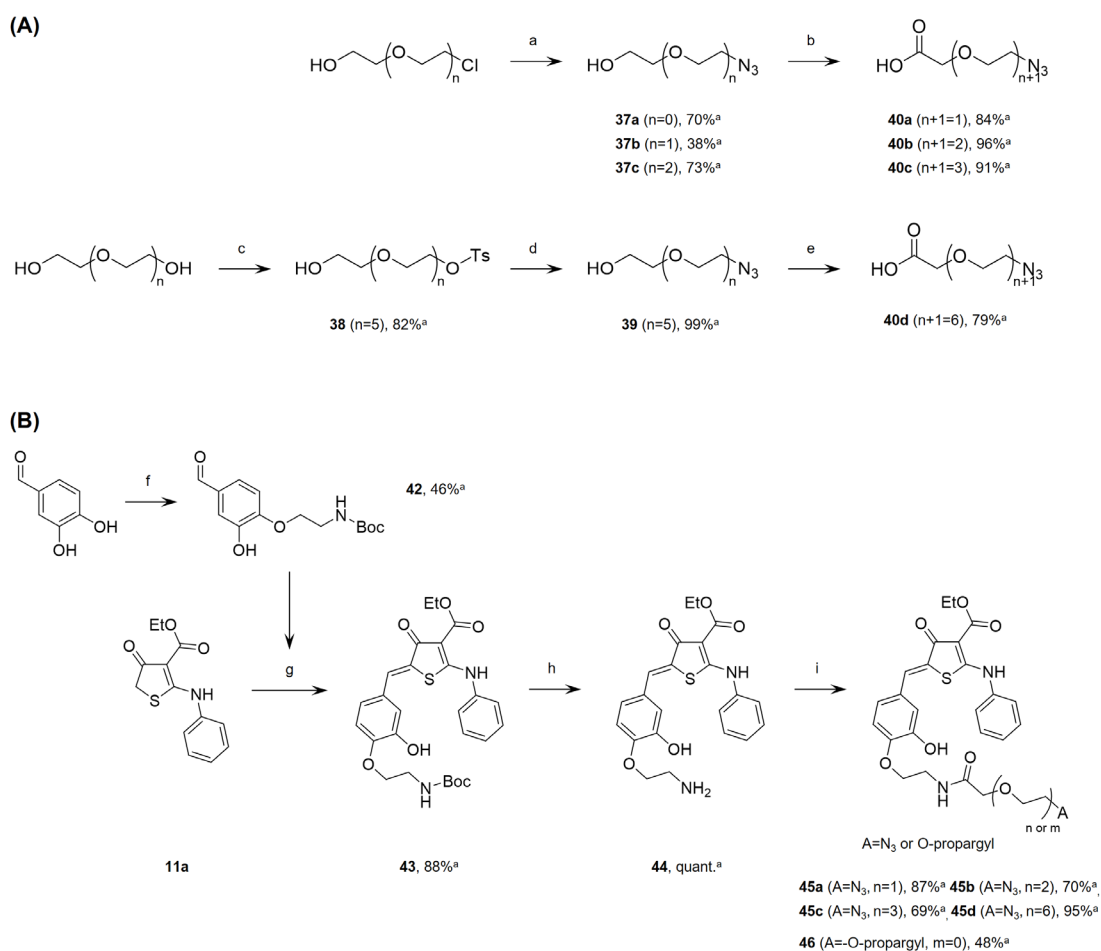
Scheme 11. The route to synthesize (A) PEG linker tagged with azide and (B) azide-tagged RNase L activator. **a**. NaN$_3$, H$_2$O, 60 °C, 2 d; **b**. bromoacetic acid, NaI, NaH, THF, rt, 2 h; **c**. p-TsCl, NaOH, H$_2$O, THF, 0 °C, 2 h; **d**. NaN$_3$, DMF, 70 °C, 1 d; **e**. bromoacetic acid, NaI, NaH, THF, rt, 2 h; **f**. 2-(Boc-amino)ethyl bromide, K$_2$CO$_3$, DMF, 50 °C, o.n.; **g**. piperidine, EtOH, reflux, 4 h; **h**. TFA, DCM, rt, 1 h; **i**. alkyne-or azide-tagged PEG linker-COOH, PyBOP, DIPEA, DMF, o.n. ªisolated yield.

To link functionalized PEG linkers and **44**, a reported condition, HATU (1.2 equiv.), HOAt (1.2 equiv.), and DIPEA (3 equiv.) in DMF at room temperature, were tested for the amide coupling. However, the conversion to desired product **45a** was less than 20%. The coupling reagents were screened to improve the conversion and PyBOP gave the best conversion among tested reagents, DCC, EDC, PyBOP, HATU, and COMU. Further detailed conditions were screened to improve reaction conversion and PyBOP (1.2 equiv.) gave full conversion with DIPEA (1.5 equiv.) in DMF at room temperature and overnight reaction time (Figure S3). The byproduct, phosphonamide, formed from PyBOP reaction is one of the typical drawbacks of PyBOP-assisted amide coupling in solution synthesis. In our synthesis, two methods helped to eliminate the phosphonamide. One is excessive washing of the organic ethyl acetate phase with 1N HCl aqueous solution. Another way is using preparative chromatography due to different retention times in an acidic ACN/H$_2$O system between products and a phosphonamide byproduct. The azide-tagged compounds **45a**, **45b**, **45c**, and **45d** were finally synthesized with optimized reaction conditions and isolated giving a good yield between 69–95%. The alkyne-tagged RNase L recruiter **46** was synthesized according to the same PyBOP conditions (Scheme 11B and Figure S4).

In the homodimerization strategy, azide-tagged thiophenones with short linker lengths **45a** and **45b** were applied in order to induce a rather rigid linkage and close proximity between RNase L monomers. Two lengths of azide-tagged PEG linker were coupled with **44** whereas one type of alkyne-tagged ligand **46** was prepared. Lastly, homobifunctional molecules **47a** and **47b** with two different linker lengths were obtained by Cu-catalyzed cycloaddition of azide and alkyne (Scheme 12).
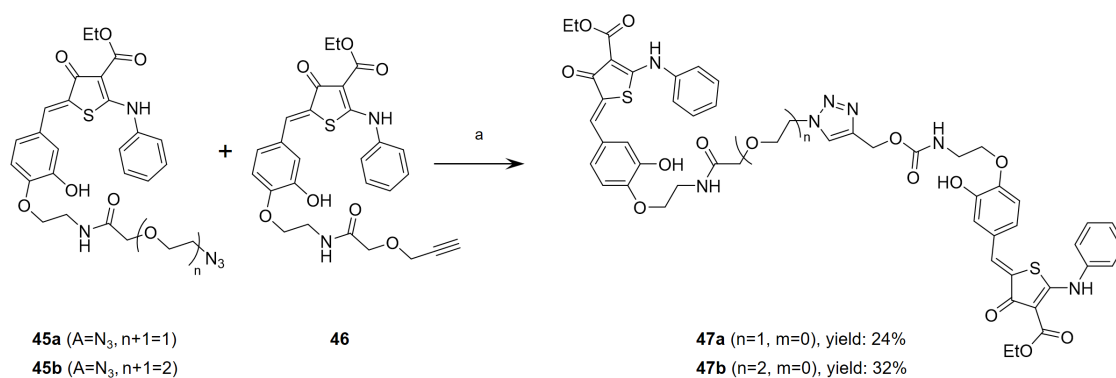
Scheme 12. Conjugation of two thiophenones via click chemistry to give homobifunctional molecules. **a**. CuSO$_4$, sodium ascorbate, THF, H$_2$O, rt, o.n.

3.2.1.3 Biological evaluation

The homobifunctional molecule **47a** was evaluated as an RNase L modulator in a biochemical gel-based RNA cleavage assay (Figure 30). Compound **47a** at 60 µM induced slight degradation of RNA with 8% of cleavage normalized with DMSO. Even though the homobifunctional molecule induced weak activation of RNase L in comparison to 2-5A, it is noteworthy that **47a** showed elevated potency to activate RNase L than the reported small molecule-activator **C1-3**. Another homobifunctional molecule might be synthesized with the recently reported activator **C6** showing improved potency than **C1-3** (Figure 7). The evaluation can be performed in *in vitro* biochemical RNA cleavage assay as well as cellular RNA cleavage assay. Additionally, the oligomerization assay to monitor the dimerization effect by homobifunctional molecules can be performed using mass photometry.
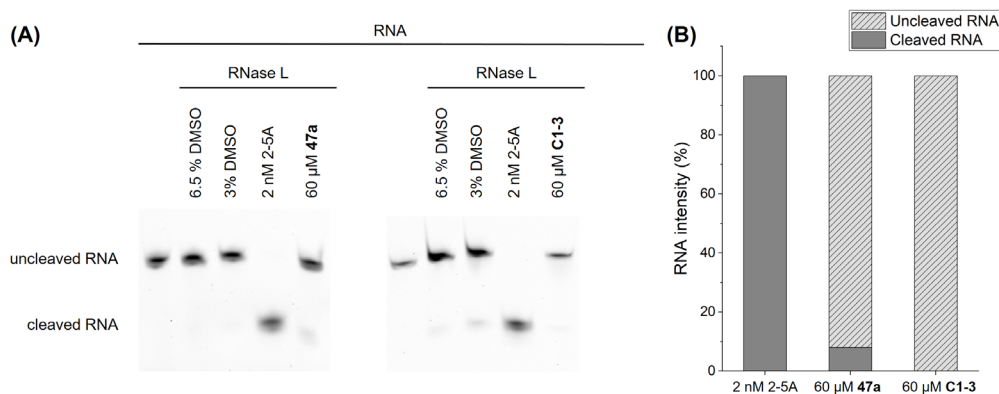
Figure 30. Evaluation of the homobifunctional molecule **47a**. (A) Gel-based RNA cleavage assay; (B) Quantification of the RNA cleavage normalized with negative DMSO control.

3.2.2 Heterobivalent molecules

Biochemical RNA cleavage assays were performed by Neele Haacke.

3.2.2.1 Design of heterobivalent molecules

The second approach in bifunctional molecule design is to synthesize a bivalent modulator targeting two different pockets in a protein. Even though RNase L has no catalytic activity as kinase, RNase L also contains an ATP-binding pocket at the PK domain where ATP analogs bind. Furthermore, RNase L contains two additional binding sites, the 2-5A binding pocket at the AKR domain where 2-5A binds and RNA binding site at the RNase domain. The only binding site in which small molecule-ligand is clearly defined via crystallography or mutation study is the ATP-binding pocket where RNase L inhibitor sunitinib binds. Even though 3 different types of activators were reported, none of them clearly described where the molecule binds. However, reported activators are assumed to bind at the AKR domain because the AKR domain is a critical part to regulate dimerization and thus activation of RNase L. Therefore, we selected compound **C1-3** as a potential 2-5A pocket binder at the AKR domain. For the ATP-pocket binder, although we obtained a more potent inhibitor in our rational design, sunitinib was selected since our 2-((pyrrol-2-yl)methylene)thiophen-4-ones inhibitor's binding pocket was not elucidated yet. In a previous homobifunctional molecule study, linker attachment to introduce azide-tags with different linker lengths for 2-5A pocket binder was established. Therefore, we adopted the same synthetic method to obtain azide-tagged 2-5A pocket binders. To couple with the azide-tagged AKR binder, sunitinib was functionalized with an alkyne tag. The linker attachment point of sunitinib was decided according to the cocrystal structure between RNase L and sunitinib (Figure 31). The oxindole moiety is located inside the ATP-binding pocket and the triethylamine tail is a solvent-exposed area. Therefore, the triethylamine tail was functionalized with an alkyne tag.
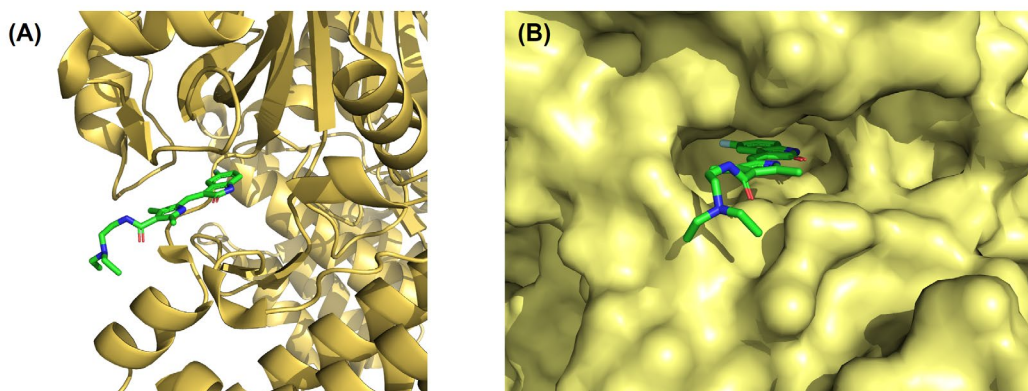
Figure 31. The cocrystal structures of RNase L PK domain and sunitinib (PDB code: 6M11).

3.2.2.2 Chemical synthesis

48a (n=3), 58%[a]
48b (n=5), 67%[a]

49a (n=3), 98%[a]
49b (n=5), 83%[a]

52a (n=3), quant.[a]
52b (n=5), quant.[a]

51a (n=3), 71%[a]
51b (n=5), 77%[a]

53, 97%[a]

54a (n=3), 64%[a]
54b (n=5), 52%[a]
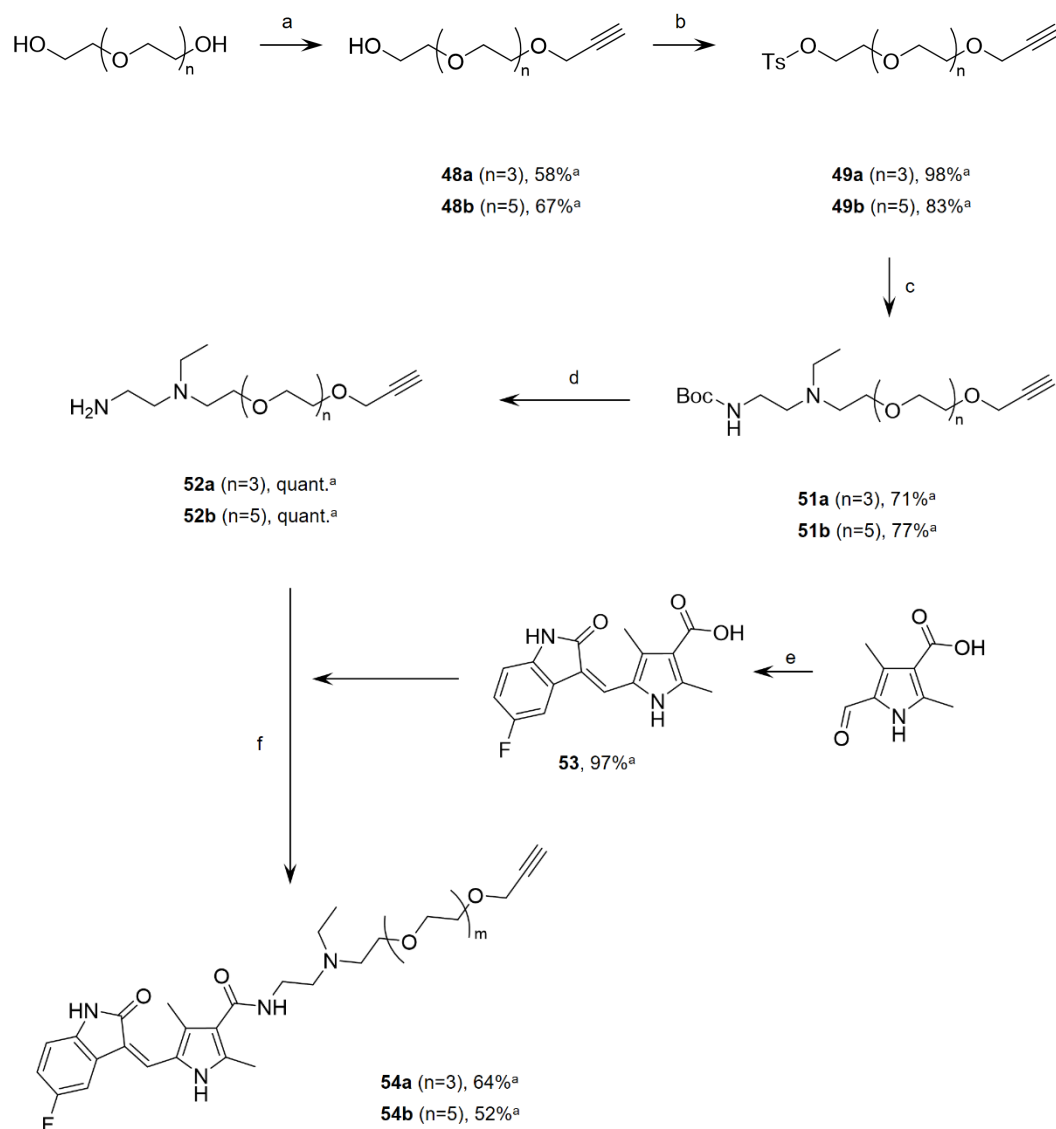
Scheme 13. The synthetic route to synthesize alkyne-tagged sunitinib. **a**. Propargyl bromide, NaH, THF, rt, o.n.; **b**. TsCl, TEA, DCM, rt, 1 h; **c**. **50**, Cs$_2$CO$_3$, NaI, ACN, rt, 2 d; **d**. TFA, DCM, rt, 1 h, **e**. 5-fluoro-2-oxindole, pyrrolidine, EtOH, reflux, 3 h; **f**. EDC, HOBt, TEA, DMF, rt, 20 h.

Firstly, a synthetic route to synthesize alkyne-tagged sunitinib was designed based on the reported study (Scheme 13).[140] Two approaches to synthesize an alkyne-tagged PEG linker were tested. The first set of trials for introducing the alkyne was tested by using a chlorinated PEG linker and propargyl alcohol with various bases, however, all the tested conditions just showed a poor isolation yield of 3–4% (Figure S5). In the second trial, the combination of substrate changed to PEG and propargyl bromide, which gave an improved yield of 60% with

the addition of NaH. Therefore, the alkyne moiety was introduced to PEG by using propargyl bromide and PEG as starting materials via nucleophilic substitution to give **48a** and **48b** with 58 and 67% yield, respectively (Scheme 14). The other hydroxide end was functionalized with the tosyl group to make hydroxide a good leaving group for the following nucleophilic substitution reaction. **50**, *N*-Boc-*N'*-ethylethylenediamine, was synthesized by protecting the primary amine of *N*-ethylethylenediamine with the Boc group to prevent the primary amine from reacting in the following step. Triethylamine tail with alkyne tag was then synthesized from PEG linker and **50** with the help of base, Cs_2CO_3, to give **51a** and **51b** with 71–77% yield. The sunitinib moiety was synthesized by Knoevenagel condensation between 5-formyl-2,4-dimethyl-1*H*-pyrrole-3-carboxylic acid and 5-fluoro-2-oxindole to give **53** in a good yield of 97%. The alkyne-tagged diethyleneamine linker was coupled with **53** to give alkyne-tagged sunitinib, **54a** and **54b**, with two different linker lengths. In this study, a long PEG linker was used to target two distant pockets simultaneously. As the last synthetic step, two ligands, azide-tagged thiophenone and alkyne-tagged sunitinib were coupled into heterobivalent molecules by click chemistry to give **55a** and **55b** with 40% and 55% yield, respectively (Scheme 14B).
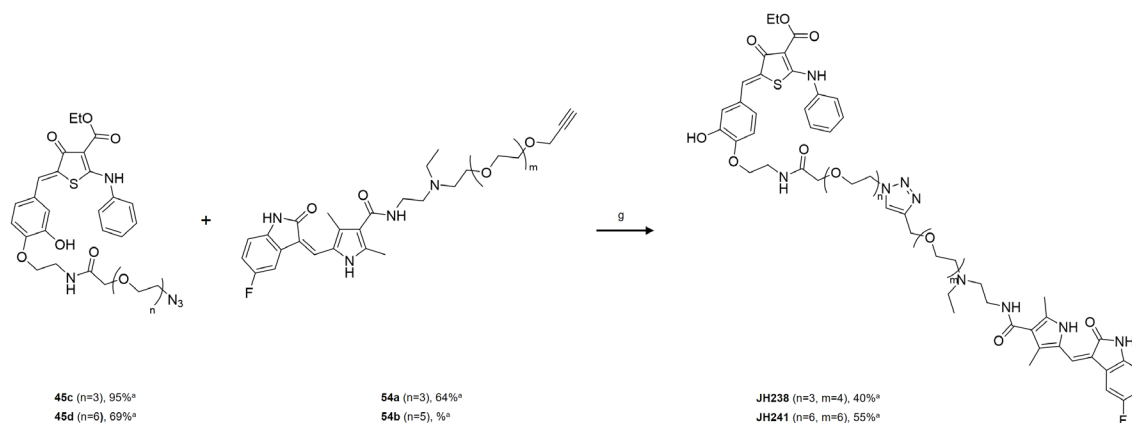
Scheme 14. The synthetic route to couple azide-tagged 2-5A-binding pocket ligand and alky-tagged ATP-binding pocket ligand by click chemistry. **a**. $CuSO_4$, sodium ascorbate, THF, H_2O, rt, o.n. [a]isolated yield.

3.2.2.3 Biological evaluation

Heterobivalent molecules were evaluated in FRET-based RNA cleavage assay (Figure 32). Two assay conditions were used for this assay. One is with 2-5A to evaluate as an inhibitor and another is without 2-5A to evaluate as an activator. Unfortunately, none of the compounds showed significant change in either activating or inhibiting RNase L activity. In the activator

assay, the known RNase L activator **C1-3** also did not show the activity while 2-5A induced RNA degradation, which points towards the same problem as with the homobifunctional molecules, the sensitivity of the biochemical assay. Meanwhile, the assay was able to detect the inhibition of RNase L activity as shown in Figure 32A. However, the synthetic bifunctional molecules did not show any inhibitory effect while sunitinib showed inhibition at 130 µM, which indicates that the formation of bifunctional molecules interfered with the binding of the isolated sunitinib moiety. The reason could be either due to the competition of the binding with the activator moiety or because the long linker design disrupts the binding of sunitinib. Once the similar binding affinity of both moieties is the origin of the problem, one moiety should have a significantly better binding affinity to avoid both moieties from competing for binding. Additional four sunitinib derivatives were synthesized and showed different levels of inhibition activity (Figure S6). Therefore, a weak inhibitor can be applied to design a heterobivalent activator while a stronger inhibitor and weak AKR binder can be conjugated to obtain a heterobivalent inhibitor. However, a ligand showing weak binding not to compete with other ligands but potent binding enough to help target both pockets is required, which makes this approach challenging.
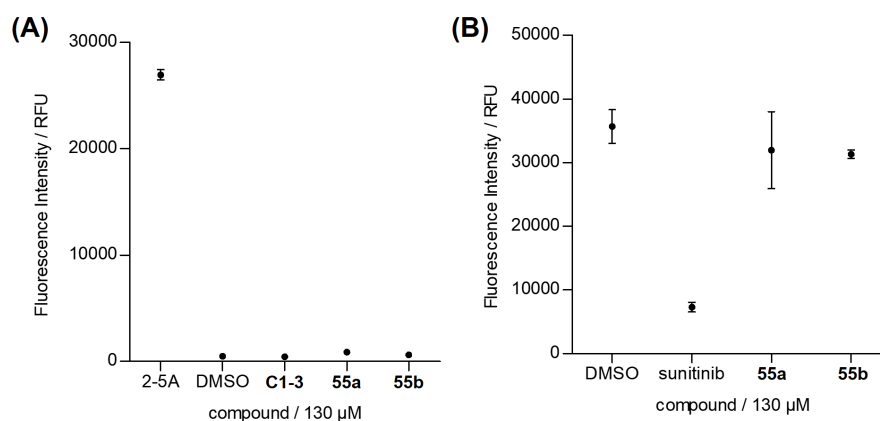
Figure 32. FRET-based RNA cleavage assay to evaluate heterobivalent molecules (A) with 0.5 nM 2-5A to evaluate as RNase L inhibitor or (B) without 2-5A.to evaluate and RNase L activator

3.2.2.4 Summary

In summary, two interesting concepts for the approach with a bifunctional molecule were designed to modulate RNase L activity. The homobifunctional molecule to recruit a monomeric RNase L to another monomer to trigger homodimerization was synthesized with optimized azide- and alkyne-tagged PEG linker attachment to known activator **C1-3** followed by a

conjugation step by click chemistry. The synthetic effort to obtain the homobifunctional molecules successfully resulted in the desired products. The homobifunctional molecule showed an improved RNA degradation than the original monomer **C1-3** in biochemical RNase cleavage assay. Despite the improvement to activate RNase L, it is still not comparable to RNase L's native activator 2-5A. Therefore, the established synthetic strategy for linker attachment can apply to the next generation of homobifunctional molecule synthesis with more potential activator moiety. Furthermore, to overcome the limitation of *in vitro* assays, the cell-based phenotype assay or rRNA degradation assay can be introduced to evaluate the homobifunctional compounds. The next bifunctional molecule strategy was a heterobivalent molecule to couple the two ligands targeting two different binding sites in RNase L. The AKR binder **C1-3** and the PK binder sunitinib were coupled to successfully obtain two heterobifunctional molecules. The *in vitro* RNA cleavage assay indicated that the heterobifunctional molecules induced neither activating nor inhibiting RNase L activity. The loss of inhibiting activity implies that the linker design restricted the action of the bivalent molecule. A possible solution for this problem is to design a new type of linker with different linker lengths. Another reason for the loss of the inhibitor effect of the sunitinib moiety is that two ligands are competing to bind each binding pocket. This problem can be solved by changing one part of a ligand with improved binding affinity.

3.2.3 Recovering RNase L activity by degrading antagonist proteins

3.2.3.1 Background and 2',5'-phosphodiesterase

Another approach in this study to modulate RNase L activity was through the degradation of the RNase L-cleaving and inhibiting protein by a PROTAC strategy. Among the various mechanisms used by viruses to antagonize the antiviral effect via the OAS-RNase L pathway is the involvement of the 2',5'-phosphodiesterase (2',5'-PDE) to degrade 2-5A and subsequently prevent RNase L activation.[40] A few 2',5'-PDEs of both viruses and humans have been characterized. Although virus 2',5'-PDE mainly plays a critical role to inhibit RNase L such as NS1 and E3L in viral infection, host 2',5'-PDEs from host cells showed the effect on 2-5A level in virus-infected cells. Therefore, one of the hosts 2',5'-PDEs was selected in this study to test the proof-of-concept. Among host proteins that showed 2',5'-PDE activity, ENPP1 and PDE12 were associated with virus infection. ENPP1 was selected to be the target for PROTAC degradation mainly because PDE12 is a mitochondrial protein, of which the degradation mechanism by proteasomal enzymes is unclear.

3.2.3.2 Design of PROTAC to degrade ENPP1

ENPP1 was initially characterized as a protein to degrade ATP and then as a cancer-promoting enzyme by degrading tumor suppressor cyclic GMP-AMP (cGAMP). ENPP1 is known to degrade both atypical 2',5'- and typical 3',5'-linked forms of cGAMP. ENPP1 is a membrane protein and mainly exists extracellular but also exists at the ER membrane to affect cytoplasmic events.[141-142] ER membrane ENPP1 is presumed to affect 2-5A degradation since 2-5A only exists in the cytoplasm. Therefore, selective targeting of ENPP1 at ER membrane was the critical point to consider when the small molecule-ligand was selected. A few types of small molecule-ligands were reported to inhibit ENPP1.[142-143] In order to selectively target ER membrane ENPP1, we chose a quinazoline scaffold containing a phosphonic acid. In the compound, the phosphonic acid is a necessary moiety to bind at the ATP-binding pocket and chelate zinc ions. In order to make the phosphonic acid-containing molecule permeable through the cell membrane, a prodrug strategy of protecting phosphonic acid as phosphate esters can be applied.[144-145] After the phosphonates penetrate the cell membrane, a cytoplasmic esterase then converts the phosphonate to give phosphonic acid. The phosphonic acid can restore the inhibitory activity and bind to ENPP1, leading to the recruitment of proteasome via PROTAC molecules to degrade the ENPP1. (Figure 33A).
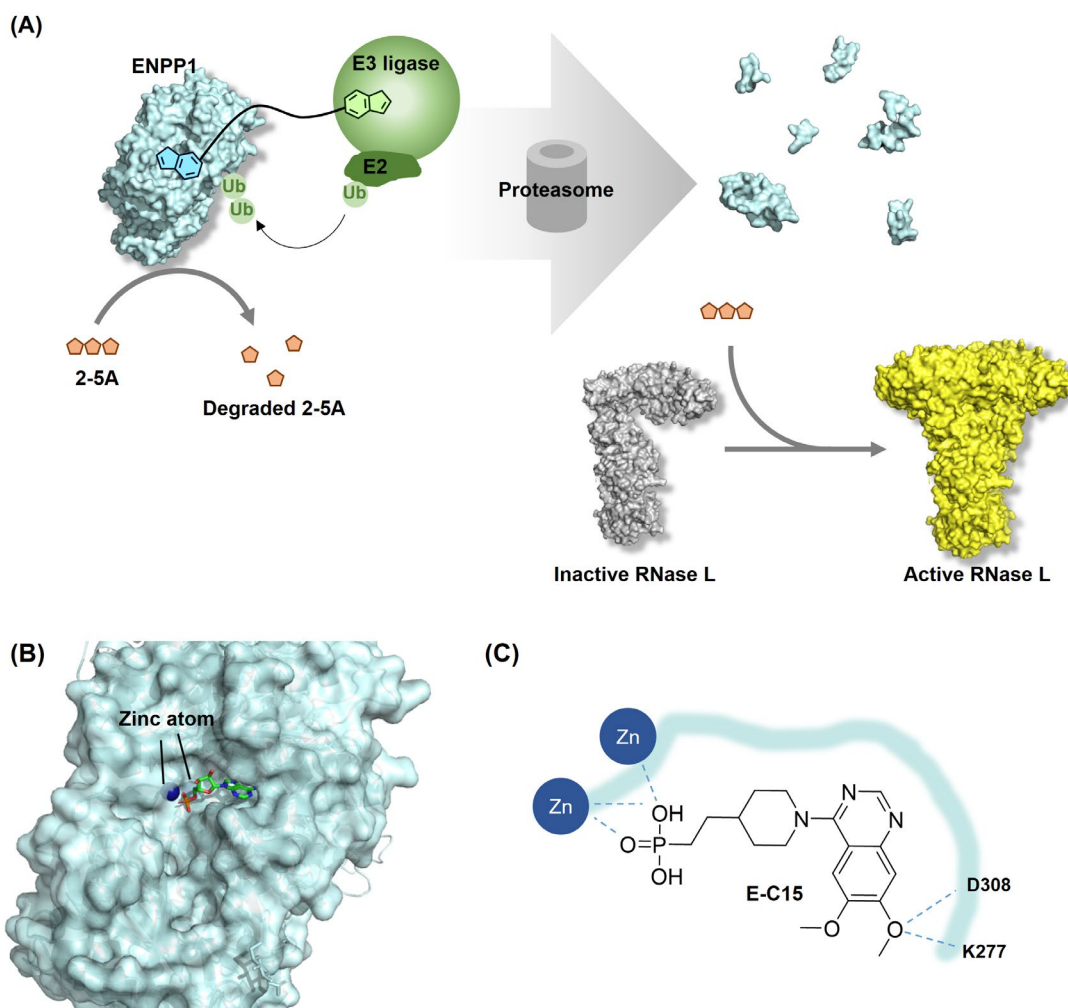
Figure 33. (A) Schematic showing the concept of ENPP1 PRTAC molecule to restore RNase L activity. (B) Co-crystal structure of ENPP1 and inhibitor **E-C15** at the catalytic domain (PDB code: 4GTW); (C) Ligand interaction of inhibitor **E-C15** with zinc atoms and residues.

As a first step to achieve the PROTAC molecule, the linker attachment position was selected according to the crystal structure between ENPP1 and reported ENPP1 inhibitor compound 15 (**E-C15**) at the ENPP1 ATP-binding pocket of the catalytic domain (Figure 33B–C). The methoxy group at 6-position of quinazoline was the solvent exposure part whereas 7-methoxy group was engaged in the formation of hydrogen bonds with the ENPP1. Therefore, the linker attachment point was designed on 6-methoxy group of quinazoline.

3.2.3.3 Chemical synthesis

Quinazolin-4-one with 6-hydroxy and 7-methoxy group were synthesized by intermolecular cyclization of 5-hydroxy-4-methoxy-2-aminobenzoic acid and formamide to give **57** which was isolated as crystal by cooling down the reaction (Scheme 15A). The next step is to protect

the hydroxy group to prevent chlorination in the following step to chlorinate ketone of quinazolin-4-one. The acetyl group was selected for the protection group of hydroxide in this step because the acetyl group is stable during the acidic chlorination step. The acetylation of phenol alcohol and chlorination of quinazoline-4-one were performed sequentially with excellent yields of 93% and 100%, respectively. Then, the acetyl group was deprotected under basic conditions with ammonia in methanol to give **60**. The linker attachment moiety was introduced to phenol by using Boc-aminoethyl bromide assisted by potassium carbonate. In this step, bromide was necessary for the aminoethyl to be more reactive than the aromatic chloride atom. The (2-(piperidin-4-yl)ethyl)phosphonic acid moiety was prepared as diethyl (2-(piperidin-4-yl)ethyl)phosphonate **63** to protect phosphonic acid into ethyl phosphonate by condensation between tetraethyl methylenediphosphonate and *N*-benzylpiperidine-4-carboxaldehyde followed by reduction of the benzyl group. The reactive aromatic chloride was coupled with **63** in mild conditions to give **64** with 86% yield. The Boc group from linker attachment moiety was deprotected to be ready to couple with E3 ligase recruiter moiety, giving the protected structure of ENPP1 recruiter moiety, **65** with quantitative yield.

Thalidomide was selected to recruit cereblon as an E3 ligase for proteasome-mediated degradation.[146-147] Thalidomide is one of the most abundantly applied E3 ligase recruiters in the PROTAC study.[148-149] The synthetic route and linker attachment design are well-established over a decade of PROTAC study.[150] Thalidomide was obtained by coupling 3-amino-2,6-piperidinedione and phthalic anhydride functionalized with 4-fluoride for linker attachment (Scheme 15B). The protected acetic acid moiety was then introduced to 4-position via nucleophilic aromatic substitution. Then **68a** was obtained by deprotection of acetic acid.
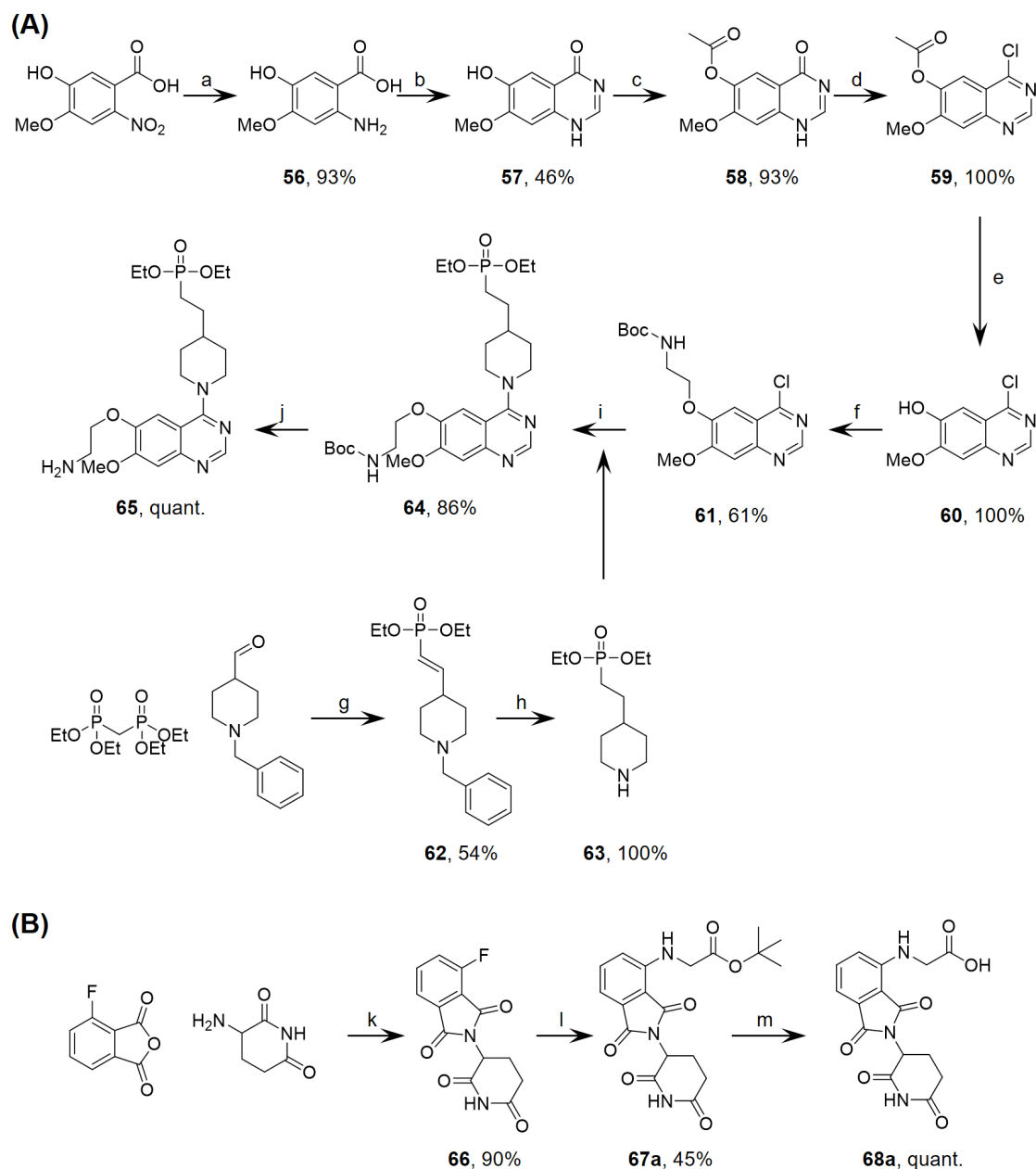
Scheme 15. Route to synthesize ENPP1 PROTAC. (A) Synthesis of ENPP1 ligand moiety with an amine for E3 ligase-recruited ligand attachment. (B) The synthesis of cereblon binder thalidomide with linker attachment design. (C) PROTAC by amide coupling and selective deprotection of ethyl phosphonate. **a**. Pd/C, MeOH, RT, o.n.; **b**. formamide, 150 °C, 1 h; **c**. Ac₂O, pyridine, 100 °C, 2 h; **d**. SOCl₂, reflux, 2 h; **e**. 7N NH₃ in MeOH, rt, 1.5 h; **f**. Boc-aminoethyl bromide, K₂CO₃, DMF, 60 °C, 2 h; **g**. NaH, toluene, rt, o.n.; **h**. Pd/C, EtOH, rt, o.n.; **i**. IPA, 90 °C, 3 h; **j**. TFA, DCM, RT, 1 h; **k**. AcONa, AcOH, reflux, o.n.; **l**. Boc-glycinate, DIPEA, DMSO, 90 °C, 1 d; **m**. TFA, DCM, RT, 1 h.

Finally, the complete PROTAC molecule was obtained by amide coupling between ENPP1 ligand **65** with free amine and cereblon ligand **68a** with a carboxylic acid (Scheme 16). Further deprotection to obtain fully deprotected phosphonic acid **70** and monoprotected ethyl phosphonate **71** was performed by adjusting the amount of bromotrimethylsilane (TMSBr) and the reaction time for selective deprotection of ethyl phosphonate. Two different deprotection modes were obtained because the monoethyl phosphonate and diethyl phosphonate showed different deprotection efficiency in a cell from previous studies.
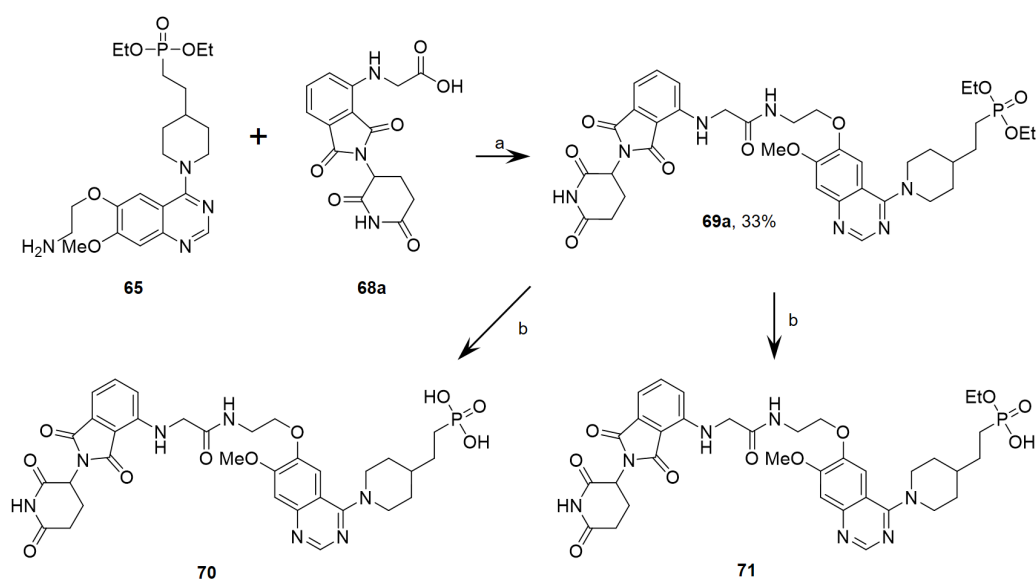
Scheme 16. The synthesis of ENPP1 PROTAC molecule by amide coupling and selective deprotection of ethyl phosphonate. **a**. EDC, DMAP, DIPEA, DMF, rt, o.n.; **b**. TMSBr, DCM, rt, 1 h–o.n.

3.2.3.4 Linker variation

Additionally, the linker variation has been conducted by changing the linker type and length (Scheme 17). Firstly, a longer aliphatic hydrocarbon linker was synthesized by using tert-butyl 4-aminobutanoate instead of tert-butyl glycinate, giving **67b** and deprotected **68b** (Scheme 17A**)**. PROTAC derivative molecule was synthesized by coupling **65** under established click chemistry conditions to yield **69b**. The second linker type was designed for different linker lengths and types. Triazole-contained PEG linker was employed to introduce more rigidity (Scheme 17). The synthesis of azide-tagged PEG linker was described in chapter 3.2.2 synthesizing **45a** and **45b**. The azide-tagged PEG linker was conjugated with ENPP1 recruiting moiety **65** by amide coupling. The thalidomide was functionalized with an alkyne tag by using propargyl amine. Two derivatives of triazole-based PROTAC molecules were synthesized by

copper-catalyzed intermolecular cycloaddition between alkyne and azide, yielding **74a** and **74b** (Scheme 18). In total, six derivatives of ENPP1 PROTAC molecules were synthesized for the initial evaluation of ENPP1 degradation and the effect.
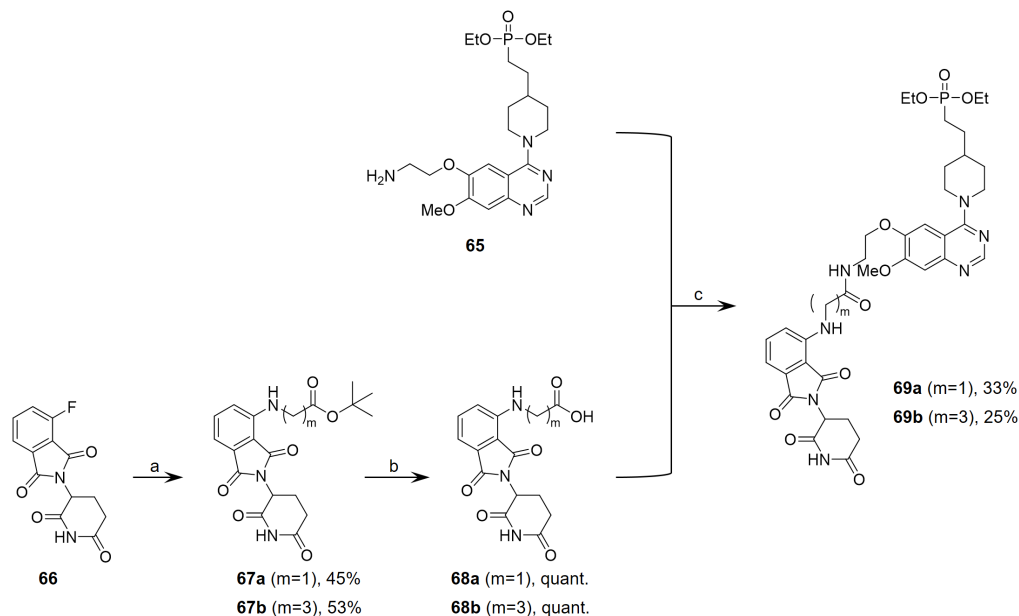
Scheme 17. Synthetic route to synthesize ENPP1 PROTAC with different lengths of alkyl linkers. **a.** Boc-glycinate, DIPEA, DMSO, 90 °C, 1 d; **b.** TFA, DCM, rt, 1 h, **c.** EDC, DMAP, DIPEA, DMPF, rt, o.n.
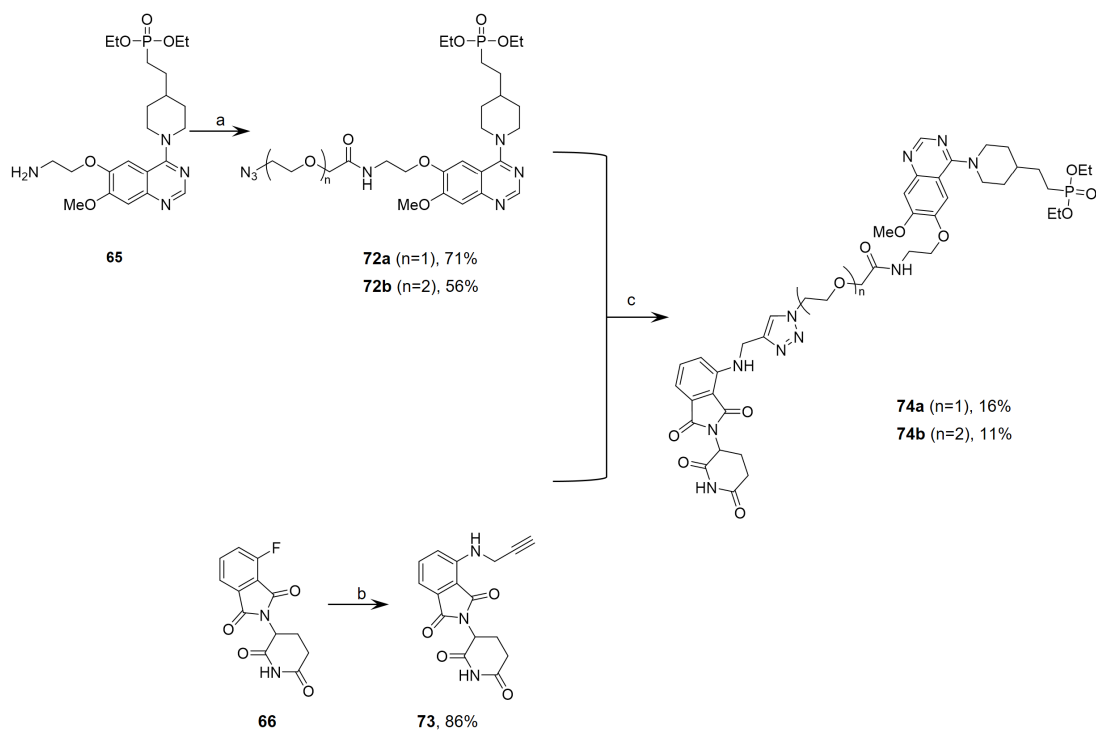
Scheme 18. Synthetic route to synthesize ENPP1 PROTAC with different linkers of triazole-based PEG linkers. **a**. **45a** or **45b**, PyBOP, DIPEA, DMF, rt, 1 h; **b**. propargyl amine, DIPEA, DMSO, 90 °C; **c**. CuSO$_4$, sodium ascorbate, THF, H$_2$O, rt, o.n.

3.2.3.5 Biological evaluation

To evaluate the protein level of ENPP1, initial immunoblotting was performed. In this experiment, we tested two conditions including and excluding membrane proteins. Unfortunately, both conditions were not able to show the degradation of ENPP1 (Figure 34). For the setup without membrane proteins, ENPP1 could not be detected with DMSO negative control, which indicated that a minor amount of ENPP1 is present in the cytoplasm of HeLa cells. The setup including membrane proteins at the right half of the gel image showed majorly ENPP1 located in the cell membrane. Therefore, the degradation of ENPP1 at ER membrane could not be detected.
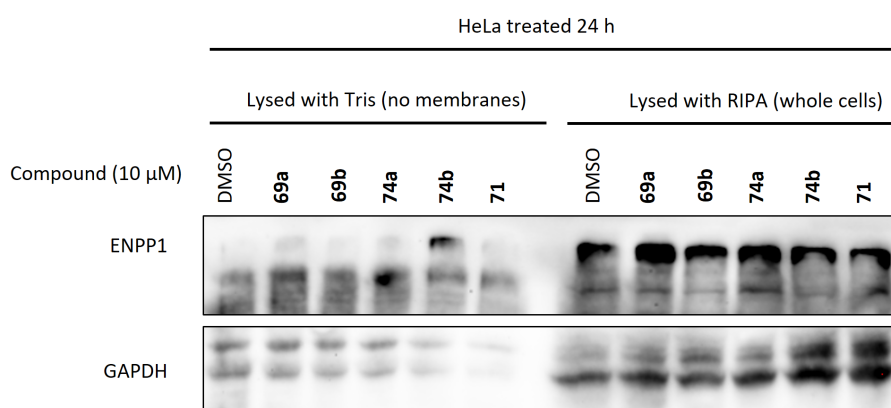
Figure 34. The Western blot showing the protein level of ENPP1

The evaluation to monitor the efficacy of the ENPP1 PROTAC molecule to restore the RNase L activity is still on-going. The assay should be further optimized to detect the ER ENPP1 level collectively. As an indirect monitor method, the 2-5A level after transfection with polyI:C or IFN can be measured.

3.2.3.6 Summary

The PROTAC molecules were obtained to indirectly activate RNase L. ENPP1 is a membrane protein which can degrade the 2',5'-linkage of nucleotide. The relation of ENPP1 with a 2-5A level in the viral infected cell was investigated in the previous study. Therefore, the degradation of ENPP1 could lead to restoring RNase L activity by increasing the 2-5A level in cells. The pre-drug form of ENPP1 PROTAC molecule was designed and obtained to selectively target and degrade ER ENPP1 while not affecting

the effect of cell membrane ENPP1 by using a phosphonate-based ENPP1 inhibitor of a prodrug form. Furthermore, different stages of phosphonate, monoester, and diester form, were synthesized to monitor the efficiency of deprotection of ethyl ester in cells. The linker type and length variation yielded three more derivatives, giving a total of six derivatives of ENPP1 PROTAC molecules. The initial investigation of ENPP1 level in cells did not reveal significant degradation of ENPP1, which was expected due to a minor level of ER ENPP1 in comparison to cell membrane ENPP1. A continuous effort is being conducted to observe the selective degradation of ER ENPP1 and the effect of PROTAC molecules at the cellular level.

4. Conclusion

In this study, a suite of small-molecule-based approaches to develop new chemical tools to modulate RNase L activity has been performed. Two types of strategies, a small molecule-binding approach and a bifunctional molecule-based design, were applied. The small molecule-binding approach incorporated three strategies: scaffold-based design of RNase L activators, structure-activity relationship study of 2-aminothiophenes, and rational design of RNase L inhibitors. The focus on the second approach was focused on the design of various bifunctional molecules: a homobifunctional molecule, a heterobivalent molecule, and a PROTAC molecule.

Scaffold-based design led to chemistry-oriented optimization of thienopyrimidines to either combine with another RNase L activator structure or modulate the core scaffold into a thienodiazepine for improvement of 3-dimensional conformation and solubility. A total of 24 derivatives of fused scaffold derivatives and 8 thienodiazepine derivatives were synthesized with the newly established combinatorial chemistry, while none of the derivatives showed significant RNase L activation ability measured by the FRET-based RNA cleavage assay. The obtained chemistry-oriented design could be further developed with the design of ligands with the assistance of a crystallographic study of small-molecule RNase L activators.

For the structure-activity relationship study, 46 derivatives of ATPC were synthesized. Biochemical i*n vitro* evaluation revealed that the RNase L activation was not significantly induced by the synthesized ATPCs in RNA cleavage assays while thermal shift measurement showed that selected ATPCs improved binding to RNase L than the reported RNase L activators. Considering the tumor-suppressing role of RNase L, the antiproliferation activity of synthesized ATPCs was evaluated in cellular assays. Selected ATPCs, such as **15l** (JH094) exhibited potent antiproliferation activity with single-digit micromolar potency against JAR cells and other human cancer cells. Moreover, a cellular evaluation showed that **15l** induced 61% apoptosis at 10 µM concentration, which correlated with RNase L-mediated apoptosis. However, further evaluations in the phenotypic and mechanistic study are required to elucidate the mode of action.

In the rational design approach, a new series of 34 RNase L inhibitors based on the 2-((pyrrol-2-yl)methylene)thiophen-4-one scaffold was designed according to structural features involved in sunitinib-binding to RNase L. Biochemical RNA cleavage assays showed the promising potency of the newly designed thiophenone compounds as RNase L inhibitor. Especially, **32a** (JH259) and **32c** (JH332) showed 30-fold improved inhibitory potency than that of sunitinib in

the FRET-based RNA cleavage assay. A subsequent docking study suggested that the high 3-dimensional complementary as well as more interactions with RNase L resulted in more potent binding to RNase L and hence improved the potency of the inhibitory effect. Furthermore, cellular rRNA cleavage assay showed that **32a** inhibited the rRNA cleavage by more than 50% at 2 µM. Further generation of RNase L inhibitors could be designed once the binding mode of 2-((pyrrol-2-yl)methylene)thiophen-4-one to RNase L can be resolved. The current structural information based on docking analysis performed at the 2-5A-binding pocket indicated that the exchange of the 3-fluorophenyl moiety into a more purine mimetic aromatic ring as well as the introduction of additional purine analog at the pyrrole position will resemble the arrangement and structure of 2-5A, which may result in the discovery of potent RNase L activators.

For the bifunctional molecule-based approaches, on the one hand, the heterobivalent molecules resulted in a loss of activity in comparison with either of the two used ligands, which indicated that the two ligands consisting of the heterobivalent molecules could potentially compete with each other for binding or the attachment of the linker inhibited ligand activity. Further work can be performed to screen for more optimal linkage or to select a less potent ligand at one end and a more potent ligand at the other side. On the other hand, homobifunctional molecules were successfully obtained and evaluated in a biochemical assay. Although the potency was still low in comparison with the native activator 2-5A, it is noteworthy that the activation by the homobifunctional molecule was improved in comparison to the reported synthetic activators. Therefore, a further generation of homobifunctional molecules could lead to more potent activator ligands. Additionally, cell-based rRNA cleavage assay and antiproliferation assay would help to overcome the limitation of *in vitro* RNA cleavage assays. Lastly, PROTAC molecules targeting the RNase L-suppressing protein ENPP1 were designed. ENPP1 is an enzyme degrading 2',5' and 3',5' linkage of nucleotide. One of the target molecules of ENPP1 is 2-5A. To analyze the efficacy of the obtained PROTAC molecules, the protein level as well as the 2-5A level should be investigated by using immunoblotting and RNA cleavage analysis.

In the course of this dissertation, synergistic small molecules-and bifunctional molecules-strategies were applied to modulate RNase L. In a successful result, promising RNase L binders showing RNase L-mediated downstream effects in cells were identified. Additionally, a new scaffold exhibited improved potency as an RNase L inhibitor. An attractive concept of a homodimerizer system using homobifunctional molecules showed improved activation of RNase L. In addition to the discussed perspectives for each of the used strategies, the discussed result can lay the foundation for the development of RNase L-targeting bifunctional molecules

with improved potency and different selectivity. In summary, the findings revealed in this study contribute to the identification of chemical tools to modulate RNase L activity, which can then be applied to the development of potential therapeutics to treat RNase L-related human diseases including immune disorders and viral infections.

5. Experimental

5.1 Chemical synthesis

5.1.1 General chemistry information

All the solvents and reagents were purchased from Fischer Scientific, TCI Chemical, VWR international GmbH, or Sigma Aldrich and used without further purification. Thin layer chromatography (TLC) was performed on silica-coated aluminum plates (Merck 60 F254) and visualized under UV irradiation (254 nm), I_2 stain, or potassium permanganate stain (1.5 g $KMnO_4$, 10 g K_2CO_3, 1.25 mL of 10% aqueous NaOH solution and 200 mL of H_2O). Chromatographic purification of products was achieved through flash column chromatography on the automated medium-pressure liquid chromatography (MPLC, Büchi Pure C-810, Büchi Pure C-835) with proper solvents or preparative chromatography (Büchi Pure C-835, Nuleodur C18 gravity VP 125/10 5 μm) with H_2O (+ 0.1% TFA) and acetonitrile (+ 0.1% TFA). Recrystallization of products from crude products was performed with indicated solvents. Yields refer to pure compounds after purification by flash column chromatography, preparative chromatography, recrystallization, or titration. LC-MS was performed on an Agilent 1260 II Infinity system equipped with a mass detector (column: InfinityLab Poroshell 120 EC-C18, 2.1×150, 2.7 μm). Appropriate gradient systems (5–95% acetonitrile in H_2O in 6 min) were applied by mixing H_2O (+ 0.1% TFA) and acetonitrile (+ 0.1% TFA). NMR spectra were obtained by Bruker AV 400 Avance III HD (^{1}H NMR: 400 MHz, ^{13}C NMR: 101 MHz), Bruker AV 500 BioSpin (^{1}H NMR: 500 MHz, ^{13}C NMR: 126 MHz), Bruker AV 700 Avance III HD (^{1}H NMR: 700 MHz). Data is reported in ppm with reference to the used deuterated solvent ($CDCl_3$: 7.26 ppm, 77.16 ppm; DMSO-d_6: 2.50 ppm, 39.52 ppm, CD_3OD: 3.31 ppm,). Multiplicities of NMR signals are abbreviated as follows; s: singlet, d: doublet, t: triplet, q: quartet, p: pentet, and m: multiplet. High-resolution mass spectrometry (HRMS) was acquired on an LTQ Orbitrap mass spectrometer coupled to an Accela HPLC-System (HPLC column: Hypersyl GOLD, 50 mm × 1 mm, particle size 1.9 μm, ionization method: electron spray ionization (ESI)).

5.1.2 Synthetic procedures and compound characterizations

5.1.2.1 Petasis products and thienodiazepines

*2-Cyano-N-ethylacetamide (**1**)*
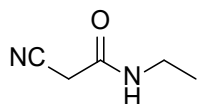
The compound was synthesized according to a literature procedure.[151] To ethyl cyanoacetate (20.0 mL, 0.19 mol) was added 70% ethylamine aqueous solution (31.2 mL, 0.37 mol) dropwise with stirring at room temperature for 15 minutes. The reaction mixture was stirred at 35 °C for 5 h. The mixture was then cooled to 0 °C overnight to give a precipitate which was filtered off and washed with cold Et_2O to give the desired product as a white solid (17. 7 g, 0.16 mol, 84%). ^{1}H NMR (400 MHz, $CDCl_3$): δ 6.16 (s, 1H), 3.38–3.32 (m, 4H), 1.21 (t, J = 7.28 Hz, 3H).

*2-Amino-N-ethyl-4,5,6,7-tetrahydrobenzo[b]thiophene-3-carboxamide (**2**)*
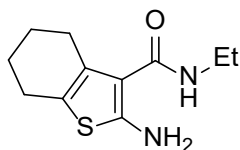
The compound was synthesized according to a literature procedure.[152] A mixture of cyclohexanone (7.0 mL, 67.78 mmol), **1** (7.6 g, 67.78 mmol), ammonium acetate (5.2 g, 67.78 mmol), and glacial acetic acid (3.9 ml, 67.78 mmol) in cyclohexane (150 mL) was refluxed overnight with molecular sieves (15.0 g). The reaction mixture was cooled to room temperature, diluted with cyclohexane, and washed sequentially with water, 10% aqueous sodium bicarbonate solution, and dried over anhydrous $MgSO_4$. The solvent was removed under vacuum to give a crude 2-cyano-2-cyclohexylidene-*N*-ethyl-acetamide (6.5 g, 33.81 mmol, 50%).

To a mixture of the crude 2-cyano-2-cyclohexylidene-N-ethyl-acetamide (3.5 g, 18.21 mmol) and sulfur (0.7 g, 21.85 mmol) in ethanol (18 mL) was added diethylamine (1.9 mL, 18.21 mmol) dropwise at room temperature. The mixture was stirred for 3 h at 48 ˚C. After the reaction completion monitored by TLC, the mixture was cooled to 4 ˚C overnight and the solid obtained was filtered and washed with cold ethanol. The crude product was recrystallized from the solvent mixture (IPA/H_2O=9:1 v/v) to give a yellow crystal (2.3 g, 10.20 mmol, 56%). ^{1}H NMR (500 MHz, $CDCl_3$): δ 5.91 (s, 2H), 5.63 (s, 1H), 3.43–3.37 (m, 2H), 2.65–2.57 (m, 2H), 2.57–2.49 (m, 2H), 1.81–1.78 (m, 4H), 1.19 (t, J = 7.25 Hz, 3H).

Ethyl 2-amino-4,5,6,7-tetrahydrobenzo[b]thiophene-3-carboxylate (**3**)
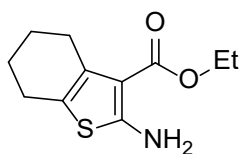
The compound was synthesized according to a literature procedure.[153] To a solution of ethyl cyanoacetate (5.0 mL, 46.86 mmol), cyclohexanone (4.9 mL, 46.86 mmol), and sulfur (1.5 g, 46.86 mmol) in absolute ethanol (310 mL) was added triethylamine (7.8 mL, 56.23 mmol) under argon. The resulting mixture was allowed to be refluxed overnight. The suspension was filtered through a pad of Celite and washed with absolute ethanol. The combined filtrate was concentrated to dryness under reduced pressure. The crude product was purified by recrystallization from the solvent mixture (IPA/H_2O=3:2 v/v) to give the desired product as an orange crystal (6.2 g, 27.58 mmol, 59%). ^1H NMR (400 MHz, $CDCl_3$): δ 5.92 (s, 2H), 4.26 (q, *J* = 7.1 Hz, 2H), 2.72–2.64 (m, 2H), 2.57–2.44 (m, 2H), 1.88–1.66 (m, 4H), 1.33 (t, *J* = 7.1 Hz, 3H).

2-Amino-4,5-dimethylthiophene-3-carboxamide (**8**)
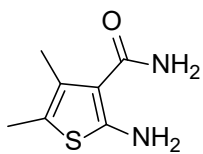
The compound was synthesized according to a literature procedure.[154] Ethyl methyl ketone (1.8 mL, 20.00 mmol), 2-cyanoacetamide (1.7 g, 20.00 mmol), and sulfur (0.6 g, 20.00 mmol) were added in EtOH (10 mL). To a reaction mixture, diethylamine (2.3 mL, 22.00 mmol) was added and the resulting mixture was stirred overnight at room temperature. The reaction mixture was diluted with H_2O and extracted several times with EA/EtOH (3:1 v/v). The combined organic layer was dried over $MgSO_4$, and the solvent was removed under reduced pressure. The crude product was purified by flash chromatography (PE/EA) to give 2-amino-4,5-dimethylthiophene-3-carboxamide as a yellow solid (494.1 mg, 2.90 mmol, 15 %). ^1H NMR (400 MHz, DMSO-d_6) δ 7.63 (s, 1H), 7.32 (s, 1H), 6.64 (s, 2H), 3.58 (s, 3H), 2.08 (s, 3H). ^{13}C NMR (151 MHz, DMSO-d_6) δ 168.5, 157.7, 128.4, 112.7, 110.3, 14.5, 12.6.

General Procedure 1

2-Aminothiophene (0.89 mmol), a respective aldehyde (1.07 mmol, 1.2 equiv.), and a boronic acid (1.07 mmol, 1.2 equiv.) were added in HFIP (0.2 mM) with molecular sieves. The mixture was stirred at room temperature for indicated reaction time. Once the reaction completion was monitored by LC-MS, the solvent was dried under reduced pressure. The crude was purified by titration (The crude product was redispersed in 5 mL of solvent mixture (ACN/H_2O=6:4 v/v)

and dried at the lyophilizer overnight. The crude solid was dispersed with a solvent mixture (ACN/H$_2$O=6:4 v/v) or Et$_2$O. When a precipitate formed, it was collected by vacuum filtration and washed with a cold mixture of 60% ACN in H$_2$O or Et$_2$O to give yellow solids. When the crude stays in a solution the product was purified by preparative chromatography.

2-((3-(Ethylcarbamoyl)-4,5,6,7-tetrahydrobenzo[b]thiophen-2-yl)amino)-2-phenylacetic acid (**4a**)
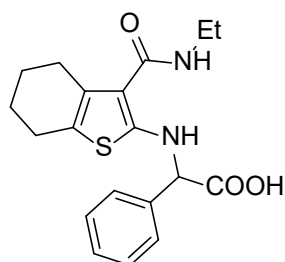
By using **2** (1.5 g, 6.69 mmol), glyoxylic acid monohydrate (0.7 g, 8.02 mmol), and phenylboronic acid (1.0 g, 8.02 mmol) according to general procedure 1 with a reaction time of 1 h and subsequent washing with 60% ACN in H$_2$O to give the desired product (1.3 g, 3.52 mmol, 53%). ^{1}H NMR (500 MHz, DMSO-d_6) δ 13.30 (s, 1H), 8.68 (d, J = 6.9 Hz, 1H), 7.55–7.21 (m, 5H), 6.81 (t, J = 5.6 Hz, 1H), 4.89 (d, J = 6.9 Hz, 1H), 3.26–3.20 (m, 2H), 2.65–2.53 (m, 2H), 2.46–2.36 (m, 2H), 1.75–1.57 (m, 4H), 1.08 (t, J = 7.1 Hz, 3H). ^{13}C NMR (126 MHz, DMSO-d_6) δ 171.0, 165.1, 156.0, 137.2, 129.8, 128.2 (2), 127.7, 126.8 (2), 117.0, 108.3, 62.3, 33.1, 25.3, 23.5, 22.2, 21.9, 14.6. HRMS-ESI (m/z): [M+H]$^+$ calculated for C$_{19}$H$_{23}$O$_3$ N$_2$S, 359.1424; found, 359.1424.

2-((3-(Ethylcarbamoyl)-4,5,6,7-tetrahydrobenzo[b]thiophen-2-yl)amino)-2-(3-hydroxyphenyl) acetic acid (**4b**)
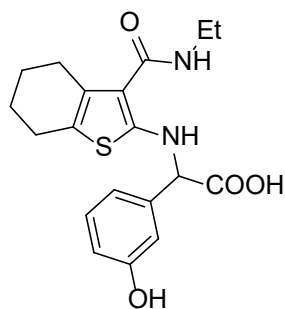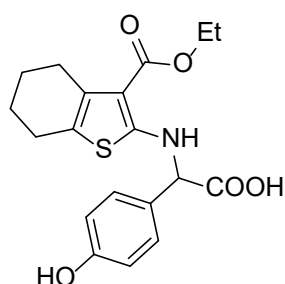
By using **2** (200.0 mg, 0.89 mmol), glyoxylic acid monohydrate (98.5 mg, 1.07 mmol), and 3-hydroxybenzeneboronic acid (147.6 mg, 1.07 mmol) according to general procedure 1 with a reaction time of 3 h and subsequent washing with 60% ACN to give the desired product (52.7 mg, 0.14 mmol, 16%). ^{1}H NMR (500 MHz, DMSO-d_6) δ 13.24 (s, 1H), 9.50 (s, 1H), 8.66 (d, J = 7.0 Hz, 1H), 7.14 (t, J = 7.8 Hz, 1H), 6.85–6.73 (m, 3H), 6.68 (d, J = 8.1 Hz, 1H), 4.77 (d, J = 7.0 Hz, 1H), 3.25–3.20 (m, 2H), 2.67–2.55 (m, 2H), 2.46–2.39 (m, 2H), 1.72–1.58 (m, 4H), 1.08 (t, J = 7.2 Hz, 3H). ^{13}C NMR (126 MHz, DMSO-d_6) δ 171.0, 165.1, 157.1, 156.2, 138.4, 129.8, 129.2, 117.7, 116.8, 114.7, 113.3, 108.0, 62.2, 33.1, 25.4, 23.5, 22.2, 22.0, 14.6. HRMS-ESI (m/z): [M+H]$^+$ calculated for C$_{19}$H$_{23}$O$_4$N$_2$S, 375.1373; found, 375.1374.

2-((3-(Ethylcarbamoyl)-4,5,6,7-tetrahydrobenzo[b]thiophen-2-yl)amino)-2-(4-methoxyphenyl)acetic acid (**4e**)
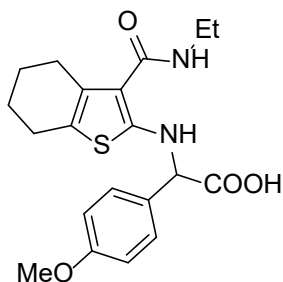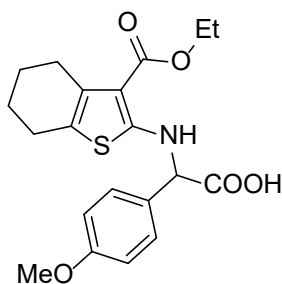
By using **2** (200.0 mg, 0.89 mmol), glyoxylic acid monohydrate (98.5 mg, 1.07 mmol), and 4-methoxyphenylboronic acid (162.6 mg, 1.07 mmol) according to general procedure 1 with a reaction time of 1 h and subsequent washing with 60% ACN to give the desired product (264.0 mg, 0.68 mmol, 76%). ^{1}H NMR (500 MHz, DMSO-d_6) δ 13.20 (s, 1H), 8.63 (d, J = 6.7 Hz, 1H), 7.29 (d, J = 8.7 Hz, 2H), 6.92 (d, J = 8.7 Hz, 2H), 6.79 (t, J = 5.6 Hz, 1H), 4.81 (d, J = 6.7 Hz, 1H), 3.73 (s, 3H), 3.25–3.20 (m, 2H), 2.64–2.57 (m, 2H), 2.47–2.37 (m, 2H), 1.72–1.59 (m, 4H), 1.08 (t, J = 7.1 Hz, 3H). ^{13}C NMR (126 MHz, DMSO-d_6) δ 171.3, 165.1, 158.6, 156.1, 129.7, 128.9, 128.0 (2), 116.9, 113.6 (2), 108.2, 61.7, 54.6, 33.1, 25.3, 23.5, 22.2, 22.0, 14.6. HRMS-ESI (m/z): [M+H]$^+$ calculated for $C_{20}H_{25}O_4N_2S$, 389.1530; found, 389.1532.

2-((3-(Ethylcarbamoyl)-4,5,6,7-tetrahydrobenzo[b]thiophen-2-yl)amino)-2-(p-tolyl)acetic acid (**4f**)
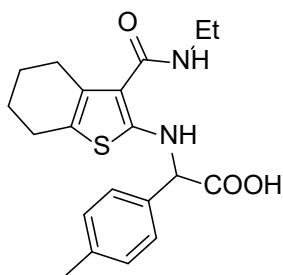
By using **2** (200.0 mg, 0.89 mmol), glyoxylic acid monohydrate (98.5 mg, 1.07 mmol), and 4-tolylboronic acid (145.5 mg, 1.07 mmol) with a reaction time of 1 h and subsequent washing with 60% ACN to give the desired product (247.5 mg, 0.66 mmol, 75%). ^{1}H NMR (700 MHz, DMSO-d_6) δ 13.20 (s, 1H), 8.64 (d, J = 6.9 Hz, 1H), 7.26 (d, J = 7.5 Hz, 2H), 7.16 (d, J = 7.5 Hz, 2H), 6.78 (t, J = 5.7 Hz, 1H), 4.83 (d, J = 6.9 Hz, 1H), 3.25–3.21 (m, 2H), 2.64–2.56 (m, 2H), 2.47–2.36 (m, 2H), 2.27 (s, 3H), 1.72–1.60 (m, 4H), 1.09 (t, J = 7.1 Hz, 3H). ^{13}C NMR (126 MHz, DMSO-d_6) δ 171.2, 165.1, 156.1, 137.0, 134.2, 129.7, 128.8 (2), 126.7 (2), 116.9, 108.3, 62.0, 33.1, 25.3, 23.5, 22.2, 21.9, 20.2, 14.6. HRMS-ESI (m/z): [M+H]$^+$ calculated for $C_{20}H_{25}O_3N_2S$, 373.1580; found, 373.1581.

2-((3-(Ethylcarbamoyl)-4,5,6,7-tetrahydrobenzo[b]thiophen-2-yl)amino)-2-(4-hydroxyphenyl)acetic acid (**4i**)
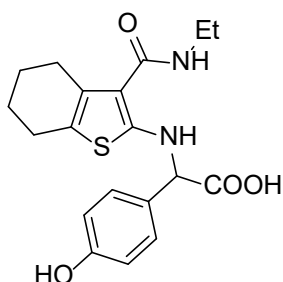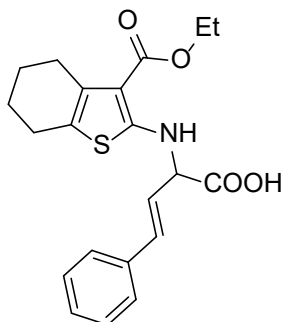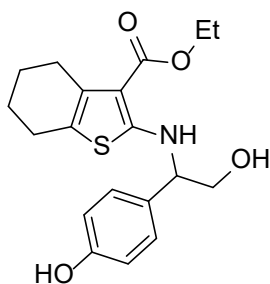
By using **2** (200.0 mg, 0.89 mmol), glyoxylic acid monohydrate (98.5 mg, 1.07 mmol), and 4-hydroxyphenylboronic acid (147.6 mg, 1.07 mmol) according to general procedure 1 with a reaction time of 1 h and subsequent washing with Et$_2$O to give the desired product (290.9 mg, 0.78 mmol, 87%). ^{1}H NMR (700 MHz, DMSO-d_6) δ 13.09 (s, 1H),

9.48 (s, 1H), 8.57 (d, J = 6.9 Hz, 1H), 7.17 (d, J = 8.6 Hz, 2H), 6.77 (t, J = 5.6 Hz, 1H), 6.73 (d, J = 8.6 Hz, 2H), 4.73 (d, J = 6.9 Hz, 1H), 3.24–3.20 (m, 2H), 2.65–2.56 (m, 2H), 2.47–2.40 (m, 2H), 1.73–1.59 (m, 4H), 1.08 (t, J = 7.2 Hz, 3H). ^{13}C NMR (176 MHz, DMSO-d_6) δ 171.6, 165.2, 157.0, 156.4, 129.8, 128.1 (2), 127.3, 117.0, 115.0 (2), 108.3, 62.0, 33.2, 25.5, 23.7, 22.3, 22.1, 14.7. HRMS-ESI (m/z): [M+H]$^+$ calculated for C$_{19}$H$_{23}$O$_4$N$_2$S, 375.1373; found, 375.1374.

2-(3,4-Dimethoxyphenyl)-2-((3-(ethylcarbamoyl)-4,5,6,7-tetrahydrobenzo[b]thiophen-2-yl) amino)acetic acid (**4k**)
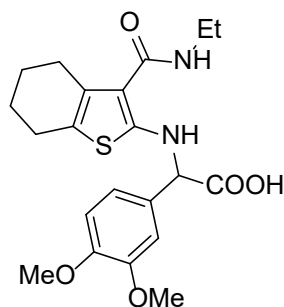
By using **2** (200.0 mg, 0.89 mmol), glyoxylic acid monohydrate (98.5 mg, 1.07 mmol), and 3,4-dimethoxyphenylboronic acid (194.7 mg, 1.07 mmol) according to general procedure 1 with a reaction time of 1 h and subsequent washing with Et$_2$O to give the desired product (245.1 mg, 0.59 mmol, 66%). ^{1}H NMR (700 MHz, DMSO-d_6) δ 13.16 (s, 1H), 8.56 (d, J = 6.9 Hz, 1H), 7.00–6.87 (m, 3H), 6.81 (t, J = 5.6 Hz, 1H), 4.81 (d, J = 6.9 Hz, 1H), 3.73 (s, 3H), 3.71 (s, 3H), 3.25–3.21 (m, 2H), 2.65–2.55 (m, 2H), 2.47–2.39 (m, 2H), 1.72–1.61 (m, 4H), 1.08 (t, J = 7.1 Hz, 3H). ^{13}C NMR (126 MHz, DMSO-d_6) δ 171.3, 165.1, 156.1, 148.2, 148.2, 129.7, 129.3, 119.0, 117.2, 111.2, 110.3, 108.6, 62.1, 55.0, 55.0, 33.1, 25.3, 23.6, 22.2, 22.0, 14.6. HRMS-ESI (m/z): [M+H]$^+$ calculated for C$_{21}$H$_{27}$O$_5$N$_2$S, 419.1635; found, 419.1635.

2-((3-(Ethylcarbamoyl)-4,5,6,7-tetrahydrobenzo[b]thiophen-2-yl)amino)-2-(thiophen-2-yl) acetic acid (**4p**)
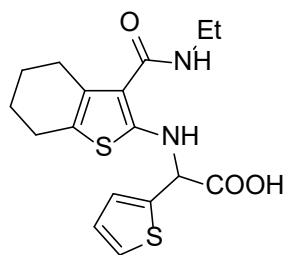
By using **2** (200.0 mg, 0.89 mmol), glyoxylic acid monohydrate (98.5 mg, 1.07 mmol), and 2-thiopheneboronic acid (136.9 mg, 1.07 mmol) according to general procedure 1 with a reaction time of 1h and subsequent washing with 60% ACN to give the desired product (244.4 mg, 75%). ^{1}H NMR (700 MHz, DMSO-d_6) δ 13.48 (s, 1H), 8.53 (d, J = 6.7 Hz, 1H), 7.48 (dd, J = 5.1 Hz, 1H), 7.15 (d, J = 3.3 Hz, 1H), 7.00 (dd, J = 5.1, 3.3 Hz, 1H), 6.86 (t, J = 5.6 Hz, 1H), 5.18 (d, J = 6.7 Hz, 1H), 3.24–3.20 (m, 2H), 2.66–2.55 (m, 2H), 2.47–2.42 (m, 2H), 1.75–1.59 (m, 4H), 1.08 (t, J = 7.2 Hz, 3H). ^{13}C NMR (126 MHz, DMSO-d_6) δ 170.3, 165.0, 155.6, 140.4, 129.8, 126.5, 126.4, 125.8, 117.6, 109.2, 58.4, 33.1, 25.3, 23.5, 22.2, 21.9, 14.6. HRMS-ESI (m/z): [M+H]$^+$ calculated for C$_{17}$H$_{21}$O$_3$N$_2$S$_2$, 365.0988; found, 365.0990.

(E)-2-((3-(Ethoxycarbonyl)-4,5,6,7-tetrahydrobenzo[b]thiophen-2-yl)amino)-4-phenylbut-3-enoic acid (**4q**)
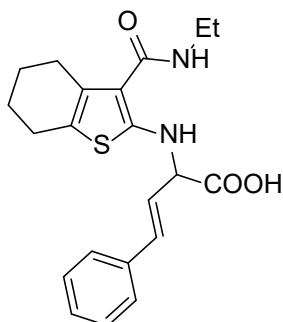
By using **2** (200.0 mg, 0.89 mmol), glyoxylic acid monohydrate (98.5 mg, 1.07 mmol), and trans-2-phenylvinylboronic acid (158.3 mg, 1.07 mmol) according to general procedure 1 with a reaction time of 40 min and subsequent washing with 60% ACN to give the desired product (212.9 mg, 62%). ^{1}H NMR (700 MHz, DMSO-d_6) δ 13.30 (s, 1H), 8.31 (d, J = 6.9 Hz, 1H), 7.46 (d, J = 7.7 Hz, 2H), 7.33 (t, J = 7.7 Hz, 2H), 7.26 (t, J = 7.7 Hz, 1H), 6.84 (t, J = 5.7 Hz, 1H), 6.70 (d, J = 15.8 Hz, 1H), 6.31 (dd, J = 15.8, 6.8 Hz, 1H), 4.52–4.51 (m, 1H), 3.25–3.21 (m, 2H), 2.67–2.58 (m, 2H), 2.48–2.46 (m, 2H), 1.74–1.62 (m, 4H), 1.09 (t, J = 7.2 Hz, 3H). ^{13}C NMR (176 MHz, DMSO-d_6) δ 171.0, 165.2, 156.4, 135.3, 132.5, 130.1, 128.3 (2), 127.7, 126.2 (2), 124.6, 117.0, 108.6, 61.1, 33.2, 25.5, 23.7, 22.3, 22.1, 14.7. HRMS-ESI (m/z): [M+H]$^+$ calculated for $C_{21}H_{25}O_3N_2S$, 385.1580; found, 385.1580.

2-((3-(Ethoxycarbonyl)-4,5,6,7-tetrahydrobenzo[b]thiophen-2-yl)amino)-2-phenylacetic acid (**5a**)
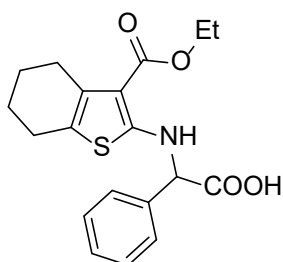
By using **3** (200.0 mg, 0.89 mmol), glyoxylic acid monohydrate (98.1 mg, 1.07 mmol), and phenylboronic acid (129.9 mg, 1.07 mmol) according to general procedure 1 and a reaction time of 1 h and subsequent washing with 60% ACN to give the desired product (233.6 mg, 73%). ^{1}H NMR (700 MHz, DMSO-d_6) δ 13.50 (s, 1H), 8.70 (d, J = 6.2 Hz, 1H), 7.42–7.35 (m, 4H), 7.32 (t, J = 6.7 Hz, 1H), 5.00 (d, J = 6.2 Hz, 1H), 4.20 (q, J = 7.1 Hz, 2H), 2.66–2.56 (m, 2H), 2.43–2.32 (m, 2H), 1.69–1.57 (m, 4H), 1.28 (t, J = 7.1 Hz, 3H). ^{13}C NMR (176 MHz, DMSO-d_6) δ 170.8, 164.9, 160.4, 136.6, 131.6, 128.4 (2), 128.0, 126.9 (2), 116.8, 102.9, 62.0, 58.7, 26.0, 23.5, 22.3, 21.9, 13.9. LCMS-ESI (m/z): [M+H]$^+$ calculated for $C_{19}H_{22}O_4NS$, 360.1; found, 360.0.

2-((3-(Ethoxycarbonyl)-4,5,6,7-tetrahydrobenzo[b]thiophen-2-yl)amino)-2-(p-tolyl)acetic acid (**5b**)
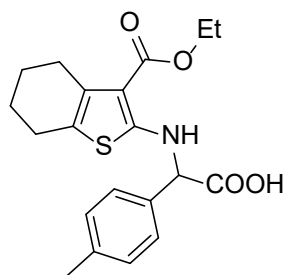
By using **3** (200.0 mg, 0.89 mmol), glyoxylic acid monohydrate (98.1 mg, 1.07 mmol), and 4-tolylboronic acid (144.8 mg, 1.07 mmol) according to general procedure 1 with a reaction time of 1 h and subsequent washing with 60% ACN to give the desired product (240.9 mg, 73%). ^{1}H NMR (700 MHz, DMSO-d_6) δ 13.43 (s, 1H), 8.67 (d, J = 6.2 Hz, 1H), 7.27 (d, J = 7.7 Hz, 2H), 7.18 (d, J = 7.7 Hz, 2H), 4.94 (d, J = 6.2 Hz, 1H), 4.20 (q, J = 7.1 Hz, 2H), 2.66–2.55 (m, 2H), 2.43–2.33 (m, 2H), 2.28 (s, 3H), 1.70–1.55 (m, 4H), 1.28 (t, J = 7.1 Hz, 3H). ^{13}C NMR (176 MHz, DMSO-d_6) δ 171.8, 165.7, 161.3, 138.2, 134.4, 132.4, 129.8 (2), 127.6 (2), 117.6, 103.7, 62.6, 59.5, 26.8, 24.3, 23.2, 22.8, 21.2, 14.8. HRMS-ESI (m/z): [M+H]$^+$ calculated for $C_{20}H_{24}O_4NS$, 374.1421; found, 374.1422.

2-(3,4-Dimethoxyphenyl)-2-((3-(ethoxycarbonyl)-4,5,6,7-tetrahydrobenzo[b]thiophen-2-yl) amino)acetic acid (**5c**)
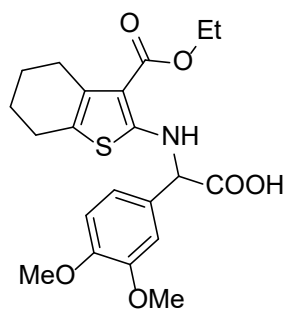
By using **3** (200.0 mg, 0.89 mmol), glyoxylic acid monohydrate (98.1 mg, 1.07 mmol), and 3,4-dimethoxyphenylboronic acid (193.8 mg, 1.07 mmol) according to general procedure 1 with a reaction time of 3 h and subsequent washing with 60% ACN to give the desired product (306.2 mg, 82%). ^{1}H NMR (700 MHz, DMSO-d_6) δ 13.37 (s, 1H), 8.63 (d, J = 6.1 Hz, 1H), 6.98–6.88 (m, 3H), 4.91 (d, J = 6.1 Hz, 1H), 4.20 (q, J = 7.1 Hz, 2H), 3.73 (s, 3H), 3.72 (s, 3H), 2.65–2.57 (m, 2H), 2.42–2.35 (m, 2H), 1.68–1.58 (m, 4H), 1.27 (t, J = 7.1 Hz, 3H). ^{13}C NMR (176 MHz, DMSO-d_6) δ 171.0, 164.9, 160.6, 148.5, 148.4, 131.5, 128.7, 119.1, 116.9, 111.5, 110.6, 103.0, 61.7, 58.7, 55.2, 55.1, 26.0, 23.5, 22.3, 21.9, 13.9. HRMS-ESI (m/z): [M+H]$^+$ calculated for $C_{21}H_{26}O_6NS$, 420.1475; found, 420.1474.

2-((3-(Ethoxycarbonyl)-4,5,6,7-tetrahydrobenzo[b]thiophen-2-yl)amino)-2-(4-hydroxyphenyl) acetic acid (**5d**)

By using **3** (200.0 mg, 0.89 mmol), glyoxylic acid monohydrate (98.1 mg, 1.07 mmol), and 4-hydroxyphenylboronic acid (146.9 mg, 1.07 mmol) according to general procedure 1 with a reaction time of 1.5 h and subsequent washing with 60% ACN to give the desired product (282.5 mg, 85%). ^{1}H NMR (700 MHz, DMSO-d_6) δ 13.32 (s, 1H),

9.54 (s, 1H), 8.63 (d, J = 6.1 Hz, 1H), 7.19 (d, J = 8.3 Hz, 2H), 6.76 (d, J = 8.3 Hz, 2H), 4.86 (d, J = 6.1 Hz, 1H), 4.20 (q, J = 7.1 Hz, 2H), 2.68–2.57 (m, 2H), 2.45–2.35 (m, 2H), 1.71–1.59 (m, 4H), 1.28 (t, J = 7.1 Hz, 3H). ^{13}C NMR (176 MHz, DMSO-d_6) δ 171.2, 164.9, 160.6, 157.1, 131.5, 128.1 (2), 126.5, 116.7, 115.2 (2), 102.7, 61.5, 58.7, 26.0, 23.5, 22.3, 21.9, 13.9. HRMS-ESI (m/z): [M+H]$^+$ calculated for $C_{19}H_{22}O_5NS$, 376.1213; found, 376.1214.

2-((3-(Ethoxycarbonyl)-4,5,6,7-tetrahydrobenzo[b]thiophen-2-yl)amino)-2-(4-methoxyphenyl) acetic acid (**5f**)

By using **3** (200.0 mg, 0.89 mmol), glyoxylic acid monohydrate (98.1 mg, 1.07 mmol), and 4-methoxyphenylboronic acid (161.9 mg, 1.07 mmol) according to general procedure 1 with a reaction time of 1 h and subsequent washing with 60% ACN to give the desired product (264.6 mg, 77%). ^{1}H NMR (700 MHz, DMSO-d_6) δ 13.40 (s, 1H), 8.65 (d, J = 6.1 Hz, 1H), 7.30 (d, J = 8.4 Hz, 2H), 6.93 (d, J = 8.4 Hz, 2H), 4.93 (d, J = 6.1 Hz, 1H), 4.19 (q, J = 7.1 Hz, 2H), 3.73 (s, 3H), 2.67–2.54 (m, 2H), 2.44–2.33 (m, 2H), 1.71–1.55 (m, 4H), 1.27 (t, J = 7.1 Hz, 3H). ^{13}C NMR (176 MHz, DMSO-d_6) δ 171.1, 164.9, 160.4, 158.9, 131.6, 128.3, 128.1 (2), 116.8, 113.8 (2), 102.8, 61.4, 58.7, 54.8, 26.0, 23.5, 22.3, 21.9, 13.9. HRMS-ESI (m/z): [M+H]$^+$ calculated for $C_{20}H_{24}O_5NS$, 390.1370; found, 390.1371.

2-((3-(Ethoxycarbonyl)-4,5,6,7-tetrahydrobenzo[b]thiophen-2-yl)amino)-2-(thiophen-2-yl) acetic acid (**5l**)
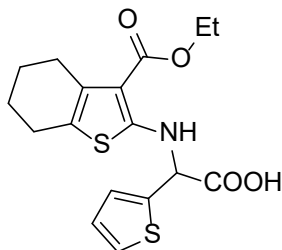
By using **3** (200.0 mg, 0.89 mmol), glyoxylic acid monohydrate (98.1 mg, 1.07 mmol), and 2-thiopheneboronic acid (136.3 mg, 1.07 mmol) according to general procedure 1 with a reaction time of 1 h the reaction was performed. The solvent was evaporated after completion and the crude was purified by preparative chromatography to give the desired product (67.4 mg, 21%). ^{1}H NMR (400 MHz, DMSO-d_6) δ 13.69 (s, 1H), 8.60 (d, J = 6.1 Hz, 1H), 7.49 (dd, J = 5.1, 1.3 Hz, 1H), 7.19 (ddd, J = 3.5, 1.3 Hz, 1H), 7.01 (dd, J = 5.1, 3.5 Hz, 1H), 5.31 (d, J = 6.1 Hz, 1H), 4.19 (q, J = 7.1 Hz, 2H), 2.65–2.59 (m, 2H), 2.44–2.38 (m, 2H), 1.71–1.59 (m, 4H), 1.27 (t, J = 7.1 Hz, 3H). LCMS-ESI (m/z): [M+H]$^+$ calculated for $C_{17}H_{20}O_4NS_2$, 366.1; found, 366.0.

(E)-2-((3-(Ethoxycarbonyl)-4,5,6,7-tetrahydrobenzo[b]thiophen-2-yl)amino)-4-phenylbut-3-enoic acid (**5m**)

By using **3** (200.0 mg, 0.89 mmol), glyoxylic acid monohydrate (98.1 mg, 1.07 mmol), and trans-2-phenylvinylboronic acid (157.6 mg, 1.07 mmol) according to general procedure 1 with a reaction time of 40 min and subsequent washing with 60% ACN to give the desired product (110.6 mg, 32%). ^{1}H NMR (700 MHz, DMSO-d_6) δ 13.53 (s, 1H), 8.40 (d, J = 6.3 Hz, 1H), 7.48 (d, J = 7.6 Hz, 2H), 7.33 (t, J = 7.6 Hz, 2H), 7.27 (t, J = 7.6 Hz, 1H), 6.73 (d, J = 15.8 Hz, 1H), 6.32 (dd, J = 15.8, 7.0 Hz, 1H), 4.64–4.63 (m, 1H), 4.20 (q, J = 7.1 Hz, 2H), 2.68–2.60 (m, 2H), 2.47–2.41 (m, 2H), 1.71–1.59 (m, 4H), 1.28 (t, J = 7.1 Hz, 3H). ^{13}C NMR (176 MHz, DMSO-d_6) δ 170.6, 164.9, 160.9, 135.2, 133.1, 131.7, 128.3 (2), 127.8, 126.3 (2), 123.8, 116.7, 102.9, 60.7, 58.7, 26.1, 23.6, 22.4, 22.0, 13.9. HRMS-ESI (m/z): [M+H]$^+$ calculated for $C_{21}H_{24}O_4NS$, 386.1421; found, 386.1423.

Ethyl 2-((2-hydroxy-1-(4-hydroxyphenyl)ethyl)amino)-4,5,6,7-tetrahydrobenzo[b]thiophene-3-carboxylate (**6a**)

By using **3** (100.0 mg, 0.44 mmol), 1,4-dioxane-2,5-diol (31.9 mg, 0.27 mmol), and 4-hydroxyphenylboronic acid (73.5 mg, 0.53 mmol) according to general procedure 1 with a reaction time of 5. The solvent was evaporated after completion and the crude was purified by preparative chromatography to give the desired product (104.2 mg, 65%). ^{1}H NMR (600 MHz, DMSO-d_6) δ 9.34 (s, 1H), 8.34 (d, J = 5.6 Hz, 1H), 7.09 (d, J = 8.5 Hz, 2H), 6.70 (d, J = 8.5 Hz, 2H), 5.20 (t, J = 5.2 Hz, 1H), 4.19–4.16 (m, 3H), 3.68–3.45 (m, 2H), 2.64–2.55 (m, 2H), 2.39–2.31 (m, 2H), 1.66–1.56 (m, 4H), 1.26 (t, J = 7.1 Hz, 3H). ^{13}C NMR (151 MHz, DMSO-d_6) δ 164.9, 162.9, 156.4, 131.2, 129.0, 127.7 (2), 116.1, 114.8 (2), 102.0, 65.2, 62.0, 58.4, 26.0, 23.5, 22.3, 21.9, 13.9. HRMS-ESI (m/z): [M+H]$^+$ calculated for $C_{19}H_{24}O_4NS$, 362.1421; found, 362.1422.

2-((3-(Ethoxycarbonyl)-4,5,6,7-tetrahydrobenzo[b]thiophen-2-yl)amino)-2-(4-hydroxyphenyl) propanoic acid (**6b**)
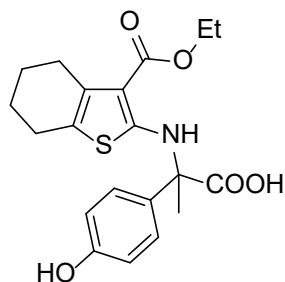
By using **3** (100.0 mg, 0.44 mmol), pyruvic acid (37.5 μl, 0.53 mmol), and 4-hydroxyphenylboronic acid (73.5 mg, 0.53 mmol) according to general procedure 1 with a reaction time of 2 h. The solvent was evaporated after completion and the crude was purified by preparative chromatography to give the desired product (80.4 mg, 47%). ^{1}H NMR (600 MHz, DMSO-d_6) δ 13.35 (s, 1H), 9.53 (s, 1H), 9.33 (s, 1H), 7.20 (d, J = 8.7 Hz, 2H), 6.73 (d, J = 8.7 Hz, 2H), 4.19 (q, J = 7.1 Hz, 2H), 2.63–2.54 (m, 2H), 2.35–2.23 (m, 2H), 1.88 (s, 3H), 1.65–1.55 (m, 4H), 1.27 (t, J = 7.1 Hz, 3H). ^{13}C NMR (151 MHz, DMSO-d_6) δ 174.2, 164.9, 158.5, 156.7, 130.5, 128.7, 127.9 (2), 117.2, 115.0 (2), 103.6, 62.7, 58.6, 26.0, 23.3, 22.3, 22.0, 20.5, 13.9. HRMS-ESI (m/z): [M+H]$^+$ calculated for C$_{20}$H$_{24}$O$_5$NS, 390.1370; found, 390.1370.

Ethyl 2-((2-ethoxy-1-(4-hydroxyphenyl)-2-oxoethyl)amino)-4,5,6,7-tetrahydrobenzo[b] thiophene-3-carboxylate (**6c**)
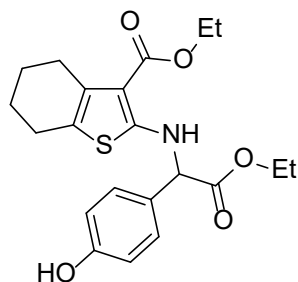
By using **3** (200.0 mg, 0.89 mmol), ethyl glyoxalate (0.21 mL, 1.07 mmol), and 4-hydroxyphenylboronic acid (146.9 mg, 1.07 mmol) according to general procedure 1 with a reaction time of 12 h. After completion, the solvent was evaporated and the crude was purified by preparative chromatography to give the desired product (78.5 mg, 22%). ^{1}H NMR (500 MHz, DMSO-d_6) δ 9.60 (s, 1H), 8.55 (d, J = 6.5 Hz, 1H), 7.18 (d, J = 8.6 Hz, 2H), 6.75 (d, J = 8.6 Hz, 2H), 4.96 (d, J = 6.5 Hz, 1H), 4.30–3.94 (m, 4H), 2.70–2.55 (m, 2H), 2.45–2.31 (m, 2H), 1.74–1.51 (m, 4H), 1.26 (t, J = 7.1 Hz, 3H), 1.11 (t, J = 7.1 Hz, 3H). ^{13}C NMR (126 MHz, DMSO-d_6) δ 169.8, 164.8, 160.3, 157.2, 131.5, 128.0 (2), 125.8, 116.9, 115.2 (2), 102.9, 61.4, 61.1, 58.7, 25.9, 23.4, 22.2, 21.8, 13.8, 13.4. HRMS-ESI (m/z): [M+H]$^+$ calculated for C$_{21}$H$_{26}$O$_5$NS, 404.1526; found, 404.1525.

Ethyl   2-((1-(4-hydroxyphenyl)-2-oxopropyl)amino)-4,5,6,7-tetrahydrobenzo[b]thiophene-3-carboxylate (**6d**)
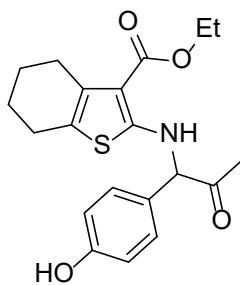
By using **3** (100.0 mg, 0.44 mmol), pyruvic aldehyde (35–45 % in H$_2$O, 91.4 µL, 0.53 mmol), and 4-hydroxyphenylboronic acid (73.5 mg, 0.53 mmol) according to general procedure 1 with a reaction time of 14 h. After completion, the solvent was evaporated and the crude was purified by preparative chromatography and subsequent washing with 60% ACN to give the desired product (14.0 mg, 8%). ^{1}H NMR (500 MHz, CD$_3$OD) δ 8.77 (d, *J* = 8.6 Hz, 2H), 8.35 (d, *J* = 8.6 Hz, 2H), 6.60 (s, 1H), 5.81 (q, *J* = 7.1 Hz, 2H), 4.28–4.15 (m, 2H), 4.03–3.93 (m, 2H), 3.63 (s, 3H), 3.26 (m, 4H), 2.93 (t, *J* = 7.1 Hz, 3H). ^{13}C NMR (126 MHz, CD$_3$OD) δ 203.7, 167.1, 162.6, 158.7, 133.1, 130.1 (2), 127.5, 118.3, 116.4 (2), 104.0, 70.0, 60.0, 27.4, 25.9, 24.8, 23.8, 23.5, 14.3. HRMS-ESI (m/z): [M+H]$^+$ calculated for C$_{20}$H$_{24}$O$_4$NS, 374.1421; found, 374.1421.

Ethyl 2-((2-(4-fluorophenyl)-1-(4-hydroxyphenyl)-2-oxoethyl)amino)-4,5,6,7-tetrahydrobenzo[b]thiophene-3-carboxylate (**6e**)
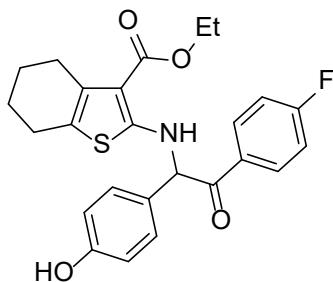
By using **3** (100.0 mg, 0.44 mmol), (4-fluorophenyl)(oxo)acetaldehyde monohydrate (92.1 mg, 0.53 mmol), and 4-hydroxyphenylboronic acid (73.5 mg, 0.53 mmol) according to general procedure 1 with a reaction time of 2 h. After completion, the solvent was evaporated and the crude was purified by preparative chromatography to give the desired product (59.3 mg, 29%). ^{1}H NMR (700 MHz, DMSO-d_6) δ 9.55 (s, 1H), 8.92 (d, *J* = 6.5 Hz, 1H), 8.18–8.16 (m, 2H), 7.32–7.30 (m, 2H), 7.24 (d, *J* = 8.0 Hz, 2H), 6.68 (d, *J* = 8.0 Hz, 2H), 6.13 (d, *J* = 6.5 Hz, 1H), 4.20 (q, *J* = 7.1 Hz, 2H), 2.66–2.55 (m, 2H), 2.45–2.36 (m, 2H), 1.71–1.56 (m, 4H), 1.29 (t, *J* = 7.1 Hz, 3H). ^{13}C NMR (176 MHz, DMSO-d_6) δ 193.5, 165.6 and 164.1 (d, $^1J$$_{C.F}$ = 252 Hz), 164.8, 160.6, 157.2, 131.7 and 131.7 (d, $^3J$$_{C.F}$ = 10 Hz), 131.6, 130.3 and 130.3 (d, $^4J$$_{C.F}$ = 2 Hz),, 129.3 (2), 125.8, 116.6, 115.6 and 115.5 (d, $^2J$$_{C.F}$ = 22 Hz), 115.4 (2), 102.8, 63.5, 58.7, 26.0, 23.6, 22.4, 21.9, 14.0. HRMS-ESI (m/z): [M+H]$^+$ calculated for C$_{25}$H$_{25}$O$_4$NFS, 454.1483; found, 454.1480.

Ethyl 2-((1-(4-hydroxyphenyl)-2-(3-methoxyphenyl)-2-oxoethyl)amino)-4,5,6,7-tetrahydro benzo[b]thiophene-3-carboxylate (**6f**)
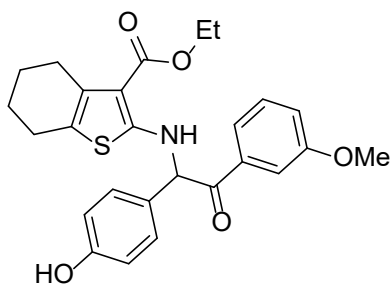
By using **3** (100.0 mg, 0.44 mmol), 2-(3-methoxyphenyl)-2-oxoacetaldehyde monohydrate (97.0 mg, 0.53 mmol), and 4-hydroxyphenylboronic acid (73.5 mg, 0.53 mmol) according to general procedure 1 with a reaction time of 3 h. After completion solvent was evaporated and the crude was purified by preparative chromatography to give the desired product (36.4 mg, 18%). ^{1}H NMR (700 MHz, DMSO-d_6) δ 9.56 (s, 1H), 8.92 (d, J = 6.5 Hz, 1H), 7.69 (d, J = 8.0 Hz, 1H), 7.53 (s, 1H), 7.41 (t, J = 8.0 Hz, 1H), 7.25 (d, J = 8.3 Hz, 2H), 7.18 (d, J = 8.0 Hz, 1H), 6.69 (d, J = 8.3 Hz, 2H), 6.14 (d, J = 6.5 Hz, 1H), 4.22 (q, J = 7.1 Hz, 2H), 3.80 (s, 3H), 2.69–2.57 (m, 2H), 2.47–2.38 (m, 2H), 1.72–1.56 (m, 4H), 1.31 (t, J = 7.1 Hz, 3H). ^{13}C NMR (176 MHz, DMSO-d_6) δ 194.7, 164.8, 160.6, 159.0, 157.1, 135.0, 131.6, 129.6, 129.3 (2), 125.8, 121.0, 119.4, 116.6, 115.4 (2), 113.1, 102.8, 63.6, 58.7, 55.0, 26.0, 23.6, 22.4, 21.9, 14.0. LCMS-ESI (m/z): [M+H]$^+$ calculated for $C_{26}H_{28}O_5NS$, 466.2; found, 466.0.

Ethyl 2-(((4-hydroxyphenyl)(4-nitrophenyl)methyl)amino)-4,5,6,7-tetrahydrobenzo[b] thio phene-3-carboxylate (**6h**)
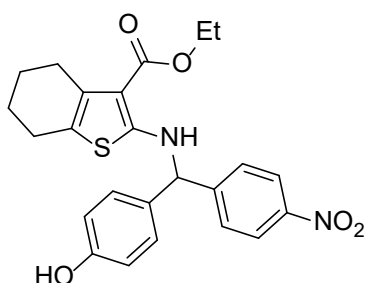
By using **3** (100.0 mg, 0.44 mmol), 4-nitrobenzaldehyde (80.5 mg, 0.53 mmol), and 4-hydroxyphenylboronic acid (73.5 mg, 0.53 mmol) according to general procedure 1 reaction mixture was refluxed with a reaction time of 2 h. After completion, the solvent was evaporated and the crude was purified by preparative chromatography to give the desired product (26.8 mg, 13%). ^{1}H NMR (700 MHz, DMSO-d_6) δ 9.55 (s, 1H), 8.37 (d, J = 6.0 Hz, 1H), 8.22 (d, J = 8.3 Hz, 2H), 7.65 (d, J = 8.3 Hz, 2H), 7.18 (d, J = 8.1 Hz, 2H), 6.75 (d, J = 8.1 Hz, 2H), 5.65 (d, J = 6.0 Hz, 1H), 4.17 (q, J = 7.1 Hz, 2H), 2.67–2.60 (m, 2H), 2.42–2.34 (m, 2H), 1.72–1.57 (m, 4H), 1.24 (t, J = 7.1 Hz, 3H). ^{13}C NMR (176 MHz, DMSO-d_6) δ 165.3, 161.5, 156.9, 149.2, 146.4, 131.5, 130.5, 127.9 (2), 127.6 (2), 123.7 (2), 117.2, 115.4 (2), 103.0, 62.9, 58.9, 26.0, 23.5, 22.3, 21.9, 13.9. HRMS-ESI (m/z): [M+H]$^+$ calculated for $C_{26}H_{28}O_5NS$, 466.1683; found, 466.1679.

2-((3-Carbamoyl-4,5-dimethylthiophen-2-yl)amino)-2-(4-hydroxyphenyl)acetic acid (**9**)
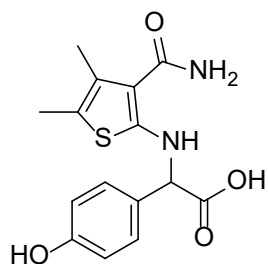
By using **8** (1.3 g, 7.6 mmol), glyoxylic acid monohydrate (0.8 g, 9.2 mmol), and 4-hydroxyphenyl boronic acid (1.3 g, 9.2 mmol) according to general procedure 1 with a reaction time of 2 h and subsequent washing with 60% ACN to give the desired product (1.60 g, 5.0 mmol, 65%). ^{1}H NMR (500 MHz, DMSO-d_6) δ 13.09 (s, 1H), 9.51 (s, 1H), 8.61 (d, J = 6.5 Hz, 1H), 7.16 (d, J = 8.5 Hz, 2H), 6.78 (s, 2H), 6.72 (d, J = 8.5 Hz, 2H), 4.73 (d, J = 6.5 Hz, 1H), 2.10 (s, 3H), 2.05 (s, 3H). ^{13}C NMR (126 MHz, DMSO-d_6) δ 171.4, 167.6, 156.9, 156.1, 128.0 (2), 127.9, 127.1, 114.9 (2), 113.2, 109.3, 61.7, 13.6, 11.7.

General Procedure 2

The Petasis product (0.28 mmol, 1 equiv.) was dissolved in THF (1.9 mM) to give a clear reaction mixture. To the reaction mixture, was added EDC·HCl (0.34 mmol, 1.2 equiv.) and stirred at room temperature overnight. The solvent was evaporated under reduced pressure and the resulting solid was redissolved in ethyl acetate. The excessive EDC and urea were removed by washing with H_2O. The organic phase was collected and dried with $MgSO_4$. The crude was purified by flash chromatography.

4-Ethyl-2-(4-hydroxyphenyl)-1,2,6,7,8,9-hexahydro-3H-benzo[4,5]thieno[2,3-e][1,4] diazepine-3,5(4H)-dione (**7a**)
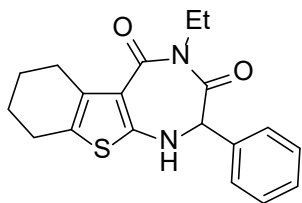
By using general procedure 2 with **4a** (100.0 mg, 0.28 mmol) and EDC·HCl (64.2 mg, 0.34 mmol) to give the desired product (78.0 mg, 75%). ^{1}H NMR (600 MHz, CDCl$_3$) δ 7.44–7.36 (m, 3H), 7.34–7.30 (m, 2H), 5.20 (d, J = 3.3 Hz, 1H), 4.84 (d, J = 3.3 Hz, 1H), 4.01–3.96 (m, 1H), 3.92–3.87 (m, 1H), 2.90–2.78 (m, 2H), 2.61–2.47 (m, 2H), 1.86–1.65 (m, 4H), 1.24 (t, J = 7.0 Hz, 3H). ^{13}C NMR (151 MHz, CDCl$_3$) δ 167.9, 163.9, 157.5, 136.0, 134.8, 128.9, 128.9 (2), 128.0 (2), 121.7, 114.4, 66.4, 40.9, 27.8, 24.8, 22.8, 22.6, 13.7. HRMS-ESI (m/z): [M+H]$^+$ calculated for C$_{19}$H$_{21}$O$_2$N$_2$S, 341.1318; found, 341.1319.

4-Ethyl-2-(p-tolyl)-1,2,6,7,8,9-hexahydro-3H-benzo[4,5]thieno[2,3-e][1,4]diazepine-3,5(4H)-dione (**7b**)
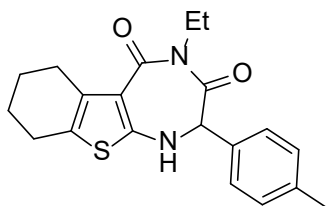
By using general procedure 2 with **4f** (50.0 mg, 0.13 mmol) and EDC·HCl (30.9 mg, 0.16 mmol) to give the desired product (35.6 mg, 75%). ^{1}H NMR (700 MHz, CDCl$_3$) δ 7.21 (s, 4H), 5.18 (d, *J* = 3.2 Hz, 1H), 4.79 (d, *J* = 3.2 Hz, 1H), 4.00–3.95 (m, 1H), 3.91–3.86 (m, 1H), 2.91–2.81 (m, 2H), 2.58–2.47 (m, 2H), 2.36 (s, 3H), 1.85–1.65 (m, 4H), 1.23 (t, *J* = 7.0 Hz, 3H). ^{13}C NMR (176 MHz, CDCl$_3$) δ 168.0, 164.1, 157.6, 138.9, 136.0, 131.8, 129.6 (2), 128.0 (2), 121.6, 114.3, 66.2, 40.9, 27.8, 24.8, 22.9, 22.6, 21.2, 13.8. HRMS-ESI (m/z): [M+H]$^+$ calculated for C$_{20}$H$_{23}$O$_2$N$_2$S, 355.1475; found, 355.1476.

4-Ethyl-2-(4-methoxyphenyl)-1,2,6,7,8,9-hexahydro-3H-benzo[4,5]thieno[2,3-e][1,4] diazepine-3,5(4H)-dione (**7c**)
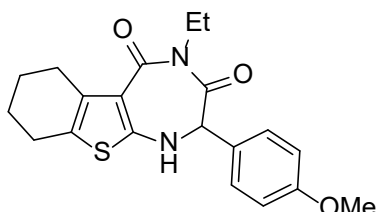
By using general procedure 2 with **4e** (100.0 mg, 0.26 mmol) and EDC·HCl (59.2 mg, 0.31 mmol) to give the desired product (84.2 mg, 88%). ^{1}H NMR (700 MHz, CDCl$_3$) δ 7.25 (d, *J* = 8.6 Hz, 2H), 6.92 (d, *J* = 8.6 Hz, 2H), 5.13 (d, *J* = 2.2 Hz, 1H), 4.75 (d, *J* = 2.2 Hz, 1H), 4.00–3.96 (m, 1H), 3.90–3.85 (m, 1H) 3.81 (s, 3H), 2.91–2.81 (m, 2H), 2.59–2.46 (m, 2H), 1.85–1.66 (m, 4H), 1.23 (t, *J* = 7.0 Hz, 3H). ^{13}C NMR (176 MHz, CDCl$_3$) δ 168.0, 164.1, 160.0, 157.6, 136.0, 129.5 (2), 126.9, 121.6, 114.3 (3), 65.9, 55.3, 40.9, 27.8, 24.8, 22.9, 22.6, 13.8. HRMS-ESI (m/z): [M+H]$^+$ calculated for C$_{20}$H$_{23}$O$_3$N$_2$S, 371.1424; found, 371.1425.

2-(3,4-Dimethoxyphenyl)-4-ethyl-1,2,6,7,8,9-hexahydro-3H-benzo[4,5]thieno[2,3-e][1,4] diazepine-3,5(4H)-dione (**7d**)
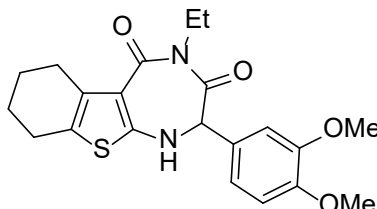
By using general procedure 2 with **4k** (100.0 mg, 0.24 mmol) and EDC·HCl (55.0 mg, 0.29 mmol) to give the desired product (53.9 mg, 56%). ^{1}H NMR (700 MHz, CDCl$_3$) δ 7.03–6.73 (m, 3H), 5.21 (d, *J* = 3.2 Hz, 1H), 4.80 (d, *J* = 3.2 Hz, 1H), 4.01–3.95 (m, 1H), 3.92–3.89 (m, 1H), 3.88 (s, 3H), 3.86 (s, 3H), 2.91–2.80 (m, 2H), 2.59–2.46 (m, 2H), 1.84–1.67 (m, 4H), 1.24 (t, *J* = 7.0 Hz, 3H). ^{13}C NMR (176 MHz, CDCl$_3$) δ 168.1, 164.0, 157.4, 149.4, 149.2, 136.0, 127.1, 121.7, 120.7, 114.5, 111.2, 111.0, 66.1, 55.9 (2), 40.9, 27.8, 24.8, 22.9, 22.6, 13.8. HRMS-ESI (m/z): [M+H]$^+$ calculated for C$_{21}$H$_{25}$O$_4$N$_2$S, 401.1530; found, 401.1528.

4-Ethyl-2-(4-hydroxyphenyl)-1,2,6,7,8,9-hexahydro-3H-benzo[4,5]thieno[2,3-e][1,4] diazepine-3,5(4H)-dione (**7e**)
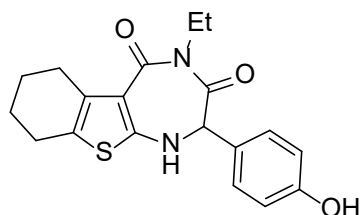
By using general procedure 2 with **4i** (100.0 mg, 0.27 mmol) and EDC·HCl (61.4 mg, 0.32 mmol) to give the desired product (81.3 mg, 85%). ^{1}H NMR (600 MHz, CDCl$_3$) δ 7.16 (d, *J* = 8.5 Hz, 2H), 6.78 (d, *J* = 8.5 Hz, 2H), 5.56 (s, 1H), 5.19 (s, 1H), 4.75 (s, 1H), 4.02–3.96 (m, 1H), 3.91–3.86 (m, 1H), 2.91–2.79 (m, 2H), 2.59–2.47 (m, 2H), 1.86–1.66 (m, 4H), 1.24 (t, *J* = 7.0 Hz, 3H). ^{13}C NMR (151 MHz, CDCl$_3$) δ 168.2, 164.2, 157.8, 156.3, 135.8, 129.5 (2), 126.6, 121.7, 115.9 (2), 114.2, 65.8, 41.0, 27.7, 24.8, 22.8, 22.6, 13.8. HRMS-ESI (m/z): [M+H]$^+$ calculated for C$_{19}$H$_{21}$O$_3$N$_2$S, 357.1267; found, 357.1268.

4-Ethyl-2-(3-hydroxyphenyl)-1,2,6,7,8,9-hexahydro-3H-benzo[4,5]thieno[2,3-e][1,4] diazepine-3,5(4H)-dione (**7f**)
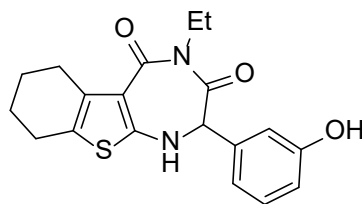
By using general procedure 2 with **4b** (30.0 mg, 0.08 mmol) and EDC·HCl (18.4 mg, 0.10 mmol) to give the desired product (17.4 mg, 61%). ^{1}H NMR (600 MHz, CDCl$_3$) δ 7.23 (t, *J* = 7.7 Hz, 1H), 6.83 (d, *J* = 7.7 Hz, 1H), 6.82–6.77 (m, 2H), 5.35 (s, 1H), 4.80 (s, 1H), 4.00–3.95 (m, 1H), 3.92–3.87 (m, 1H), 2.88–2.78 (m, 2H), 2.59–2.46 (m, 2H), 1.84–1.67 (m, 4H), 1.24 (t, *J* = 7.0 Hz, 3H). ^{13}C NMR (151 MHz, CDCl$_3$) δ 168.1, 164.0, 157.6, 156.2, 136.1, 135.9, 130.1, 121.8, 120.1, 116.2, 114.8, 114.3, 66.0, 41.0, 27.7, 24.8, 22.8, 22.6, 13.7. HRMS-ESI (m/z): [M+H]$^+$ calculated for C$_{19}$H$_{21}$O$_3$N$_2$S, 357.1267; found, 357.1268.

4-Ethyl-2-(thiophen-2-yl)-1,2,6,7,8,9-hexahydro-3H-benzo[4,5]thieno[2,3-e][1,4]diazepine-3,5(4H)-dione (**7g**)
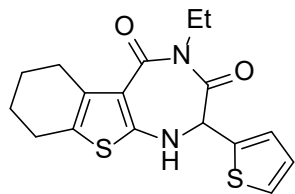
By using general procedure 2 with **4p** (100.0 mg, 0.27 mmol) and EDC·HCl (63.1 mg, 0.33 mmol) to give the desired product (67.6 mg, 71%). ^{1}H NMR (700 MHz, CDCl$_3$) δ 7.39 (d, *J* = 5.0 Hz, 1H), 7.09 (d, *J* = 3.5 Hz, 1H), 7.01 (dd, *J* = 5.0, 3.5 Hz, 1H), 5.19 (s, 1H), 5.18 (s, 1H), 4.03–3.98 (m, 1H), 3.93–3.88 (m, 1H), 2.92–2.80 (m, 2H), 2.60–2.47 (m, 2H), 1.84–1.68 (m, 4H), 1.25 (t, *J* = 7.0 Hz, 3H). ^{13}C NMR (176 MHz, CDCl$_3$) δ 166.9, 163.8, 156.6, 136.1, 136.0, 128.2, 127.5, 126.6, 122.1, 114.7, 61.8, 41.0, 27.8, 24.8, 22.9, 22.6, 13.8. HRMS-ESI (m/z): [M+H]$^+$ calculated for C$_{17}$H$_{19}$O$_2$N$_2$S$_2$, 347.0883; found, 347.0884.

(E)-4-Ethyl-2-styryl-1,2,6,7,8,9-hexahydro-3H-benzo[4,5]thieno[2,3-e][1,4]diazepine-3,5 (4H)-dione (**7h**)
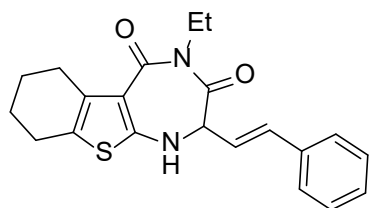
By using general procedure 2 with **4q** (100.0 mg, 0.26 mmol) and EDC·HCl (59.8 mg, 0.31 mmol) to give a desired product (67.8 mg, 71%). ^{1}H NMR (700 MHz, CDCl$_3$) δ 7.41 (d, *J* = 7.4 Hz, 2H), 7.34 (t, *J* = 7.4 Hz, 2H), 7.29 (t, *J* = 7.4 Hz, 1H), 6.69 (d, *J* = 16.1 Hz, 1H), 6.60 (dd, *J* = 16.1, 7.3 Hz, 1H), 4.99 (d, *J* = 2.5 Hz, 1H), 4.42 (dd, *J* = 7.3, 2.5 Hz, 1H), 4.02–3.97 (m, 1H), 3.89–3.84 (m, 1H), 2.92–2.85 (m, 2H), 2.60–2.48 (m, 2H), 1.87–1.69 (m, 4H), 1.23 (t, *J* = 7.0 Hz, 3H). ^{13}C NMR (176 MHz, CDCl$_3$) δ 168.0, 164.0, 157.2, 136.5, 136.1, 135.5, 128.7 (2), 128.6, 126.8 (2), 122.0, 121.7, 114.3, 63.9, 40.5, 27.9, 24.8, 22.9, 22.7, 13.8. HRMS-ESI (m/z): [M+H]$^{+}$ calculated for C$_{21}$H$_{23}$O$_2$N$_2$S, 367.1475; found, 367.1475.

2-(4-Hydroxyphenyl)-6,7-dimethyl-1,2-dihydro-3H-thieno[2,3-e][1,4]diazepine-3,5(4H)-dione (**10**)
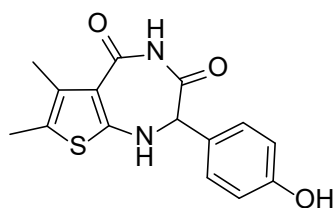
By using general procedure 2 with **9** (320.0 mg, 1.00 mmol) and EDC·HCl (230.0 mg, 1.20 mmol) to give the desired product (151.9 mg, 0.50 mmol, 50%). ^{1}H NMR (500 MHz, DMSO-d_6) δ 10.43 (s, 1H), 9.50 (s, 1H), 8.24 (d, *J* = 4.3 Hz, 1H), 7.04 (d, *J* = 8.6 Hz, 2H), 6.72 (d, *J* = 8.6 Hz, 2H), 4.86 (d, *J* = 4.3 Hz, 1H), 2.10 (s, 3H), 2.07 (s, 3H). ^{13}C NMR (126 MHz, DMSO) δ 169.0, 160.7, 158.2, 156.6, 131.3, 128.4 (2), 124.7, 116.6, 114.6 (2), 112.4, 62.9, 14.5, 11.5. HRMS-ESI (m/z): [M+H]$^{+}$ calculated for C$_{15}$H$_{15}$O$_3$N$_2$S, 303.0798; found, 303.0799.

5.1.2.2 SAR study of ATPCs

General procedure 3

The compounds were synthesized according to the previously reported method.[125] To a solution of NaH (60% in oil, 22.5 mmol, 1.1 equiv.) in 1,4-dioxane (1 M) was added the ethyl 4-chloroacetoacetate (20.0 mmol, 1.0 equiv.) and stirred for 30 min at room temperature. A solution of aryl isothiocyanate or aryl isocyanate (20.0 mmol, 1.0 equiv.) was added to the reaction mixture. The temperature was allowed to heat to 40 °C. After 2 h of stirring, the mixture was poured into a cold 1 M HCl aqueous solution and the solid precipitate was

collected, washed with H_2O, and recrystallized from ethanol to give the desired product. All derivatives were synthesized with the general method unless it is mentioned in detail.

Ethyl 4-oxo-2-(phenylamino)-4,5-dihydrothiophene-3-carboxylate (**11a**)
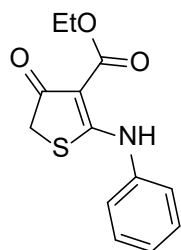
By using general procedure 3 with ethyl 4-chloroacetoacetate (30 mmol), NaH (33 mmol), and phenyl isothiocyanate (30 mmol) in dioxane (30 mL) to give the desired product (4.1 g, 16 mmol, 52%). ^{1}H NMR (400 MHz, CDCl$_3$): δ 11.49 (s, 1H), 7.47–7.43 (m, 2H), 7.37–7.32 (m, 3H), 4.41 (q, *J* = 7.08 Hz, 2H), 3.63 (s, 2H), 1.42 (t, *J* = 7.08 Hz, 3H).

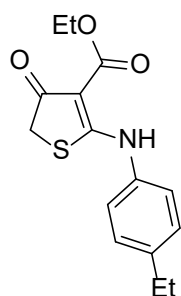*Ethyl 2-((4-methoxyphenyl)amino)-4-oxo-4,5-dihydrothiophene-3-carboxylate* (**11b**)
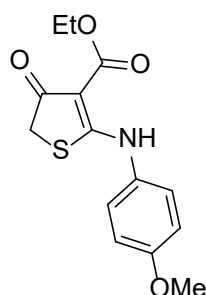
By using general procedure 3 with 4-methoxyphenyl isothiocyanate to give the desired product (677 mg, 2.3 mmol, 46%). ^{1}H NMR (400 MHz, CDCl$_3$) δ 11.21 (s, 1H), 7.27 (d, *J* = 9.2 Hz, 2H), 6.95 (d, *J* = 8.9 Hz, 2H), 4.37 (q, *J* = 7.2 Hz, 2H), 3.84 (s, 3H), 3.61 (s, 2H), 1.40 (t, *J* = 7.1 Hz, 3H).

Ethyl 2-((3-methoxyphenyl)amino)-4-oxo-4,5-dihydrothiophene-3-carboxylate (**11c**)
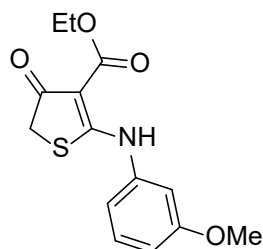
By using general procedure 3 with 3-methoxyphenyl isothiocyanate to give the desired product (619 mg, 2.1 mmol, 42%). ^{1}H NMR (400 MHz, CDCl$_3$) δ 11.50 (s, 1H), 7.34 (t, *J* = 8.0 Hz, 1H), 6.97–6.85 (m, 3H), 4.38 (q, *J* = 7.1 Hz, 2H), 3.83 (s, 3H), 3.64 (s, 2H), 1.40 (t, *J* = 7.1 Hz, 3H).

*Ethyl 2-((3,4-dimethoxyphenyl)amino)-4-oxo-4,5-dihydrothiophene-3-carboxylate* (**11d**)
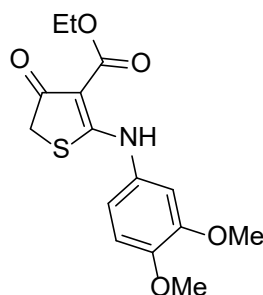
By using general procedure 3 with 3,4-dimethoxyphenyl isothiocyanate to give the desired product (530 mg, 1.6 mmol, 33%). ^{1}H NMR (700 MHz, CDCl$_3$) δ 11.13 (s, 1H), 7.35 (d, *J* = 8.7 Hz, 1H), 6.55 (d, *J* = 2.6 Hz, 1H), 6.50 (dd, *J* = 8.7, 2.6 Hz, 1H), 4.38 (q, *J* = 7.1 Hz, 2H), 3.87 (s, 3H), 3.84 (s, 3H), 3.63 (s, 2H), 1.40 (t, *J* = 7.1 Hz, 3H). ^{13}C NMR (176 MHz, CDCl$_3$) δ 191.2, 183.6, 166.4, 160.1, 154.0, 125.3, 119.3, 103.9, 99.5, 97.9, 60.3, 55.9, 55.6, 37.9, 14.5.

Ethyl 2-((4-bromophenyl)amino)-4-oxo-4,5-dihydrothiophene-3-carboxylate (**11e**)
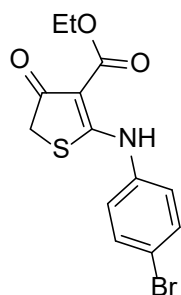
By using general procedure 3 with 4-bromophenyl isothiocyanate to give the desired product (1.0 g, 3.0 mmol, 60%). ^{1}H NMR (700 MHz, CDCl$_3$) δ 11.48 (s, 1H), 7.57 (d, *J* = 8.7 Hz, 2H), 7.25 (d, *J* = 8.7 Hz, 2H), 4.38 (q, *J* = 7.1 Hz, 2H), 3.65 (s, 2H), 1.40 (t, *J* = 7.1 Hz, 3H). ^{13}C NMR (176 MHz, CDCl$_3$) δ 191.0, 183.1, 166.6, 135.9, 132.9 (2), 125.6 (2), 121.2, 98.2, 60.6, 38.1, 14.4.

Ethyl 2-((2-bromophenyl)amino)-4-oxo-4,5-dihydrothiophene-3-carboxylate (**11f**)
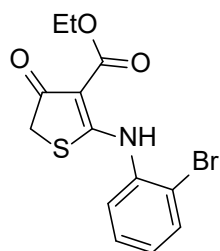
By using general procedure 3 with 2-bromophenyl isothiocyanate to give the desired product (927 mg, 2.7 mmol, 54%). ^{1}H NMR (700 MHz, CDCl$_3$) δ 11.51 (s, 1H), 7.71 (dd, *J* = 8.0, 1.4 Hz, 1H), 7.59 (dd, *J* = 8.0, 1.5 Hz, 1H), 7.40 (td, *J* = 7.8, 1.4 Hz, 1H), 7.23 (td, *J* = 7.8, 1.5 Hz, 1H), 4.40 (q, *J* = 7.1 Hz, 2H), 3.65 (s, 2H), 1.41 (t, *J* = 7.1 Hz, 3H). ^{13}C NMR (176 MHz, CDCl$_3$) δ 191.1, 183.3, 166.4, 135.8, 133.8, 129.0, 128.3, 125.5, 119.5, 98.7, 60.6, 38.1, 14.4.

*Ethyl 2-((4-fluorophenyl)amino)-4-oxo-4,5-dihydrothiophene-3-carboxylate* (**11g**)
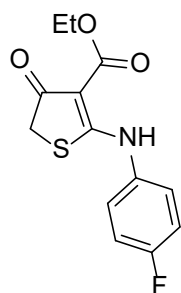
By using general procedure 3 with 4-fluorophenyl isothiocyanate to give the desired product (909 mg, 3.2 mmol, 65%). ^{1}H NMR (700 MHz, CDCl$_3$) δ 11.34 (s, 1H), 7.34 (dd, *J* = 8.8, 4.7 Hz, 2H), 7.14 (dd, *J* = 8.9, 8.0 Hz, 2H), 4.38 (q, *J* = 7.1 Hz, 2H), 3.63 (s, 2H), 1.40 (t, *J* = 7.1 Hz, 3H). ^{13}C NMR (176 MHz, CDCl$_3$) δ 191.1, 183.9, 166.6, 162.4 and 161.0 (d, $^1J_{C-F}$ = 249 Hz), 132.8 and 132.8 (d, $^4J_{C-F}$ = 3 Hz), 126.6 and 126.5 (d, $^3J_{C-F}$ = 9 Hz) (2), 116.7 and 116.6 (d, $^2J_{C-F}$ = 23 Hz) (2), 97.9, 60.6, 38.0, 14.4.

Ethyl 2-((3-fluorophenyl)amino)-4-oxo-4,5-dihydrothiophene-3-carboxylate (**11h**)
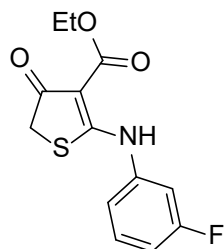
By using general procedure 3 with 3-fluorophenyl isothiocyanate to give the desired product (911 mg, 3.2 mmol, 65%). ^{1}H NMR (700 MHz, CDCl$_3$) δ 11.59 (s, 1H), 7.42 (td, *J* = 8.2, 6.2 Hz, 1H), 7.16 (dd, *J* = 8.0, 1.3 Hz, 1H), 7.13 (dt, *J* = 9.5, 2.3 Hz, 1H), 7.05 (tdd, *J* = 8.4, 2.5, 0.9 Hz, 1H), 4.38 (q, *J* = 7.1 Hz, 2H), 3.66 (s, 2H), 1.40 (t, *J* = 7.1 Hz, 3H).

Ethyl 4-oxo-2-((4-(trifluoromethyl)phenyl)amino)-4,5-dihydrothiophene-3-carboxylate (**11i**)
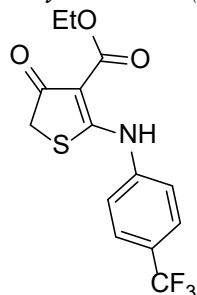
By using general procedure 3 with 4-(trifluoromethyl)phenyl isothiocyanate to give the desired product (947 mg, 2.9 mmol, 57%). ^{1}H NMR (600 MHz, CDCl$_3$) δ 11.77 (s, 1H), 7.72 (d, J = 8.4 Hz, 2H), 7.50 (d, J = 8.4 Hz, 2H), 4.39 (q, J = 7.1 Hz, 2H), 3.69 (s, 2H), 1.41 (t, J = 7.1 Hz, 3H). ^{13}C NMR (151 MHz, CDCl$_3$) δ 190.9, 182.5, 166.6, 140.0, 129.5 and 129.3 and 129.1 and 128.8 (q, $^3J_{C-F}$ = 4 Hz) (2), 127.0 and 126.9 and 126.9 and 126.9 (q, $^2J_{C-F}$ = 33 Hz), 126.2 and 124.4 and 122.6 and 120.8 (q, $^1J_{C-F}$ = 272 Hz), 123.4 (2), 98.7, 60.8, 38.1, 14.4.

Ethyl 4-oxo-2-((3-(trifluoromethyl)phenyl)amino)-4,5-dihydrothiophene-3-carboxylate (**11j**)
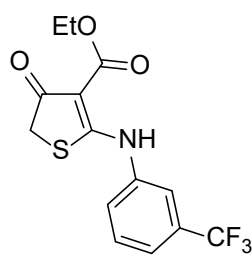
By using general procedure 3 with 3-(trifluoromethyl)phenyl isothiocyanate to give the desired product (1.1 g, 3.4 mmol, 69%). ^{1}H NMR (600 MHz, CDCl$_3$) δ 11.66 (s, 1H), 7.65 (s, 1H), 7.59 (dd, J = 12.9, 6.0 Hz, 3H), 4.39 (q, J = 7.1 Hz, 2H), 3.68 (s, 2H), 1.41 (t, J = 7.1 Hz, 3H). ^{13}C NMR (151 MHz, CDCl$_3$) δ 190.9, 183.0, 166.6, 137.4, 132.6 and 132.4 and 132.2 and 131.9 (q, $^2J_{C-F}$ = 33 Hz), 130.4, 127.0, 126.0 and 124.2 and 122.4 and 120.6 (q, $^1J_{C-F}$ = 273 Hz), 124.2 and 124.2 and 124.2 and 124.1 (q, $^3J_{C-F}$ = 4 Hz), 120.9 and 120.8 and 120.8 and 120.8 (q, $^3J_{C-F}$ = 4 Hz), 98.5, 60.7, 38.1, 14.4.

Ethyl 2-((4-nitrophenyl)amino)-4-oxo-4,5-dihydrothiophene-3-carboxylate (**11k**)
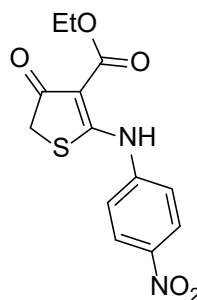
By using general procedure 3 with 4-nitrophenyl isothiocyanate to give the desired product (888 mg, 2.9 mmol, 58%). ^{1}H NMR (600 MHz, CDCl$_3$) δ 12.05 (s, 1H), 8.33 (d, J = 9.0 Hz, 2H), 7.55 (d, J = 9.0 Hz, 2H), 4.40 (q, J = 7.1 Hz, 2H), 3.73 (s, 2H), 1.41 (t, J = 7.1 Hz, 3H). ^{13}C NMR (151 MHz, CDCl$_3$) δ 190.7, 181.8, 166.6, 145.5, 142.6, 125.4 (2), 122.7 (2), 99.5, 61.0, 38.2, 14.3.

Ethyl 2-((3-nitrophenyl)amino)-4-oxo-4,5-dihydrothiophene-3-carboxylate (**11l**)
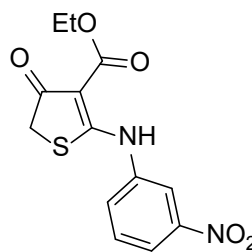
By using general procedure 3 with 3-nitrophenyl isothiocyanate to give the desired product (1.1 g, 3.5 mmol, 69%). ^{1}H NMR (400 MHz, CDCl$_3$) δ 11.80 (s, 1H), 8.31 (d, J = 2.1 Hz, 1H), 8.19 (dt, J = 8.0, 1.3 Hz, 1H), 7.71 (dt, J = 8.0, 1.3 Hz, 1H), 7.65 (t, J = 8.0 Hz, 1H), 4.39 (q, J = 7.1 Hz, 2H), 3.70 (s, 2H), 1.41 (t, J = 7.1 Hz, 3H).

Ethyl 4-oxo-2-(p-tolylamino)-4,5-dihydrothiophene-3-carboxylate (**11m**)
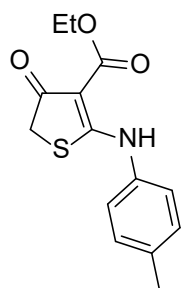
By using general procedure 3 with p-tolyl isothiocyanate to give the desired product (853 mg, 3.1 mmol, 61%). ^{1}H NMR (400 MHz, CDCl$_3$) δ 11.36 (s, 1H), 7.27–7.21 (m, 4H), 4.38 (q, J = 7.1 Hz, 2H), 3.62 (s, 2H), 2.39 (s, 3H), 1.40 (t, J = 7.1 Hz, 3H).

Ethyl 2-((4-ethylphenyl)amino)-4-oxo-4,5-dihydrothiophene-3-carboxylate (**11n**)

By using general procedure 3 with 4-ethylphenyl isothiocyanate to give the desired product (550 mg, 1.9 mmol, 38%). ^{1}H NMR (400 MHz, CDCl$_3$) δ 11.38 (s, 1H), 7.29–7.24 (m, 4H), 4.38 (q, J = 7.1 Hz, 2H), 3.62 (s, 2H), 2.69 (q, J = 7.6 Hz, 2H), 1.40 (t, J = 7.1 Hz, 3H), 1.26 (t, J = 7.6 Hz, 3H).

Ethyl 2-((3-chlorophenyl)amino)-4-oxo-4,5-dihydrothiophene-3-carboxylate (**11o**)
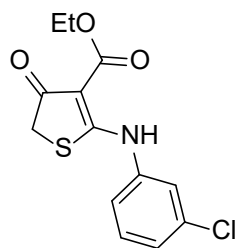
By using general procedure 3 with 3-chlorophenyl isothiocyanate (20.0 mmol) to give the desired product as solid (4.4 g, 14.9 mmol, 75%). ^{1}H NMR (700 MHz, CDCl$_3$) δ 11.55 (s, 1H), 7.41–7.37 (m, 2H), 7.34–7.30 (m, 1H), 7.29–7.26 (m, 1H), 4.38 (q, J = 7.1 Hz, 2H), 3.67 (s, 2H), 1.40 (t, J = 7.1 Hz, 3H). ^{13}C NMR (176 MHz, CDCl$_3$) δ 191.0, 183.1, 166.6, 138.0, 135.3, 130.7, 127.8, 124.1, 122.0, 98.3, 60.7, 38.1, 14.4.

Ethyl 4-oxo-2-(phenylamino)-4,5-dihydrofuran-3-carboxylate (**11p**)
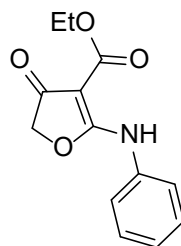
By using general procedure 3 with phenyl isothiocyanate (20.0 mmol) to give the desired product as solid (2.2 g, 8.9 mmol, 44%). ^{1}H NMR (700 MHz, CDCl$_3$) δ 10.28 (s, 1H), 7.43–7.37 (m, 4H), 7.26–7.22 (m, 1H), 4.69 (s, 2H), 4.39 (q, J = 7.1 Hz, 2H), 1.40 (t, J = 7.1 Hz, 3H). ^{13}C NMR (176 MHz, CDCl$_3$) δ 188.4, 177.7, 165.6, 134.8, 129.5 (2), 126.2, 121.5 (2), 87.7, 77.2, 60.6, 14.5.

Ethyl 2-((3-fluorophenyl)amino)-4-oxo-4,5-dihydrofuran-3-carboxylate (**11q**)
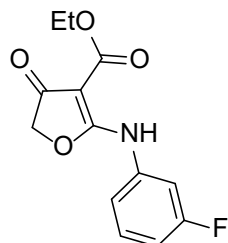
By using general procedure 3 with 3-fluorophenyl isothiocyanate (20.0 mmol) to give the desired product as solid (3.7 g, 13.9 mmol, 70%). ^{1}H NMR (500 MHz, CDCl$_3$) δ 10.38 (s, 1H), 7.36 (td, J = 8.3, 6.3 Hz, 1H), 7.22 (dt, J = 10.1, 2.4 Hz, 1H), 7.11 (dd, J = 8.1, 1.7 Hz, 2H), 6.95 (td, J =

8.3, 2.4 Hz, 1H), 4.72 (s, 2H), 4.38 (q, J = 7.1 Hz, 2H), 1.40 (t, J = 7.1 Hz, 3H). ^{13}C NMR (126 MHz, CDCl$_3$) δ 188.23, 177.69, 165.48, 163.9 and 161.9 (d, $^1J_{C-F}$ = 247 Hz), 136.2 and 136.1 (d, $^3J_{C-F}$ = 10 Hz), 130.7 and 130.7 (d, $^3J_{C-F}$ = 9 Hz), 116.6 and 116.6 (d, $^4J_{C-F}$ = 3 Hz), 112.9 and 112.8 (d, $^2J_{C-F}$ = 21 Hz), 108.8 and 108.7 (d, $^2J_{C-F}$ = 26 Hz), 87.9, 75.5, 60.7, 14.4.

General procedure 4

The compounds were synthesized according to the previously reported method.[155] To the solution of NaH (60% in oil, 12.70 mmol, 1.5 equiv.) in THF (0.85 M) was added azaindole (8.47 mmol, 1 equiv.) in THF (4.2 M) dropwise over 5 min at 0 °C under Ar atmosphere. After the reaction mixture was stirred at 0 °C for 30 min, benzenesulfonyl chloride (9.31 mmol, 1.1 equiv.) was added dropwise at 0 °C with following stirring for 2 h at room temperature until the starting material had been completely consumed by monitoring TLC. The mixture was poured into H$_2$O and extracted with EA. The organic layer was washed with brine, dried over MgSO$_4$, and filtered. The solvent was evaporated under reduced pressure to give the crude product which was purified by flash chromatography (PE/EA) to give the desired product as a white solid.

1-(Phenylsulfonyl)-1H-pyrrolo[3,2-b]pyridine (**12a**)
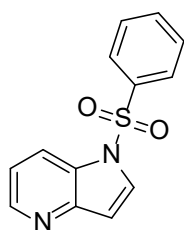
By using general procedure 4 with 4-azaindole (8.5 mmol) to give the title compound (2.0 g, 7.6 mmol, 90%). ^{1}H NMR (400 MHz, CDCl$_3$) δ 8.54 (dd, J = 4.8, 1.5 Hz, 1H), 8.30 (dd, J = 8.4, 1.5 Hz, 1H), 7.88 (d, J = 7.7 Hz, 1H), 7.81 (d, J = 3.8 Hz, 1H), 7.58 (t, J = 7.7 Hz, 1H), 7.47 (t, J = 7.7 Hz, 2H), 7.26 (dd, J = 8.4, 4.8 Hz, 2H), 6.91 (d, J = 3.8 Hz, 1H).

1-(Phenylsulfonyl)-1H-pyrrolo[3,2-c]pyridine (**12b**)
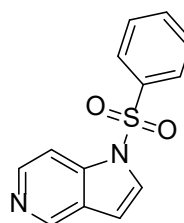
By using general procedure 4 with 5-azaindole (8.5 mmol) to give the title compound (1.9 g, 7.2 mmol, 86%). 1H NMR (400 MHz, CDCl$_3$) δ 8.88 (s, 1H), 8.49 (d, J = 5.8 Hz, 1H), 7.94–7.88 (m, 3H), 7.64–7.56 (m, 2H), 7.53–7.46 (m, 2H), 6.76 (d, J = 3.7 Hz, 1H).

1-(Phenylsulfonyl)-1H-pyrrolo[2,3-c]pyridine (**12c**)
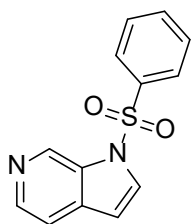
By using general procedure 4 with 6-azaindole (8.5 mmol) to give the title compound (2.0 g, 7.5 mmol, 89%). 1H NMR (400 MHz, CDCl$_3$) δ 9.33 (s, 1H), 8.41 (d, J = 5.3 Hz, 1H), 8.00–7.91 (m, 2H), 7.71 (d, J = 3.6 Hz, 1H), 7.63–7.54 (m, 1H), 7.52–7.45 (m, 3H), 6.69 (dt, J = 3.6, 0.8 Hz, 1H).

1-(Phenylsulfonyl)-1H-pyrrolo[2,3-b]pyridine (**12d**)
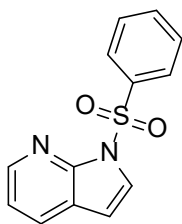
By using general procedure 4 with 7-azaindole (8.5 mmol) to give the title compound (2.1 g, 7.9 mmol, 94%). 1H NMR (400 MHz, CDCl$_3$) δ 8.43 (dd, J = 4.8, 1.6 Hz, 1H), 8.21–8.19 (m, 1H), 7.84 (dd, J = 7.8, 1.6 Hz, 1H), 7.73 (d, J = 4.0 Hz, 1H), 7.60–7.54 (m, 1H), 7.51–7.45 (m, 2H), 7.17 (dd, J = 7.8, 4.8 Hz, 2H), 6.60 (d, J = 4.0 Hz, 1H).

General procedure 5

The compounds were synthesized according to the previously reported method.[156] To a solution of lithium diisopropylamide (1 M in THF, 5.25 mmol, 1.5 equiv.) diluted in THF (0.6 M), was added a solution of *N*-phenylsulfonyl azaindole (3.50 mmol, 1 equiv.) in THF (1.2 M) dropwise. The resulting reaction was stirred at -78 °C for 2 h and then a solution of DMF (14.00 mmol, 4 equiv.) was added dropwise. The reaction was stirred at -78 °C for 1 h and warmed up to -10 °C and stirred for 1 h. The reaction was quenched with saturated aqueous NH$_4$Cl solution after monitoring the completion of the reaction with TLC. The mixture was extracted with EA, and the combined organic layers were dried over MgSO$_4$ and concentrated under reduced pressure. Purification of the crude by silica gel chromatography (PE/EA) afforded the title compounds as a white solid.

1-(Phenylsulfonyl)-1H-pyrrolo[3,2-b]pyridine-2-carbaldehyde (**13a**)
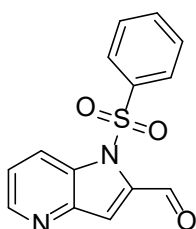
By using general procedure 5 with **12a** (3.5 mmol) to give the title compound (601.5 mg, 2.1 mmol, 60%). ^{1}H NMR (400 MHz, CDCl$_3$) δ 10.56 (s, 1H), 8.68 (ddd, J = 4.6, 1.5, 0.6 Hz, 1H), 8.56 (ddt, J = 8.6, 1.5, 0.6 Hz, 1H), 7.83–7.78 (m, 2H), 7.63–7.56 (m, 2H), 7.51–7.42 (m, 3H).

1-(Phenylsulfonyl)-1H-pyrrolo[3,2-c]pyridine-2-carbaldehyde (**13b**)
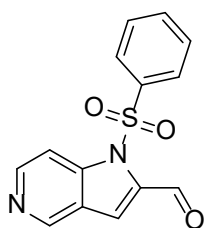
By using general procedure 5 with **12b** (3.5 mmol) to give the title compound (744 mg, 2.6 mmol, 74%). ^{1}H NMR (400 MHz, CDCl$_3$) δ 10.49 (s, 1H), 9.02 (s, 1H), 8.66 (d, *J* = 6.0 Hz, 1H), 8.15 (d, *J* = 6.0 Hz, 0H), 7.88–7.83 (m, 2H), 7.66–7.59 (m, 1H), 7.54 (s, 1H), 7.53–7.47 (m, 1H).

1-(Phenylsulfonyl)-1H-pyrrolo[2,3-c]pyridine-2-carbaldehyde (**13c**)
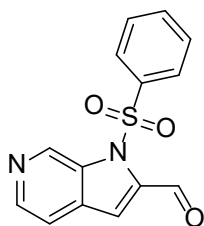
By using general procedure 5 with **12c** (3.5 mmol) to give the title compound (726.3 mg, 2.5 mmol, 72%). ^{1}H NMR (400 MHz, CDCl$_3$) δ 10.59 (s, 1H), 9.62 (d, *J* = 1.2 Hz, 1H), 8.53 (d, *J* = 5.3 Hz, 1H), 7.88–7.83 (m, 2H), 7.64–7.56 (m, 1H), 7.55 (dd, *J* = 5.3, 1.2 Hz, 1H), 7.51–7.45 (m, 2H), 7.41 (s, 1H).

1-(Phenylsulfonyl)-1H-pyrrolo[2,3-b]pyridine-2-carbaldehyde (**13d**)
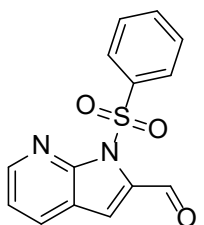
By using general procedure 5 with **12d** (4.4 mmol) to give the title compound (1.03 g, 3.6 mmol, 82%). ^{1}H NMR (400 MHz, CDCl$_3$) δ 10.64 (s, 1H), 8.62 (dd, *J* = 4.7, 1.7 Hz, 1H), 8.25–8.13 (m, 2H), 7.98 (dd, *J* = 8.0, 1.7 Hz, 1H), 7.62–7.56 (m, 1H), 7.52–7.47 (m, 2H), 7.40 (s, 1H), 7.27 (dd, *J* = 8.0, 4.7 Hz, 1H).

General procedure 6

The compounds were synthesized according to the previously reported method.[157] To a solution of **13a**–**13d** (1.50 mmol, 1 equiv.) in MeOH (0.17 M) was added a solution of 7M KOH in H$_2$O (6.00 mmol, 4 equiv.) dropwise slowly under Ar at room temperature. The reaction mixture was stirred at room temperature for 30 min. After the completion of the reaction monitored by TLC, the saturated NH$_4$Cl solution was added and extracted with DCM. The organic layer was washed with H$_2$O and saturated brine, dried over MgSO$_4$, and evaporated in vacuo to give the title compound as a yellow solid which was used in the next reaction without further purification.

1H-pyrrolo[3,2-b]pyridine-2-carbaldehyde (**14a**)
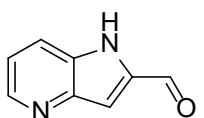
By using general procedure 6 with **13a** (1.50 mmol) to give the title compound (96 mg, 0.66 mmol, 44%). ^{1}H NMR (400 MHz, CDCl$_3$) δ 9.98 (s, 1H), 9.22 (s, 1H), 8.63 (d, *J* = 4.6 Hz, 1H), 7.82 (d, *J* = 8.5 Hz, 1H), 7.49 (s,

1H), 7.33 (dd, *J* = 8.5, 4.6 Hz, 1H).

1H-pyrrolo[3,2-c]pyridine-2-carbaldehyde (**14b**)
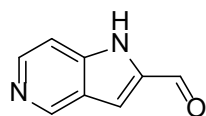
By using general procedure 6 with **13b** (1.50 mmol) to give the title compound (110 mg, 0.76 mmol, 50%). ¹H NMR (400 MHz, CD₃OD) δ 11.47 (s, 1H), 10.55 (s, 1H), 9.84 (d, *J* = 6.0 Hz, 1H), 9.07 (s, 1H), 9.04 (d, *J* = 6.0 Hz, 1H).

1H-pyrrolo[2,3-c]pyridine-2-carbaldehyde (**14c**)
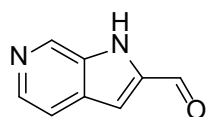
By using general procedure 6 with **13c** (1.50 mmol) to give the title compound (19 mg, 0.14 mmol, 9%). ¹H NMR (400 MHz, CDCl₃) δ 10.01 (s, 1H), 9.39 (s, 1H), 9.00 (s, 1H), 8.38 (d, *J* = 5.6 Hz, 1H), 7.66 (d, *J* = 5.6 Hz, 1H), 7.28 (s, 1H).

1H-pyrrolo[2,3-b]pyridine-2-carbaldehyde (**14d**)
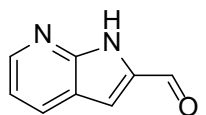
By using general procedure 6 with **13d** (1.50 mmol) to give the title compound (59 mg, 0.40 mmol, 27%). ¹H NMR (500 MHz, CDCl₃) δ 12.67 (s, 1H), 10.00 (s, 1H), 8.84 (dd, *J* = 4.7, 1.6 Hz, 1H), 8.19 (dd, *J* = 8.0, 1.6 Hz, 1H), 7.30 (s, 1H), 7.27 (dd, *J* = 8.0, 4.7 Hz, 1H).

General procedure 7

The synthetic method to obtain title compounds was modified from the previously reported method.[105, 125] A mixture of **14a**–**14q** (0.38 mmol, 1 equiv.), an aldehyde (or ketone, 0.42 mmol, 1.1 equiv.), and piperidine (0.38 mmol, 1 equiv.) in ethanol (0.13 M) was refluxed for the indicated reaction time as described individually. After the reaction completion was monitored by TLC, The reaction mixture was cooled down to room temperature. The purification was performed in either of the following two methods.

Purification 1. When the product was crystalized as a solid during the reaction or the cooling down of the reaction mixture, the precipitate is collected by using vacuum filtration with washing cold EtOH. The collected product was dried under low pressured vacuum to give the desired product.

Purification 2. When the product was present as dissolved in the reaction mixture, the reaction mixture was shaken with H₂O and chloroform without removing the reaction solvent EtOH.

The organic layer was collected, washed with 1N HCl, and dried over MgSO$_4$. The organic solvent was evaporated under reduced pressure and the crude was purified by flash chromatography (PE/EA) to give the desired product.

*Ethyl (Z)-5-(3-hydroxybenzylidene)-4-oxo-2-(phenylamino)-4,5-dihydrothiophene-3-carboxylate* (**C1**, **15a**)[104]
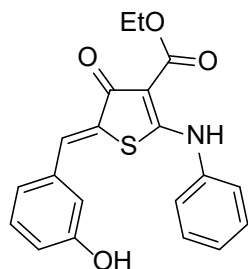
By using general procedure 7 with **11a** (0.57 mmol), 3-hydroxybenzaldehyde (77 mg, 0.63 mmol), and piperidine (56.3 µL, 0.57 mmol) with a reaction time of 4 h. The product was purified with purification method 1 to give the desired product (175 mg, 0.48 mmol, 84%). ^{1}H NMR (400 MHz, DMSO-d_6) δ 11.27 (s, 1H), 9.73 (s, 1H), 7.59–7.47 (m, 5H), 7.27–7.23 (m, 1H), 7.25 (t, J = 7.9 Hz, 1H), 6.95 (d, J = 7.9 Hz, 1H), 6.89 (s, 1H), 6.80 (d, J = 7.9 Hz, 1H), 4.27 (q, J = 7.0 Hz, 2H), 1.29 (t, J = 7.0 Hz, 3H). ^{13}C NMR (176 MHz, DMSO-d_6) δ 180.4, 175.2, 164.4, 157.4, 137.1, 134.4, 130.0, 129.4, 129.3 (2), 127.9, 127.1, 125.3 (2), 120.8, 116.8, 115.3, 96.5, 59.2, 14.0. HRMS-ESI (m/z): calculated for [M+H]$^+$ C$_{20}$H$_{18}$O$_4$NS, 368.0951; found, 368.0953.

Ethyl (Z)-5-(3-hydroxy-4-methoxybenzylidene)-4-oxo-2-(phenylamino)-4,5-dihydrothiophene-3-carboxylate (**C1-3**, **15b**)[105]
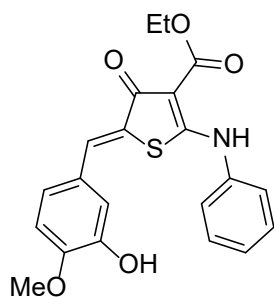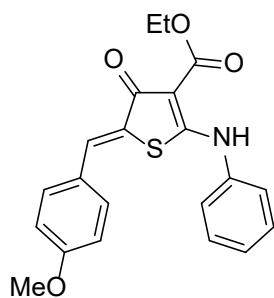
By using general procedure 7 with **11a** (100 mg, 0.38 mmol), 3-hydroxy-4-methoxybenzaldehyde (64 mg, 0.42 mmol), and piperidine (37.5 µL, 0.38 mmol) in ethanol (3.5 mL) with a reaction time of 4 h. The product was purified with purification method 2 to give the desired product (128 mg, 0.32 mmol, 85%). ^{1}H NMR (500 MHz, CDCl$_3$): δ 11.49 (s, 1H), 7.74 (s, 1H), 7.51 (t, J = 7.45 Hz, 2H), 7.40 (d, J = 8.2 Hz, 1H), 7.13 (d, J = 2.1 Hz, 3H), 7.08 (dd, J = 8.4 Hz, 2.1 Hz, 1H), 6.88 (d, J = 8.4 Hz, 1H), 5.79 (s, 1H), 4.43 (q, J = 7.15 Hz, 2H), 3.92 (s, 3H), 1.45 (t, J = 7.1 Hz, 3H). ^{13}C NMR (126 MHz, CDCl$_3$): δ 182.4, 176.3, 167.2, 148.1, 146.0, 137.3, 131.7, 130.0, 129.9, 127.9, 127.7, 125.7, 124.3, 124.2, 115.5, 110.9, 98.1, 60.8, 56.2, 14.6. HRMS-ESI (m/z): calculated for [M+H]$^+$ C$_{21}$H$_{20}$O$_5$NS, 398.1057; found, 398.1050.

Ethyl (Z)-5-(4-hydroxy-3-methoxybenzylidene)-4-oxo-2-(phenylamino)-4,5-dihydrothiophene-3-carboxylate (**C1-4**, **15c**)[105]
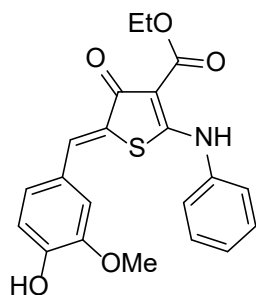
By using general procedure 7 with **11a** (150 mg, 0.38 mmol), 3-methoxy-4-hydroxybenzaldehyde (95 mg, 0.63 mmol), and piperidine (56.3 μL, 0.57 mmol) in ethanol (5.0 mL) with a reaction time of 4 h. The product was purified with purification method 2 to give the desired product (172 mg, 0.43 mmol, 76%). ^{1}H NMR (700 MHz, DMSO-d_6) δ 11.23 (s, 1H), 9.75 (s, 1H), 7.56 (s, 1H), 7.54–7.49 (m, 4H), 7.45–7.40 (m, 1H), 7.15 (d, J = 2.1 Hz, 1H), 6.98 (dd, J = 8.3, 2.1 Hz, 1H), 6.86 (d, J = 8.3 Hz, 1H), 4.27 (q, J = 7.1 Hz, 2H), 3.75 (s, 3H), 1.29 (t, J = 7.1 Hz, 3H). ^{13}C NMR (176 MHz, DMSO-d_6) δ 180.6, 174.7, 164.5, 148.5, 147.5, 137.2, 130.0, 129.2 (2), 127.7, 125.0 (2), 124.6, 123.7, 122.6, 115.8, 114.6, 96.6, 59.1, 55.2, 14.1. HRMS-ESI (m/z): calculated for [M+H]$^+$ C$_{21}$H$_{20}$O$_5$NS, 398.1057; found, 398.1050.

Ethyl (Z)-5-benzylidene-4-oxo-2-(phenylamino)-4,5-dihydrothiophene-3-carboxylate (**15d**)
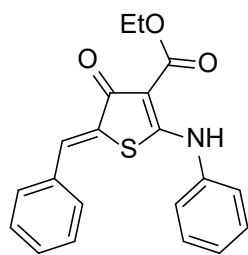
By using general procedure 7 with **11a** (100 mg, 0.38 mmol), benzaldehyde (42.2 μL, 0.42 mmol), and piperidine (37.5 μL, 0.38 mmol) in ethanol (3.5 mL) with a reaction time of 4 h. The product was purified with purification method 2 to give the desired product (87 mg, 0.25 mmol, 65%). ^{1}H NMR (700 MHz, DMSO-d_6) δ 11.30 (s, 1H), 7.63 (s, 1H), 7.56–7.36 (m, 10H), 4.28 (q, J = 7.1 Hz, 2H), 1.29 (t, J = 7.1 Hz, 3H). ^{13}C NMR (176 MHz, DMSO-d_6) δ 181.2, 176.0, 165.2, 137.9, 134.1, 130.3, 130.3 (2), 130.1 (2), 130.0, 129.7 (2), 128.8, 128.2, 126.2 (2), 97.3, 60.0, 14.9. HRMS-ESI (m/z): calculated for [M+H]$^+$ C$_{20}$H$_{18}$O$_3$NS, 352.1002; found, 352.1003.

Ethyl (Z)-5-(3,4-dihydroxybenzylidene)-4-oxo-2-(phenylamino)-4,5-dihydrothiophene-3-carboxylate (**15e**)
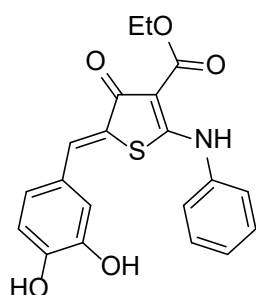
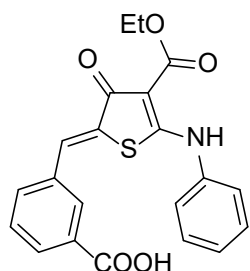By using general procedure 7 with **11a** (100 mg, 0.38 mmol), 3,4-dihydroxybenzaldehyde (58 mg, 0.42 mmol), and piperidine (37.5 μL, 0.38 mmol) in ethanol (3.5 mL) with a reaction time of 4 h. The product was purified with purification method 2 to give the desired product (21 mg, 0.05 mmol, 14%). ^{1}H NMR (400 MHz, DMSO-d_6) δ 11.20 (s, 1H), 9.63 (s, 1H), 9.36 (s, 1H), 7.59–7.47 (m, 4H), 7.47–7.40 (m, 2H), 6.92 (d, J = 2.2 Hz, 1H), 6.88 (dd, J = 8.4, 2.2 Hz, 1H), 6.80 (d, J = 8.2 Hz, 1H), 4.26 (q, J =

7.1 Hz, 2H), 1.28 (t, J = 7.1 Hz, 3H). ^{13}C NMR (126 MHz, DMSO-d_6) δ 180.5, 174.7, 164.4, 147.6, 145.3, 137.1, 130.0, 129.2 (2), 127.6, 125.1 (2), 124.3, 123.2, 122.9, 115.7, 115.7, 96.4, 59.0, 13.9. HRMS-ESI (m/z): calculated for [M+H]$^+$ C$_{20}$H$_{18}$O$_5$NS, 384.0900; found, 384.0904.

Ethyl (Z)-5-(4-methoxybenzylidene)-4-oxo-2-(phenylamino)-4,5-dihydrothiophene-3-carboxylate (**15f**)

By using general procedure 7 with **11a** (100 mg, 0.38 mmol), 4-methoxybenzaldehyde (58 μL, 0.42 mmol), and piperidine (37.5 μL, 0.38 mmol) in ethanol (3.5 mL) with a reaction time of 4 h. The product was purified with purification method 1 to give the desired product (120 mg, 0.32 mmol, 83%). ^{1}H NMR (700 MHz, CDCl$_3$) δ 11.48 (s, 1H), 7.79 (s, 1H), 7.53–7.45 (m, 4H), 7.41–7.35 (m, 3H), 6.96–6.91 (m, 2H), 4.41 (q, J = 7.1 Hz, 2H), 3.83 (s, 3H), 1.44 (t, J = 7.1 Hz, 3H). ^{13}C NMR (176 MHz, CDCl$_3$) δ 182.3, 176.1, 167.0, 160.8, 137.3, 132.0 (2), 131.3, 129.9 (2), 127.8, 126.7, 125.0, 124.2 (2), 114.5 (2), 98.0, 60.6, 55.4, 14.5. HRMS-ESI (m/z): calculated for [M+H]$^+$ C$_{21}$H$_{20}$O$_4$NS, 382.1108; found, 382.1118.

Ethyl (Z)-5-(3-hydroxy-4-nitrobenzylidene)-4-oxo-2-(phenylamino)-4,5-dihydrothiophene-3-carboxylate (**15g**)
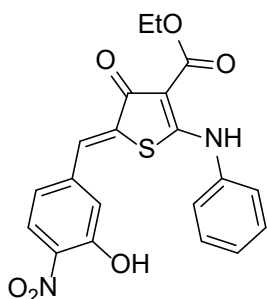
By using general procedure 7 with **11a** (100 mg, 0.38 mmol), 3-hydroxy-4-nitrobenzaldehyde (70 mg, 0.42 mmol), and piperidine (37.5 μL, 0.38 mmol) in ethanol (3.5 mL) with a reaction time of 5 h. The product was purified with purification method 1 to give the desired product (124 mg, 0.30 mmol, 79%). ^{1}H NMR (700 MHz, DMSO-d_6) δ 11.32 (s, 2H), 7.94 (d, J = 8.5 Hz, 1H), 7.58 (s, 1H), 7.57–7.51 (m, 4H), 7.49–7.45 (m, 1H), 7.24 (d, J = 1.9 Hz, 1H), 7.13 (dd, J = 8.5, 1.9 Hz, 1H), 4.30 (q, J = 7.1 Hz, 2H), 1.31 (t, J = 7.1 Hz, 3H). ^{13}C NMR (176 MHz, DMSO-d_6) δ 180.0, 175.1, 164.2, 151.8, 139.5, 137.0, 136.4, 130.9, 129.3 (2), 128.1, 126.9, 125.8, 125.5 (2), 120.3, 118.6, 96.4, 59.3, 14.0. HRMS-ESI (m/z): calculated for [M+H]$^+$ C$_{20}$H$_{17}$O$_6$N$_2$S, 413.0802; found, 413.0800.

Ethyl (Z)-5-(4-bromo-3-hydroxybenzylidene)-4-oxo-2-(phenylamino)-4,5-dihydrothiophene-3-carboxylate (**15h**)

By using general procedure 7 with **11a** (100 mg, 0.38 mmol), 4-bromo-3-hydroxybenzaldehyde (84 mg, 0.42 mmol), and piperidine (37.5 μL, 0.38 mmol) in ethanol (3.0 mL) with a reaction
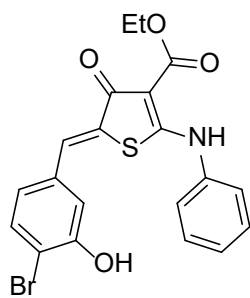
time of 4 h. The product was purified with purification method 1 to give the desired product (158 mg, 0.35 mmol, 93%). ^{1}H NMR (700 MHz, DMSO-d_6) δ 11.30 (s, 1H), 10.60 (s, 1H), 7.56 (d, J = 8.3 Hz, 1H), 7.55–7.43 (m, 6H), 7.07 (d, J = 2.1 Hz, 1H), 6.91 (dd, J = 8.3, 2.1 Hz, 1H), 4.27 (q, J = 7.1 Hz, 2H), 1.29 (t, J = 7.1 Hz, 3H). ^{13}C NMR (176 MHz, DMSO-d_6) δ 180.3, 175.0, 164.3, 154.1, 137.1, 133.7, 133.3, 129.3 (2), 128.4, 127.9, 127.8, 125.3 (2), 122.1, 115.7, 111.0, 96.4, 59.2, 14.0. HRMS-ESI (m/z): calculated for [M+H]$^+$ $C_{20}H_{17}O_4NBrS$, 446.0056; found, 446.0055.

(Z)-4-((4-(ethoxycarbonyl)-3-oxo-5-(phenylamino)thiophen-2(3H)-ylidene)methyl)benzoic acid (**15i**)
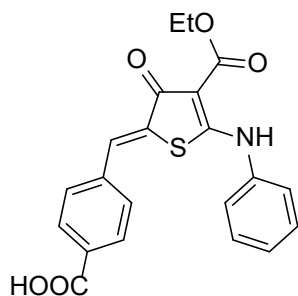
By using general procedure 7 with **11a** (100 mg, 0.38 mmol), 4-formylbenzoic acid (63 mg, 0.42 mmol), and piperidine (37.5 µL, 0.38 mmol) in ethanol (3.0 mL) with a reaction time of 4 h. The product was purified with purification method 1 to give the desired product (100 mg, 0.25 mmol, 66%). ^{1}H NMR (700 MHz, DMSO-d_6) δ 13.08 (s, 1H), 11.35 (s, 1H), 7.98 (d, J = 8.4 Hz, 2H), 7.67 (s, 1H), 7.63 (d, J = 8.4 Hz, 2H), 7.56–7.47 (m, 4H), 7.47–7.41 (m, 1H), 4.28 (q, J = 7.1 Hz, 2H), 1.30 (t, J = 7.1 Hz, 3H). ^{13}C NMR (176 MHz, DMSO-d_6) δ 180.2, 175.0, 166.3, 164.3, 137.3, 137.2, 130.9, 129.7 (2), 129.6, 129.4 (2), 129.3 (2), 127.9, 127.9, 125.3 (2), 96.4, 59.2, 14.0. HRMS-ESI (m/z): calculated for [M+H]$^+$ $C_{21}H_{18}O_5NS$, 396.0900; found, 396.0889.

*(Z)-3-((4-(ethoxycarbonyl)-3-oxo-5-(phenylamino)thiophen-2(3H)-ylidene)methyl)benzoic acid* (**15j**)

By using general procedure 7 with **11a** (100 mg, 0.38 mmol), 3-carboxybenzaldehyde (63 mg, 0.42 mmol), and piperidine (37.5 µL, 0.38 mmol) in ethanol (3.5 mL) with a reaction time of 5 h. The product was purified with purification method 1 to give the desired product (97 mg, 0.24 mmol, 64%). ^{1}H NMR (700 MHz, DMSO-d_6) δ 13.15 (s, 1H), 11.32 (s, 1H), 8.06 (t, J = 1.6 Hz, 1H), 7.93 (dt, J = 7.9, 164 Hz, 1H), 7.77 (dt, J = 7.9, 1.6 Hz, 1H), 7.69 (s, 1H), 7.59 (t, J = 7.9 Hz, 1H), 7.54–7.50 (m, 4H), 7.47–7.41 (m, 1H), 4.28 (q, J = 7.1 Hz, 2H), 1.30 (t, J = 7.1 Hz, 3H). ^{13}C NMR (176 MHz, DMSO-d_6) δ 180.2, 175.1, 166.2, 164.3, 137.1, 133.6, 133.4, 131.3, 129.9, 129.8, 129.3, 129.2 (2), 128.5, 128.2, 128.0, 125.4 (2), 96.4, 59.2, 14.0. HRMS-ESI (m/z): calculated for [M+H]$^+$ $C_{21}H_{18}O_5NS$, 396.0900;

found, 396.0889.

*Ethyl (Z)-4-oxo-2-(phenylamino)-5-(4-(trifluoromethyl)benzylidene)-4,5-dihydrothiophene-3-carboxylate* (**15k**, JH092)
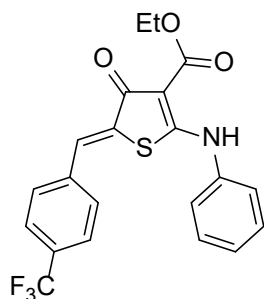
By using general procedure 7 with **11a** (50 mg, 0.19 mmol), 4-(Trifluoromethyl)benzaldehyde (28.0 μL, 0.21 mmol), and piperidine (18.8 μL, 0.19 mmol) in ethanol (1.8 mL) with a reaction time of 5 h. The product was purified with purification method 2 to give the desired product (53 mg, 0.13 mmol, 66%). ^{1}H NMR (700 MHz, CDCl$_3$) δ 11.55 (s, 1H), 7.82 (s, 1H), 7.65 (d, J = 8.2 Hz, 2H), 7.61 (d, J = 8.2 Hz, 2H), 7.52–7.48 (m, 2H), 7.44–7.38 (m, 3H), 4.43 (q, J = 7.1 Hz, 2H), 1.45 (t, J = 7.1 Hz, 3H). ^{13}C NMR (176 MHz, CDCl$_3$) δ 181.5, 176.3, 166.8, 137.6, 136.9, 130.6 and 130.2 and 129.9 and 129.6 (q, $^2J_{\text{C-F}}$ = 61 Hz), 130.0 (2), 129.9 (2), 129.7, 129.3, 128.2, 126.0 and 124.5 and 122.9 and 121.4 (q, $^1J_{\text{C-F}}$ = 272 Hz), 125.9 and 125.9 and 125.9 and 125.8 (q, $^3J_{\text{C-F}}$ = 4 Hz) (2), 124.3 (2), 97.8, 60.8, 14.4. HRMS-ESI (m/z): calculated for [M+H]$^+$ C$_{21}$H$_{17}$O$_3$NF$_3$S, 420.0876; found, 420.0879.

Ethyl (Z)-5-(3-cyano-4-fluorobenzylidene)-4-oxo-2-(phenylamino)-4,5-dihydrothiophene-3-carboxylate (**15l**, JH094)
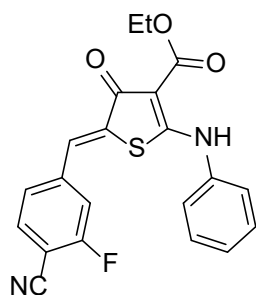
By using general procedure 7 with **11a** (100 mg, 0.38 mmol), 3-cyano-4-fluorobenzaldehyde (62 mg, 0.42 mmol), and piperidine (37.5 μL, 0.38 mmol) in ethanol (3.5 mL) with a reaction time of 4 h. The product was purified by following purification method 1 except for using flash chromatography. The product was purified by preparative chromatography to give the desired product (19 mg, 0.05 mmol, 13%). ^{1}H NMR (600 MHz, CDCl$_3$) δ 11.35 (s, 1H), 8.15 (dd, J = 6.2, 2.4 Hz, 1H), 7.87 (ddd, J = 9.0, 5.1, 2.4 Hz, 1H), 7.64 (s, 1H), 7.62 (t, J = 9.0 Hz, 1H), 7.55–7.47 (m, 4H), 7.47–7.43 (m, 1H), 4.28 (q, J = 7.1 Hz, 2H), 1.29 (t, J = 7.1 Hz, 3H). ^{13}C NMR (151 MHz, DMSO-d_6) δ 180.0, 175.0, 164.1, 162.7 and 161.0 (d, $^1J_{\text{C-F}}$ = 260 Hz), 137.0, 135.6 and 135.5 (d, $^3J_{\text{C-F}}$ = 9 Hz), 135.4, 131.0 and 131.0 (d, $^3J_{\text{C-F}}$ = 4 Hz), 129.4 and 129.4 (d, $^3J_{\text{C-F}}$ = 2 Hz), 129.2 (2), 128.0, 126.0, 125.4 (2), 117.3 and 117.2 ($^2J_{\text{C-F}}$ = 20 Hz), 113.1, 100.9 and 100.8 (d, $^2J_{\text{C-F}}$ = 16 Hz), 96.3, 59.2, 14.0. HRMS-ESI (m/z): calculated for [M+H]$^+$ C$_{21}$H$_{16}$O$_3$N$_2$FS, 395.0860; found, 395.0863.

Ethyl (Z)-5-(2,5-dimethoxybenzylidene)-4-oxo-2-(phenylamino)-4,5-dihydrothiophene-3-carboxylate (**15m**)
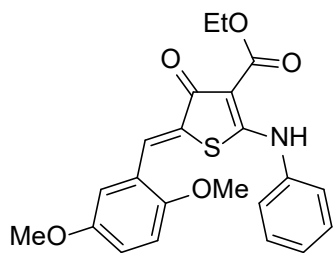
By using general procedure 7 with **11a** (100 mg, 0.38 mmol), 2,5-dimethoxybenzaldehyde (69 mg, 0.42 mmol), and piperidine (37.5 μL, 0.38 mmol) in ethanol (3.5 mL) with a reaction time of 4 h. The product was purified with purification method 1 to give the desired product (121 mg, 0.29 mmol, 77%). ^{1}H NMR (700 MHz, DMSO-d_6) δ 11.26 (s, 1H), 7.81 (s, 1H), 7.54–7.47 (m, 4H), 7.44–7.40 (m, 1H), 7.04 (d, J = 9.0 Hz, 1H), 7.00 (dd, J = 9.0, 2.9 Hz, 1H), 6.86 (d, J = 2.9 Hz, 1H), 4.27 (q, J = 7.1 Hz, 2H), 3.79 (s, 3H), 3.65 (s, 3H), 1.29 (t, J = 7.1 Hz, 3H). ^{13}C NMR (176 MHz, DMSO-d_6) δ 180.3, 175.1, 164.4, 152.5, 151.9, 137.1, 129.2 (2), 128.0, 127.9, 125.3 (2), 124.0, 122.5, 115.6, 113.9, 112.5, 96.6, 59.1, 55.7, 55.0, 14.0. HRMS-ESI (m/z): calculated for [M+H]$^+$ $C_{22}H_{22}O_5NS$, 412.1213; found, 412.1217.

Ethyl (Z)-5-(2-hydroxybenzylidene)-4-oxo-2-(phenylamino)-4,5-dihydrothiophene-3-carboxylate (**15n**)
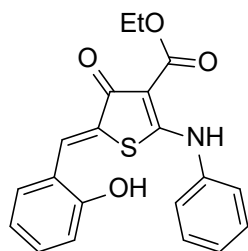
By using general procedure 7 with **11a** (100 mg, 0.38 mmol), 3-carboxybenzaldehyde (44.0 μL, 0.42 mmol), and piperidine (37.5 μL, 0.38 mmol) in ethanol (3.5 mL) refluxed for 4 h. The product was purified with method 1 to give the desired product (90 mg, 0.25 mmol, 64%). ^{1}H NMR (700 MHz, DMSO-d_6) δ 11.24 (s, 1H), 10.32 (s, 1H), 7.91 (s, 1H), 7.54–7.47 (m, 4H), 7.45–7.40 (m, 1H), 7.28 (dd, J = 7.6, 1.6 Hz, 1H), 7.22 (td, J = 7.6, 1.6 Hz, 1H), 6.91 (dd, J = 8.2, 1.2 Hz, 1H), 6.85 (td, J = 7.6, 1.2 Hz, 1H), 4.27 (q, J = 7.1 Hz, 2H), 1.29 (t, J = 7.1 Hz, 3H). ^{13}C NMR (176 MHz, DMSO-d_6) δ 180.5, 175.1, 164.5, 156.6, 137.2, 131.2, 129.2 (2), 128.2, 127.8, 126.1, 125.2 (2), 124.8, 120.2, 119.2, 115.7, 96.6, 59.1, 14.0. HRMS-ESI (m/z): calculated for [M+H]$^+$ $C_{20}H_{18}O_4NS$, 368.0951; found, 368.0951.

Ethyl (Z)-4-oxo-2-(phenylamino)-5-(2-(trifluoromethyl)benzylidene)-4,5-dihydrothiophene-3-carboxylate (**15o**)
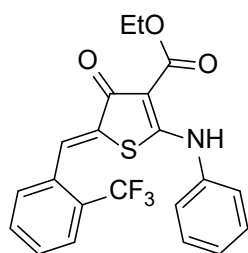
By using general procedure 7 with **11a** (100 mg, 0.38 mmol), 2-(trifluoromethyl)benzaldehyde (55.0 μL, 0.42 mmol), and piperidine (37.5 μL, 0.38 mmol) in ethanol (3.5 mL) with a reaction time of 6 h. The product was purified with purification method 2 to give the desired product (113 mg, 0.27 mmol, 71%). ^{1}H NMR (700 MHz, CDCl$_3$) δ 11.54

114

(s, 1H), 8.10 (q, J = 2.3 Hz, 1H), 7.72 (d, J = 7.8 Hz, 1H), 7.60–7.52 (m, 2H), 7.49–7.41 (m, 3H), 7.39–7.32 (m, 3H), 4.41 (q, J = 7.1 Hz, 2H), 1.45 (t, J = 7.1 Hz, 3H). ^{13}C NMR (176 MHz, CDCl$_3$) δ 180.9, 176.8, 166.9, 136.9, 133.4 and 133.4 and 133.3 and 133.3 (d, $^4J_{C-F}$ = 2 Hz), 132.4, 132.0, 129.8 (2), 129.8 and 129.7 and 129.5 and 129.3 (q, $^2J_{C-F}$ = 31 Hz), 129.3, 129.0, 128.0, 127.5 and 127.5 and 127.4 and 127.4 (q, $^4J_{C-F}$ = 2 Hz), 126.5 and 126.5 and 126.5 and 126.4 (q, $^3J_{C-F}$ = 5 Hz), 126.0 and 124.4 and 122.9 and 121.3 (q, $^1J_{C-F}$ = 274 Hz), 124.3 (2), 98.1, 60.7, 14.4. HRMS-ESI (m/z): calculated for [M+H]$^+$ C$_{21}$H$_{17}$O$_3$NF$_3$S, 420.0876; found, 420.0874.

Ethyl (Z)-5-(4-hydroxy-3,5-dimethoxybenzylidene)-4-oxo-2-(phenylamino)-4,5-dihydrothio phene-3-carboxylate (**15p**)[105]
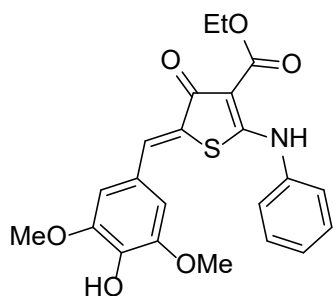
By using general procedure 7 with **11a** (100 mg, 0.38 mmol), 3,5-dimethoxy-4-hydroxybenzaldehyde (76 mg, 0.42 mmol), and piperidine (37.5 μL, 0.38 mmol) in ethanol (3.5 mL) with a reaction time of 4 h. The product was purified with purification method 1 to give the desired product (92 mg, 0.22 mmol, 57%). ^{1}H NMR (700 MHz, DMSO-d_6) δ 11.26 (s, 1H), 9.18 (s, 1H), 7.57 (s, 1H), 7.56–7.50 (m, 4H), 7.45–7.40 (m, 1H), 6.85 (s, 2H), 4.29 (q, J = 7.1 Hz, 2H), 3.74 (s, 6H), 1.31 (t, J = 7.1 Hz, 3H). ^{13}C NMR (176 MHz, DMSO-d_6) δ 180.5, 174.6, 164.5, 147.8 (2), 137.8, 137.2, 130.2, 129.1 (2), 127.6, 124.9 (2), 124.2, 123.5, 107.7 (2), 96.6, 59.1, 55.7 (2), 14.1. HRMS-ESI (m/z): calculated for [M+H]$^+$ C$_{22}$H$_{22}$O$_6$NS, 428.1162; found, 428.1161.

Ethyl (Z)-5-(furan-2-ylmethylene)-4-oxo-2-(phenylamino)-4,5-dihydrothiophene-3-carboxy late (**16a**)
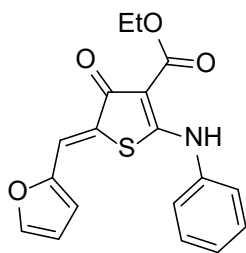
By using general procedure 7 with **11a** (100 mg, 0.38 mmol), 2-furaldehyde (34.6 μL, 0.42 mmol), and piperidine (37.5 μL, 0.38 mmol) in ethanol (3.5 mL) with a reaction time of 5 h. The product was purified with purification method 1 to give the desired product (99 mg, 0.29 mmol, 77%). ^{1}H NMR (700 MHz, DMSO-d_6) δ 11.23 (s, 1H), 7.93 (d, J = 1.8 Hz, 1H), 7.57–7.47 (m, 4H), 7.47–7.41 (m, 2H), 7.02 (d, J = 3.5 Hz, 1H), 6.67 (dd, J = 3.5, 1.8 Hz, 1H), 4.27 (q, J = 7.1 Hz, 2H), 1.28 (t, J = 7.1 Hz, 3H). ^{13}C NMR (176 MHz, DMSO-d_6) δ 180.2, 175.6, 164.4, 149.4, 146.3, 137.1, 129.3 (2), 127.9, 125.5 (2), 124.4, 117.4, 115.7, 112.9, 96.6, 59.1, 14.1. LCMS-ESI (m/z): [M+H]$^+$ calculated for C$_{18}$H$_{16}$O$_4$NS, 342.1; found, 342.0.

*Ethyl (Z)-4-oxo-2-(phenylamino)-5-(thiophen-2-ylmethylene)-4,5-dihydrothiophene-3-carboxylate* (**16b**)
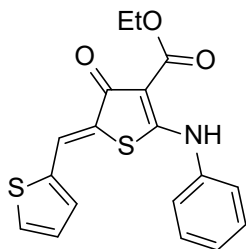
By using general procedure 7 with **11a** (100 mg, 0.38 mmol), 2-thenaldehyde (39 μL, 0.42 mmol), and piperidine (37.5 μL, 0.38 mmol) in ethanol (3.5 mL) with a reaction time of 4 h. The product was purified with purification method 1 to give the desired product (116 mg, 0.32 mmol, 85%). ^{1}H NMR (700 MHz, DMSO-d_6) δ 11.27 (s, 1H), 7.85 (s, 1H), 7.82 (dt, J = 5.0, 1.1 Hz, 1H), 7.58 (dt, J = 3.7, 1.1 Hz, 1H), 7.56–7.49 (m, 4H), 7.48–7.43 (m, 1H), 7.20 (dd, J = 5.0, 3.7 Hz, 1H), 4.27 (q, J = 7.1 Hz, 2H), 1.29 (t, J = 7.1 Hz, 3H). ^{13}C NMR (176 MHz, DMSO-d_6) δ 180.2, 174.4, 164.3, 137.2 (2), 133.6, 131.4, 129.2 (2), 128.4, 127.9, 125.4 (2), 125.2, 122.1, 96.8, 59.2, 14.1. HRMS-ESI (m/z): calculated for [M+H]$^+$ $C_{18}H_{16}O_3NS_2$, 358.0566; found, 358.0568.

Ethyl (Z)-5-((1H-pyrrol-2-yl)methylene)-4-oxo-2-(phenylamino)-4,5-dihydrothiophene-3-carboxylate (**16c**)
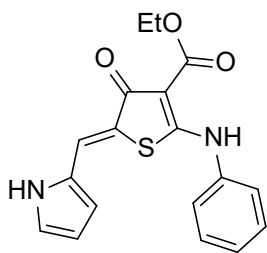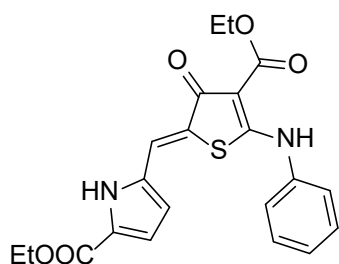
By using general procedure 7 with **11a** (100 mg, 0.38 mmol), pyrrole-2-carboxaldehyde (40 mg, 0.42 mmol), and piperidine (37.5 μL, 0.38 mmol) in ethanol (3.0 mL) with a reaction time of 5 h. The product was purified with purification method 1 to give the desired product (118 mg, 0.35 mmol, 91%, d.r. 7.5:1). ^{1}H NMR (700 MHz, DMSO-d_6) δ 11.61 (s, 1H), 11.20 (s, 1H), 7.55 (s, 1H), 7.54–7.49 (m, 4H), 7.45–7.39 (m, 1H), 7.10–7.09 (m, 1H), 6.35–6.33 (m, 1H), 6.25–6.23 (m, 1H), 4.26 (q, J = 7.1 Hz, 2H), 1.28 (t, J = 7.1 Hz, 3H). ^{13}C NMR (176 MHz, DMSO-d_6) δ 180.5, 173.8, 164.7, 137.3, 129.2 (2), 127.5, 126.7, 124.8 (2), 123.2, 120.0, 119.7, 112.3, 111.1, 97.0, 59.0, 14.1. HRMS-ESI (m/z): calculated for [M+H]$^+$ $C_{18}H_{17}O_3N_2S$, 341.0954; found, 341.0954.

Ethyl (Z)-5-((1H-pyrrol-3-yl)methylene)-4-oxo-2-(phenylamino)-4,5-dihydrothiophene-3-carboxylate (**16d**)
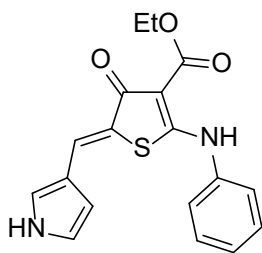
By using general procedure 7 with **11a** (100 mg, 0.38 mmol), pyrrole-3-carboxaldehyde (40 mg, 0.42 mmol), and piperidine (37.5 μL, 0.38 mmol) in ethanol (3.0 mL) with a reaction time of 4 h. The product was purified with purification method 2 to give the desired product (103 mg, 0.30 mmol, 80%). ^{1}H NMR (700 MHz, CDCl$_3$) δ 11.43 (s, 1H), 8.90 (s, 1H), 7.82 (s, 1H), 7.50–7.45 (m, 2H), 7.42–7.39 (m, 2H), 7.38–7.35 (m, 1H), 7.16–

7.15 (m, 1H), 6.85–6.84 (m, 1H), 6.45–6.44 (m, 1H), 4.40 (q, J = 7.1 Hz, 2H), 1.42 (t, J = 7.1 Hz, 3H). ^{13}C NMR (176 MHz, CDCl$_3$) δ 182.4, 175.3, 167.0, 137.4, 129.8 (2), 127.5, 126.7, 123.9 (2), 123.5, 122.3, 120.3, 119.5, 109.1, 98.6, 60.5, 14.4. HRMS-ESI (m/z): calculated for [M+H]$^+$ C$_{18}$H$_{17}$O$_3$N$_2$S, 341.0954; found, 341.0910.

*Ethyl (Z)-5-((4-(ethoxycarbonyl)-3-oxo-5-(phenylamino)thiophen-2(3H)-ylidene)methyl)-1H-pyrrole-2-carboxylate* (**16e**)

By using general procedure 7 with **11a** (100 mg, 0.38 mmol), ethyl-5-formyl-1H-pyrrole-2-carboxaldehyde (70 mg, 0.42 mmol), and piperidine (37.5 μL, 0.38 mmol) in ethanol (3.0 mL) with a reaction time of 4 h. The product was purified with purification method 1 to give the desired product (140 mg, 0.34 mmol, 89%). ^{1}H NMR (700 MHz, DMSO-d_6) δ 12.52 (s, 1H), 11.29 (s, 1H), 7.64 (s, 1H), 7.57–7.50 (m, 4H), 7.47–7.43 (m, 1H), 6.87 (t, J = 4.0, 2.3 Hz, 1H), 6.35 (dd, J = 4.0, 2.3 Hz, 1H), 4.30–4.24 (m, 4H), 1.33–1.27 (m, 6H). ^{13}C NMR (176 MHz, DMSO-d_6) δ 180.2, 174.2, 164.4, 159.5, 137.1, 131.2, 129.2 (2), 127.8, 125.3, 125.1 (2), 124.7, 118.5, 116.5, 112.1, 96.7, 59.8, 59.1, 14.0, 13.9. HRMS-ESI (m/z): calculated for [M+H]$^+$ C$_{21}$H$_{21}$O$_5$N$_2$S, 413.1166; found, 413.1162.

Ethyl (Z)-4-oxo-2-(phenylamino)-5-(pyridin-3-ylmethylene)-4,5-dihydrothiophene-3-carboxylate (**16f**)
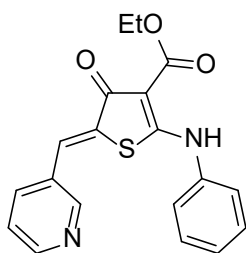
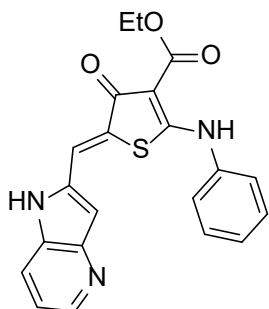By using general procedure 7 with **11a** (100 mg, 0.38 mmol), 3-pyridinecarboxaldehyde (39 μL, 0.42 mmol), and piperidine (37.5 μL, 0.38 mmol) in ethanol (3.0 mL) with a reaction time of 8 h. The product was purified with purification method 2 to give the desired product (70 mg, 0.20 mmol, 52%, d.r. 9:1). ^{1}H NMR (700 MHz, DMSO-d_6) δ 11.34 (s, 1H), 8.76 (d, J = 2.0 Hz, 1H), 8.55 (dd, J = 4.8, 2.0 Hz, 1H), 7.89 (dt, J = 7.9, 2.0 Hz, 1H), 7.66 (s, 1H), 7.55–7.47 (m, 5H), 7.47–7.42 (m, 1H), 4.29 (q, J = 7.1 Hz, 2H), 1.30 (t, J = 7.1 Hz, 3H). ^{13}C NMR (176 MHz, CDCl$_3$) δ 181.3, 176.1, 166.8, 150.4, 149.4, 136.9, 136.8, 130.5, 130.3, 129.9 (2), 128.2, 127.0, 124.3 (2), 123.8, 97.7, 60.8, 14.4. HRMS-ESI (m/z): calculated for [M+H]$^+$ C$_{19}$H$_{17}$O$_3$N$_2$S, 353.0954; found, 353.0959.

*Ethyl (Z)-5-((1H-indol-3-yl)methylene)-4-oxo-2-(phenylamino)-4,5-dihydrothiophene-3-carboxylate* (**16g**)
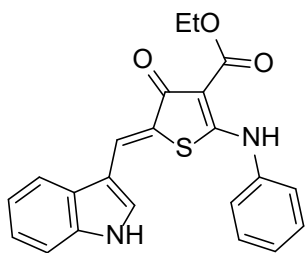
By using general procedure 7 with **11a** (100 mg, 0.38 mmol), indole-3-carboxaldehyde (61 mg, 0.42 mmol), and piperidine (37.5 μL, 0.38 mmol) in ethanol (3.0 mL) with a reaction time of 4 h. The product was purified with purification method 1 to give the desired product (134 mg, 0.34 mmol, 91%). ^{1}H NMR (700 MHz, DMSO-d_6) δ 11.84 (s, 1H), 11.23 (s, 1H), 7.91 (s, 1H), 7.78 (d, J = 7.9 Hz, 1H), 7.63 (d, J = 2.7 Hz, 1H), 7.56–7.51 (m, 4H), 7.48 (d, J = 8.0 Hz, 1H), 7.45–7.40 (m, 1H), 7.22 (t, J = 7.5 Hz, 1H), 7.17 (t, J = 7.5 Hz, 1H), 4.28 (q, J = 7.1 Hz, 2H), 1.30 (t, J = 7.1 Hz, 3H). ^{13}C NMR (176 MHz, DMSO-d_6) δ 180.4, 173.5, 164.7, 137.3, 135.8, 129.3 (2), 127.4, 127.4, 126.6, 124.7 (2), 122.5, 121.3, 121.2, 120.4, 117.7, 112.0, 109.9, 97.1, 59.1, 14.0. HRMS-ESI (m/z): calculated for [M+H]$^+$ $C_{22}H_{19}O_3N_2S$, 391.1110; found, 391.1113.

Ethyl (Z)-5-((1H-pyrrolo[3,2-b]pyridin-2-yl)methylene)-4-oxo-2-(phenylamino)-4,5-dihydrothiophene-3-carboxylate (**17a**)

By using general procedure 7 with **11a** (50 mg, 0.19 mmol), **14a** (31 mg, 0.21 mmol), and piperidine (18.8 μL, 0.19 mmol) in ethanol (1.5 mL) with a reaction time of 4 h. The product was purified with purification method 1 to give the desired product (47 mg, 0.12 mmol, 64%). ^{1}H NMR (600 MHz, DMSO-d_6) δ 11.85 (s, 1H), 11.38 (s, 1H), 8.36 (dd, J = 4.5, 1.3 Hz, 1H), 7.80 (dt, J = 8.2, 1.3 Hz, 1H), 7.65 (s, 1H), 7.59–7.52 (m, 4H), 7.49–7.43 (m, 1H), 7.17 (dd, J = 8.2, 4.5 Hz, 1H), 6.71 (s, 1H), 4.29 (q, J = 7.1 Hz, 2H), 1.30 (t, J = 7.1 Hz, 3H). ^{13}C NMR (151 MHz, DMSO-d_6) δ 179.9, 174.3, 164.3, 145.4, 143.8, 137.1, 134.9, 129.7, 129.2 (2), 128.5, 127.8, 125.1 (2), 118.6, 118.5, 118.0, 104.0, 96.6, 59.2, 14.0. HRMS-ESI (m/z): calculated for [M+H]$^+$ $C_{21}H_{18}O_3N_3S$, 392.1063; found, 392.1055.

Ethyl (Z)-5-((1H-pyrrolo[2,3-c]pyridin-2-yl)methylene)-4-oxo-2-(phenylamino)-4,5-dihydrothiophene-3-carboxylate (**17b**)
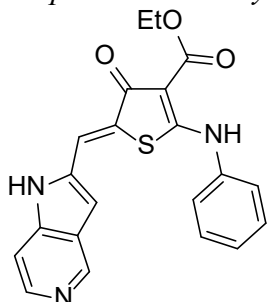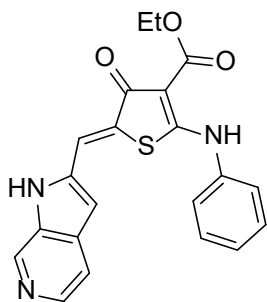
By using general procedure 7 with **11a** (30 mg, 0.11 mmol), **14b** (18 mg, 0.13 mmol), and piperidine (11.3 μL, 0.11 mmol) in ethanol (1 mL) with a reaction time of 4 h. The product was purified with purification method 1 to give the desired product (28 mg, 0.07 mmol, 63%). ^{1}H NMR (400 MHz, DMSO-d_6) δ 11.99 (s, 1H), 11.39 (s, 1H), 8.90 (s, 1H),

8.19 (d, J = 5.6 Hz, 1H), 7.65 (s, 1H), 7.61–7.40 (m, 5H), 7.38 (d, J = 5.8 Hz, 1H), 6.79 (s, 1H), 4.28 (q, J = 7.1 Hz, 2H), 1.30 (t, J = 7.1 Hz, 3H). HRMS-ESI (m/z): calculated for [M+H]$^+$ $C_{21}H_{18}O_3N_3S$, 392.1063; found, 392.1066.

Ethyl (Z)-5-((1H-pyrrolo[3,2-c]pyridin-2-yl)methylene)-4-oxo-2-(phenylamino)-4,5-dihydro thiophene-3-carboxylate (**17c**)

By using general procedure 7 with **11a** (50 mg, 0.19 mmol), **14c** (31 mg, 0.21 mmol), and piperidine (18.8 μL, 0.19 mmol) in ethanol (1.5 mL) with a reaction time of 4 h. The product was purified with purification method 1 to give the desired product (58 mg, 0.15 mmol, 77%). ^{1}H NMR (600 MHz, DMSO-d_6) δ 12.08 (s, 1H), 11.45 (s, 1H), 8.79 (s, 1H), 8.10 (d, J = 5.6 Hz, 1H), 7.67 (s, 1H), 7.60–7.51 (m, 5H), 7.49–7.41 (m, 1H), 6.68 (s, 1H), 4.29 (q, J = 7.1 Hz, 2H), 1.31 (t, J = 7.1 Hz, 3H). ^{13}C NMR (151 MHz, DMSO-d_6) δ 180.8, 170.8, 165.1, 138.8, 136.3, 135.5, 134.3, 132.8, 130.6, 130.1, 130.0, 128.6, 126.0 (2), 118.9, 115.5 (2), 103.6, 97.4, 60.0, 14.9. HRMS-ESI (m/z): calculated for [M+H]$^+$ $C_{21}H_{18}O_3N_3S$, 392.1063; found, 392.1056.

*Ethyl (Z)-5-((1H-pyrrolo[2,3-b]pyridin-2-yl)methylene)-4-oxo-2-(phenylamino)-4,5-dihydro thiophene-3-carboxylate* (**17d**)
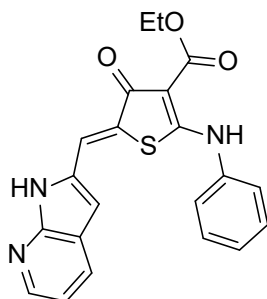
By using general procedure 7 with **11a** (50 mg, 0.19 mmol), **14d** (31 mg, 0.21 mmol), and piperidine (18.8 μL, 0.19 mmol) in ethanol (1.5 mL) with a reaction time of 4 h. The product was purified with purification method 1 to give the desired product (58 mg, 0.15 mmol, 78%). ^{1}H NMR (700 MHz, DMSO-d_6) δ 12.13 (s, 1H), 11.35 (s, 1H), 8.28 (dd, J = 4.6, 1.3 Hz, 1H), 8.02 (dd, J = 7.9, 1.3 Hz, 1H), 7.66 (s, 1H), 7.58–7.53 (m, 4H), 7.49–7.46 (m, 1H), 7.08 (dd, J = 7.9, 4.6 Hz, 1H), 6.64 (d, J = 1.7 Hz, 1H), 4.29 (q, J = 7.1 Hz, 2H), 1.30 (t, J = 7.1 Hz, 3H). ^{13}C NMR (176 MHz, DMSO-d_6) δ 180.0, 174.4, 164.3, 148.5, 144.9, 137.1, 132.4, 129.3 (2), 129.0, 127.9, 127.8, 125.3 (2), 120.3, 118.7, 116.3, 102.7, 96.7, 59.2, 14.1. HRMS-ESI (m/z): calculated for [M+H]$^+$ $C_{21}H_{18}O_3N_3S$, 392.1063; found, 392.1064.

*Ethyl 5-cyclohexylidene-4-oxo-2-(phenylamino)-4,5-dihydrothiophene-3-carboxylate* (**18a**)
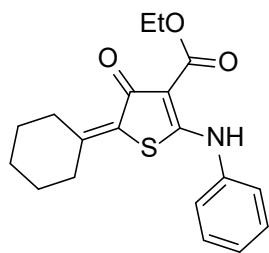
By using general procedure 7 with **11a** (100 mg, 0.38 mmol), cyclohexanone (39 μL, 0.42 mmol), and piperidine (37.5 μL, 0.38 mmol) in ethanol (3.0 mL) with a reaction time of 4 h. The product was purified with purification method 2 to give the desired product (64 mg, 0.19 mmol, 49%). ^{1}H NMR (600 MHz, CDCl$_3$) δ 11.36 (s, 1H), 7.48–7.41 (m, 2H), 7.39–7.30 (m, 3H), 4.38 (q, J = 7.1 Hz, 2H), 3.27 (d, J = 6.1 Hz, 2H), 2.26 (t, J = 6.1 Hz, 2H), 1.76–1.57 (m, 6H), 1.43 (t, J = 7.1 Hz, 3H). ^{13}C NMR (151 MHz, CDCl$_3$) δ 182.7, 173.6, 167.2, 154.8, 137.4, 129.6 (2), 127.2, 123.8 (2), 122.4, 100.9, 60.3, 37.8, 29.6, 28.1, 27.9, 26.2, 14.4. HRMS-ESI (m/z): calculated for [M+H]$^+$ C$_{19}$H$_{22}$O$_3$NS, 344.1315; found, 344.1317.

Ethyl 5-cyclobutylidene-4-oxo-2-(phenylamino)-4,5-dihydrothiophene-3-carboxylate (**18e**)
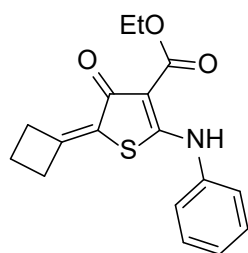
By using general procedure 7 with **11a** (100 mg, 0.38 mmol), cyclobutanone (56 μL, 0.42 mmol), and piperidine (37.6 μL, 0.38 mmol) in ethanol (3.0 mL) with a reaction time of 4 h. The product was purified with purification method 2 to give the desired product (60 mg, 0.19 mmol, 50%). ^{1}H NMR (500 MHz, CDCl$_3$) δ 11.34 (s, 1H), 7.48–7.40 (m, 2H), 7.39–7.29 (m, 3H), 4.35 (q, J = 7.1 Hz, 2H), 3.33 (t, J = 7.9 Hz, 2H), 2.80 (t, J = 7.9 Hz, 2H), 2.23 (p, J = 7.9 Hz, 2H), 1.40 (t, J = 7.1 Hz, 3H). ^{13}C NMR (126 MHz, CDCl3) δ 182.1, 175.2, 166.9, 155.8, 137.2, 129.5 (2), 127.2, 123.6 (2), 120.0, 99.0, 60.2, 33.8, 31.9, 19.0, 14.3. HRMS-ESI (m/z): calculated for [M+H]$^+$ C$_{17}$H$_{18}$O$_3$NS, 316.1002; found, 316.1006.

Ethyl (Z)-5-(cyclohexylmethylene)-4-oxo-2-(phenylamino)-4,5-dihydrothiophene-3-carboxylate (**19**)
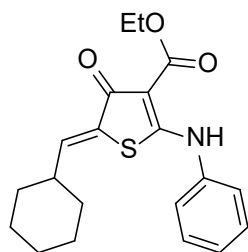
By using general procedure 7 with **11a** (100 mg, 0.38 mmol), cyclohexanecarboxaldehyde (51 μL, 0.42 mmol), and piperidine (37.5 μL, 0.38 mmol) in ethanol (3.0 mL) with a reaction time of 5 h. The product was purified with purification method 2 to give the desired product (92 mg, 0.28 mmol, 68%). ^{1}H NMR (700 MHz, DMSO-d_6) δ 11.21 (s, 1H), 7.51 (t, J = 7.6 Hz, 2H), 7.45 (d, J = 7.6 Hz, 2H), 7.42 (t, J = 7.6 Hz, 1H), 6.57 (d, J = 9.7 Hz, 1H), 4.24 (q, J = 7.1 Hz, 2H), 2.14–2.05 (m, 1H), 1.67–1.53 (m, 5H), 1.26 (t, J = 7.1 Hz, 3H), 1.24–1.11 (m, 5H). ^{13}C NMR (176 MHz, DMSO-d_6) δ 179.7, 175.0, 164.4, 137.6, 137.2, 129.2 (2), 128.5, 127.8, 125.2 (2), 97.5, 59.0, 30.7 (2), 30.1, 24.8, 24.3 (2), 14.0.

HRMS-ESI (m/z): calculated for $[M+H]^+$ $C_{20}H_{24}O_3NS$, 358.1471; found, 358.1476.

Ethyl-5-((1H-pyrrol-2-yl)methylene)-2-((4-methoxyphenyl)amino)-4-oxo-4,5-dihydrothio phene-3-carboxylate (**20a**)
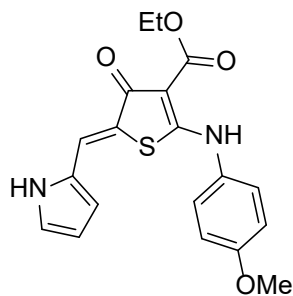
By using general procedure 7 with **11b** (100 mg, 0.34 mmol), pyrrol-1-carboxyaldehyde (35 mg, 0.37 mmol), and piperidine (33.6 µL, 0.34 mmol) in ethanol (3.3 mL) with a reaction time of 2 h. The product was purified with purification method 1 to give the desired product (99.8 mg, 0.27 mmol, 79%, d.r. 9:1). ^{1}H NMR (600 MHz, CDCl$_3$) δ 13.48 (s, 1H), 11.11 (s, 1H), 7.29 (d, *J* = 8.8 Hz, 2H), 7.04–7.02 (m, 1H), 6.97 (d, *J* = 8.8 Hz, 2H), 6.76 (s, 1H), 6.54 -6.52 (m, 1H), 6.32 - 6.30 (m, 1H), 4.47 (q, *J* = 7.1 Hz, 2H), 3.85 (s, 3H), 1.46 (t, *J* = 7.1 Hz, 3H). ^{13}C NMR (151 MHz, CDCl$_3$) δ 181.7, 175.5, 167.1, 159.1, 130.3, 129.6, 126.3, 125.9 (2), 124.1, 119.7, 118.8, 115.0 (2), 111.5, 100.6, 60.8, 55.7, 14.9. HRMS-ESI (m/z): calculated for $[M+H]^+$ $C_{19}H_{19}O_4N_2S$, 371.1060; found, 371.1062.

Ethyl-5-((1H-pyrrol-2-yl)methylene)-2-((3-methoxyphenyl)amino)-4-oxo-4,5-dihydrothio phene-3-carboxylate (**20b**)
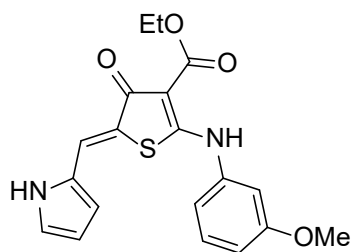
By using general procedure 7 with **11c** (100 mg, 0.34 mmol), pyrrol-1-carboxyaldehyde (35 mg, 0.37 mmol), and piperidine (33.6 µL, 0.34 mmol) in ethanol (3.3 mL) with a reaction time of 2 h. The product was purified with purification method 1 to give the desired product (99.9 mg, 0.27 mmol, 79%, d.r. 5:1). ^{1}H NMR (500 MHz, CDCl$_3$) δ 13.50 (s, 1H), 11.44 (s, 1H), 7.35 (t, *J* = 8.0 Hz, 1H), 7.06–7.04 (m, 1H), 6.97 (dd, *J* = 8.0, 2.3 Hz, 1H), 6.91 (t, *J* = 2.3 Hz, 1H), 6.87 (dd, dd, *J* = 8.0, 2.3 Hz, 1H), 6.82 (s, 1H), 6.58–6.54 (m, 1H), 6.33–6.31 (m, 1H), 4.48 (q, *J* = 7.1 Hz, 2H), 3.85 (s, 3H), 1.46 (t, *J* = 7.1 Hz, 3H). ^{13}C NMR (126 MHz, CDCl$_3$) δ 181.5, 173.9, 167.2, 160.7, 138.7, 130.7, 129.7, 126.6, 124.3, 119.4, 119.1, 115.3, 113.1, 111.6, 108.9, 101.1, 60.9, 55.7, 14.8. HRMS-ESI (m/z): calculated for $[M+H]^+$ $C_{19}H_{19}O_4N_2S$, 371.1060; found, 371.1062.

*Ethyl-5-((1H-pyrrol-2-yl)methylene)-2-((3,4-dimethoxyphenyl)amino)-4-oxo-4,5-dihydro thiophene-3-carboxylate* (**20c**)
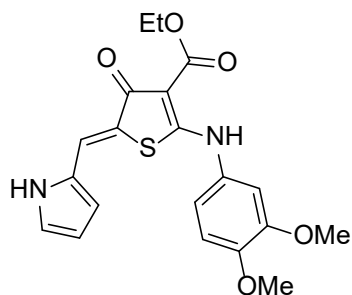
By using general procedure 7 with **11d** (100 mg, 0.31 mmol), pyrrol-1-carboxyaldehyde (32 mg, 0.33 mmol), and piperidine (30.5 µL, 0.31 mmol) in ethanol (3.3 mL) with a reaction time of 6 h The product was purified with purification method 1 to give the desired product (86.7 mg, 0.22 mmol, 70%, d.r. 6:1). ^{1}H NMR (600 MHz, CDCl$_3$) δ 13.53 (s, 1H), 11.10 (s, 1H), 7.39 (d, J = 8.6 Hz, 1H), 7.05–7.00 (m, 1H), 6.77 (s, 1H), 6.56 (d, J = 2.6 Hz, 1H), 6.53–6.51 (m, 2H), 6.30 (dt, J = 3.5, 2.6 Hz, 1H), 4.48 (q, J = 7.1 Hz, 2H), 3.88 (s, 3H), 3.85 (s, 3H), 1.46 (t, J = 7.1 Hz, 3H). ^{13}C NMR (151 MHz, CDCl$_3$) δ 181.6, 174.5, 166.9, 159.9, 153.8, 129.7, 126.1, 124.5, 124.0, 120.1, 119.9, 118.6, 111.4, 104.0, 101.0, 99.7, 60.7, 56.1, 55.8, 14.9. HRMS-ESI (m/z): calculated for [M+H]$^{+}$ C$_{20}$H$_{21}$O$_5$N$_2$S, 401.1166; found, 401.1167.

Ethyl-5-((1H-pyrrol-2-yl)methylene)-2-((4-bromophenyl)amino)-4-oxo-4,5-dihydrothiophene-3-carboxylate (**20d**)
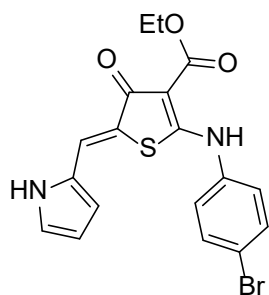
By using general procedure 7 with **11e** (100 mg, 0.29 mmol), pyrrol-1-carboxyaldehyde (30 mg, 0.32 mmol), and piperidine (28.9 µL, 0.29 mmol) in ethanol (3.3 mL) with a reaction time of 1 h. The product was purified with purification method 1 to give the desired product (103.6 mg, 0.25 mmol, 84%, d.r. 2:1). ^{1}H NMR (700 MHz, DMSO-d_6) δ 11.61 (s, 1H), 11.14 (s, 1H), 7.71 (m, J = 8.7 Hz, 2H), 7.55 (s, 1H), 7.49 (d, J = 8.7 Hz, 2H), 7.12–7.10 (m, 1H), 6.39–6.39 (m, 1H), 6.26–6.25 (m, 1H), 4.26 (q, J = 7.1 Hz, 2H), 1.29 (t, J = 7.1 Hz, 3H). ^{13}C NMR (176 MHz, DMSO-d_6) δ 180.9, 174.0, 164.9, 132.4 (2), 127.4 (2), 127.2, 127.0, 123.7, 120.5, 120.3, 120.2, 112.9, 111.5, 97.7, 59.4, 14.4. HRMS-ESI (m/z): calculated for [M+H]$^{+}$ C$_{18}$H$_{16}$O$_3$N$_2$BrS, 419.0060; found, 419.0061.

*Ethyl-5-((1H-pyrrol-2-yl)methylene)-2-((2-bromophenyl)amino)-4-oxo-4,5-dihydrothiophene-3-carboxylate* (**20e**)
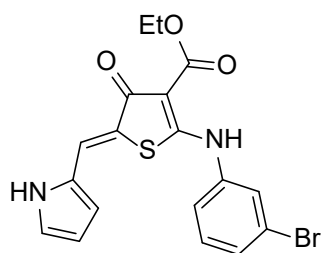
By using general procedure 7 with **11f** (100 mg, 0.29 mmol), pyrrol-1-carboxyaldehyde (30 mg, 0.32 mmol), and piperidine (28.9 µL, 0.29 mmol) in ethanol (3.3 mL) with a reaction time of 2 h. The product was purified with purification method 1 to give the desired product (98.7 mg, 0.24 mmol, 81%, d.r. 3:1). ^{1}H NMR (700

MHz, DMSO-d_6) δ 11.62 (s, 1H), 11.17 (s, 1H), 7.85 (dd, J = 7.7, 1.3 Hz, 1H), 7.72 (d, J = 7.7 Hz, 1H), 7.59–7.55 (m, 2H), 7.42 (td, J = 7.7, 1.3 Hz, 1H), 7.12 - 7.10 (m, 1H), 6.32–6.32 (m, 1H), 6.25–6.23 (m, 1H), 4.28 (q, J = 7.1 Hz, 2H), 1.30 (t, J = 7.1 Hz, 3H). ^{13}C NMR (176 MHz, DMSO-d_6) δ 180.9, 164.9, 133.5, 133.4, 130.1, 129.0, 128.0, 127.0, 123.7, 120.6, 120.4, 120.2, 112.8, 111.5, 100.0, 97.6, 59.5, 14.4. HRMS-ESI (m/z): calculated for [M+H]$^+$ C$_{18}$H$_{16}$O$_3$N$_2$BrS, 419.0060; found, 419.0060.

Ethyl-5-((1H-pyrrol-2-yl)methylene)-2-((4-fluorophenyl)amino)-4-oxo-4,5-dihydrothiophene-3-carboxylate (**20f**)
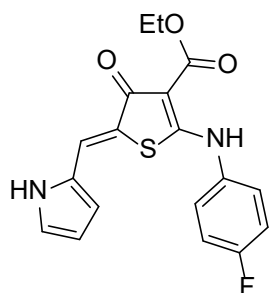
By using general procedure 7 with **11g** (100 mg, 0.36 mmol), pyrrol-1-carboxyaldehyde (37 mg, 0.36 mmol), and piperidine (35.1 μL, 0.36 mmol) in ethanol (3.3 mL) with a reaction time of 2 h. The product was purified with purification method 1 to give the desired product (98.1 mg, 0.27 mmol, 77%, d.r. 4:1). ^{1}H NMR (700 MHz, CDCl$_3$) δ 13.47 (s, 1H), 11.24 (s, 1H), 7.37–7.35 (m, 2H), 7.17–7.14 (m, 2H), 7.06–7.04 (m, 1H), 6.80 (s, 1H), 6.57–6.55 (m, 1H), 6.33 - 6.32 (m, 1H), 4.48 (q, J = 7.1 Hz, 2H), 1.46 (t, J = 7.1 Hz, 3H). ^{13}C NMR (176 MHz, CDCl$_3$) δ 181.6, 175.0, 167.1, 162.4 and 160.9 (d, $^1J_{\text{C-F}}$ = 162 Hz), 133.5 and 133.5 (d, $^4J_{\text{C-F}}$ = 4 Hz), 129.6, 126.7, 126.1 and 126.1 (d, $^3J_{\text{C-F}}$ = 9 Hz) (2), 124.4, 119.2, 119.2, 117.0 and 116.9 (d, $^2J_{\text{C-F}}$ = 23 Hz) (2), 111.7, 101.0, 60.9, 14.8. HRMS-ESI (m/z): calculated for [M+H]$^+$ C$_{18}$H$_{16}$O$_3$N$_2$FS, 359.0860; found, 359.0863.

Ethyl-5-((1H-pyrrol-2-yl)methylene)-2-((3-fluorophenyl)amino)-4-oxo-4,5-dihydrothiophene-3-carboxylate (**20g**)
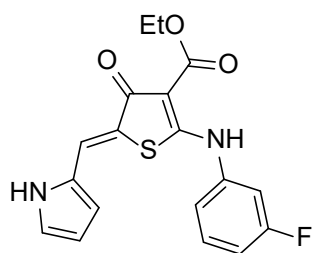
By using general procedure 7 with **11h** (100 mg, 0.36 mmol), pyrrol-1-carboxyaldehyde (37 mg, 0.36 mmol), and piperidine (35.1 μL, 0.36 mmol) in ethanol (3.3 mL) with a reaction time of 2 h. The product was purified with purification method 1 to give the desired product (96.5 mg, 0.27 mmol, 76%, d.r. 3.5:1). ^{1}H NMR (700 MHz, CDCl$_3$) δ 13.49 (s, 1H), 11.53 (s, 1H), 7.42 (td, J = 8.2, 7.9 Hz, 1H), 7.17 (dd, J = 8.2, 2.1 Hz, 1H), 7.14 (dt, J = 7.9, 2.1 Hz, 1H), 7.08–7.05 (m, 1H), 7.02 (td, J = 8.2, 2.1 Hz, 1H), 6.85 (s, 1H), 6.59- 6.57 (m, 1H), 6.34 (m, 1H), 4.48 (q, J = 7.1 Hz, 2H), 1.46 (t, J = 7.1 Hz, 3H). ^{13}C NMR (176 MHz, CDCl$_3$) δ 181.4, 173.5, 167.1, 164.0 and 162.6 (d, $^1J_{\text{C-F}}$ = 249 Hz), 139.1 and 139.1 (d, $^3J_{\text{C-F}}$ = 10 Hz), 131.3 and 131.3 (d, $^3J_{\text{C-F}}$ = 10 Hz), 129.7, 127.0, 124.6, 119.5, 118.9, 118.8 and 118.7 (d, $^4J_{\text{C-F}}$ = 3 Hz), 114.2 and 114.1 (d, $^2J_{\text{C-F}}$ = 22 Hz), 111.8, 110.6 and 110.4 (d,

$^2J_{C-F}$ = 22 Hz), 101.5, 61.0, 14.8. HRMS-ESI (m/z): calculated for [M+H]$^+$ C$_{18}$H$_{16}$O$_3$N$_2$FS, 359.0860; found, 359.0861.

Ethyl-5-((1H-pyrrol-2-yl)methylene)-4-oxo-2-((4-(trifluoromethyl)phenyl)amino)-4,5-dihydro thiophene-3-carboxylate (**20h**)
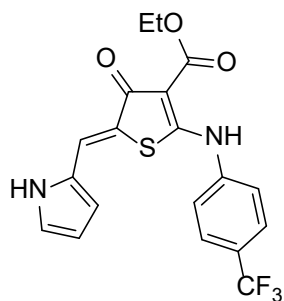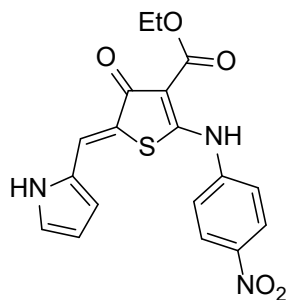
By using general procedure 7 with **11i** (100 mg, 0.30 mmol), pyrrol-1-carboxyaldehyde (31 mg, 0.33 mmol), and piperidine (29.8 µL, 0.30 mmol) in ethanol (3.3 mL) with a reaction time of 2 h. The product was purified with purification method 1 to give the desired product (86.9 mg, 0.21 mmol, 71%, d.r. 3:1). ^{1}H NMR (700 MHz, CDCl$_3$) δ 13.50 (s, 1H), 11.72 (s, 1H), 7.72 (d, *J* = 8.5 Hz, 2H), 7.50 (d, *J* = 8.5 Hz, 2H), 7.08 (s, 1H), 6.87 (s, 1H), 6.62–6.59 (m, 1H), 6.35 (m, 1H), 4.49 (q, *J* = 7.1 Hz, 2H), 1.47 (t, *J* = 7.1 Hz, 3H). ^{13}C NMR (176 MHz, CDCl$_3$) δ 181.2, 172.9, 167.2, 140.8, 129.7, 129.0 and 128.8 and 128.6 and 128.4 (q, $^2J_{C-F}$ = 33 Hz) 127.3, 127.3 and 127.2 and 127.2 and 127.2 (q, $^3J_{C-F}$ = 4 Hz) (2), 126.2 and 124.8 and 123.1 and 121.5 (q, $^1J_{C-F}$ = 272 Hz), 124.8, 122.6 (2), 119.9, 118.5, 112.0, 102.0, 61.2, 14.8. HRMS-ESI (m/z): calculated for [M+H]$^+$ C$_{19}$H$_{16}$O$_3$N$_2$F$_3$S, 409.0828; found, 409.0830.

*Ethyl-5-((1H-pyrrol-2-yl)methylene)-4-oxo-2-((3-(trifluoromethyl)phenyl)amino)-4,5-dihydro thiophene-3-carboxylate* (**20i**)
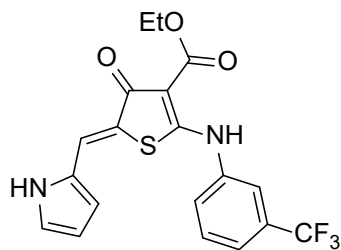
By using general procedure 7 with **11j** (100 mg, 0.30 mmol), pyrrol-1-carboxyaldehyde (31 mg, 0.33 mmol), and piperidine (29.8 µL, 0.30 mmol) in ethanol (3.3 mL) with a reaction time of 2 h. The product was purified with purification method 1 to give the desired product (83.8 mg, 0.21 mmol, 68%, d.r. 4:1). ^{1}H NMR (700 MHz, CDCl$_3$) δ 13.48 (s, 1H), 11.61 (s, 1H), 7.66 (s, 1H), 7.61–7.56 (m, 3H), 7.08 - 7.07 (m, 1H), 6.87 (s, 1H), 6.60–6.59 (m, 1H), 6.34 (m, 1H), 4.49 (q, *J* = 7.1 Hz, 2H), 1.47 (t, *J* = 7.1 Hz, 3H). ^{13}C NMR (176 MHz, CDCl$_3$) δ 181.3, 173.6, 167.2, 138.3, 132.8 and 132.7 and 132.5 and 132.3 (q, $^2J_{C-F}$ = 33 Hz), 130.7, 129.7, 127.2, 126.3, 125.9 and 124.3 and 122.8 and 121.2 (q, $^1J_{C-F}$ = 273 Hz), 124.7, 123.8 and 123.8 and 123.7 and 123.7 (q, $^3J_{C-F}$ = 4 Hz), 120.1 and 120.1 and 120.1 and 120.0 (q, $^3J_{C-F}$ = 4 Hz), 119.7, 118.6, 111.9, 101.7, 61.1, 14.8. HRMS-ESI (m/z): calculated for [M+H]$^+$ C$_{19}$H$_{16}$O$_3$N$_2$F$_3$S, 409.0828; found, 409.0830.

*Ethyl-5-((1H-pyrrol-2-yl)methylene)-2-((4-nitrophenyl)amino)-4-oxo-4,5-dihydrothiophene-3-carboxylate* (**20j**)

By using general procedure 7 with **11k** (100 mg, 0.32 mmol), pyrrol-1-carboxyaldehyde (33 mg, 0.35 mmol), and piperidine (32.0 μL, 0.32 mmol) in ethanol (3.3 mL) with a reaction time of 2 h. The product was purified with purification method 1 to give the desired product (106.0 mg, 0.28 mmol, 85%, d.r. 99:1). ^{1}H NMR (600 MHz, DMSO-d_6) δ 11.22 (s, 1H), 11.03 (s, 1H), 7.89 (d , J = 9.0 Hz, 2H), 7.34 (d, J = 9.0 Hz, 2H), 7.15 (s, 1H), 6.70–6.69 (m, 1H), 6.05–6.05 (m, 1H), 5.83–5.31 (m, 1H), 3.81 (q, J = 7.1 Hz, 2H), 0.82 (t, J = 7.1 Hz, 3H). ^{13}C NMR (151 MHz, DMSO-d_6) δ 180.8, 172.6, 164.8, 145.2, 143.4, 127.0, 125.1 (2), 124.6 (2), 124.2, 121.2, 119.5, 113.4, 111.8, 99.4, 59.8, 14.4. HRMS-ESI (m/z): calculated for [M+H]$^+$ C$_{18}$H$_{16}$O$_5$N$_3$S, 386.0805; found, 386.0807.

Ethyl-5-((1H-pyrrol-2-yl)methylene)-2-((3-nitrophenyl)amino)-4-oxo-4,5-dihydrothiophene-3-carboxylate (**20k**)
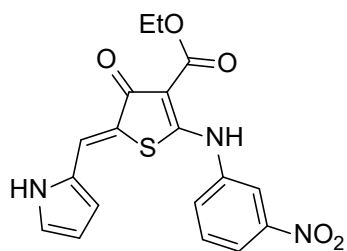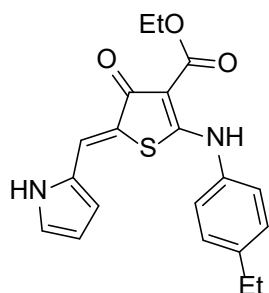
By using general procedure 7 with **11l** (100 mg, 0.32 mmol), pyrrol-1-carboxyaldehyde (33 mg, 0.35 mmol), and piperidine (32.0 μL, 0.32 mmol) in ethanol (3.3 mL) with a reaction time of 2 h. The product was purified with purification method 1 to give the desired product (102.7 mg, 0.27 mmol, 82%, d.r. 99:1). ^{1}H NMR (600 MHz, DMSO-d_6) δ 11.65 (s, 1H), 11.29 (s, 1H), 8.39 (t, J = 1.6 Hz, 1H), 8.25 (dd, J = 8.1, 1.6 Hz, 1H), 8.02 (dd, J = 8.13, 1.63 Hz, 1H), 7.81 (t, J = 8.1 Hz, 1H), 7.58 (s, 1H), 7.12 (m, 1H), 6.42–6.37 (m, 1H), 6.27–6.24 (m, 1H), 4.28 (q, J = 7.1 Hz, 2H), 1.30 (t, J = 7.1 Hz, 3H). ^{13}C NMR (151 MHz, DMSO-d_6) δ 198.4, 191.4, 182.1, 165.6, 156.3, 149.4, 148.4, 144.4, 141.3, 139.7, 138.0, 137.9, 137.3, 130.4, 129.1, 115.9, 77.0, 31.9. HRMS-ESI (m/z): calculated for [M+H]+ C$_{18}$H$_{16}$O$_5$N$_3$S, 386.0805; found, 386.0808.

Ethyl-5-((1H-pyrrol-2-yl)methylene)-4-oxo-2-(p-tolylamino)-4,5-dihydrothiophene-3-carboxylate (**20l**)
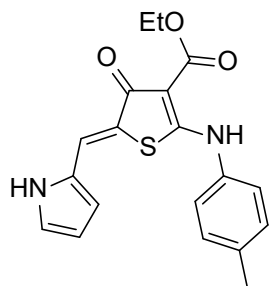
By using general procedure 7 with **11m** (100 mg, 0.36 mmol), pyrrol-1-carboxyaldehyde (37 mg, 0.39 mmol), and piperidine (35.6 μL, 0.36 mmol) in ethanol (3.3 mL) with a reaction time of 2 h. The product was purified with purification method 1 to give the desired product (56.7 mg, 0.16 mmol, 44%, d.r. 5:1). ^{1}H NMR (700 MHz, DMSO-d_6) δ 11.60 (s, 1H), 11.12 (s, 1H), 7.54 (s, 1H), 7.38 (d, J = 8.1 Hz, 2H), 7.33 (d, J = 8.1 Hz, 2H), 7.09 (m, 1H), 6.33 (s, 1H), 6.26–6.22 (m, 1H), 4.26 (q, J = 7.1 Hz, 2H), 2.37 (s, 3H), 1.29 (t, J = 7.1 Hz, 3H). ^{13}C NMR (176 MHz, DMSO-d_6) δ 180.9, 174.5, 165.0, 137.5, 135.1, 130.0 (2), 127.1, 125.1 (2), 123.4, 120.6, 119.9, 112.6, 111.4, 97.1, 59.4, 20.7, 14.4. HRMS-ESI (m/z): calculated for [M+H]+ $C_{19}H_{19}O_3N_2S$, 355.1111; found, 355.1112.

*Ethyl-5-((1H-pyrrol-2-yl)methylene)-2-((4-ethylphenyl)amino)-4-oxo-4,5-dihydrothiophene-3-carboxylate* (**20m**)

By using general procedure 7 with **11n** (100 mg, 0.36 mmol), pyrrol-1-carboxyaldehyde (37 mg, 0.39 mmol), and piperidine (35.6 μL, 0.36 mmol) in ethanol (3.3 mL) with a reaction time of 2 h. The product was purified with purification method 2 to give the desired product (80.5 mg, 0.22 mmol, 64%, d.r. 17:1). 1H NMR (600 MHz, DMSO-d_6) δ 11.61 (s, 1H), 11.14 (s, 1H), 7.54 (s, 1H), 7.41 (d, J = 8.5 Hz, 2H), 7.36 (d, J = 8.5Hz, 2H), 7.10–7.09 (m, 1H), 6.34 (s, 1H), 6.26–6.24 (m, 1H), 4.26 (q, J = 7.1 Hz, 2H), 2.67 (d, J = 7.6 Hz, 2H), 1.29 (t, J = 7.1 Hz, 3H), 1.23 (q, J = 7.6 Hz, 3H). ^{13}C NMR (151 MHz, DMSO-d_6) δ 180.9, 174.3, 165.1, 143.6, 135.3, 128.8 (2), 127.1, 125.1 (2), 123.5, 120.5, 112.0, 112.6, 111.4, 97.2, 59.4, 27.7, 15.4, 14.4. HRMS-ESI (m/z): calculated for [M+H]$^+$ $C_{20}H_{21}O_3N_2S$, 369.1267; found, 369.1268.

### 5.1.2.3 2-((Pyrrol-2-yl)methylene)thiophen-4-one

General procedure 8

The compounds were synthesized according to the previously reported method.[158-159] To a solution of 2-aminothiophenone-3-carboxylates or 2-aminofuranone-3-carboxylates (10.00 mmol) in EtOH (0.2 M) was added aqueous 50% w/w KOH solution (0.4 M) at room temperature. The mixture was stirred at 95° C for the given reaction time until the reaction mixture becomes transparent. The reaction mixture was cooled down to room temperature and neutralized under pH3 with 1M HCl solution. The precipitate was collected by filtration, washed with H_2O (KOH volume × 10), and dried overnight in ambient air or reduced pressure to afford the titled compound as solid.

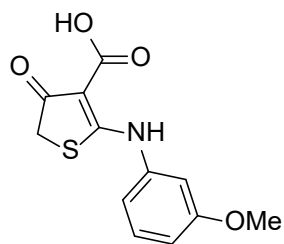*4-Oxo-2-(phenylamino)-4,5-dihydrothiophene-3-carboxylic acid* (**21a**)
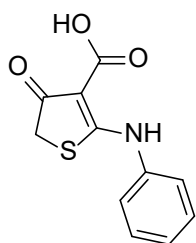
By using general procedure 8 with **11a** (10.0 mmol) for 1 h to give the desired product as an off-white solid (1.8 g, 6.6 mmol, 66%). ^{1}H NMR (700 MHz, DMSO-d_6) δ 12.81 (s, 1H), 11.28 (s, 1H), 7.53–7.49 (m, 2H), 7.47–7.45 (m, 2H), 7.44–7.40 (m, 1H), 4.04 (s, 2H). ^{13}C NMR (176 MHz, DMSO) δ 196.5, 182.3, 164.4, 136.7, 129.2 (2), 127.9, 124.6 (2), 97.6, 38.6.

*2-((3-Fluorophenyl)amino)-4-oxo-4,5-dihydrothiophene-3-carboxylic acid* (**21b**)
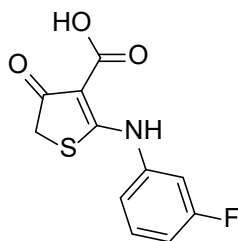
By using general procedure 8 with **11h** (10.0 mmol) for 1 h min to give the desired product as an off-white solid (2.2 g, 7.5 mmol, 75%). ^{1}H NMR (700 MHz, DMSO-d_6) δ 12.77 (s, 1H), 11.30 (s, 1H), 7.55 (td, J = 8.2, 6.5 Hz, 1H), 7.40 (dt, J = 10.0, 2.1 Hz, 1H), 7.34 (ddd, J = 8.2, 2.1, 0.9 Hz, 1H), 7.28 (tdd, J = 8.2, 2.1, 0.9 Hz, 1H), 4.05 (s, 2H). ^{13}C NMR (176 MHz, DMSO-d_6) δ 196.5, 182.4, 182.3, 164.3, 162.4 and 161.0 (d, $^1J_{C\text{-}F}$ = 246 Hz), 138.3 and 138.2 (d, $^3J_{C\text{-}F}$ = 10 Hz), 130.9 and 130.9 (d, $^3J_{C\text{-}F}$ = 9 Hz), 120.8 and 120.8 (d, $^4J_{C\text{-}F}$ = 3 Hz), 114.8 and 114.7 (d, $^2J_{C\text{-}F}$ = 21 Hz), 112.3 and 112.2 (d, $^2J_{C\text{-}F}$ = 24 Hz), 97.9, 38.7.

2-((3-Chlorophenyl)amino)-4-oxo-4,5-dihydrothiophene-3-carboxylic acid (**21c**)
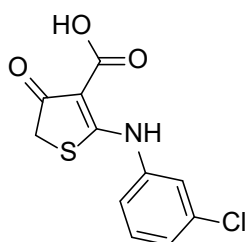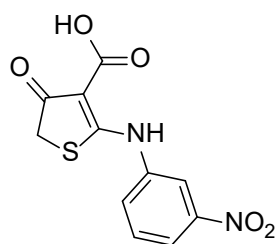
By using general procedure 8 with **11o** (10.0 mmol) for 30 min to give the desired product as an off-white solid (2.6 g, 8.5 mmol, 85%). ^{1}H NMR (700 MHz, DMSO-d_6) δ 14.37 (s, 1H), 7.27 (t, J = 8.0 Hz, 1H), 7.02 (d, J = 8.0 Hz, 1H), 6.89 (s, 1H), 6.83 (d, J = 8.0 Hz, 1H), 3.46 (s, 2H).

2-((3-Methoxyphenyl)amino)-4-oxo-4,5-dihydrothiophene-3-carboxylic acid (**21d**)
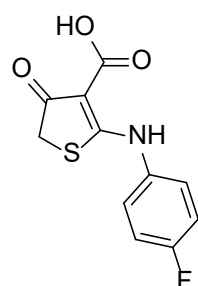
By using general procedure 8 with **11c** (5.7 mmol), EtOH (30 mL), and 50% w/w KOH solution (15 mL) for 1 h to give the desired product as an off-white solid (1.0 g, 3.2 mmol, 56%). ^{1}H NMR (700 MHz, DMSO-d_6) δ 12.82 (s, 1H), 11.25 (s, 1H), 7.42 (t, J = 8.1 Hz, 1H), 7.07 (t, J = 2.1 Hz, 1H), 7.05 (ddd, J = 8.1, 2.1, 0.8 Hz, 1H), 6.99 (ddd, J = 8.1, 2.1, 0.8 Hz, 1H), 4.06 (s, 2H), 3.80 (s, 3H). ^{13}C NMR (176 MHz, DMSO-d_6) δ 196.5, 182.2, 164.5, 159.6, 137.7, 130.1, 116.2, 113.5, 110.0, 97.6, 55.1, 38.7.

4-oxo-2-((3-(trifluoromethyl)phenyl)amino)-4,5-dihydrothiophene-3-carboxylic acid (**21e**)
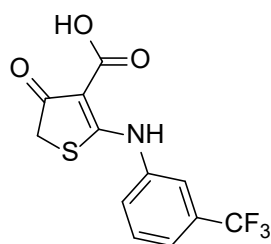
By using general procedure 8 with **11j** (2.6 mmol), EtOH (13 mL), and 50% w/w KOH solution (6.5 mL) for 1 h to give the desired product as an off-white solid (0.7 g, 2.1 mmol, 80%). ^{1}H NMR (700 MHz, DMSO-d_6) δ 12.72 (s, 1H), 11.43 (s, 1H), 7.88 (s, 1H), 7.81–7.77 (m, 2H), 7.74 (t, J = 7.8 Hz, 1H), 4.05 (s, 2H). ^{13}C NMR (176 MHz, DMSO-d_6) δ 196.5, 182.5, 164.1, 137.8, 130.4, 129.9 and 129.8 and 129.6 and 129.4 (q, $^2J_{C-F}$ = 32 Hz), 129.2, 125.6 and 124.0 and 122.5 and 120.9 (q, $^1J_{C-F}$ = 273 Hz), 124.4 and 124.4 and 124.4 and 124.4 (q, $^3J_{C-F}$ = 4 Hz), 122.0 and 122.0 and 122.0 and 122.0 (q, $^3J_{C-F}$ = 3 Hz), 98.1, 38.7.

2-((3-Nitrophenyl)amino)-4-oxo-4,5-dihydrothiophene-3-carboxylic acid (**21f**)

By using general procedure 8 with **11l** (2.6 mmol), EtOH (13 mL), and 50% w/w KOH solution (6.5 mL) for 1 h to give the desired product as an off-white solid (0.4 g, 1.3 mmol, 51%). ^{1}H NMR (700 MHz, DMSO-d_6) δ 12.77 (s, 1H), 11.43 (s, 1H), 8.36 (t, J = 2.2 Hz, 1H), 8.25 (ddd, J = 8.2, 2.2, 1.0 Hz, 1H), 7.96 (ddd, J = 8.2, 2.2, 1.0 Hz, 1H), 7.80 (t, J = 8.2 Hz, 1H), 4.08 (s, 2H). ^{13}C NMR (176 MHz, DMSO-d_6) δ 196.6, 182.6, 164.1, 147.7, 137.8, 131.6, 130.6, 122.4, 119.9, 98.4, 38.8.

2-((4-Fluorophenyl)amino)-4-oxo-4,5-dihydrothiophene-3-carboxylic acid (**21g**)

By using general procedure 8 with **11g** (2.4 mmol), EtOH (12 mL), and 50% w/w KOH solution (6.0 mL) for 1 h to give the desired product as an off-white solid (0.5 g, 1.8 mmol, 76%). ^{1}H NMR (700 MHz, DMSO-d_6) δ 12.78 (s, 1H), 11.11 (s, 1H), 7.51 (dd, J = 8.8, 4.9 Hz, 2H), 7.34 (t, J = 8.8 Hz, 2H), 4.02 (s, 2H). ^{13}C NMR (176 MHz, DMSO-d_6) δ 196.5, 182.9, 164.2, 161.6

and 160.2 (d, $^1J_{\text{C-F}}$ = 246 Hz), 133.3, 127.6 and 127.5 (d, $^3J_{\text{C-F}}$ = 9 Hz) (2), 116.0 and 115.9 (d, $^2J_{\text{C-F}}$ = 23 Hz) (2), 97.6, 38.6.

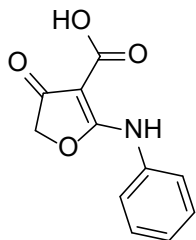*4-Oxo-2-(phenylamino)-4,5-dihydrofuran-3-carboxylic acid* (**22a**)

By using general procedure 8 with **11p** (5.0 mmol), EtOH (30 mL), and 50% w/w KOH solution (15.0 mL) for 1 h to give the desired product as an off-white solid (0.7 g, 2.7 mmol, 54%). ^{1}H NMR (700 MHz, DMSO-d_6) δ 11.98 (s, 1H), 10.40 (s, 1H), 7.47–7.45 (m, 2H), 7.43–7.40 (m, 2H), 7.28–7.24 (m, 1H), 4.77 (s, 2H). ^{13}C NMR (176 MHz, DMSO-d_6) δ 190.3, 176.3, 164.3, 134.6, 128.7 (2), 125.8, 122.9 (2), 87.1, 74.9.

2-((3-Fluorophenyl)amino)-4-oxo-4,5-dihydrofuran-3-carboxylic acid (**22b**)
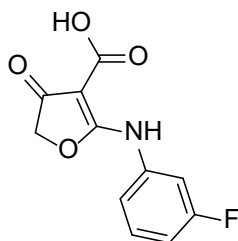
By using general procedure 8 with **11q** (10.0 mmol) for 30 min to give the desired product as an off-white solid (2.3 g, 8.4 mmol, 84%). ^{1}H NMR (600 MHz, DMSO-d_6) δ 13.51 (s, 1H), 7.25–7.17 (m, 1H), 6.96–6.88 (m, 2H), 6.76–6.65 (m, 1H), 4.31 (s, 2H).

General procedure 9

3-Carboxylate- or 3-carboxamide- functionalized 2-aminothiophenones or 2-aminofuranones (0.7 mmol, 1 equiv.), PyBOP (1.1 mmol, 1.6 equiv.), and DIPEA (2.8 mmol, 4 equiv.) were dissolved in DMF (0.2 M). After 10 min of stirring at room temperature, an amine (0.84 mmol, 1.2 equiv.) was added to the mixture and further stirred for 1 h at room temperature. The reaction mixture was diluted with ethyl acetate and continuously washed with 1M HCl to remove DMF and phosphonamide, followed by washing with brine. The organic layer was dried over MgSO₄ and purified by column chromatography (10–40% EA in PE).

N-Methyl-4-oxo-2-(phenylamino)-4,5-dihydrothiophene-3-carboxamide (**23a**)
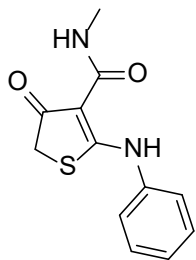
By using general procedure 9 with **21a** (524 mg, 1.9 mmol), methylamine (2 M in THF, 1.2 mL, 2.3 mmol), PyBOP (1.6 g, 3.0 mmol), DIPEA (1.3 mL, 7.6 mmol) in DMF (9 mL) to give the desired product (233 mg, 0.9 mmol, 49%). ^{1}H NMR (600 MHz, CDCl₃) δ 12.69 (s, 1H), 8.75 (s, 1H), 7.43 (t, *J* = 7.4 Hz, 2H), 7.36 (d, *J* = 7.4 Hz, 2H), 7.30 (t, *J* = 7.4 Hz, 1H), 3.70 (s, 2H),

2.92 (d, J = 4.9 Hz, 3H). ^{13}C NMR (151 MHz, CDCl$_3$) δ 193.6, 181.2, 166.4, 137.3, 129.6 (2), 127.1, 123.1 (2), 99.4, 38.4, 24.9.

2-((3-Fluorophenyl)amino)-N-methyl-4-oxo-4,5-dihydrothiophene-3-carboxamide (**23b**)
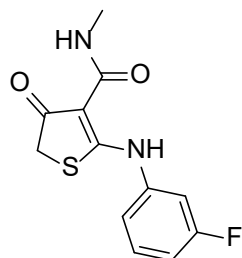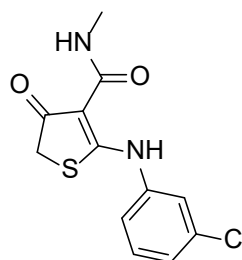
By using general procedure 9 with **21b** (542 mg, 1.9 mmol), methylamine (2 M in THF, 1.1 mL, 2.2 mmol), PyBOP (1.6 g, 3.0 mmol), DIPEA (1.3 mL, 7.6 mmol) in DMF (9 mL) to give the desired product (219 mg, 0.8 mmol, 44%). ^{1}H NMR (500 MHz, CDCl$_3$) δ 12.86 (s, 1H), 8.73 (s, 1H), 7.42–7.36 (m, 1H), 7.16–7.10 (m, 2H), 7.03–6.97 (m, 1H), 3.73 (s, 2H), 2.92 (d, J = 4.9 Hz, 3H). ^{13}C NMR (126 MHz, CDCl$_3$) δ 193.7, 180.9, 166.2, 163.9 and 161.9 (d, $^1J_{C-F}$ = 248 Hz), 138.7 and 138.7 (d, $^3J_{C-F}$ = 10 Hz), 130.9 and 130.9 (d, $^3J_{C-F}$ = 9 Hz), 118.4 and 118.4 (d, $^4J_{C-F}$ = 3 Hz), 113.8 and 113.7 (d, $^2J_{C-F}$ = 21 Hz), 110.2 and 110.0 (d, $^2J_{C-F}$ = 25 Hz), 99.7, 38.4, 24.9.

2-((3-Chlorophenyl)amino)-N-methyl-4-oxo-4,5-dihydrothiophene-3-carboxamide (**23c**)

By using general procedure 9 with **21c** (216 mg, 0.7 mmol), methylamine (2 M in THF, 420 μL, 0.8 mmol), PyBOP (474 mg, 0.9 mmol), DIPEA (488 μL, 2.8 mmol) in DMF (3.5 mL) to give the desired product (35 mg, 0.1 mmol, 17%). ^{1}H NMR (700 MHz, CDCl$_3$) δ 12.82 (s, 1H), 8.71 (s, 1H), 7.43−7.34 (m, 2H), 7.29−7.23 (m, 2H), 3.72 (s, 2H), 2.92 (d, J = 4.9 Hz, 3H). ^{13}C NMR (176 MHz, CDCl$_3$) δ 193.7, 181.0, 166.3, 138.5, 135.3, 130.6, 127.1, 123.1, 121.1, 99.8, 38.5, 25.0.

2-((3-Methoxyphenyl)amino)-N-methyl-4-oxo-4,5-dihydrothiophene-3-carboxamide (**23d**)
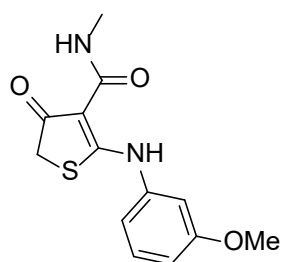
By using general procedure 9 with **21d** (352 mg, 1.2 mmol), methylamine (2 M in THF, 0.7 mL, 1.4 mmol), PyBOP (1.0 g, 1.9 mmol), DIPEA (0.84 mL, 4.8 mmol) in DMF (6 mL) to give the desired product (150 mg, 0.5 mmol, 46%). ^{1}H NMR (600 MHz, CDCl$_3$) δ 12.72 (s, 1H), 8.75 (s, 1H), 7.32 (t, J = 8.1 Hz, 1H), 6.95 (dd, J = 8.1, 1.0 Hz, 1H), 6.88 (t, J = 2.3 Hz, 1H), 6.83 (ddd, J = 8.1, 2.3, 1.0 Hz, 1H), 3.82 (s, 3H), 3.71 (s, 2H), 2.92 (d, J = 4.9 Hz, 3H). ^{13}C NMR (151 MHz, CDCl$_3$) δ 193.6, 181.0, 166.4, 160.5, 138.4, 130.4, 114.9, 112.8, 108.5, 99.4, 55.4, 38.4, 24.9.

N-Methyl-4-oxo-2-((3-(trifluoromethyl)phenyl)amino)-4,5-dihydrothiophene-3-carboxamide
(**23e**)
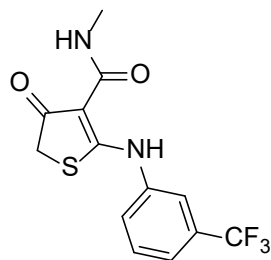
By using **21e** (238 mg, 0.7 mmol), methylamine (2 M in THF, 420 μL, 0.8 mmol), PyBOP (474 mg, 0.9 mmol), DIPEA (488 μL, 2.8 mmol) in DMF (3.5 mL) to give the desired product (126 mg, 0.4 mmol, 57%). ^{1}H NMR (700 MHz, CDCl$_3$) δ 12.98 (s, 1H), 8.71 (s, 1H), 7.64 (s, 1H), 7.58–7.53 (m, 3H), 3.74 (s, 2H), 2.93 (d, J = 4.9 Hz, 3H). ^{13}C NMR (176 MHz, CDCl$_3$) δ 193.7, 181.0, 166.3, 138.0, 132.5 and 132.3 and 132.1 and 131.9 (q, $^2J_{\text{C-F}}$ = 33 Hz), 130.3, 125.9, 125.7 and 124.1 and 122.6 and 121.0 (q, $^1J_{\text{C-F}}$ = 273 Hz), 123.5 and 123.5 and 123.5 and 123.4 (d, $^3J_{\text{C-F}}$ = 4 Hz), 119.8 and 119.8 and 119.8 and 119.7 (q, $^3J_{\text{C-F}}$ = 4 Hz), 99.9, 38.5, 25.0.

N-Methyl-2-((3-nitrophenyl)amino)-4-oxo-4,5-dihydrothiophene-3-carboxamide (**23f**)

By using general procedure 9 with **21f** (222 mg, 0.7 mmol), methylamine (2 M in THF, 420 μL, 0.8 mmol), PyBOP (474 mg, 0.9 mmol), DIPEA (488 μL, 2.8 mmol) in DMF (3.5 mL) to give the desired product (48 mg, 0.2 mmol, 23%). ^{1}H NMR (600 MHz, CDCl$_3$) δ 13.18 (s, 1H), 8.71 (s, 1H), 8.31 (t, J = 2.1 Hz, 1H), 8.14 (ddd, J = 8.1, 2.1, 1.1 Hz, 1H), 7.67 (ddd, J = 8.0, 2.1, 1.1 Hz, 1H), 7.63 (t, J = 8.1 Hz, 1H), 3.78 (s, 2H), 2.93 (d, J = 4.9 Hz, 3H). ^{13}C NMR (151 MHz, CDCl$_3$) δ 193.8, 180.8, 166.2, 148.8, 138.6, 130.6, 128.3, 121.2, 117.3, 100.3, 38.6, 25.0.

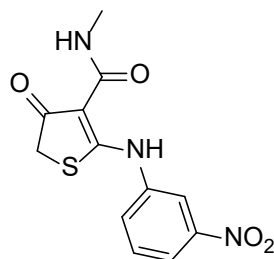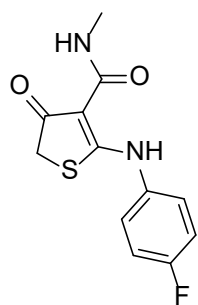*2-((4-Fluorophenyl)amino)-N-methyl-4-oxo-4,5-dihydrothiophene-3-carboxamide* (**23g**)

By using general procedure 9 with **21g** (203 mg, 0.7 mmol), methylamine (2 M in THF, 420 μL, 0.8 mmol), PyBOP (474 mg, 0.9 mmol), DIPEA (488 μL, 2.8 mmol) in DMF (3.5 mL) to give the desired product (46 mg, 0.2 mmol, 25%). ^{1}H NMR (700 MHz, CDCl$_3$) δ 12.52 (s, 1H), 8.70 (s, 1H), 7.32 (dd, J = 8.9, 4.6 Hz, 2H), 7.14–7.10 (m, 2H), 3.70 (s, 2H), 2.92 (d, J = 4.9 Hz, 3H). ^{13}C NMR (176 MHz, CDCl$_3$) δ 193.7, 181.9, 166.4, 162.0 and 160.6 (d, $^1J_{\text{C-F}}$ = 248 Hz), 133.3 and 133.3 (d, $^4J_{\text{C-F}}$ = 3 Hz), 125.6 and 125.5 (d, $^3J_{\text{C-F}}$ = 9 Hz) (2), 116.6 and 116.5 (d, $^2J_{\text{C-F}}$ = 23 Hz) (2), 99.4, 38.4, 25.0.

Tert-butyl (2-(4-oxo-2-(phenylamino)-4,5-dihydrothiophene-3-carboxamido)ethyl)carbamate (**24a**)
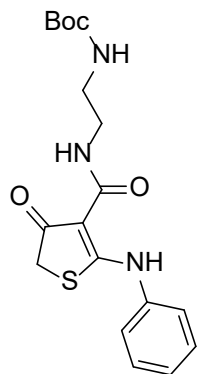
By using general procedure 9 with **21a** (217 mg, 0.8 mmol), N-Boc-ethylenediamine (151 μL, 1.0 mmol), PyBOP (833 mg, 1.6 mmol), DIPEA (697 μL, 4.0 mmol) in DMF (4.0 mL) to give the desired product (137 mg, 0.4 mmol, 45%). ^{1}H NMR (600 MHz, CDCl$_3$) δ 12.54 (s, 1H), 8.98 (t, J = 6.3 Hz, 1H), 7.44 (t, J = 7.8 Hz, 2H), 7.36 (d, J = 7.8 Hz, 2H), 7.31 (t, J = 7.8 Hz, 1H), 4.98 (s, 1H), 3.71 (s, 2H), 3.49 (q, J = 6.3 Hz, 2H), 3.32 (t, J = 5.9 Hz, 2H), 1.45 (s, 9H). ^{13}C NMR (151 MHz, CDCl$_3$) δ 193.6, 181.5, 166.5, 155.9, 137.2, 129.6 (2), 127.2, 123.2 (2), 99.2, 79.4, 41.1, 38.4, 38.4, 28.3 (3).

Tert-butyl (2-(2-((3-fluorophenyl)amino)-4-oxo-4,5-dihydrothiophene-3-carboxamido)ethyl) carbamate (**24b**)
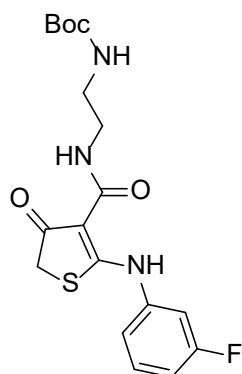
By using general procedure 9 with **21b** (1.4 g, 5.0 mmol), N-Boc-ethylenediamine (950 μL, 6.0 mmol), PyBOP (3.4 g, 6.5 mmol), DIPEA (3.5 mL, 20.0 mmol) in DMF (25.0 mL) to give the desired product (1.2 g, 3.1 mmol, 61%). ^{1}H NMR (600 MHz, CDCl$_3$) δ 12.72 (s, 1H), 8.96 (t, J = 6.0 Hz, 1H), 7.40 (td, J = 8.3, 6.2 Hz, 1H), 7.14 (dd, J = 8.0, 1.7 Hz, 1H), 7.12 (dt, J = 9.6, 2.4 Hz, 1H), 7.01 (td, J = 8.3, 2.4 Hz, 1H), 4.94 (s, 1H), 3.73 (s, 2H), 3.48 (q, J = 6.0 Hz, 2H), 3.32 (t, J = 5.8 Hz, 2H), 1.45 (s, 9H). ^{13}C NMR (151 MHz, CDCl$_3$) δ 193.7, 181.2, 166.3, 163.8 and 162.1 (d, $^1J_{C-F}$ = 249 Hz), 155.9, 138.7 and 138.6 (d, $^3J_{C-F}$ = 10 Hz), 131.0 and 130.9 (d, $^3J_{C-F}$ = 9 Hz), 118.6 and 118.6 (d, $^4J_{C-F}$ = 3 Hz), 114.1 and 113.9 (d, $^2J_{C-F}$ = 21 Hz), 110.4 and 110.3 (d, $^2J_{C-F}$ = 25 Hz), 99.5, 79.3, 40.9, 38.5, 38.5, 28.3 (3).

Tert-butyl (2-(2-((3-chlorophenyl)amino)-4-oxo-4,5-dihydrothiophene-3-carboxamido)ethyl) carbamate (**24c**)
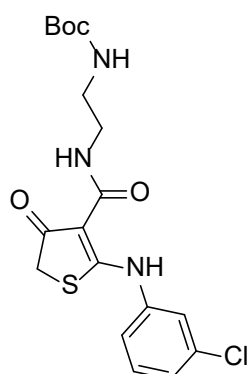
By using general procedure 9 with **21c** (306 mg, 1.0 mmol), N-Boc-ethylenediamine (189 μL, 1.2 mmol), PyBOP (781 mg, 1.5 mmol), DIPEA (697 μL, 4.0 mmol) in DMF (5.0 mL) to give the desired product (88 mg, 0.2 mmol, 21%). ^{1}H NMR (600 MHz, CDCl$_3$) δ 12.67 (s, 1H), 8.95 (t, J = 5.7 Hz, 1H), 7.39 (t, J = 1.9 Hz, 1H), 7.37 (t, J = 8.1 Hz, 1H), 7.29 (ddd, J = 8.1, 1.9, 1.0 Hz, 1H), 7.25 (ddd, J = 8.1, 1.9, 1.0 Hz, 1H), 5.05 (s, 2H), 3.73 (s, 2H), 3.48 (q, J = 6.0 Hz, 2H), 3.32 (t, J = 5.4 Hz,

2H), 1.45 (s, 9H). ^{13}C NMR (151 MHz, CDCl$_3$) δ 193.7, 181.3, 166.3, 156.0, 138.3, 135.3, 130.6, 127.2, 123.2, 121.2, 99.5, 79.6, 41.1, 38.5, 38.5, 28.3 (3).

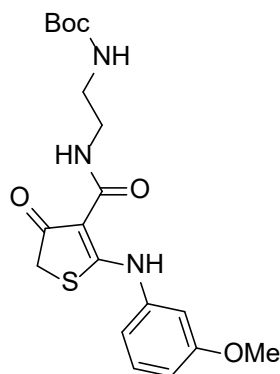*Tert-butyl (2-(2-((3-methoxyphenyl)amino)-4-oxo-4,5-dihydrothiophene-3-carboxamido)ethyl) carbamate* (**24d**)

By using general procedure 9 with **21d** (217 mg, 0.8 mmol), N-Boc-ethylenediamine (96 μL, 0.6 mmol), PyBOP (458 mg, 0.9 mmol), DIPEA (697 μL, 4.0 mmol) in DMF (4.0 mL) to give the desired product (86 mg, 0.2 mmol, 35%). ^{1}H NMR (400 MHz, CDCl$_3$) δ 12.57 (s, 1H), 8.99 (t, J = 6.2 Hz, 1H), 7.33 (t, J = 8.1 Hz, 1H), 6.95 (dd, J = 8.1, 2.0 Hz, 1H), 6.88 (t, J = 2.0 Hz, 1H), 6.84 (dd, J = 8.3, 2.0 Hz, 1H), 4.95 (s, 1H), 3.82 (s, 3H), 3.70 (s, 2H), 3.49 (q, J = 5.9 Hz, 2H), 3.32 (t, J = 5.9 Hz, 2H), 1.45 (s, 9H).

N-benzoyl-4-oxo-2-(phenylamino)-4,5-dihydrothiophene-3-carboxamide (**25**)
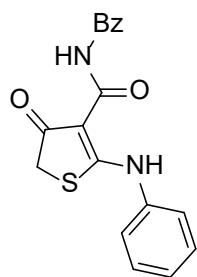
By using general procedure 9 with **21a** (203 mg, 0.7 mmol), benzylamine (92 μL, 0.8 mmol), PyBOP (846 mg, 1.1 mmol), DIPEA (362 μL, 2.8 mmol) in DMF (3.5 mL) to give the desired product (116 mg, 0.3 mmol, 48%). ^{1}H NMR (600 MHz, CDCl$_3$) δ 12.78 (s, 1H), 9.23 (t, J = 6.2 Hz, 1H), 7.39 (td, J = 8.1, 6.2 Hz, 1H), 7.34 (d, J = 4.4 Hz, 4H), 7.28–7.24 (m, 1H), 7.15 (ddd, J = 8.1, 2.2, 0.9 Hz, 1H), 7.12 (dt, J = 9.6, 2.2 Hz, 1H), 7.00 (tdd, J = 8.1, 2.2, 0.9 Hz, 1H), 4.58 (d, J = 6.0 Hz, 2H), 3.74 (s, 2H). ^{13}C NMR (151 MHz, CDCl$_3$) δ 193.7, 181.2, 165.7, 163.7 and 162.1 (d, $^1J_{\text{C-F}}$ = 249 Hz), 138.7 and 138.7 (d, $^3J_{\text{C-F}}$ = 10 Hz), 138.4, 131.0 and 130.9 (d, $^3J_{\text{C-F}}$ = 9 Hz), 128.6 (2), 127.3 (2), 127.2, 118.6 and 118.6 (d, $^4J_{\text{C-F}}$ = 3 Hz), 114.0 and 113.9 (d, $^2J_{\text{C-F}}$ = 21 Hz), 110.4 and 110.3 (d, $^2J_{\text{C-F}}$ = 25 Hz), 99.6, 42.2, 38.5.

N-methyl-4-oxo-2-(phenylamino)-4,5-dihydrofuran-3-carboxamide (**26**)
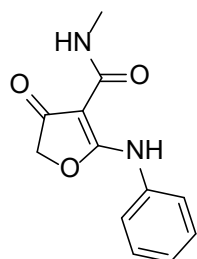
By using general procedure 9 with **22a** (205 mg, 0.8 mmol), methylamine (2 M in THF, 480 μL, 1.0 mmol), PyBOP (458 mg, 0.9 mmol), DIPEA (697 μL, 4.0 mmol) in DMF (4.0 mL) to give the desired product (95 mg, 0.4 mmol, 51%). ^{1}H NMR (500 MHz, CDCl$_3$) δ 10.82 (s, 1H), 7.72–7.63 (m, 1H), 7.40–7.37 (m, 4H), 7.24–7.20 (m, 1H), 4.75 (s, 2H), 2.94 (d, J = 4.9 Hz, 3H). ^{13}C NMR (126 MHz, CDCl$_3$) δ 190.3, 176.1, 164.8, 135.0, 129.4 (2), 125.7, 120.9 (2), 89.3, 75.4, 25.0.

Tert-butyl (2-(4-oxo-2-(phenylamino)-4,5-dihydrofuran-3-carboxamido)ethyl)carbamate (**27a**)
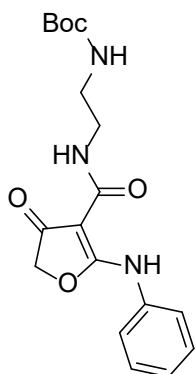
By using general procedure 9 with **22a** (205 mg, 0.8 mmol), N-Boc-ethylenediamine (151 µL, 1.0 mmol), PyBOP (458 mg, 0.9 mmol), DIPEA (697 µL, 4.0 mmol) in DMF (4.0 mL) to give the desired product (179 mg, 0.5 mmol, 62%). ^{1}H NMR (500 MHz, CDCl$_3$) δ 10.69 (s, 1H), 7.92 (t, *J* = 6.1 Hz, 1H), 7.42–7.36 (m, 5H), 7.24–7.20 (m, 1H), 4.74 (s, 2H), 3.49 (q, *J* = 6.1 Hz, 2H), 3.32 (t, *J* = 5.9 Hz, 2H), 1.44 (s, 9H). ^{13}C NMR (126 MHz, CDCl$_3$) δ 190.3, 176.1, 164.9, 155.9, 134.9, 129.4 (2), 125.8, 121.0 (2), 89.1, 79.5, 75.5, 41.1, 38.5, 28.3 (3).

Tert-butyl (2-(2-((3-fluorophenyl)amino)-4-oxo-4,5-dihydrofuran-3-carboxamido)ethyl)carbamate (**27b**)
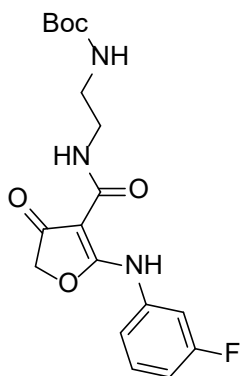
By using **22b** (547 mg, 2.0 mmol), N-Boc-ethylenediamine (378 µL, 2.4 mmol), PyBOP (1.2 g, 2.4 mmol), DIPEA (1.7 mL, 10.0 mmol) in DMF (10.0 mL) to give the desired product (364 mg, 1.0 mmol, 48%). ^{1}H NMR (500 MHz, CDCl$_3$) δ 10.81 (s, 1H), 7.89 (t, *J* = 5.6 Hz, 1H), 7.34 (td, *J* = 8.2, 6.3 Hz, 1H), 7.22 (dt, *J* = 10.2, 2.2 Hz, 1H), 7.10 (dd, *J* = 8.1, 1.7 Hz, 1H), 6.92 (td, *J* = 8.3, 2.4 Hz, 1H), 6.08 (s, 1H), 4.76 (s, 2H), 3.49 (q, *J* = 6.0 Hz, 2H), 3.32 (t, *J* = 5.9 Hz, 2H), 1.45 (s, 9H). ^{13}C NMR (126 MHz, CDCl$_3$) δ 190.4, 176.2, 164.7, 163.9 and 161.9 (d, $^1J_{C-F}$ = 247 Hz), 155.9, 136.4 and 136.4 (d, $^3J_{C-F}$ = 10 Hz), 130.7 and 130.6 (d, $^3J_{C-F}$ = 10 Hz), 116.3 and 116.3 (d, $^4J_{C-F}$ = 3 Hz), 112.6 and 112.4 (d, $^2J_{C-F}$ = 21 Hz), 108.4 and 108.2 (d, $^2J_{C-F}$ = 26 Hz), 89.4, 79.5, 75.6, 40.7, 38.6, 28.3 (3).

N-(2-(diethylamino)ethyl)-5-formyl-2,4-dimethyl-1H-pyrrole-3-carboxamide (**28**)
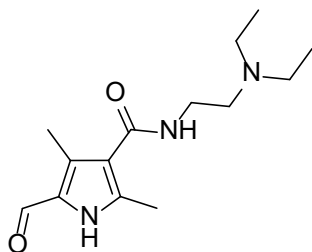
The compound was synthesized according to the previously reported method.[110] To a solution of 5-formyl-2,4-dimethyl-1H-pyrrole-3-carboxylic acid (1.0 g, 6.0 mmol) in DMF (5 mL) was added EDC (1.7 g, 9.0 mmol), HOBt hydrate (1.4 g, 9.0 mmol), TEA (1.7 mL, 12.0 mmol), and *N,N*-diethylethylenediamine (1.0 mL, 7.2 mmol) at room temperature. The reaction mixture was stirred overnight, was diluted with water and sodium bicarbonate solution. The pH was adjusted to higher than 10 with 2 N NaOH solution. The crude was extracted with 10% methanol in DCM and the combined

organic layer was dried over MgSO₄. The organic layer was evaporated under reduced pressure and excess DMF was co-evaporated with toluene. The precipitates were formed by adding hexane and Et₂O mixture (3:1 v/v), collected, and washed with EtOAc to give the desired product (0.8 g, 3.0 mmol, 50%). The product was used in further steps without further purification. ¹H NMR (400 MHz, DMSO-d_6) δ 11.79 (s, 1H), 9.52 (s, 1H), 7.29 (t, J = 5.6 Hz, 1H), 3.23 (q, J = 5.6 Hz, 2H), 2.50 (t, J = 5.6 Hz, 2H), 2.46 (p, J = 7.1 Hz, 4H), 2.35 (s, 3H), 2.30 (s, 3H), 0.94 (t, J = 7.1 Hz, 6H).

General procedure 10

A mixture of thiophenones (0.19 mmol), **28** (0.21 mmol), and pyrrolidine (0.19 mmol) in ethanol (2.0 ml) was refluxed for 2 h. After reaction completion monitored by TLC, the purification was performed by either of the following two methods.

Purification 1. When the product was crystalized as solid during the reaction, the reaction mixture was cooled, and the obtained precipitate was collected by using vacuum filtration with washing cold EtOH. The collected product was dried under low pressured vacuum to give the desired product.

Purification 2. When the product was present as a dissolved form in the reaction mixture, the reaction mixture was cooled down to room temperature. The organic solvent was evaporated under reduced pressure and the residue was purified by flash chromatography (2–10% MeOH in DCM) to give the desired product.

The Boc deprotection to give **32a**–**32d** and **36a**–**36b** was performed by stirring either in 4M HCl in 1,4-dioxane and MeOH or in TFA/DCM (1:2 v/v) at room temperature for 30 min from corresponding compounds as described below. The excess acids and solvents were removed by air blow and further drying under reduced pressure.

Ethyl (E)-5-((4-((2-(diethylamino)ethyl)carbamoyl)-3,5-dimethyl-1H-pyrrol-2-yl)methylene)-4-oxo-2-(phenylamino)-4,5-dihydrothiophene-3-carboxylate (**29a**)
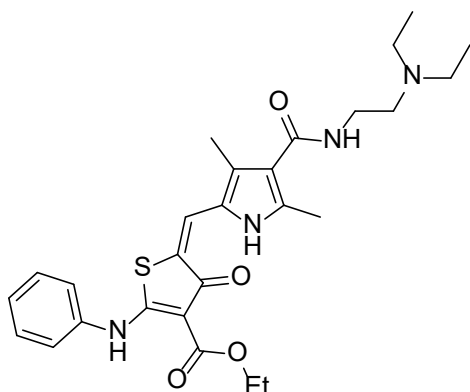
By using general procedure 10 with **11a** (50 mg, 0.19 mmol). The product was purified with purification method 2 to give the desired product (83 mg, 0.16 mmol, 85%, d.r. 5:1). ^{1}H NMR (700 MHz, CDCl$_3$) δ 13.58 (s, 1H), 11.37 (s, 1H), 7.48–7.44 (m, 2H), 7.41–7.36 (m, 2H), 7.34–7.30 (m, 1H), 6.77 (s, 1H), 6.54 (s, 1H), 4.47 (q, *J* = 7.1 Hz, 2H), 3.57–3.48 (m, 2H), 2.78–2.68 (m, 2H), 2.68–2.61 (m, 4H), 2.57 (s, 3H), 2.35 (s, 3H), 1.48 (t, *J* = 7.1 Hz, 3H), 1.17–1.04 (m, 6H). ^{13}C NMR (176 MHz, CDCl$_3$) δ 181.3, 173.6, 166.9, 137.5, 136.6, 129.7 (2), 127.6, 127.2, 125.9, 124.1, 123.3, 123.2 (2), 118.8, 117.7, 101.1, 60.8, 51.7, 46.7 (2), 36.5, 14.6, 14.2, 11.4 (2), 11.1. HRMS-ESI (m/z): calculated for [M+H]$^+$ C$_{27}$H$_{35}$O$_4$N$_4$S, 511.2374; found, 511.2382.

Ethyl (E)-5-((4-((2-(diethylamino)ethyl)carbamoyl)-3,5-dimethyl-1H-pyrrol-2-yl)methylene)-2-((4-fluorophenyl)amino)-4-oxo-4,5-dihydrothiophene-3-carboxylate (**29b**)
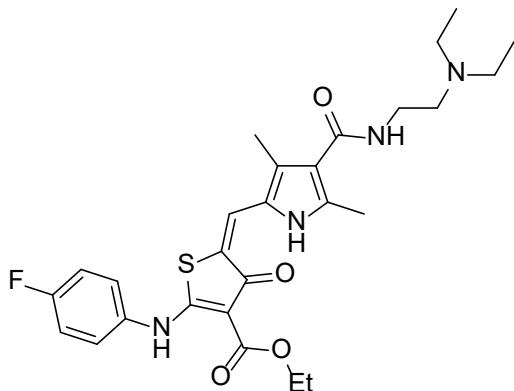
By using general procedure 10 with **11g** (50 mg, 0.18 mmol), **28** (52 mg, 0.20 mmol), and pyrrolidine (14.6 μL, 0.18 mmol) in ethanol (2.0 mL). The product was purified with purification method 2 to give the desired product (94 mg, 0.18 mmol, 100%, d.r. 3:1). ^{1}H NMR (700 MHz, CDCl$_3$) δ 13.55 (s, 1H), 11.19 (s, 1H), 7.39–7.32 (m, 2H), 7.21–7.12 (m, 2H), 6.76 (s, 1H), 6.62 (s, 1H), 4.46 (q, *J* = 7.1 Hz, 2H), 3.57–3.48 (m, 2H), 2.81–2.71 (m, 2H), 2.71–2.62 (m, 4H), 2.57 (s, 3H), 2.35 (s, 3H), 1.47 (t, *J* = 7.1 Hz, 3H), 1.15–1.03 (m, 6H). HRMS-ESI (m/z): calculated for [M+H]$^+$ C$_{27}$H$_{34}$O$_4$N$_4$FS, 529.2279; found, 529.2283.

Ethyl (E)-5-((4-((2-(diethylamino)ethyl)carbamoyl)-3,5-dimethyl-1H-pyrrol-2-yl)methylene)-2-((3-fluorophenyl)amino)-4-oxo-4,5-dihydrothiophene-3-carboxylate (**29c**)
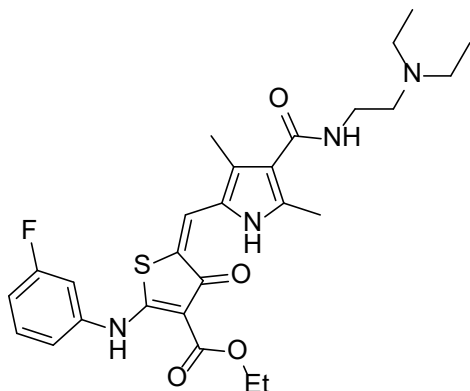
By using general procedure 10 with **11h** (50 mg, 0.19 mmol). The product was purified with purification method 2 to give the desired product (94 mg, 0.18 mmol, 93%, d.r. 10:1). ^{1}H NMR (700 MHz, CDCl$_3$) δ 13.58 (s, 1H), 11.49 (s, 1H), 7.48–7.37 (m, 1H), 7.18–7.11 (m, 2H), 7.05–6.99 (m, 1H), 6.82 (s, 1H), 6.52 (s, 1H), 4.47 (q, *J* = 7.1 Hz, 2H), 3.54–3.45 (m, 2H), 2.76–2.68 (m, 2H), 2.67–2.60 (m, 4H), 2.58 (s, 3H), 2.37 (s, 3H), 1.48 (t, *J* = 7.1 Hz, 3H), 1.12–1.00 (m, 6H). ^{13}C NMR (176 MHz, CDCl$_3$) δ 181.2, 172.8, 166.9, 165.7, 163.8 and 162.4 (d, $^1J_{C-F}$ = 249 Hz), 139.0 and 139.0 (d, $^3J_{C-F}$ = 10 Hz), 136.9, 131.1 and 131.0 (d, $^3J_{C-F}$ = 9 Hz), 128.1, 126.0, 123.7, 119.2, 118.5 and 118.5 (d, $^4J_{C-F}$ = 3 Hz), 117.2, 113.9 and 113.8 (d, $^2J_{C-F}$ = 21 Hz), 110.2 and 110.1 (d, $^2J_{C-F}$ = 25 Hz), 101.6, 61.0, 51.6, 46.7 (2), 36.6, 14.5, 14.2, 11.4 (2), 11.1. HRMS-ESI (m/z): calculated for [M+H]$^+$ C$_{27}$H$_{34}$O$_4$N$_4$FS, 529.2279; found, 529.2291.

Ethyl (E)-5-((4-((2-(diethylamino)ethyl)carbamoyl)-3,5-dimethyl-1H-pyrrol-2-yl)methylene)-4-oxo-2-((4-(trifluoromethyl)phenyl)amino)-4,5-dihydrothiophene-3-carboxylate (**29d**)
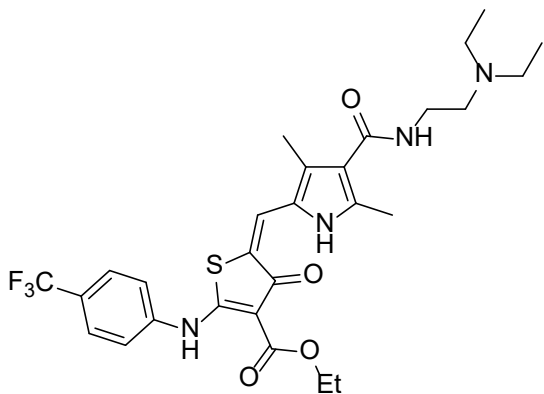
By using general procedure 10 with **11i** (50 mg, 0.19 mmol). The product was purified with purification method 2 to give the desired product (101 mg, 0.17 mmol, 92%, d.r. 12:1). ^{1}H NMR (700 MHz, CDCl$_3$) δ 13.59 (s, 1H), 11.68 (s, 1H), 7.71 (d, *J* = 8.4 Hz, 2H), 7.50 (d, *J* = 8.4 Hz, 2H), 6.84 (s, 1H), 6.54 (s, 1H), 4.48 (q, *J* = 7.1 Hz, 2H), 3.55–3.49 (m, 2H), 2.75–2.69 (m, 2H), 2.68–2.61 (m, 4H), 2.58 (s, 3H), 2.38 (s, 3H), 1.48 (t, *J* = 7.1 Hz, 3H), 1.11–1.04 (m, 6H). ^{13}C NMR (176 MHz, CDCl$_3$) δ 181.0, 172.2, 167.0, 165.6, 140.7, 137.2, 128.7 and 128.5 and 128.3 and 128.1 (q, $^2J_{C-F}$ = 33 Hz), 128.5, 127.0 and 127.0 and 127.0 and 127.0 (q, $^3J_{C-F}$ = 3 Hz) (2), 126.1, 126.0 and 124.4 and 122.9 and 121.3 (q, $^1J_{C-F}$ = 272 Hz), 124.0, 122.3 (2), 119.3, 116.8, 102.1, 61.1, 51.6, 46.7 (2), 36.5, 14.5, 14.2, 11.4 (2), 11.2. HRMS-ESI (m/z): calculated for [M+H]$^+$ C$_{28}$H$_{38}$O$_4$N$_4$FS, 579.2271; found, 579.2258.

Ethyl (E)-5-((4-((2-(diethylamino)ethyl)carbamoyl)-3,5-dimethyl-1H-pyrrol-2-yl)methylene)-2-((4-methoxyphenyl)amino)-4-oxo-4,5-dihydrothiophene-3-carboxylate (**29e**)
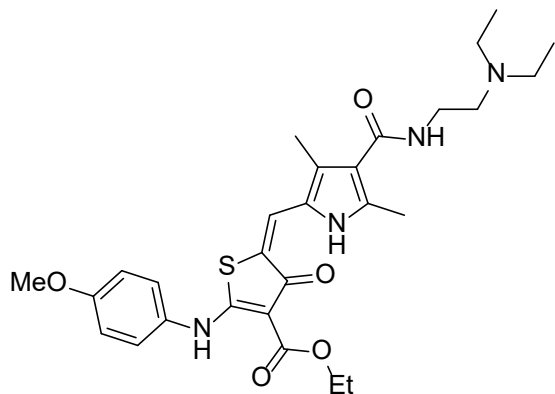
By using general procedure 10 with **11b** (56 mg, 0.19 mmol). The product was purified with purification method 2 to give the desired product (96 mg, 0.18 mmol, 93%, d.r. 2.5:1). ^{1}H NMR (500 MHz, CDCl$_3$) δ 13.56 (s, 1H), 11.05 (s, 1H), 7.29 (d, J = 8.9 Hz, 2H), 6.96 (d, J = 8.9 Hz, 2H), 6.73 (s, 1H), 6.62 (s, 1H), 4.46 (q, J = 7.1 Hz, 2H), 3.85 (s, 3H), 3.58–3.49 (m, 2H), 2.78–2.71 (m, 2H), 2.71–2.62 (m, 4H), 2.56 (s, 3H), 2.34 (s, 3H), 1.47 (t, J = 7.1 Hz, 3H), 1.16–1.04 (m, 6H). ^{13}C NMR (126 MHz, CDCl$_3$) δ 181.4, 174.8, 166.8, 158.8, 130.1, 127.3, 126.3, 125.6 (2), 123.2, 122.9, 118.5, 118.3, 118.0, 114.7 (2), 100.6, 60.7, 55.5, 51.7, 46.7 (2), 36.3, 14.5, 14.1, 11.1 (2), 11.1. HRMS-ESI (m/z): calculated for [M+H]$^+$ C$_{28}$H$_{37}$O$_5$N$_4$S, 541.2479; found, 541.2483.

Ethyl (E)-5-((4-((2-(diethylamino)ethyl)carbamoyl)-3,5-dimethyl-1H-pyrrol-2-yl)methylene)-2-((3-methoxyphenyl)amino)-4-oxo-4,5-dihydrothiophene-3-carboxylate (**29f**)
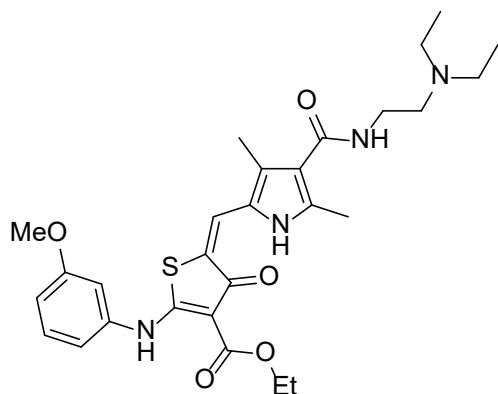
By using general procedure 10 with **11c** (56 mg, 0.19 mmol). The product was purified with purification method 2 to give the desired product (92 mg, 0.17 mmol, 89%, d.r. 5:1). ^{1}H NMR (500 MHz, CDCl$_3$) δ 13.59 (s, 1H), 11.39 (s, 1H), 7.35 (t, J = 8.1 Hz, 1H), 6.96 (dd, J = 8.1, 2.2 Hz, 1H), 6.91 (t, J = 2.2 Hz, 1H), 6.85 (dd, J = 8.1, 2.2 Hz, 1H), 6.78 (s, 1H), 6.58 (s, 1H), 4.47 (q, J = 7.1 Hz, 2H), 3.84 (s, 3H), 3.59–3.46 (m, 2H), 2.76–2.68 (m, 2H), 2.68–2.60 (m, 4H), 2.57 (s, 3H), 2.36 (s, 3H), 1.48 (t, J = 7.1 Hz, 3H), 1.14–1.00 (m, 6H). ^{13}C NMR (126 MHz, CDCl$_3$) δ 181.2, 173.2, 166.9, 165.7, 160.5, 138.5, 136.6, 130.4, 127.6, 125.8, 123.2, 118.8, 117.6, 115.0, 112.7, 108.5, 101.1, 60.8, 55.4, 51.5, 46.6 (2), 36.4, 14.5, 14.1, 11.3 (2), 11.1. HRMS-ESI (m/z): calculated for [M+H]$^+$ C$_{28}$H$_{37}$O$_5$N$_4$S, 541.2479; found, 541.2485.

Ethyl (E)-2-((4-bromophenyl)amino)-5-((4-((2-(diethylamino)ethyl)carbamoyl)-3,5-dimethyl-1H-pyrrol-2-yl)methylene)-4-oxo-4,5-dihydrothiophene-3-carboxylate (**29g**)

By using general procedure 10 with **11e** (65 mg, 0.19 mmol). The product was purified with purification method 2 to give the desired product (87 mg, 0.15 mmol, 77%, d.r. 5:1).^{1}H NMR (500 MHz, CDCl$_3$) δ 13.57 (s, 1H), 11.37 (s, 1H), 7.57 (d, J = 8.5 Hz, 2H), 7.27 (d, J = 8.5 Hz, 2H), 6.79 (s, 1H), 6.58 (s, 1H), 4.47 (q, J = 7.1 Hz, 2H), 3.60–3.49 (m, 2H), 2.80–2.71 (m, 2H), 2.71–2.64 (m, 4H), 2.57 (s, 3H), 2.37 (s, 3H), 1.47 (t, J = 7.1 Hz, 3H), 1.15–1.04 (m, 6H). ^{13}C NMR (126 MHz, CDCl$_3$) δ 181.1, 173.0, 166.9, 138.1, 136.5, 133.0, 132.8 (2), 128.0, 125.9, 125.6, 124.6 (2), 123.6, 120.3, 117.2, 101.4, 60.9, 51.7, 46.9 (2), 36.3, 14.5, 14.1, 11.1 (2), 11.0. HRMS-ESI (m/z): calculated for [M+H]$^+$ C$_{27}$H$_{34}$O$_4$N$_4$^{79}BrS, 589.1479; found, 589.1497 and C$_{27}$H$_{34}$O$_4$N$_4$^{81}BrS, 591.1458; found, 591.1474.

Ethyl (E)-2-((2-bromophenyl)amino)-5-((4-((2-(diethylamino)ethyl)carbamoyl)-3,5-dimethyl-1H-pyrrol-2-yl)methylene)-4-oxo-4,5-dihydrothiophene-3-carboxylate (**29h**)
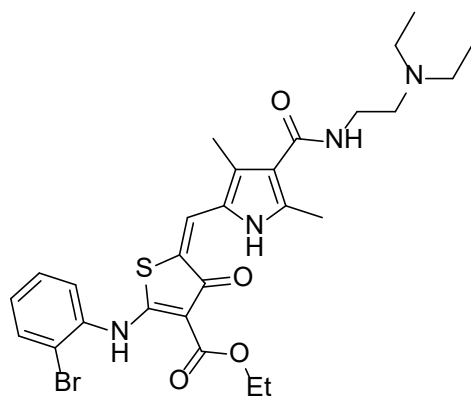
By using general procedure 10 with **11f** (95 mg, 0.19 mmol). The product was purified with purification method 2 to give the desired product (92 mg, 0.16 mmol, 82%, d.r. 6:1). ^{1}H NMR (500 MHz, CDCl$_3$) δ 13.60 (s, 1H), 11.43 (s, 1H), 7.71 (dd, J = 8.1, 1.4 Hz, 1H), 7.65 (dd, J = 8.1, 1.4 Hz, 1H), 7.41 (td, J = 8.1, 1.4 Hz, 1H), 7.19 (td, J = 8.1, 1.4 Hz, 1H), 6.79 (s, 1H), 6.59 (s, 1H), 4.50 (q, J = 7.1 Hz, 2H), 3.61–3.48 (m, 2H), 2.83–2.73 (m, 2H), 2.73–2.64 (m, 4H), 2.58 (s, 3H), 2.36 (s, 3H), 1.48 (t, J = 7.1 Hz, 3H), 1.20–1.05 (m, 6H). ^{13}C NMR (126 MHz, CDCl$_3$) δ 181.2, 172.9, 166.4, 137.3, 136.3, 133.7, 128.3, 128.2, 128.0, 126.2, 125.9, 123.9, 123.6, 118.8, 118.5, 117.3, 101.9, 60.9, 51.7, 46.6 (2), 36.3, 14.5, 14.1, 11.1 (2), 10.5. HRMS-ESI (m/z): calculated for [M+H]$^+$ C$_{27}$H$_{34}$O$_4$N$_4$^{79}BrS, 589.1479; found, 589.1494 and C$_{27}$H$_{34}$O$_4$N$_4$^{81}BrS, 591.1458; found, 591.1468.

Ethyl (E)-5-((4-((2-(diethylamino)ethyl)carbamoyl)-3,5-dimethyl-1H-pyrrol-2-yl)methylene)-2-((4-nitrophenyl)amino)-4-oxo-4,5-dihydrothiophene-3-carboxylate (**29i**)
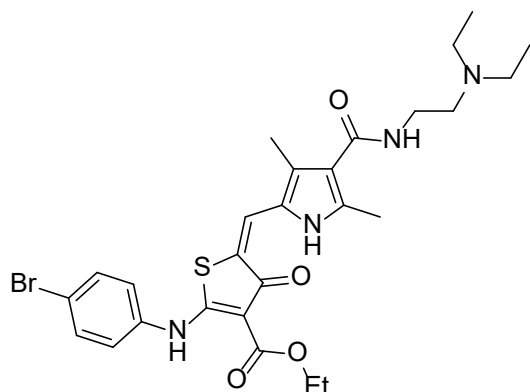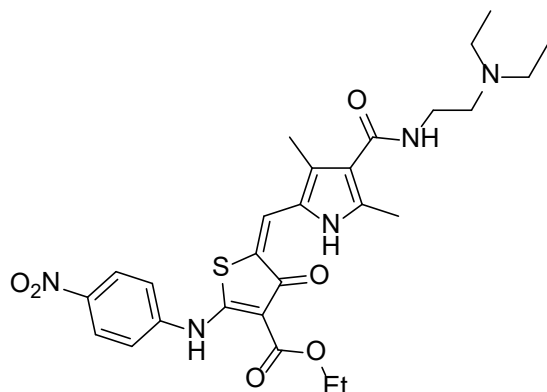
By using general procedure 10 with **11k** (59 mg, 0.19 mmol). The product was purified with purification method 2 to give the desired product (82 mg, 0.15 mmol, 77%, d.r. 15:1). ^{1}H NMR (500 MHz, CDCl$_3$) δ 13.63 (s, 1H), 12.01 (s, 1H), 8.32 (d, J = 9.1 Hz, 2H), 7.52 (d, J = 9.1 Hz, 2H), 6.90 (s, 1H), 6.59 (s, 1H), 4.49 (q, J = 7.1 Hz, 2H), 3.59–3.47 (m, 2H), 2.81–2.70 (m, 2H), 2.68–2.62 (m, 4H), 2.59 (s, 3H), 2.40 (s, 3H), 1.49 (t, J = 7.1 Hz, 3H), 1.13–1.03 (m, 6H). ^{13}C NMR (126 MHz, CDCl$_3$) δ 180.6, 170.6, 166.9, 144.5, 143.2, 137.8, 129.3, 126.2, 125.5 (2), 124.6, 123.8, 121.0 (2), 119.5, 116.2, 102.9, 61.3, 52.9, 46.6 (2), 36.4, 14.4, 14.2, 11.1 (2), 11.0. HRMS-ESI (m/z): calculated for [M+H]$^+$ C$_{27}$H$_{34}$O$_6$N$_5$S, 556.2224; found, 556.2230.

Ethyl (E)-5-((4-((2-(diethylamino)ethyl)carbamoyl)-3,5-dimethyl-1H-pyrrol-2-yl)methylene)-2-((3-nitrophenyl)amino)-4-oxo-4,5-dihydrothiophene-3-carboxylate (**29j**)
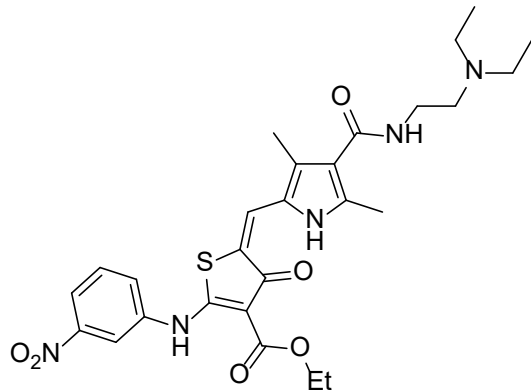
By using general procedure 10 with **11l** (59 mg, 0.19 mmol). The product was purified with purification method 2 to give the desired product (108 mg, 0.19 mmol, 100%, d.r. 15:1). ^{1}H NMR (500 MHz, CDCl$_3$) δ 13.58 (s, 1H), 11.73 (s, 1H), 8.33 (t, J = 2.1 Hz, 1H), 8.14 (dd, J = 8.0, 2.1 Hz, 1H), 7.72–7.67 (m, 1H), 7.64 (t, J = 8.0 Hz, 1H), 6.87 (s, 1H), 6.58 (s, 1H), 4.49 (q, J = 7.1 Hz, 2H), 3.55–3.49 (m, 2H), 2.76–2.69 (m, 2H), 2.69–2.62 (m, 4H), 2.58 (s, 3H), 2.39 (s, 3H), 1.49 (t, J = 7.1 Hz, 3H), 1.15–1.03 (m, 6H). ^{13}C NMR (126 MHz, CDCl$_3$) δ 180.9, 172.1, 166.9, 165.5, 148.8, 138.7, 137.4, 130.7, 128.8, 128.1, 126.0, 124.3, 121.0, 119.3, 117.0, 116.3, 102.2, 61.1, 51.5, 46.6 (2), 36.4, 14.4, 14.1, 11.3 (2), 11.1. HRMS-ESI (m/z): calculated for [M+H]$^+$ C$_{27}$H$_{34}$O$_6$N$_5$S, 556.2224; found, 556.2233.

Ethyl (E)-5-((4-((2-(diethylamino)ethyl)carbamoyl)-3,5-dimethyl-1H-pyrrol-2-yl)methylene)-4-oxo-2-(p-tolylamino)-4,5-dihydrothiophene-3-carboxylate (**29k**)
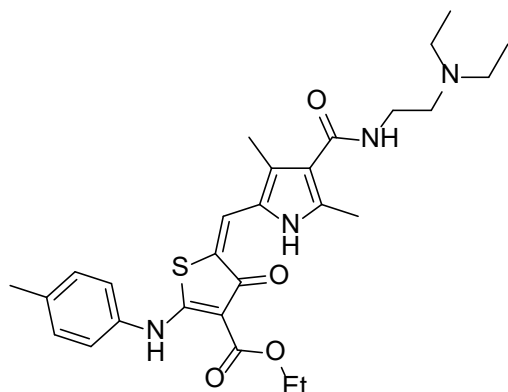
By using general procedure 10 with **11m** (53 mg, 0.19 mmol). The product was purified with purification method 2 to give the desired product (96 mg, 0.18 mmol, 97%, d.r. 4:1). ^{1}H NMR (700 MHz, CDCl$_3$) δ 13.57 (s, 1H), 11.23 (s, 1H), 7.29–7.24 (m, 4H), 6.75 (s, 1H), 6.45 (s, 1H), 4.47 (q, *J* = 7.1 Hz, 2H), 3.51–3.46 (m, 2H), 2.70–2.64 (m, 2H), 2.64–2.58 (m, 4H), 2.57 (s, 3H), 2.39 (s, 3H), 2.34 (s, 3H), 1.48 (t, *J* = 7.1 Hz, 3H), 1.04 (t, *J* = 7.1 Hz, 6H). ^{13}C NMR (176 MHz, CDCl$_3$) δ 181.4, 174.0, 166.9, 165.7, 137.5, 136.4, 134.9, 130.3 (2), 127.4, 125.9, 123.4 (2), 123.1, 118.9, 117.9, 100.9, 60.8, 51.5, 46.6 (2), 36.6, 21.1, 14.6, 14.1, 11.5 (2), 11.1. HRMS-ESI (m/z): calculated for [M+H]$^+$ C$_{28}$H$_{37}$O$_4$N$_4$S, 525.2530; found, 525.2528.

Ethyl (E)-5-((4-((2-(diethylamino)ethyl)carbamoyl)-3,5-dimethyl-1H-pyrrol-2-yl)methylene)-2-((3,4-dimethoxyphenyl)amino)-4-oxo-4,5-dihydrothiophene-3-carboxylate (**29l**)
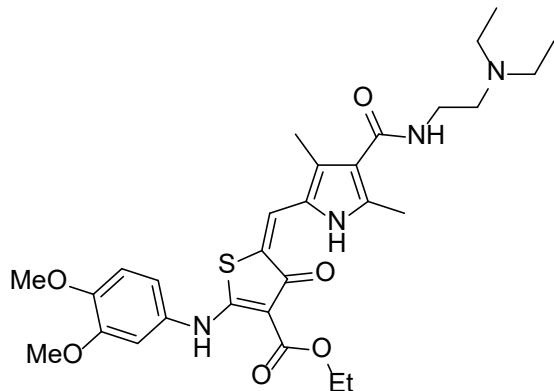
By using general procedure 10 with **11d** (61 mg, 0.19 mmol). The product was purified with purification method 2 to give the desired product (101 mg, 0.18 mmol, 93%, d.r. 3.5:1). ^{1}H NMR (700 MHz, CDCl$_3$) δ 13.60 (s, 1H), 11.06 (s, 1H), 7.40 (d, *J* = 8.7 Hz, 1H), 6.74 (s, 1H), 6.56 (d, *J* = 2.6 Hz, 1H), 6.52 (dd, *J* = 8.7, 2.6 Hz, 1H), 6.45 (s, 1H), 4.47 (q, *J* = 7.1 Hz, 2H), 3.89 (s, 3H), 3.85 (s, 3H), 3.52–3.46 (m, 2H), 2.70–2.64 (m, 2H), 2.64–2.57 (m, 4H), 2.56 (s, 3H), 2.34 (s, 3H), 1.47 (t, *J* = 7.1 Hz, 3H), 1.07–1.02 (m, 6H). ^{13}C NMR (176 MHz, CDCl$_3$) δ 181.4, 173.8, 166.6, 165.8, 159.6, 153.5, 136.2, 127.1, 125.9, 124.1, 122.8, 120.0, 118.7, 118.2, 103.9, 101.1, 99.5, 60.6, 55.9, 55.6, 51.6, 46.6 (2), 36.6, 14.6, 14.1, 11.5 (2), 11.1. HRMS-ESI (m/z): calculated for [M+H]$^+$ C$_{29}$H$_{39}$O$_6$N$_4$S, 571.2585; found, 571.592.

Ethyl (E)-5-((4-((2-(diethylamino)ethyl)carbamoyl)-3,5-dimethyl-1H-pyrrol-2-yl)methylene)-2-((4-ethylphenyl)amino)-4-oxo-4,5-dihydrothiophene-3-carboxylate (**29m**)
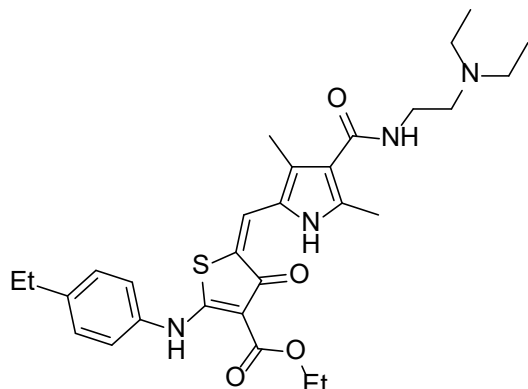
By using general procedure 10 with **11n** (55 mg, 0.19 mmol). The product was purified with purification method 2 to give the desired product (99 mg, 0.18 mmol, 97%, d.r. 3:1). ^{1}H NMR (700 MHz, CDCl₃) δ 13.58 (s, 1H), 11.25 (s, 1H), 7.32–7.27 (m, 4H), 6.83 (s, 1H), 6.75 (s, 1H), 4.46 (q, *J* = 7.1 Hz, 2H), 3.62–3.55 (m, 2H), 2.88–2.80 (m, 2H), 2.80–2.72 (m, 4H), 2.69 (q, *J* = 7.6 Hz, 2H),

2.57 (s, 3H), 2.36 (s, 3H), 1.47 (t, *J* = 7.1 Hz, 3H), 1.27 (t, *J* = 7.6 Hz, 3H), 1.18–1.12 (m, 6H). ^{13}C NMR (176 MHz, CDCl₃) δ 181.4, 173.9, 166.9, 166.0, 143.7, 136.6, 135.0, 129.1 (2), 127.5, 125.9, 123.4 (2), 123.1, 118.5, 118.0, 100.9, 60.8, 52.0, 47.2 (2), 36.3, 28.4, 15.4, 14.6, 14.2, 11.2, 10.7 (2). HRMS-ESI (m/z): calculated for [M+H]⁺ $C_{29}H_{39}O_4N_4S$, 539.2687; found, 539.2699.

(E)-N-(2-(Diethylamino)ethyl)-2,4-dimethyl-5-((4-(methylcarbamoyl)-3-oxo-5-(phenylamino)thiophen-2(3H)-ylidene)methyl)-1H-pyrrole-3-carboxamide (**30a**)
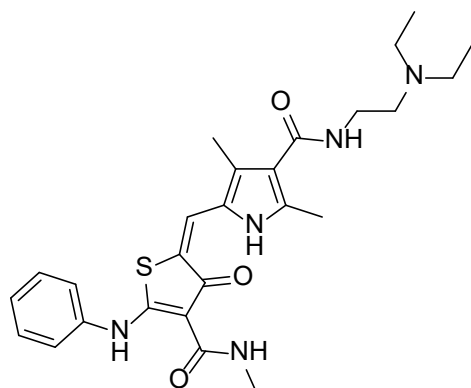
By using general procedure 10 with **23a** (30 mg, 0.12 mmol), **28** (35 mg, 0.13 mmol), and pyrrolidine (9.9 μL, 0.12 mmol) in ethanol (1.5 mL). The product was purified with purification method 2 to give the desired product (52 mg, 0.11 mmol, 87%, d.r. 5:1). ^{1}H NMR (700 MHz, CDCl₃) δ 13.66 (s, 1H), 12.65 (s, 1H), 9.23 (q, *J* = 4.8 Hz, 1H), 7.50–7.33 (m, 4H), 7.26–7.24 (m, 1H), 7.02 (s, 1H), 6.82 (s, 1H), 3.77–3.67 (m, 2H), 2.99

(d, *J* = 4.8 Hz, 3H), 3.06–2.82 (m, 6H), 2.62 (s, 3H), 2.41 (s, 3H), 1.32–1.22 (m, 6H). ^{13}C NMR (176 MHz, CDCl₃) δ 181.7, 171.0, 167.1, 138.0, 137.1, 129.8, 129.7 (2), 127.0, 126.3, 126.1, 123.6, 123.1, 122.1 (2), 118.5, 102.9, 52.7, 48.1 (2), 36.0, 25.0, 14.3, 11.3, 9.6 (2). HRMS-ESI (m/z): calculated for [M+H]⁺ $C_{26}H_{34}O_3N_5S$, 496.2377; found, 496.2383.

(E)-N-(2-(Diethylamino)ethyl)-5-((5-((3-methoxyphenyl)amino)-4-(methylcarbamoyl)-3-oxothiophen-2(3H)-ylidene)methyl)-2,4-dimethyl-1H-pyrrole-3-carboxamide (**30b**)
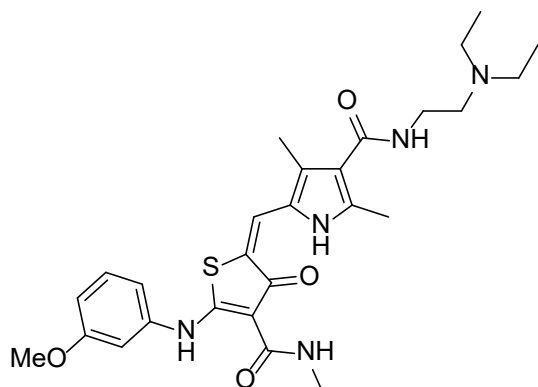
By using general procedure 10 with **23d** (33 mg, 0.12 mmol), **28** (35 mg, 0.13 mmol), and pyrrolidine (9.9 µL, 0.12 mmol) in ethanol (1.5 mL). The product was purified with purification method 2 to give the desired product (59 mg, 0.11 mmol, 94%, d.r. 3:1). ^{1}H NMR (700 MHz, CDCl$_3$) δ 13.66 (s, 1H), 12.69 (s, 1H), 9.25 (q, J = 4.7 Hz, 1H), 7.32 (t, J = 8.0 Hz, 1H), 6.95 (dd, J = 8.0, 2.1 Hz, 1H), 6.89 (t, J = 2.1 Hz, 1H), 6.87 (s, 1H), 6.83 (s, 1H), 6.79 (dd, J = 8.0, 2.1 Hz, 1H), 3.83 (s, 3H), 3.76–3.69 (m, 2H), 2.99 (d, J = 4.7 Hz, 3H), 3.05–2.90 (m, 6H), 2.62 (s, 3H), 2.42 (s, 3H), 1.37–1.23 (m, 6H). ^{13}C NMR (176 MHz, CDCl$_3$) δ 181.7, 170.7, 167.1, 160.6, 139.1, 137.2, 130.4, 126.1, 123.6, 118.6, 115.0, 114.0, 112.7, 112.1, 108.7, 107.4, 102.9, 55.4, 53.0, 48.2 (2), 35.7, 25.1, 14.4, 11.3, 9.8 (2). HRMS-ESI (m/z): calculated for [M+H]$^+$ C$_{27}$H$_{36}$O$_4$N$_5$S, 526.2483; found, 526.2490.

(E)-N-(2-(Diethylamino)ethyl)-5-((5-((3-fluorophenyl)amino)-4-(methylcarbamoyl)-3-oxothiophen-2(3H)-ylidene)methyl)-2,4-dimethyl-1H-pyrrole-3-carboxamide (**30c**)

By using general procedure 10 with **23b** (32 mg, 0.12 mmol), **28** (35 mg, 0.13 mmol), and pyrrolidine (9.9 µL, 0.12 mmol) in ethanol (1.5 mL). The product was purified with purification method 2 to give the desired product (55 mg, 0.11 mmol, 90%, d.r. 8:1). ^{1}H NMR (600 MHz, CDCl$_3$) δ 13.65 (s, 1H), 12.83 (s, 1H), 9.23 (q, J = 4.7 Hz, 1H), 7.41–7.35 (m, 1H), 7.15–7.10 (m, 2H), 7.02 (s, 1H), 6.97–6.92 (m, 1H), 6.86 (s, 1H), 3.76–3.65 (m, 2H), 2.99 (d, J = 4.7 Hz, 3H), 2.97–2.85 (m, 6H), 2.62 (s, 3H), 2.42 (s, 3H), 1.31–1.20 (m, 6H). ^{13}C NMR (151 MHz, CDCl$_3$) δ 181.6, 170.2, 166.9 and 163.9 (d, $^1J_{C-F}$ = 248 Hz), 162.3, 139.5 and 139.5 (d, $^3J_{C-F}$ = 10 Hz), 137.4, 131.0 and 130.9 (d, $^3J_{C-F}$ = 9 Hz), 128.7, 126.2, 124.1, 123.3, 118.6, 118.0, 117.3 and 117.3 (d, $^4J_{C-F}$ = 3 Hz), 112.9 and 112.8 (d, $^2J_{C-F}$ = 21 Hz), 109.0 and 108.8 (d, $^2J_{C-F}$ = 25 Hz), 103.2, 52.6, 47.7 (2), 35.9, 25.0, 14.3, 11.3, 9.9 (2). HRMS-ESI (m/z): calculated for [M+H]$^+$ C$_{26}$H$_{33}$O$_3$N$_5$FS, 514.2283; found,

514.2295.

(E)-N-(2-(Diethylamino)ethyl)-5-((5-((4-fluorophenyl)amino)-4-(methylcarbamoyl)-3-oxothiophen-2(3H)-ylidene)methyl)-2,4-dimethyl-1H-pyrrole-3-carboxamide (**30d**)
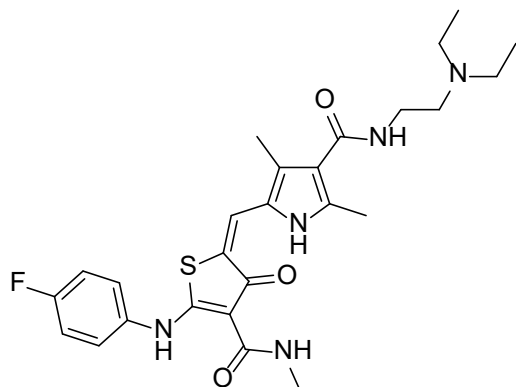
By using general procedure 10 with **23g** (30 mg, 0.15 mmol), **28** (44 mg, 0.17 mmol), and pyrrolidine (12.3 μL, 0.15 mmol) in ethanol (1.5 mL). The product was purified with purification method 2 to give the desired product (50 mg, 0.10 mmol, 65%, d.r. 15:1). ^{1}H NMR (700 MHz, CDCl$_3$) δ 13.61 (s, 1H), 12.46 (s, 1H), 9.19 (q, J = 4.9 Hz, 1H), 7.36–7.31 (m, 2H), 7.15–7.11 (m, 2H), 6.81 (s, 1H), 6.47 (s, 1H), 3.52–3.46 (m, 2H), 2.99 (d, J = 4.9 Hz, 3H), 2.70–2.65 (m, 2H), 2.59 (s, 3H), 2.58–2.54 (m, 4H), 2.36 (s, 3H), 1.07–0.99 (m, 6H). ^{13}C NMR (176 MHz, CDCl$_3$) δ 181.8, 171.7, 167.0, 165.6, 161.6 and 160.2 (d, $^1J_{C\text{-}F}$ = 248 Hz), 136.9, 134.0 and 134.0 (d, $^4J_{C\text{-}F}$ = 3 Hz), 127.8, 126.0, 124.6 and 124.5 (d, $^3J_{C\text{-}F}$ = 8 Hz) (2), 123.6, 119.1, 118.1, 116.6 and 116.5 (d, $^2J_{C\text{-}F}$ = 23 Hz) (2), 102.8, 51.5, 46.5 (2), 36.6, 25.0, 14.2, 11.7 (2), 11.1. HRMS-ESI (m/z): calculated for [M+H]$^+$ C$_{26}$H$_{33}$O$_3$N$_5$FS, 514.2283; found, 514.2287.

(E)-5-((5-((3-Chlorophenyl)amino)-4-(methylcarbamoyl)-3-oxothiophen-2(3H)-ylidene)methyl)-N-(2-(diethylamino)ethyl)-2,4-dimethyl-1H-pyrrole-3-carboxamide (**30e**)
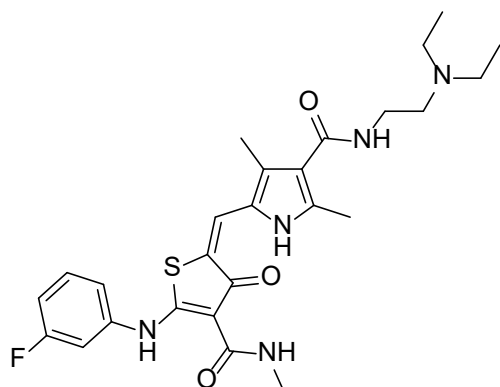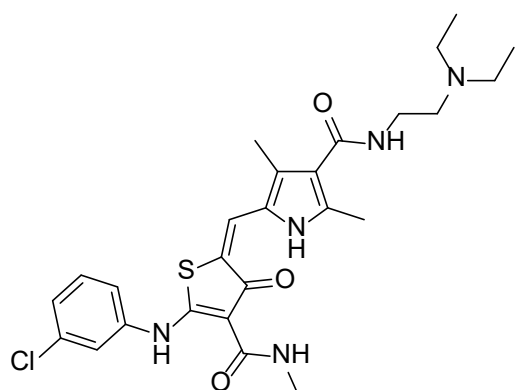
By using general procedure 10 with **23c** (35 mg, 0.12 mmol), **28** (36 mg, 0.13 mmol), and pyrrolidine (10.0 μL, 0.12 mmol) in ethanol (1.5 mL). The product was purified with purification method 2 to give the desired product (39 mg, 0.07 mmol, 61%, d.r. 6:1). ^{1}H NMR (600 MHz, CDCl$_3$) δ 13.63 (s, 1H), 12.79 (s, 1H), 9.23 (q, J = 4.9 Hz, 1H), 7.40 (t, J = 1.9 Hz, 1H), 7.35 (t, J = 8.0 Hz, 1H), 7.23 (td, J = 8.0, 1.9 Hz, 2H), 6.87 (s, 1H), 6.53 (s, 1H), 3.54–3.46 (m, 2H), 2.99 (d, J = 4.9 Hz, 3H), 2.72–2.66 (m, 2H), 2.65–2.60 (m, 4H), 2.60 (s, 3H), 2.38 (s, 3H), 1.11–1.00 (m, 6H). ^{13}C NMR (151 MHz, CDCl$_3$) δ 181.6, 170.3, 166.9, 165.5, 139.2, 137.2, 135.3, 130.6, 128.3, 126.1, 124.0, 123.1, 121.7, 121.0, 119.9, 117.8, 103.2, 51.5, 46.5 (2), 36.6, 25.0, 14.1, 11.5 (2), 11.1. HRMS-ESI (m/z): calculated for [M+H]$^+$ C$_{26}$H$_{33}$O$_3$N$_5$^{35}ClS, 530.1987; found, 530.1998 and

$C_{26}H_{33}O_3N_5{}^{37}ClS$, 532.1958; found, 532.1969.

(E)-N-(2-(Diethylamino)ethyl)-2,4-dimethyl-5-((4-(methylcarbamoyl)-3-oxo-5-((3-(trifluoromethyl)phenyl)amino)thiophen-2(3H)-ylidene)methyl)-1H-pyrrole-3-carboxamide **(30f)**

By using general procedure 10 with **23e** (63 mg, 0.20 mmol), **28** (58 mg, 0.22 mmol), and pyrrolidine (16.4 μL, 0.20 mmol) in ethanol (2.0 mL). The product was purified with purification method 2 to give the desired product (93 mg, 0.16 mmol, 82%, d.r. 2:1). ^{1}H NMR (600 MHz, CDCl$_3$) δ 13.63 (s, 1H), 12.95 (s, 1H), 9.23 (q, J = 5.0 Hz, 1H), 7.61–7.46 (m, 4H), 6.88 (s, 1H), 6.75 (s, 1H), 3.58–3.51 (m, 2H), 2.99 (d, J = 4.9 Hz, 3H), 2.81–2.74 (m, 2H), 2.71–2.65 (m, 4H), 2.60 (s, 3H), 2.39 (s, 3H), 1.14–1.07 (m, 6H). ^{13}C NMR (151 MHz, CDCl$_3$) δ 181.6, 170.1, 166.9, 165.6, 138.7, 137.4, 132.5 and 132.3 and 132.1 and 131.8 (q, $^2J_{C\text{-}F}$ = 32 Hz), 130.3, 128.6, 126.1 and 124.3 and 122.5 and 120.7 (q, $^1J_{C\text{-}F}$ = 273 Hz), 125.7 and 125.7 and 125.7 and 125.7 (q, $^4J_{C\text{-}F}$ = 1 Hz), 124.7 and 124.7 and 124.6 and 124.6 (q, $^4J_{C\text{-}F}$ = 1 Hz), 124.3, 123.2, 122.5 and 122.4 and 122.4 and 122.4 (q, $^3J_{C\text{-}F}$ = 4 Hz), 119.2, 118.4 and 118.3 and 118.3 and 118.3 (q, $^3J_{C\text{-}F}$ = 4 Hz), 103.4, 51.7, 46.8 (2), 36.4, 25.1, 14.2, 11.2, 11.0 (2). HRMS-ESI (m/z): calculated for [M+H]$^+$ $C_{27}H_{33}O_3N_5F_3S$, 564.2251; found, 564.2261.

(E)-N-(2-(Diethylamino)ethyl)-2,4-dimethyl-5-((4-(methylcarbamoyl)-5-((3-nitrophenyl)amino)-3-oxothiophen-2(3H)-ylidene)methyl)-1H-pyrrole-3-carboxamide **(30g)**
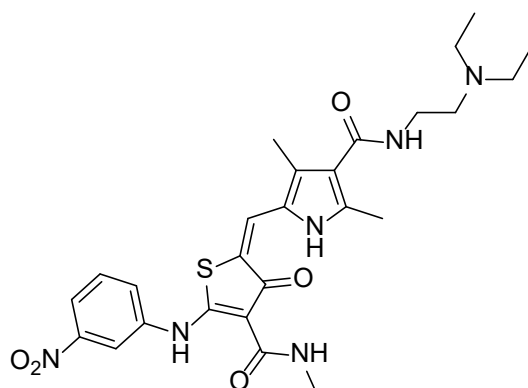
By using general procedure 10 with **23f** (44 mg, 0.15 mmol), **28** (44 mg, 0.17 mmol), and pyrrolidine (12.3 μL, 0.15 mmol) in ethanol (1.5 mL). The product was purified with purification method 2 to give the desired product (26 mg, 0.05 mmol, 31%, d.r. 25:1). ^{1}H NMR (600 MHz, CDCl$_3$) δ 13.64 (s, 1H), 13.17 (s, 1H), 9.25 (q, J = 4.9 Hz, 1H), 8.30 (t, J = 2.1 Hz, 1H), 8.07 (ddd, J = 8.0, 2.1, 1.3 Hz, 1H), 7.63 (ddd, J = 8.0, 2.1, 1.3 Hz, 1H), 7.60 (t, J = 8.0 Hz, 1H), 6.93 (s, 1H), 6.55 (s, 1H), 3.57–3.47 (m, 2H), 3.00 (d, J = 4.9 Hz, 3H), 2.75–2.66 (m, 2H), 2.64–2.59 (m,

4H), 2.61 (s, 3H), 2.41 (s, 3H), 1.10–1.02 (m, 6H). ^{13}C NMR (151 MHz, CDCl$_3$) δ 181.4, 169.4, 166.8, 165.4, 148.9, 139.4, 137.8, 130.6, 129.0, 127.0, 126.2, 124.7, 120.0, 119.5, 117.1, 115.5, 103.8, 51.5, 46.6 (2), 36.6, 25.1, 14.2, 11.5 (2), 11.2. HRMS-ESI (m/z): calculated for [M+H]$^+$ C$_{26}$H$_{33}$O$_5$N$_6$S, 541.2228; found, 541.2239.

Tert-butyl (E)-(2-(5-((4-((2-(diethylamino)ethyl)carbamoyl)-3,5-dimethyl-1H-pyrrol-2-yl) methylene)-2-((3-fluorophenyl)amino)-4-oxo-4,5-dihydrothiophene-3-carboxamido)ethyl) carbamate (**31a**)

By using general procedure 10 with **24b** (50 mg, 0.13 mmol), **28** (37 mg, 0.14 mmol), and pyrrolidine (10.4 µL, 0.13 mmol) in ethanol (1.5 mL). The product was purified with purification method 2 to give the desired product (47 mg, 0.07 mmol, 58%, d.r. 4:1). ^{1}H NMR (400 MHz, CDCl$_3$) δ 13.60 (s, 1H), 12.67 (s, 1H), 9.48 (t, J = 5.9 Hz, 1H), 7.45–7.35 (m, 1H), 7.20–7.08 (m, 2H), 6.99–6.92 (m, 1H), 6.87 (s, 1H), 6.77 (s, 1H), 5.01 (s, 1H), 3.66–3.48 (m, 4H), 3.42–3.31 (m, 2H), 2.88–2.68 (m, 6H), 2.62 (s, 3H), 2.41 (s, 3H), 1.45 (s, 9H), 1.21–1.12 (m, 6H). ^{13}C NMR (151 MHz, CDCl$_3$) δ 181.5, 170.4, 166.9, 166.0, 163.9 and 162.3 (d, $^1J_{C-F}$ = 245 Hz), 156.0, 139.4 and 139.3 (d, $^3J_{C-F}$ = 10 Hz), 137.4, 131.0 and 130.9 (d, $^3J_{C-F}$ = 9 Hz), 128.4, 126.1, 124.0, 119.5, 117.8, 117.5 and 117.4 (d, $^4J_{C-F}$ = 3 Hz), 113.1 and 112.9 (d, $^2J_{C-F}$ = 21 Hz), 109.1 and 108.9 (d, $^2J_{C-F}$ = 25 Hz), 102.9, 79.3, 52.0, 46.8 (2), 40.9, 38.5, 36.7, 28.3 (3), 14.2, 11.3 (2), 11.1. HRMS-ESI (m/z): calculated for [M+H]$^+$ C$_{32}$H$_{44}$O$_5$N$_6$FS, 643.3072; found, 643.3079.

Tert-butyl (E)-(2-(5-((4-((2-(diethylamino)ethyl)carbamoyl)-3,5-dimethyl-1H-pyrrol-2-yl) methylene)-4-oxo-2-(phenylamino)-4,5-dihydrothiophene-3-carboxamido)ethyl)carbamate (**31b**)
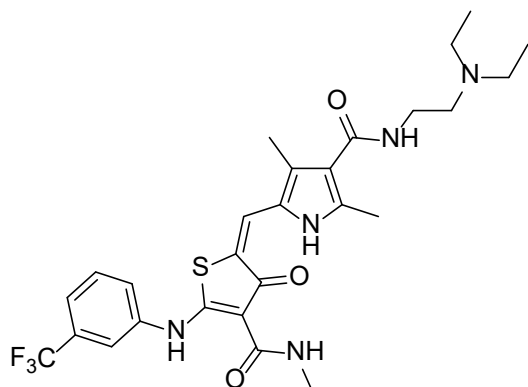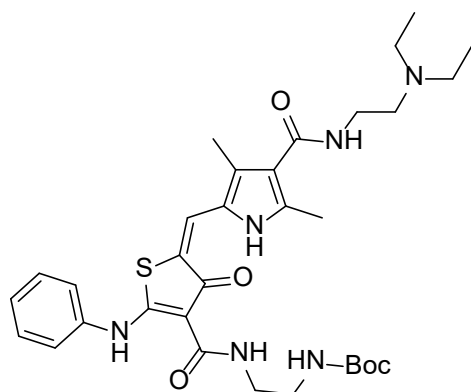
By using general procedure 10 with **24a** (75 mg, 0.20 mmol), **28** (64 mg, 0.24 mmol), and pyrrolidine (16.4 µL, 0.20 mmol) in ethanol (2.0 mL). The product was purified with purification method 2 to give the desired product (70 mg, 0.11 mmol, 56%, d.r. 7:1). ^{1}H NMR (500 MHz, CDCl$_3$) δ 13.60 (s, 1H), 12.48 (s, 1H), 9.48 (t, J = 6.2 Hz, 1H), 7.45–7.40 (m, 2H), 7.37–7.33 (m,

2H), 7.29–7.26 (m, 1H), 6.90 (s, 1H), 6.81 (s, 1H), 5.07 (t, J = 5.8 Hz, 1H), 3.64–3.58 (m, 2H), 3.58–3.49 (m, 2H), 3.41–3.32 (m, 2H), 2.92–2.80 (m, 2H), 2.80–2.69 (m, 4H), 2.61 (s, 3H), 2.38 (d, J = 1.8 Hz, 3H), 1.45 (s, 9H), 1.20–1.10 (m, 6H). ^{13}C NMR (126 MHz, CDCl$_3$) δ 181.6, 171.1, 167.0, 165.8, 155.9, 137.8, 129.6 (2), 128.0, 126.4, 125.9, 123.5, 123.1, 122.1 (2), 118.6, 118.1, 102.5, 79.2, 51.9, 47.1 (2), 41.0, 38.4, 36.2, 28.3 (3), 14.2, 11.1, 10.6 (2). HRMS-ESI (m/z): calculated for [M+H]$^+$ C$_{32}$H$_{45}$O$_5$N$_6$S, 625.3167; found, 625.3177.

Tert-butyl (E)-(2-(2-((3-chlorophenyl)amino)-5-((4-((2-(diethylamino)ethyl)carbamoyl)-3,5-dimethyl-1H-pyrrol-2-yl)methylene)-4-oxo-4,5-dihydrothiophene-3-carboxamido)ethyl)carbamate (**31c**)
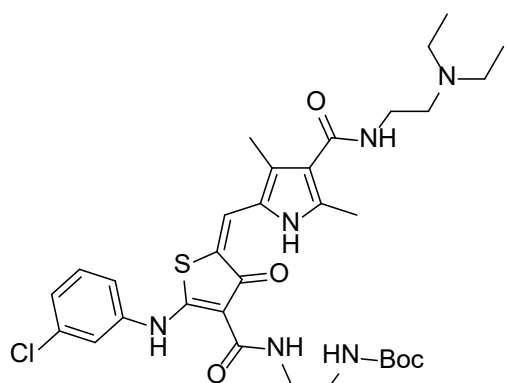
By using general procedure 10 with **24c** (82 mg, 0.20 mmol), **28** (58 mg, 0.22 mmol), and pyrrolidine (16.4 µL, 0.20 mmol) in ethanol (2.0 mL). The product was purified with purification method 2 to give the desired product (75 mg, 0.11 mmol, 57%, d.r. 6:1). ^{1}H NMR (700 MHz, CDCl$_3$) δ 13.61 (s, 1H), 12.63 (s, 1H), 9.46 (t, J = 6.1 Hz, 1H), 7.39 (t, J = 1.9 Hz, 1H), 7.35 (t, J = 8.0 Hz, 1H), 7.23 (td, J = 8.0, 1.9 Hz, 2H), 6.86 (s, 1H), 6.80 (s, 1H), 5.03 (s, 1H), 3.78–3.69 (m, 2H), 3.61–3.48 (m, 2H), 3.43–3.33 (m, 2H), 3.12–3.00 (m, 2H), 3.00–2.88 (m, 4H), 2.63 (s, 3H), 2.42 (s, 3H), 1.45 (s, 9H), 1.36–1.23 (m, 6H). ^{13}C NMR (176 MHz, CDCl$_3$) δ 181.6, 170.6, 167.0, 166.1, 156.0, 139.1, 137.7, 135.4, 130.7, 129.0, 126.3, 126.2, 124.2, 121.9, 120.0, 118.6, 117.8, 103.0, 79.3, 52.7, 48.1 (2), 41.0, 38.5, 35.9, 28.4 (3), 14.4, 11.3, 9.6 (2). HRMS-ESI (m/z): calculated for [M+H]$^+$ C$_{32}$H$_{44}$O$_5$N$_6$^{35}ClS, 659.2777; found, 659.2794 and C$_{32}$H$_{44}$O$_5$N$_6$^{37}ClS, 661.2747; found, 661.2769.

Tert-butyl (E)-(2-(5-((4-((2-(diethylamino)ethyl)carbamoyl)-3,5-dimethyl-1H-pyrrol-2-yl)methylene)-2-((3-methoxyphenyl)amino)-4-oxo-4,5-dihydrothiophene-3-carboxamido)ethyl)carbamate (**31d**)
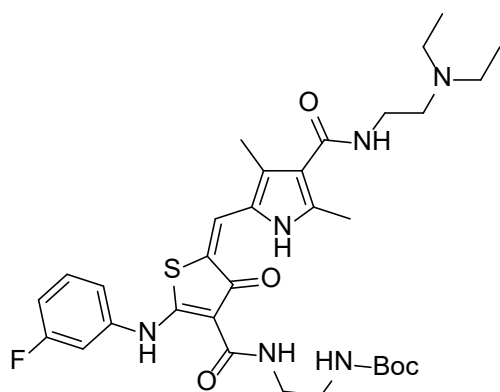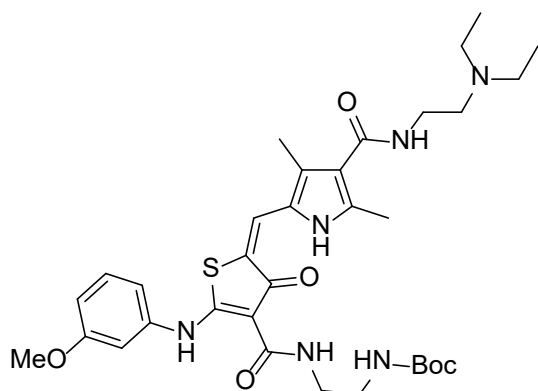
By using general procedure 10 with **24d** (26 mg, 0.06 mmol), **28** (19 mg, 0.07 mmol), and pyrrolidine (5.2 µL, 0.06 mmol) in ethanol (1.0 mL). The product was purified with purification method 2 to give the desired product (31 mg, 0.05 mmol, 75%, d.r. 9:1). ^{1}H NMR (700 MHz, CDCl$_3$)

δ 13.61 (s, 1H), 12.52 (s, 1H), 9.49 (t, J = 6.2 Hz, 1H), 7.32 (t, J = 8.0 Hz, 1H), 6.95 (dd, J = 8.0, 2.1 Hz, 1H), 6.89 (t, J = 2.1 Hz, 1H), 6.87 (s, 1H), 6.83 (s, 1H), 6.80 (dd, J = 8.0, 2.1 Hz, 1H), 5.05 (s, 1H), 3.83 (s, 3H), 3.74–3.65 (m, 2H), 3.59–3.52 (m, 2H), 3.40–3.35 (m, 2H), 3.06–2.95 (m, 2H), 2.95–2.83 (m, 4H), 2.63 (s, 3H), 2.41 (s, 3H), 1.45 (s, 9H), 1.31–1.20 (m, 6H). ^{13}C NMR (176 MHz, CDCl$_3$) δ 181.7, 170.9, 167.1, 166.0, 160.6, 156.0, 139.0, 137.3, 130.5, 128.4, 126.1, 123.7, 118.5, 118.3, 114.1, 112.2, 107.6, 102.6, 79.3, 55.5, 52.5, 47.7 (2), 41.0, 38.5, 36.0, 28.4 (3), 14.3, 11.3, 10.0 (2). HRMS-ESI (m/z): calculated for [M+H]$^+$ C$_{33}$H$_{47}$O$_6$N$_6$S, 655.3272; found, 655.3283.

(E)-5-((4-((2-Aminoethyl)carbamoyl)-5-((3-fluorophenyl)amino)-3-oxothiophen-2(3H)-yli dene)methyl)-N-(2-(diethylamino)ethyl)-2,4-dimethyl-1H-pyrrole-3-carboxamide (**32a**, JH259)
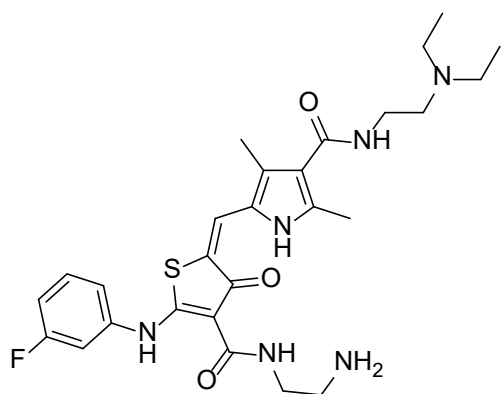
The Boc group of **31a** was deprotected by using 4M HCl in dioxane and MeOH (d.r. 2:1). The residue was washed or titrated by EtOH/n-hexane and dried under vacuum to give the pure isomeric product as HCl salt (Protonated triethylamine). ^{1}H NMR (600 MHz, DMSO-d_6) δ 13.51 (s, 1H), 12.34 (s, 1H), 10.47 (s, 1H), 9.28 (t, J = 6.1 Hz, 1H), 8.09–7.97 (m, 3H), 7.55 (td, J = 8.2, 6.4 Hz, 1H), 7.48 (s, 1H), 7.38 (dt, J = 10.1, 2.3 Hz, 1H), 7.31 (ddd, J = 8.2, 2.3, 0.9 Hz, 1H), 7.20 (tdd, J = 8.2, 2.3, 0.9 Hz, 1H), 3.62–3.55 (m, 4H), 3.21–3.12 (m, 6H), 3.00 (t, J = 6.4 Hz, 2H), 2.48 (s, 3H), 2.31 (s, 3H), 1.23 (t, J = 7.2 Hz, 6H). ^{13}C NMR (151 MHz, DMSO-d_6) δ 180.8, 170.7, 165.6, 164.7, 162.8 and 161.2 (d, $^1J_{\text{C-F}}$ = 245 Hz), 138.9 and 138.8 (d, $^3J_{\text{C-F}}$ = 10 Hz), 135.7, 131.2 and 131.2 (d, $^3J_{\text{C-F}}$ = 9 Hz), 128.8, 125.3, 124.8, 119.4, 118.5 and 118.5 (d, $^4J_{\text{C-F}}$ = 3 Hz), 116.6, 113.2 and 113.1 (d, $^2J_{\text{C-F}}$ = 21 Hz), 109.7 and 109.5 (d, $^2J_{\text{C-F}}$ = 25 Hz), 101.9, 49.8, 46.4 (2), 38.2, 35.6, 33.6, 13.2, 10.1, 8.1 (2). HRMS-ESI (m/z): calculated for [M+H]$^+$ C$_{27}$H$_{36}$O$_3$N$_6$FS, 543.2548; found, 543.2555.

(E)-5-((4-((2-Aminoethyl)carbamoyl)-3-oxo-5-(phenylamino)thiophen-2(3H)-ylidene)methyl) -N-(2-(diethylamino)ethyl)-2,4-dimethyl-1H-pyrrole-3-carboxamide (**32b**)

By using **31b** following the same procedure described in **32a** (d.r. 2:1). ^{1}H NMR (600 MHz, DMSO-d_6) δ 13.52 (s, 1H), 12.29 (s, 1H), 9.41 (s, 1H), 9.28 (t, J = 6.2 Hz, 1H), 7.91–7.82 (m, 2H), 7.79 (t, J = 5.7 Hz, 1H), 7.56–7.43 (m, 4H), 7.43 (s, 1H), 7.42–7.33 (m, 1H), 3.61–3.51 (m, 4H), 3.25–3.16 (m, 6H), 3.07–2.97 (m, 2H), 2.46 (s, 3H), 2.29 (s, 3H), 1.22 (t, J = 7.2 Hz,
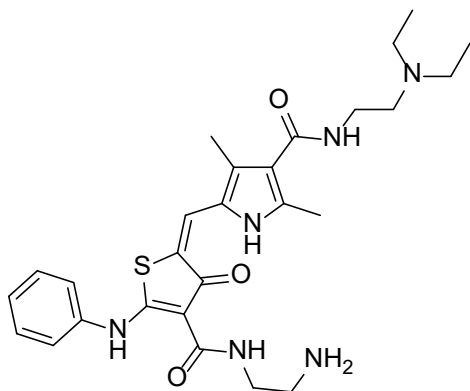
6H). ^{13}C NMR (151 MHz, DMSO-d_6) δ 180.8, 171.2, 165.7, 157.6, 137.2, 135.3, 129.5 (2), 128.2, 126.6, 125.2, 124.4, 123.0, 122.5 (2), 119.1, 117.1, 101.5, 49.5, 46.5 (2), 35.6, 33.7, 13.0, 10.0, 8.2 (2). ^{13}C NMR (126 MHz, DMSO-d_6) δ 180.8, 170.8, 165.5, 165.0, 138.6, 135.5, 133.4, 131.0, 128.6, 126.2, 125.2, 124.7, 122.1, 121.2, 119.1, 116.7, 101.9, 49.4, 46.4 (2), 38.3, 35.5, 33.5, 12.9, 9.9, 8.1 (2).HRMS-ESI (m/z): calculated for [M+H]+ $C_{27}H_{37}O_3N_6S$, 525.2642; found, 525.2653.

(E)-5-((4-((2-Aminoethyl)carbamoyl)-5-((3-chlorophenyl)amino)-3-oxothiophen-2(3H)-yli dene)methyl)-N-(2-(diethylamino)ethyl)-2,4-dimethyl-1H-pyrrole-3-carboxamide (**32c**, JH332)
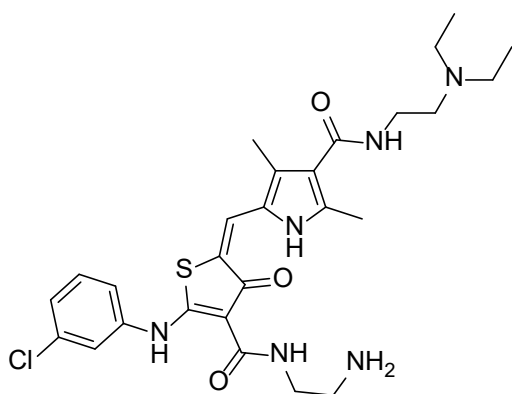
By using **31c** following the same procedure as described for **32a** (d.r. 5:1). ^{1}H NMR (500 MHz, DMSO-d_6) δ 13.50 (s, 1H), 12.32 (s, 1H), 9.63–9.54 (m, 1H), 9.28 (t, J = 6.1 Hz, 1H), 7.97–7.91 (m, 2H), 7.83 (t, J = 5.7 Hz, 1H), 7.62–7.51 (m, 2H), 7.49 (s, 1H), 7.44–7.39 (m, 2H), 3.61–3.52 (m, 4H), 3.26–3.14 (m, 6H), 3.05–2.97 (m, 2H), 2.46 (s, 3H), 2.29 (s, 3H), 1.22 (t, J = 7.2 Hz, 6H). HRMS-ESI (m/z): calculated for [M+H]$^+$ $C_{27}H_{36}O_3N_6{}^{35}ClS$, 559.2253; found, 559.2260 and $C_{27}H_{36}O_3N_6{}^{37}ClS$, 561.2223; found, 561.2227.

(E)-5-((4-((2-Aminoethyl)carbamoyl)-5-((3-methoxyphenyl)amino)-3-oxothiophen-2(3H)-yli dene)methyl)-N-(2-(diethylamino)ethyl)-2,4-dimethyl-1H-pyrrole-3-carboxamide (**32d**, JH333)
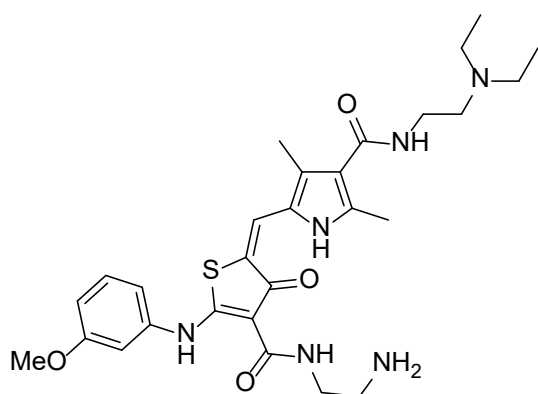
By using **31d** following the same procedure as described for **32a** (d.r. 1.5:1). ^{1}H NMR (700 MHz, DMSO-d_6) δ 13.53 (s, 1H), 12.34 (s, 1H), 10.57–10.42 (m, 1H), 9.31 (t, J = 6.1 Hz, 1H), 8.06–8.04 (m, 2H), 8.02 (t, J = 5.7 Hz, 1H), 7.47–7.41 (m, 2H), 7.11–7.01 (m, 2H), 6.97–6.92 (m, 1H), 3.82 (s, 3H), 3.63–3.58 (m, 4H), 3.23–3.11 (m, 6H), 3.05–2.91 (m, 2H), 2.49 (s, 3H), 2.33 (s, 3H), 1.25 (t, J = 7.2 Hz, 6H). ^{13}C NMR (176 MHz, DMSO-d_6) δ 180.8, 170.8, 165.8, 164.8, 159.9, 138.4,

149

135.5, 130.4, 128.5, 125.3, 121.8, 119.3, 118.2, 117.0, 114.1, 112.1, 107.8, 101.7, 55.1, 49.8, 46.4 (2), 38.3, 35.6, 33.6, 13.2, 10.2, 8.1 (2). HRMS-ESI (m/z): calculated for [M+H]$^+$ $C_{28}H_{39}O_4N_6S$, 555.2748; found, 555.2757.

(E)-5-((4-(Benzylcarbamoyl)-5-((3-fluorophenyl)amino)-3-oxothiophen-2(3H)-ylidene)methyl)-N-(2-(diethylamino)ethyl)-2,4-dimethyl-1H-pyrrole-3-carboxamide (**33**)
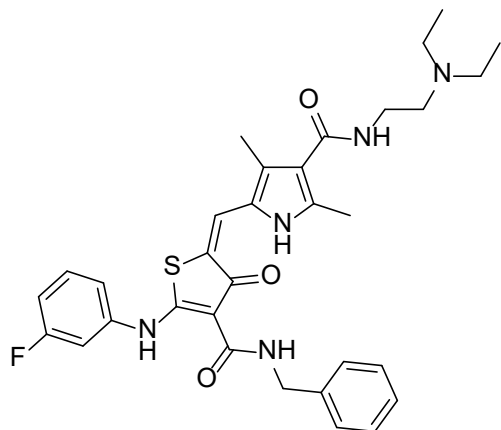
By using general procedure 10 with **25** (68 mg, 0.20 mmol), **28** (58 mg, 0.22 mmol), and pyrrolidine (16.4 µL, 0.20 mmol) in ethanol (2.0 mL). The product was purified with purification method 2 to give the desired product (105 mg, 0.18 mmol, 89%, d.r. 99:1). ^{1}H NMR (600 MHz, CDCl$_3$) δ 13.56 (s, 1H), 12.75 (s, 1H), 9.74 (t, *J* = 6.1 Hz, 1H), 7.42–7.35 (m, 5H), 7.30–7.27 (m, 1H), 7.16–7.11 (m, 2H), 6.97–6.93 (m, 1H), 6.87 (s, 1H), 6.45 (s, 1H), 4.66 (d, *J* = 6.0 Hz, 2H), 3.51–3.44 (m, 2H), 2.71–2.63 (m, 2H), 2.61–2.53 (m, 4H), 2.58 (s, 3H), 2.38 (s, 3H), 1.08–0.99 (m, 6H). ^{13}C NMR (151 MHz, CDCl$_3$) δ 181.6, 170.5, 166.4, 165.4, 163.9 and 162.3 (d, $^1J_{C\text{-}F}$ = 248 Hz), 139.5 and 139.4 (d, $^3J_{C\text{-}F}$ = 10 Hz), 138.7, 137.2, 131.0 and 130.9 (d, $^3J_{C\text{-}F}$ = 9 Hz), 128.6 (2), 128.3, 127.3 (2), 127.1, 126.1, 124.0, 119.3, 117.7, 117.5 and 117.5 (d, $^4J_{C\text{-}F}$ = 3 Hz), 113.0 and 112.9 (d, $^3J_{C\text{-}F}$ = 21 Hz), 109.1 and 109.0 (d, $^3J_{C\text{-}F}$ = 25 Hz), 103.0, 51.4, 46.4 (2), 42.2, 36.6, 14.2, 11.6 (2), 11.1. HRMS-ESI (m/z): calculated for [M+H]$^+$ $C_{32}H_{37}O_3N_5FS$, 590.2596; found, 590.2603.

(E)-N-(2-(diethylamino)ethyl)-2,4-dimethyl-5-((4-(methylcarbamoyl)-3-oxo-5-(phenylamino)furan-2(3H)-ylidene)methyl)-1H-pyrrole-3-carboxamide (**34**)
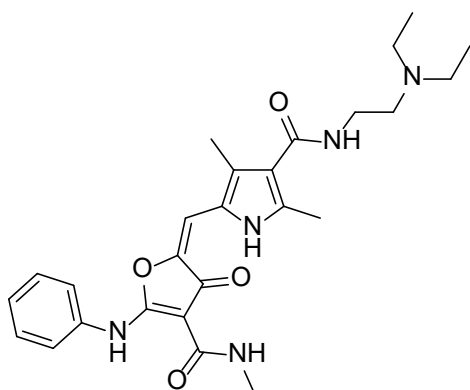
By using general procedure 10 with **26** (30 mg, 0.13 mmol), **28** (38 mg, 0.14 mmol), and pyrrolidine (10.7 µL, 0.13 mmol) in ethanol (1.5 mL). The product was purified with purification method 2 to give the desired product (31 mg, 0.07 mmol, 50%, d.r. 2.5:1). ^{1}H NMR (700 MHz, CDCl$_3$) δ 12.98 (s, 1H), 10.63 (s, 1H), 7.92 (q, *J* = 4.9 Hz, 1H), 7.46–7.37 (m, 4H), 7.24–7.18 (m, 1H), 6.95 (s, 1H), 6.83 (s, 1H), 3.67–3.56 (m, 2H), 2.98 (d, *J* = 5.0 Hz, 3H), 2.91–2.84 (m, 2H), 2.83–2.76 (m, 4H), 2.58 (s, 3H), 2.40 (s, 3H), 1.22–1.12 (m, 6H). ^{13}C NMR (176 MHz, CDCl$_3$) δ 176.3, 167.4, 166.0, 165.1, 142.6, 136.4, 135.4,

129.5 (2), 127.1, 125.6, 121.7, 120.7 (2), 118.2, 109.8, 92.5, 52.2, 47.3 (2), 36.2, 25.1, 14.2, 11.3, 10.5 (2). HRMS-ESI (m/z): calculated for $[M+H]^+$ $C_{26}H_{34}O_4N_5$, 480.2605; found, 480.2609.

Tert-butyl (E)-(2-(5-((4-((2-(diethylamino)ethyl)carbamoyl)-3,5-dimethyl-1H-pyrrol-2-yl) methylene)-4-oxo-2-(phenylamino)-4,5-dihydrofuran-3-carboxamido)ethyl)carbamate (**35a**)
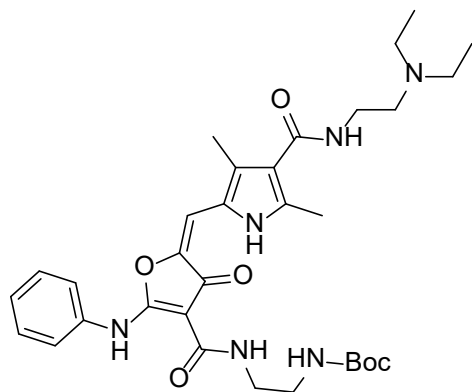
By using general procedure 10 with **27a** (47 mg, 0.13 mmol), **28** (38 mg, 0.14 mmol), and pyrrolidine (10.7 µL, 0.13 mmol) in ethanol (1.5 mL). The product was purified with purification method 2 to give the desired product (28 mg, 0.05 mmol, 35%, d.r. 3:1). ^{1}H NMR (700 MHz, CDCl$_3$) δ 12.98 (s, 1H), 10.52 (s, 1H), 8.16 (t, J = 6.4 Hz, 1H), 7.45–7.40 (m, 4H), 7.25–7.21 (m, 1H), 6.82 (s, 1H), 6.73 (s, 1H), 5.03 (s, 1H), 3.84–3.73 (m, 2H), 3.56–3.50 (m, 2H), 3.39–3.34 (m, 2H), 3.22–3.13 (m, 2H), 3.13–2.99 (m, 4H), 2.61 (s, 3H), 2.43 (s, 3H), 1.45 (s, 9H), 1.40–1.32 (m, 6H). ^{13}C NMR (176 MHz, CDCl$_3$) δ 176.3, 167.4, 166.4, 165.2, 156.0, 142.5, 136.8, 135.3, 129.6 (2), 127.5, 125.7, 121.8, 120.8 (2), 117.7, 109.9, 92.3, 79.4, 53.2, 48.5 (2), 41.0, 38.7, 35.7, 28.4 (3), 14.3, 11.4, 9.0 (2). HRMS-ESI (m/z): calculated for $[M+H]^+$ $C_{32}H_{45}O_6N_6$, 609.3395; found, 609.3397.

Tert-butyl (E)-(2-(5-((4-((2-(diethylamino)ethyl)carbamoyl)-3,5-dimethyl-1H-pyrrol-2-yl) methylene)-2-((3-fluorophenyl)amino)-4-oxo-4,5-dihydrofuran-3-carboxamido)ethyl)carbamate (**35b**)
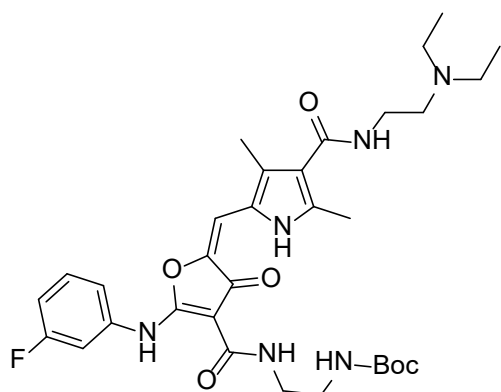
By using general procedure 10 with **27b** (86 mg, 0.23 mmol), **28** (66 mg, 0.25 mmol), and pyrrolidine (18.7 µL, 0.23 mmol) in ethanol (2.5 mL). The product was purified with purification method 2 to give the desired product (21 mg, 0.03 mmol, 15%, d.r. 6:1). ^{1}H NMR (500 MHz, CDCl$_3$) δ 12.95 (s, 1H), 10.62 (s, 1H), 8.16 (t, J = 6.1 Hz, 1H), 7.37 (td, J = 8.2, 6.3 Hz, 1H), 7.28 (dt, J = 8.2, 2.2 Hz, 1H), 7.15 (dd, J = 8.2, 2.2 Hz, 1H), 6.92 (td, J = 8.2, 2.2 Hz, 1H), 6.88 (s, 1H), 6.77 (s, 1H), 5.02 (s, 1H), 3.81–3.69 (m, 2H), 3.57–3.51 (m, 2H), 3.40–3.33 (m, 2H), 3.14–3.04 (m, 2H), 3.03–2.89 (m, 4H), 2.60 (s, 3H), 2.44 (s, 3H), 1.45 (s, 9H), 1.36–1.27 (m, 6H). 13C NMR (126 MHz, CDCl3)

δ 176.2, 167.1, 166.1, 165.0, 164.0 and 162.0 (d, $^1J_{C-F}$ = 247 Hz), 155.9, 142.2, 136.9, 136.7 and 136.6 (d, $^3J_{C-F}$ = 10 Hz), 130.8 and 130.7 (d, $^3J_{C-F}$ = 10 Hz), 127.9, 121.6, 118.0, 116.0 and 116.0 (d, $^4J_{C-F}$ = 3 Hz), 112.3 and 112.1 (d, $^2J_{C-F}$ = 21 Hz), 110.4, 107.9 and 107.7 (d, $^2J_{C-F}$ = 26 Hz), 92.4, 79.3, 52.7, 48.1 (2), 40.9, 38.7, 35.8, 28.3 (3), 14.2, 11.3, 9.4 (2). HRMS-ESI (m/z): calculated for [M+H]$^+$ $C_{32}H_{44}O_6N_6F$, 627.3301; found, 627.3314.

(E)-5-((4-((2-Aminoethyl)carbamoyl)-3-oxo-5-(phenylamino)furan-2(3H)-ylidene)methyl)-N-(2-(diethylamino)ethyl)-2,4-dimethyl-1H-pyrrole-3-carboxamide (**36a**)
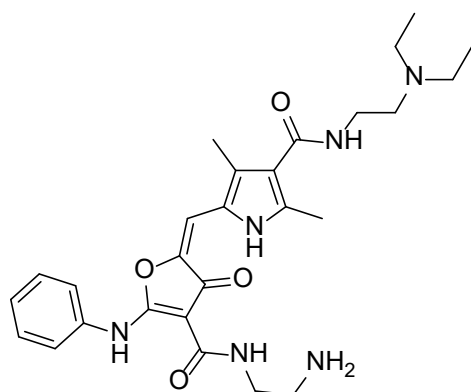
By using **35a** following the same procedure as described for **32a** (d.r. 3.5:1). ^{1}H NMR (600 MHz, DMSO-d_6) δ 13.01 (s, 1H), 10.68 (s, 1H), 10.58–10.51 (m, 1H), 8.23 (t, J = 6.1 Hz, 1H), 8.09–8.02 (m, 2H), 7.93 (t, J = 5.7 Hz, 1H), 7.58 (d, J = 7.5 Hz, 2H), 7.46 (d, J = 7.5 Hz, 2H), 7.28 (t, J = 7.5 Hz, 1H), 7.21 (s, 1H), 3.62–3.55 (m, 4H), 3.23–3.10 (m, 6H), 3.02–2.93 (m, 2H), 2.44 (s, 3H), 2.30 (s, 3H), 1.24 (t, J = 7.2 Hz, 6H). ^{13}C NMR (151 MHz, DMSO-d_6) δ 175.4, 166.8, 164.9, 163.5, 141.4, 134.8, 134.2, 129.0 (2), 126.7, 125.5, 121.6 (2), 120.8, 118.7, 109.7, 91.6, 49.8, 46.4 (2), 38.3, 35.6, 33.5, 13.0, 10.1, 8.0 (2). HRMS-ESI (m/z): calculated for [M+H]$^+$ $C_{27}H_{37}O_4N_6$, 509.2871; found, 509.2874.

Tert-butyl (E)-(2-(5-((4-((2-(diethylamino)ethyl)carbamoyl)-3,5-dimethyl-1H-pyrrol-2-yl)methylene)-2-((3-fluorophenyl)amino)-4-oxo-4,5-dihydrofuran-3-carboxamido)ethyl)carbamate (**36b**)
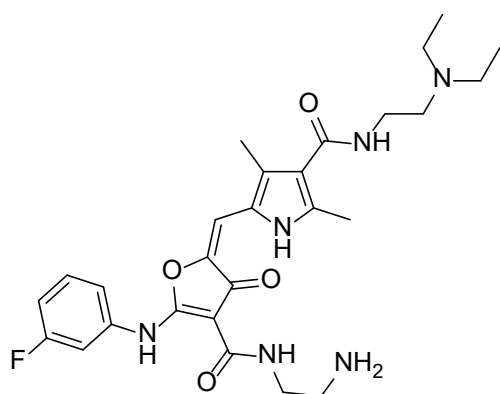
By using **35b** following the same procedure as described for **32a** (d.r. 3.5:1). ^{1}H NMR (500 MHz, DMSO-d_6) δ 13.00 (s, 1H), 10.74 (s, 1H), 10.51–10.44 (m, 1H), 8.24 (t, J = 6.1 Hz, 1H), 8.14–7.99 (m, 2H), 7.93 (t, J = 5.7 Hz, 1H), 7.57–7.38 (m, 3H), 7.31 (s, 1H), 7.17–7.04 (m, 1H), 3.62–3.52 (m, 4H), 3.22–3.09 (m, 6H), 3.04–2.95 (m, 2H), 2.44 (s, 3H), 2.32 (s, 3H), 1.24 (t, J = 7.2 Hz, 6H). ^{13}C NMR (126 MHz, DMSO-d_6) δ 175.4, 166.6, 164.8, 163.3, 162.7 and 160.8 (d, $^1J_{C-F}$ = 243 Hz), 141.2, 136.3 and 136.2 (d, $^3J_{C-F}$ = 11 Hz), 134.3, 130.6 and 130.5 (d, $^3J_{C-F}$ = 10 Hz), 127.0, 120.8, 118.7, 117.5
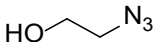
and 117.4 (d, $^4J_{C-F}$ = 3 Hz), 112.0 and 111.8 (d, $^2J_{C-F}$ = 21 Hz), 110.2, 108.7 and 108.5 (d, $^2J_{C-F}$ = 26 Hz), 91.8, 49.7, 46.3 (2), 38.2, 35.5, 33.4, 12.9, 10.1, 7.9 (2). HRMS-ESI (m/z): calculated for [M+H]$^+$ $C_{27}H_{36}O_4N_6F$, 527.2777; found, 527.2786.

5.1.2.4 Homobifunctional molecules
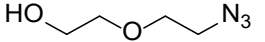
General procedure 11

The compound was synthesized according to the previously reported method.[160] Corresponding halogenated ethyl alcohol (10.00 mmol, 1 equiv.) was dissolved in H_2O (1 M). Sodium azide (10.0 mmol, 1 equiv.) was added in one portion, and the mixture was stirred at 60 °C for 1–3 days. Upon completion of the reaction, the mixture was cooled down, diluted with H_2O, and extracted with DCM. The organic layer was dried over $MgSO_4$, and the solvent was removed under reduced pressure to give the desired product as an oil.
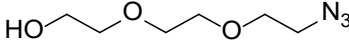
2-Azidoethan-1-ol (**37a**)

 By using general procedure 11 with 2-bromoethanol (0.7 mL, 10.0 mmol) to give the desired product (612.3 mg, 7.0 mmol, 70%). ^{1}H NMR (500 MHz, CDCl$_3$) δ 3.84–3.71 (m, 2H), 3.45 (d, J = 5.2 Hz, 2H), 1.83 (s, 1H).

2-(2-Azidoethoxy)ethan-1-ol (**37b**)

 By using general procedure 11 with 2-(2-chloroethoxy)ethanol (1.1 mL, 10.0 mmol) to give the desired product (496.8 mg, 3.8 mmol, 38%). ^{1}H NMR (700 MHz, CDCl$_3$) δ 3.80–3.74 (m, 2H), 3.72–3.68 (m, 2H), 3.68–3.60 (m, 2H), 3.41 (t, J = 5.0 Hz, 2H), 1.96 (s, 1H).

2-(2-(2-Azidoethoxy)ethoxy)ethan-1-ol (**37c**)

 By using general procedure 11 with 2-[2-(2-chloroethoxy)ethoxy]ethanol (1.5 mL, 10.0 mmol) to give the desired product (1.3 g, 7.5 mmol, 75%). ^{1}H NMR (400 MHz, CDCl$_3$) δ 3.80–3.58 (m, 10H), 3.40 (t, J = 5.0 Hz, 2H), 2.02 (s, 1H).

17-Hydroxy-3,6,9,12,15-pentaoxaheptadecyl 4-methylbenzenesulfonate (**38**)

The compound was synthesized according to the previously reported method.[161] Hexaethylen glycol (3.3 mL, 13.1 mmol) was dissolved in THF (1 mL) and cool the mixture to 0 °C. 2M NaOH aqueous (1.3 mL, 2.6 mmol) was slowly added to the solution, and stir the mixture for a further 1 h. Para-toluenesulfonylchloride (0.5 g, 2.6 mmol) in 1 mL of THF was added dropwise to the mixture. The reaction mixture was stirred for 2 h at 0 °C. Once reaction completion was monitored by TLC, the residue was dissolved in DCM and wash the residue with H_2O and brine. The organic layer was dried over $MgSO_4$ to give the product (941.4 mg, 2.2 mmol, 82%). The crude was used in the next step without further purification. ^{1}H NMR (500 MHz, $CDCl_3$) δ 7.80 (d, J = 8.3 Hz, 2H), 7.34 (d, J = 8.3 Hz, 2H), 4.18 – 4.15 (m, 2H), 3.76 – 3.56 (m, 22H), 2.44 (s, 3H), 2.16 (s, 1H).

17-Azido-3,6,9,12,15-pentaoxaheptadecan-1-ol (**39**)

The compound was synthesized according to the previously reported method.[162] **38** (436.5 mg, 1.0 mmol) and NaN_3 (130 mg, 2.0 mmol) were dispersed in DMF (1.5 mL). The reaction mixture was allowed to stir for 3 days at 70 °C under Ar atmosphere. After reaction completion, the mixture was cooled to room temperature and H_2O was added. The product was extracted with DCM and the organic phase was washed with H_2O to remove DMF, followed by dry over $MgSO_4$ and solvent evaporation under reduced vacuum to give the desired product as an oil (305.0 mg, 1.0 mmol, 99%). ^{1}H NMR (700 MHz, $CDCl_3$) δ 3.74–3.71 (m, 2H), 3.68–3.65 (m, 18H), 3.63–3.60 (m, 2H), 3.39 (t, J = 5.1 Hz, 2H), 2.34 (s, 1H).

General procedure 12

The compound was synthesized according to the previously reported method.[163] To a stirred solution of NaH (60% in oil, 15.0 mmol, 3 equiv.) and NaI (0.05 mmol, 0.01 equiv.) in THF (0.4 M) was added azide-tagged PEG linker (5.0 mmol, 1 equiv.) in THF (1 M) over 10 min at 0 °C under Ar atmosphere. After stirring for 15 min, 2-bromoacetic acid (6.0 mmol, 1.2 equiv.) in THF (1 M) was added dropwise over 30 min. The reaction mixture was stirred at room temperature for 2 h and then poured into water in an ice bath. The resulting mixture was acidified with 1N HCl to pH 3 and extracted with DCM. The combined organic layer was washed with H_2O and dried over $MgSO_4$ and concentrated under reduced pressure to afford the

title compound as an oil. The crude was used in the next step without further purification.

2-(2-Azidoethoxy)acetic acid (**40a**)

By using general procedure 12 with **37a** (435 mg, 10.0 mmol) to give the desired product (625 mg, 4.3 mmol, 86%). ^{1}H NMR (400 MHz, CDCl$_3$) δ 4.21 (s, 2H), 3.76 (d, *J* = 5.1 Hz, 2H), 3.48 (t, *J* = 5.1 Hz, 2H).

2-(2-(2-Azidoethoxy)ethoxy)acetic acid (**40b**)

By using general procedure 12 with **37b** (459 mg, 3.5 mmol), NaH (60% in oil, 420 mg, 10.5 mmol), NaI (5.2 mg, 0.04 mmol), and 2-bromoacetic acid (584 mg, 4.2 mmol) in THF (18 mL) to give the desired product (636 mg, 3.4 mmol, 96%). ^{1}H NMR (400 MHz, CDCl$_3$) δ 4.19 (s, 2H), 3.83–3.76 (m, 2H), 3.75–3.68 (m, 4H), 3.43 (t, *J* = 5.0 Hz, 2H).
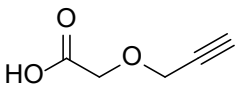
2-(2-(2-(2-Azidoethoxy)ethoxy)ethoxy)acetic acid (**40c**)

By using general procedure 12 with **37c** (613 mg, 3.5 mmol), NaH (60% in oil, 420 mg, 10.5 mmol), NaI (5.2 mg, 0.04 mmol), and 2-bromoacetic acid (584 mg, 4.2 mmol) in THF (18 mL) to give the desired product (740 mg, 3.2 mmol, 91%). ^{1}H NMR (400 MHz, CDCl$_3$) δ 4.17 (s, 2H), 3.78 (d, *J* = 6.3 Hz, 2H), 3.74–3.65 (m, 8H), 3.40 (t, *J* = 5.0 Hz, 2H).

20-Azido-3,6,9,12,15,18-hexaoxaicosanoic acid (**40d**)

By using general procedure 12 with **39** (307 mg, 1.0 mmol), NaH (60% in oil, 120 mg, 3.0 mmol), NaI (1.5 mg, 0.01 mmol), and 2-bromoacetic acid (167 mg, 1.2 mmol) in THF (5 mL) to give the desired product (290 mg, 0.8 mmol, 79%). ^{1}H NMR (500 MHz, CDCl$_3$) δ 4.09 (s, 2H), 3.71–3.67 (m, 2H), 3.64–3.55 (m, 20H), 3.32 (t, *J* = 5.1 Hz, 2H).

2-(Prop-2-yn-1-yloxy)acetic acid (**41**)

The compound was synthesized according to the previously reported method.[164] To the solution of NaH (60% in oil, 0.8 g, 20.0 mmol) in 20 mL of THF was added propargyl alcohol (0.48 mL, 8.3 mmol) dropwise to the mixture at room temperature under Ar. Once gas formation ceased, bromoacetic acid (1.3 g, 9.4 mmol) in 10

mL of THF was added dropwise. The reaction was stirred overnight at room temperature. H_2O was added to the reaction and acidified to pH 2 with 1N HCl. The aqueous phase was extracted with Et_2O three times. The combined organic layer was dried over $MgSO_4$ and concentrated under reduced pressure and purified by column chromatography (MeOH/DCM) to give the desired product (620.9 mg, 5.4 mmol, 66%). ^{1}H NMR (400 MHz, $CDCl_3$) δ 9.03 (s, 1H), 4.33 (d, J = 2.4 Hz, 2H), 4.27 (s, 2H), 2.51 (t, J = 2.4 Hz, 1H).

Tert-butyl (2-(4-formyl-2-hydroxyphenoxy)ethyl)carbamate (**42**)
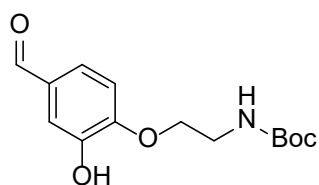
A solution of 3,4-dihydroxyphenylacetaldehyde (414 mg, 3.0 mmol), tert-Butyl N-(2-bromoethyl)carbamate (740 mg, 3.3 mmol), and K_2CO_3 (622 mg, 4.5 mmol) in DMF (10 mL) was stirred at 55 °C overnight. The reaction was diluted with H_2O and extracted with EA. The combined organic layer was washed with 1N HCl and brine, followed by drying over $MgSO_4$ and concentration under reduced pressure. The crude was purified by silica column chromatography (PE/EA) to give the desired product (386 mg, 1.4 mmol, 46%). ^{1}H NMR (400 MHz, $CDCl_3$) δ 9.84 (s, 1H), 7.44 (d, J = 2.0 Hz, 1H), 7.39 (dd, J = 8.3, 2.0 Hz, 1H), 6.92 (d, J = 8.3 Hz, 1H), 6.42 (s, 1H), 4.95 (s, 1H), 4.18 (t, J = 5.0 Hz, 2H), 3.60–3.58 (m, 2H), 1.46 (s, 9H). ^{13}C NMR (176 MHz, $CDCl_3$) δ 186.3, 151.9, 146.4, 142.0, 126.3, 119.3, 109.9, 106.5, 75.5, 64.7, 35.4, 23.6 (3).

Ethyl (Z)-5-(4-(2-((tert-butoxycarbonyl)amino)ethoxy)-3-hydroxybenzylidene)-4-oxo-2-(phenylamino)-4,5-dihydrothiophene-3-carboxylate (**43**)
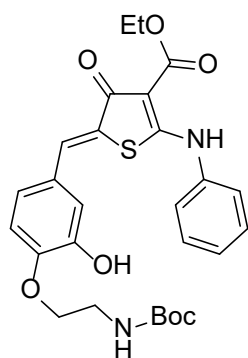
The compound **43** was synthesized by using general procedure 4 with **11a** (1.1 g, 4.2 mmol), **42** (1.3 g, 4.6 mmol), and piperidine (413 μL, 4.2 mmol) in EtOH (32 mL) to give the desired product (1.8 g, 3.4 mmol, 82%). 1H NMR (700 MHz, DMSO-d_6) δ 11.24 (s, 1H), 9.11 (s, 1H), 7.57–7.50 (m, 5H), 7.48–7.44 (m, 1H), 7.09–7.05 (m, 1H), 7.02–6.98 (m, 2H), 6.97–6.95 (m, 1H), 4.28 (q, J = 7.1 Hz, 2H), 3.97 (t, J = 5.4 Hz, 2H), 3.35–3.33 (m, 2H), 1.39 (s, 9H), 1.30 (t, J = 7.1 Hz, 3H). ^{13}C NMR (176 MHz, DMSO-d_6) δ 181.4, 175.7, 165.3, 156.0, 148.7, 147.2, 138.0, 130.4, 130.1 (2), 128.7, 127.0, 126.1 (2), 125.3, 123.4, 116.4, 113.7, 97.3, 78.4, 68.0, 60.0, 40.5, 28.7 (3), 14.9.

Ethyl (Z)-5-(4-(2-aminoethoxy)-3-hydroxybenzylidene)-4-oxo-2-(phenylamino)-4,5-dihydro thiophene-3-carboxylate (**44**)
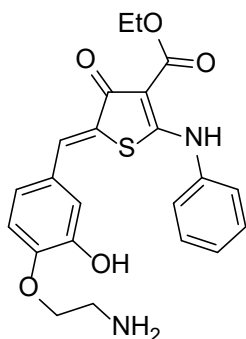
To a solution of **43** (213.9 mg, 0.4 mmol) in 4 mL of dichloromethane was added TFA (2 mL). The mixture was stirred at room temperature for 30 min, followed by evaporation of the solvent to give a product as an orange solid in TFA salt with quantitative yield. ^{1}H NMR (500 MHz, DMSO-d_6) δ 11.26 (s, 1H), 9.15–9.04 (m, 1H), 7.94 (t, *J* = 5.8 Hz, 3H), 7.59–7.50 (m, 5H), 7.49–7.40 (m, 1H), 7.08 (d, *J* = 8.5 Hz, 1H), 7.03 (dd, *J* = 8.5, 2.1 Hz, 1H), 6.99 (d, *J* = 2.1 Hz, 1H), 4.28 (q, *J* = 7.1 Hz, 2H), 4.18 (t, *J* = 5.0 Hz, 2H), 3.27 (h, *J* = 5.5 Hz, 2H), 1.30 (t, *J* = 7.1 Hz, 3H). ^{13}C NMR (126 MHz, DMSO-d_6) δ 181.4, 175.8, 165.2, 147.8, 147.1, 138.0, 130.2, 130.1 (2), 128.8, 127.7, 126.3 (2), 125.7, 123.3, 116.5, 113.8, 97.3, 65.3, 60.0, 38.9, 14.9.

General procedure 13

A solution of respective functionalized PEG linker (0.57 mmol, 1.2 equiv.), PyBOP (0.57 mmol, 1.2 equiv.), and DIPEA (0.71 mmol, 1.5 equiv.) in DMF (0.2 M) was stirred for 10 min, and a solution of **44** (0.48 mmol, 1 equiv.) and DIPEA (0.71 mmol, 1.5 equiv.) was added in 2 mL of DMF. The mixture was stirred at room temperature for 24 h. The solvent was evaporated and the product was purified by flash chromatography (PE/EA) to give the desired product as a yellow solid.

Ethyl (Z)-5-(4-(2-(2-(2-azidoethoxy)acetamido)ethoxy)-3-hydroxybenzylidene)-4-oxo-2-(phenylamino)-4,5-dihydrothiophene-3-carboxylate (**45a**)
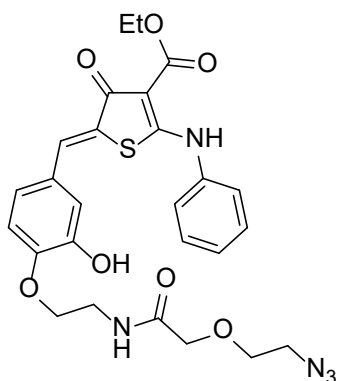
By using general procedure 13 with **40a** (24 mg, 0.16 mmol), PyBOP (92.4 mg, 0.18 mmol), DIPEA (77.4 µL, 0.44 mmol), and **44** (80 mg, 0.15 mmol) in DMF (3 mL) to give the desired product (71.5 mg, 0.13 mmol, 87%). ^{1}H NMR (400 MHz, DMSO-d_6) δ 11.21 (s, 1H), 9.22 (s, 1H), 7.94 (t, *J* = 5.7 Hz, 1H), 7.56–7.38 (m, 6H), 7.02–6.90 (m, 3H), 4.26 (q, *J* = 7.1 Hz, 2H), 3.99 (t, *J* = 5.7 Hz, 2H), 3.92 (s, 2H), 3.66–3.58 (m, 2H), 3.48 (q, *J* = 5.7 Hz, 2H), 3.44 (d, *J* = 4.6 Hz, 2H), 1.27 (t, *J* = 7.1 Hz, 3H).

Ethyl (Z)-5-(4-(2-(2-(2-(2-azidoethoxy)ethoxy)acetamido)ethoxy)-3-hydroxybenzylidene)-4-oxo-2-(phenylamino)-4,5-dihydrothiophene-3-carboxylate (**45b**)
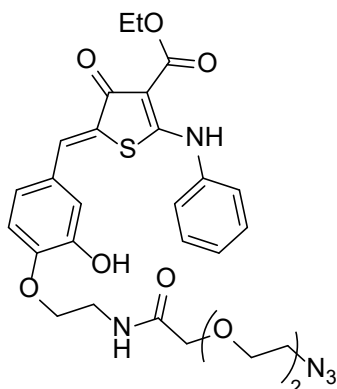
By using general procedure 13 with **40b** (41.6 mg, 0.22 mmol), PyBOP (124.9 mg, 0.24 mmol), DIPEA (104.5 µL, 0.60 mmol), and **44** (92.6 mg, 0.20 mmol) in DMF (4 mL) to give the desired product (84.1 mg, 0.14 mmol, 70%). ^{1}H NMR (400 MHz, CDCl$_3$) δ 11.52 (s, 1H), 7.75 (s, 1H), 7.60–7.53 (m, 1H), 7.50 (t, J = 7.6 Hz, 2H), 7.39 (d, J = 7.6 Hz, 2H), 7.38 (s, 1H), 7.10 (s, 1H), 7.04 (d, J = 8.3 Hz, 1H), 6.85 (d, J = 8.3 Hz, 1H), 4.40 (q, J = 7.1 Hz, 2H), 4.17 (t, J = 4.9 Hz, 2H), 4.02 (s, 2H), 3.80–3.64 (m, 8H), 3.46 (d, J = 4.3 Hz, 2H), 1.43 (t, J = 7.1 Hz, 3H).

Ethyl (Z)-5-(4-((14-azido-4-oxo-6,9,12-trioxa-3-azatetradecyl)oxy)-3-hydroxybenzylidene)-4-oxo-2-(phenylamino)-4,5-dihydrothiophene-3-carboxylate (**45c**)
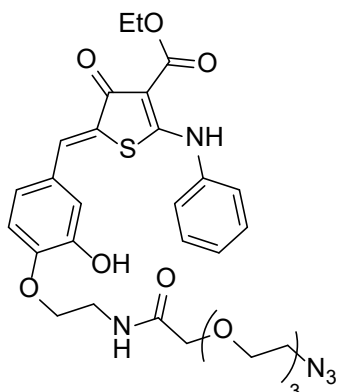
By using general procedure 13 with **40c** (132.8 mg, 0.57 mmol), PyBOP (2963 mg, 0.57 mmol), DIPEA (247.9 µL, 1.42 mmol), and **44** (256.2 mg, 0.48 mmol) in DMF (4 mL) to give the desired product (209.7 mg, 0.33 mmol, 69%). ^{1}H NMR (400 MHz, CDCl$_3$) δ 11.48 (s, 1H), 8.40 (s, 1H), 7.89–7.81 (m, 1H), 7.72 (s, 1H), 7.53–7.45 (m, 2H), 7.44–7.34 (m, 3H), 7.08 (s, 1H), 7.03 (d, J = 8.3 Hz, 1H), 6.84 (d, J = 8.3 Hz, 1H), 4.40 (q, J = 7.1 Hz, 2H), 4.16 (t, J = 5.0 Hz, 2H), 3.98 (s, 2H), 3.79–3.57 (m, 12H), 3.35 (d, J = 4.2 Hz, 2H), 1.43 (d, J = 7.1 Hz, 3H).

Ethyl (Z)-5-(4-((23-azido-4-oxo-6,9,12,15,18,21-hexaoxa-3-azatricosyl)oxy)-3-hydroxybenzylidene)-4-oxo-2-(phenylamino)-4,5-dihydrothiophene-3-carboxylate (**45d**)
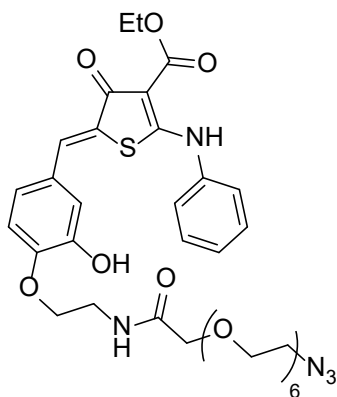
By using general procedure 13 with **40d** (219.2 mg, 0.60 mmol), PyBOP (312.2 mg, 0.60 mmol), DIPEA (261.3 µL, 1.5 mmol), and **44** (270.3 mg, 0.50 mmol) in DMF (3 mL) to give the desired product (368.3 mg, 0.48 mmol, 95%). ^{1}H NMR (500 MHz, DMSO-d_6) δ 11.23 (s, 1H), 9.23 (s, 1H), 7.95–7.89 (m, 1H), 7.57–7.48 (m, 5H), 7.48–7.40 (m, 1H), 7.04–6.93 (m, 3H), 4.27 (q, J = 7.1 Hz, 2H), 4.01 (t, J = 5.7 Hz, 2H), 3.89 (s, 2H), 3.63–3.44 (m, 24H), 3.37 (d, J = 4.3 Hz, 2H), 1.29 (t, J = 7.1 Hz, 3H). ^{13}C NMR

(126 MHz, DMSO-d_6) δ 180.4, 174.8, 169.0, 164.3, 147.8, 146.4, 137.0, 129.5, 129.1 (2), 127.7, 126.9, 126.1, 125.1 (2), 122.4, 115.3, 112.9, 96.4, 69.7, 69.5, 69.3, 69.3, 69.2, 69.2 (5), 69.0, 68.7, 66.7, 59.0, 49.5, 37.0, 13.9.

Ethyl (Z)-5-(3-hydroxy-4-(2-(2-(prop-2-yn-1-yloxy)acetamido)ethoxy)benzylidene)-4-oxo-2-(phenylamino)-4,5-dihydrothiophene-3-carboxylate (**46**)
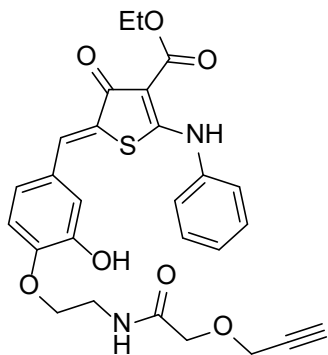
By using general procedure 13 with **41** (20.5 mg, 0.18 mmol), PyBOP (93.6 mg, 0.18 mmol), DIPEA (78.3 μL, 0.45 mmol), and **44** (81.0 mg, 0.15 mmol) in DMF (1.3 mL) to give the desired product (37.5 mg, 0.07 mmol, 48%). ^{1}H NMR (400 MHz, DMSO-d_6) δ 11.21 (s, 1H), 9.20 (s, 1H), 8.02 (t, J = 5.7 Hz, 1H), 7.57–7.40 (m, 6H), 7.04–6.92 (m, 3H), 4.26 (q, J = 7.1 Hz, 2H), 4.20 (d, J = 2.1 Hz, 2H), 3.98 (t, J = 5.7 Hz, 2H), 3.92 (s, 2H), 3.50–3.45 (m, 2H), 2.50 (d, J = 2.1 Hz, 1H), 1.27 (t, J = 7.1 Hz, 3H).

General procedure 14

To a solution of **45a** or **45b** (0.05 mmol) and **46** (20.0 mg, 0.04 mmol) in THF (1 mL) was added CuSO$_4$ • 5H$_2$O (10.5 mg, 0.04 mmol) and sodium ascorbate (15.2 mg, 0.08 mmol) with a few drop of H$_2$O. The mixture was stirred at room temperature for 24 h. The solvent was evaporated and the crude was purified by HPLC.

Ethyl 5-((Z)-4-(2-(2-((1-(2-(2-((2-(4-((Z)-(4-(ethoxycarbonyl)-3-oxo-5-(phenylamino)thio phen-2(3H)-ylidene)methyl)-2-hydroxyphenoxy)ethyl)amino)-2-oxoethoxy)ethyl)-1H-1,2,3-triazol-4-yl)methoxy)acetamido)ethoxy)-3-hydroxybenzylidene)-4-oxo-2-(phenylamino)-4,5-dihydrothiophene-3-carboxylate (**47a**)
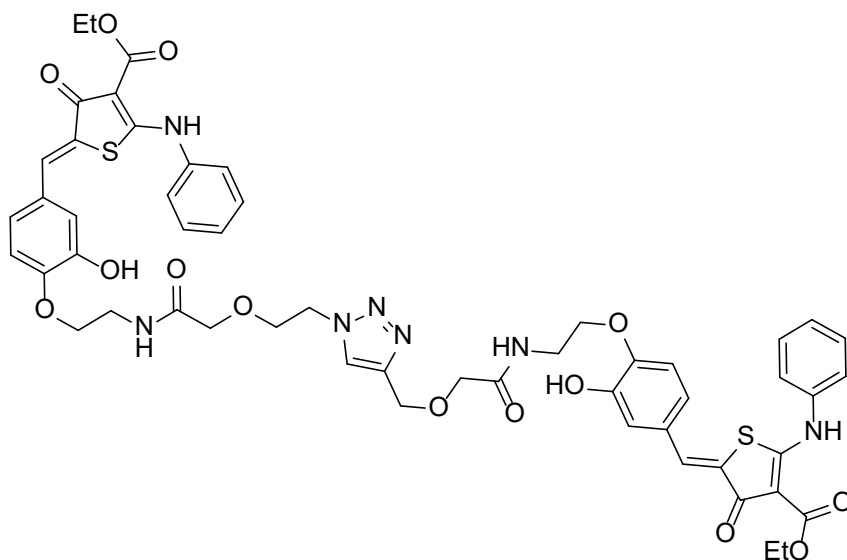
By using general procedure 14 with **45a** (25.4 mg, 0.05 mmol) to give the desired product (9.8 mg, 10 μmol, 24%). ^{1}H NMR (500 MHz, DMSO-d_6) δ 11.21 (s, 2H), 9.23 (s, 2H), 8.05 (s, 1H), 8.00 (d, J = 5.7 Hz, 1H), 7.88 (t, J = 6.0 Hz, 1H), 7.56–7.45 (m, 8H), 7.46 (s, 2H), 7.45–7.38 (m, 2H), 7.01–6.93 (m, 6H), 4.57 (s, 2H), 4.46 (t, J = 5.2 Hz, 2H), 4.22 (q, J = 7.1 Hz, 4H), 3.97 (t, J = 5.7 Hz, 4H), 3.90 (s, 2H), 3.81 (s, 2H), 3.75 (t, J = 5.2 Hz, 2H), 3.48–3.42 (m, 4H), 1.25 (t, J = 7.1 Hz, 6H). ^{13}C NMR (126 MHz, DMSO-d_6) δ 180.9 (2), 175.3 (2), 169.2, 168.9, 164.4 (2), 148.2, 148.2, 146.9, 146.9, 143.0, 137.5 (2), 129.7 (2), 129.5 (4), 127.9 (2), 126.5 (2), 125.1 (4), 124.6 (2), 124.7, 122.9 (2), 115.6 (2), 113.1 (2), 96.8 (2), 69.4, 68.8, 68.7, 66.5 (2), 63.9, 59.5 (2), 49.2, 37.6 (2), 14.3 (2). HRMS-ESI (m/z): [M+H]$^{+}$ calculated for C$_{53}$H$_{54}$O$_{14}$N$_7$S$_2$, 1076.3165; found, 1076.3202.

Ethyl 5-((Z)-4-(2-(2-((1-(2-(2-(2-((2-(4-((Z)-(4-(ethoxycarbonyl)-3-oxo-5-(phenylamino)thiophen-2(3H)-ylidene)methyl)-2-hydroxyphenoxy)ethyl)amino)-2-oxoethoxy)ethoxy)ethyl)-1H-1,2,3-triazol-4-yl)methoxy)acetamido)ethoxy)-3-hydroxybenzylidene)-4-oxo-2-(phenylamino)-4,5-dihydrothiophene-3-carboxylate (**47b**)
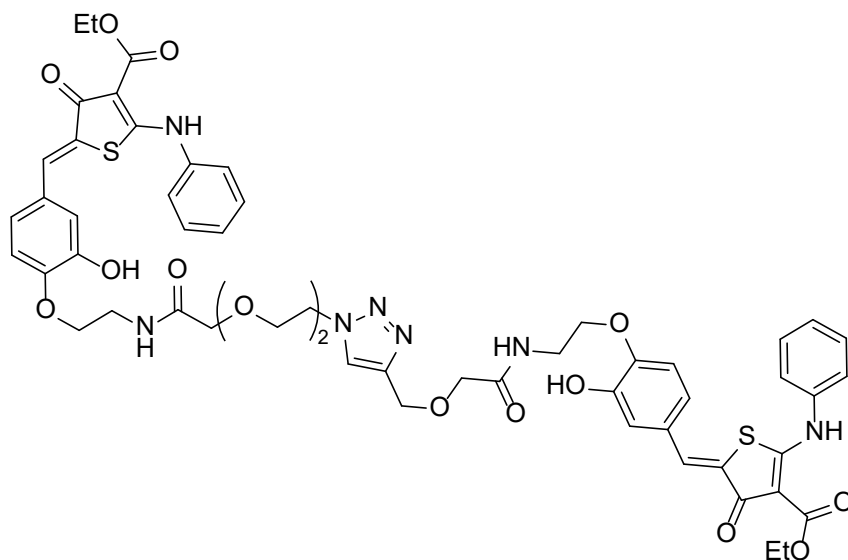
By using general procedure 14 with **45b** (0.09 mmol) to give the desired product (21.4 mg, 20 μmol, 32%). ^{1}H NMR (500 MHz, DMSO-d_6) δ 11.23 (s, 2H), 9.26 (s, 2H), 8.08 (s, 1H), 8.02 (d, J = 5.7 Hz, 1H), 7.91 (t, J = 6.0 Hz, 1H), 7.56–7.49 (m, 8H), 7.48 (s, 2H), 7.46–7.40 (m, 2H), 7.01–6.92 (m, 6H), 4.57 (s, 2H), 4.48 (t, J = 5.2 Hz, 2H), 4.26 (q, J = 7.1 Hz, 4H), 3.98 (t, J = 5.7 Hz, 4H), 3.90 (s, 2H), 3.84 (s, 2H), 3.77 (t, J = 5.2 Hz, 2H), 3.56–3.50 (m, 4H), 3.50–3.45 (m, 4H), 1.28 (t, J = 7.1 Hz, 6H). ^{13}C NMR (126 MHz, DMSO-d_6) δ 180.4 (2), 174.8 (2), 168.9, 168.6, 164.4 (2), 147.8, 147.8, 146.4, 146.4, 142.6, 137.0 (2), 129.5 (2), 129.1 (4), 127.7 (2), 126.0 (2), 125.2 (4), 124.3 (2), 124.2, 122.5 (2), 115.3 (2), 112.8 (2), 96.4 (2), 69.5, 68.8 (2), 68.4, 68.2, 66.7 (2), 63.1, 59.0 (2), 48.8, 37.1 (2), 13.9 (2). HRMS-ESI (m/z): [M+H]$^+$ calculated for $C_{55}H_{58}O_{15}N_7S_2$, 1120.3427; found, 1120.3469.

5.1.2.5 Heterobivalent molecules

General procedure 15

The compound was synthesized according to the previously reported method.[165] To a solution of polyethylene glycol (30.0 mmol, 2 equiv.) in THF (2.5 M) at 0 °C, NaH (60% in mineral oil, 20.0 mmol, 1.3 equiv.) was added portionwise. The mixture was stirred for 20 min at room temperature. Propargyl bromide (15.0 mmol, 1 equiv.) was added dropwise to the mixture. The reaction was quenched with ice-cold water (50 mL) and the pH was adjusted to pH 2 with 1N HCl solution. The aqueous solution was extracted with DCM three times. The combined organic layer was washed with brine and dried over MgSO4. The solvent was removed in vacuo and the crude product was purified by flash chromatography (MeOH/DCM) to give the product as an oil.

3,6,9,12-Tetraoxapentadec-14-yn-1-ol (**48a**)
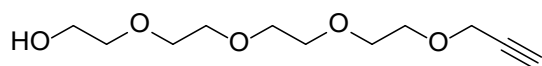
By using general procedure 15 with tetraethylene glycol (5.2 mL, 30.0 mmol) to give the desired product (2.0 g, 8.7 mmol, 58%). ^{1}H NMR (400 MHz, CDCl$_3$) δ 4.21 (d, J = 2.4 Hz, 2H), 3.74–3.72 (m, 2H), 3.74–3.64 (m, 12H), 3.63–3.60 (m, 2H), 2.43 (t, J = 2.4 Hz, 1H), 2.14 (s, 1H).

3,6,9,12,15,18-Hexaoxahenicos-20-yn-1-ol (**48b**)
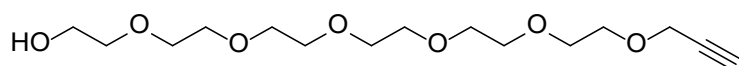
By using general procedure 15 with hexaethylene glycol (2.5 mL, 10.0 mmol), NaH (60% in mineral oil, 0.26 g, 6.5 mmol), and propargyl bromide (0.56 mL, 5.0 mmol) in THF (3 mL) to give the desired product (1.0 g, 3.2 mmol, 64%). ^{1}H NMR (400 MHz, CDCl$_3$) δ 4.20 (d, J = 2.4 Hz, 2H), 3.74–3.63 (m, 22H), 3.63–3.58 (m, 2H), 2.42 (t, J = 2.4 Hz, 1H), 2.22 (s, 1H).

General procedure 16

The compound was synthesized according to the previously reported method.[165] To a solution of alkyne-tagged PEG linker (5.0 mmol) in DCM (8 mL) was added TEA (2.1 mL, 15.0 mmol) and p-toluenesulfonyl chloride (1.4 g, 7.5 mmol). The mixture was stirred at room temperature for 1 h. The reaction mixture was diluted with H$_2$O. The crude was extracted with DCM and the organic layer was dried over MgSO4 and the residue was purified by column

chromatography (PE/EA) to yield the title products.

3,6,9,12-Tetraoxapentadec-14-yn-1-yl 4-methylbenzenesulfonate (**49a**)
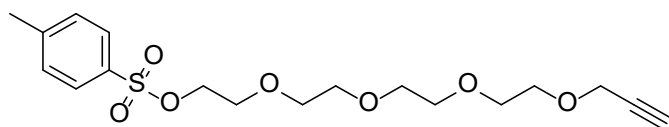
By using general procedure 16 with **48a** (1.16 g, 5.0 mmol) to give the desired product (1.92 g, 5.0 mmol, 100%). ^{1}H NMR (500 MHz, CDCl$_3$) δ 7.79 (d, *J* = 8.3 Hz, 2H), 7.34 (d, *J* = 8.3 Hz, 2H), 4.19 (d, *J* = 2.4 Hz, 2H), 4.17 – 4.14 (m, 2H), 3.71 – 3.59 (m, 11H), 3.58 (s, 3H), 2.44 (s, 3H), 2.42 (t, *J* = 2.4 Hz, 1H).

3,6,9,12,15,18-Hexaoxahenicos-20-yn-1-yl 4-methylbenzenesulfonate (**49b**)
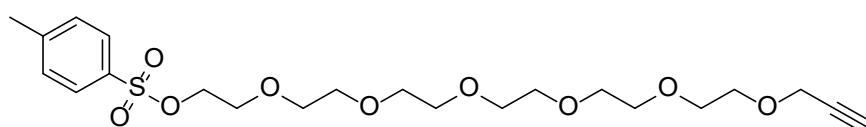
By using general procedure 16 with **48b** (480.6 mg, 1.5 mmol), p-toluenesulfonyl chloride (429.0 mg, 2.3 mmol), and TEA (0.63 mL, 4.5 mmol) in DCM (2.5 mL) to give the desired product (594.3 mg, 1.3 mmol, 83%). ^{1}H NMR (500 MHz, CDCl$_3$) δ 7.73 (d, *J* = 8.8 Hz, 2H), 7.28 (d, *J* = 8.8 Hz, 2H), 4.13 (d, *J* = 2.4 Hz, 2H), 4.11–4.06 (m, 2H), 3.65–3.50 (m, 22H), 2.38 (s, 3H), 2.36 (t, *J* = 2.4 Hz, 1H).

Tert-butyl (2-(ethylamino)ethyl)carbamate (**50**)
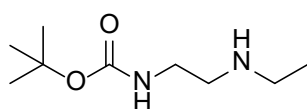
The compound was synthesized according to the previously reported method.[166] To a solution of *N*-ethylethylenediamine (10.5 mL, 100.0 mmol) in THF (200 mL) was added a solution of Boc$_2$O (6.5 g, 30.0 mmol) in THF (60 mL) dropwise at 0 °C. The reaction mixture was stirred at room temperature for 5 h and then concentrated in *vacuo*. The obtained residue was subsequently diluted with EA and sat. NaHCO$_3$ aqueous solution. The obtained mixture was extracted three times with EA. The combined organic layer was washed with brine, dried over MgSO$_4$, filtrated, and concentrated in vacuo to obtain the crude product as pale yellow solid (5.3 g, 28.4 mmol, 95%). The obtained crude carbamate was used for the next step without further purification. ^{1}H NMR (400 MHz, CDCl$_3$) δ 5.00 (s, 1H), 3.24 (q, *J* = 5.8 Hz, 2H), 2.76 (t, *J* = 5.8 Hz, 2H), 2.68 (q, *J* = 7.1 Hz, 2H), 1.46 (s, 2H), 1.44 (s, 9H), 1.12 (t, *J* = 7.1 Hz, 3H).

General procedure 17

The compound was synthesized according to the previously reported method.[140] To a stirred solution of **49a** or **49b** (1.8 mmol) and **50** (1.36 g, 7.2 mmol) in dry ACN (13 ml) was added Cs_2CO_3 (1.18 g, 3.6 mmol) and NaI (108.4 mg, 0.7 mmol). The reaction mixture was allowed to stir under Ar at room temperature for 2 days and at 65 °C for 2 further days. The reaction mixture was diluted with H_2O and extracted with DCM. The organic layer was dried over $MgSO_4$. The crude product was purified by silica gel flash chromatography (MeOH/DCM).

Tert-butyl (3-ethyl-6,9,12,15-tetraoxa-3-azaoctadec-17-yn-1-yl)carbamate (**51a**)
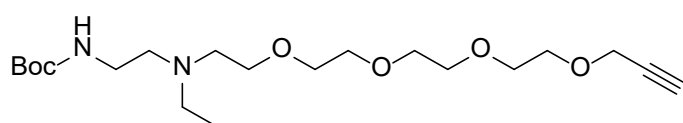
By using general procedure 17 with **49a** (698.9 mg, 1.8 mmol) to give the desired product (496.2 mg, 1.3 mmol, 71%). ^{1}H NMR (700 MHz, CDCl₃) δ 5.29 (s, 1H), 4.20 (d, *J* = 2.4 Hz, 2H), 3.78–3.50 (m, 14H), 3.18 (s, 2H), 2.68 (s, 2H), 2.65–2.54 (m, 4H), 2.42 (t, *J* = 2.4 Hz, 1H), 1.44 (s, 9H), 1.09–0.99 (m, 3H).

Tert-butyl (3-ethyl-6,9,12,15,18,21-hexaoxa-3-azatetracos-23-yn-1-yl)carbamate (**51b**)
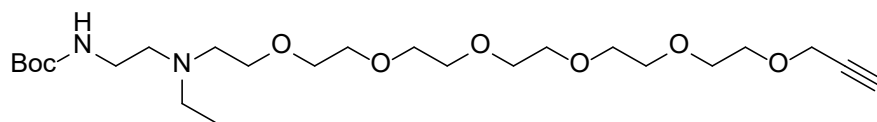
By using general procedure 17 with **49b** (655.8 mg, 1.4 mmol), **50** (1.04 g, 5.5 mmol), Cs_2CO_3 (0.9 g, 2.8 mmol), and NaI (82.9 mg, 0.55 mmol) in ACN (9 mL) to give the desired product (504.0 mg, 1.1 mmol, 77%). ^{1}H NMR (700 MHz, CDCl₃) δ 5.24 (s, 1H), 4.20 (d, *J* = 2.4 Hz, 2H), 3.77–3.57 (m, 22H), 3.41–3.25 (m, 2H), 3.19 (s, 2H), 2.67 (s, 4H), 2.43 (t, J = 2.4 Hz, 1H), 1.44 (s, 9H), 1.08–0.98 (m, 3H).

(Z)-5-((5-fluoro-2-oxoindolin-3-ylidene)methyl)-2,4-dimethyl-1H-pyrrole-3-carboxylic acid (**53**)
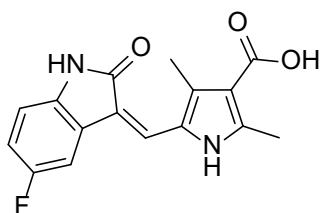
The compound was synthesized according to the previously reported method.[167] A mixture of 5-fluoro-2-oxindole (1.33 g, 8.8 mmol), 5-formyl-2,4-dimethyl-1*H*-pyrrole-3-carboxylic acid (1.47 g, 8.8 mmol), and pyrrolidine (1.5 mL, 18.0 mmol) in EtOH (30

mL) was refluxed for 3 h. After completion, the mixture was cooled to room temperature and 1N HCl (15 mL, 2M) was added to the suspension. A crude precipitate was filtered and washed with EtOH to yield the crude product without further purification (2.6 g, 8.6 mmol, 97%). ^{1}H NMR (700 MHz, DMSO-d_6) δ 13.86 (s, 1H), 12.15 (s, 1H), 10.93 (s, 1H), 7.78 (dd, J = 9.5, 2.6 Hz, 1H), 7.75 (s, 1H), 6.93 (ddd, J = 9.5, 8.4, 2.6 Hz, 1H), 6.84 (dd, J = 8.4, 4.5 Hz, 1H), 2.53 (s, 3H), 2.50 (s, 3H).

(Z)-N-(2-(Diethylamino)ethyl)-5-((5-fluoro-2-oxoindolin-3-ylidene)methyl)-2,4-dimethyl-1H-pyrrole-3-carboxamide (sunitinib)
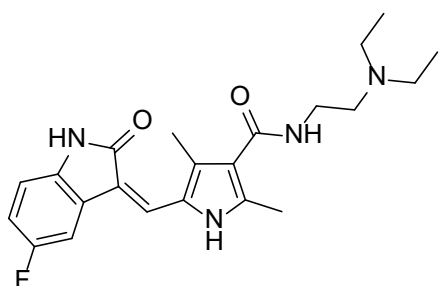
The compound was synthesized according to the previously reported method.[110] A mixture of **28** (50.0 mg, 0.18 mmol), 5-fluoro-2-oxindole (31.3 mg, 0.21 mmol), pyrrolidine (0.77 µL, 10 µmol) in EtOH (2 mL) was refluxed for 3 h. Upon the completion of the reaction, the solution is cooled down and the crystal formed during cooling was collected by vacuum filtration and washed with cold EtOH to give the title compound (16 mg, 40 µmol, 21%). ^{1}H NMR (500 MHz, DMSO-d_6) δ 13.67 (s, 1H), 10.89 (s, 1H), 7.75 (dd, J = 9.6, 2.6 Hz, 1H), 7.71 (s, 1H), 7.43 (t, J = 6.2 Hz, 1H), 6.92 (ddd, J = 9.6, 8.4, 2.6 Hz, 1H), 6.83 (dd, J = 8.4, 4.5 Hz, 1H), 3.27 (q, J = 6.2 Hz, 2H), 2.55–2.51 (m, 6H), 2.43 (s, 3H), 2.41 (s, 3H), 0.96 (t, J = 7.1 Hz, 6H).

General procedure 18

The compounds **52a** and **52b** were prepared by stirring **51a** or **51b** in TFA/DCM (1:2 v/v) at room temperature for 1 h, followed by the removal of solvents to dryness. A mixture of **53** (0.15 mmol, 1 equiv.), EDC HCl (0.22 mmol, 1.5 equiv.), 4-(dimethylamino)pyridine (0.27 mmol, 1.8 equiv.), and DIPEA (0.44 mmol, 3 equiv.) in 0.5 mL of DMF at room temperature for 10 min. **52a** or **52b** (0.16 mmol, 1.1 equiv.) in 0.5 mL of DMF was added to the reaction mixture and stirred at room temperature overnight. The products were purified by preparative chromatography.

(Z)-N-(3-ethyl-6,9,12,15-tetraoxa-3-azaoctadec-17-yn-1-yl)-5-((5-fluoro-2-oxoindolin-3-ylidene)methyl)-2,4-dimethyl-1H-pyrrole-3-carboxamide (**54a**)
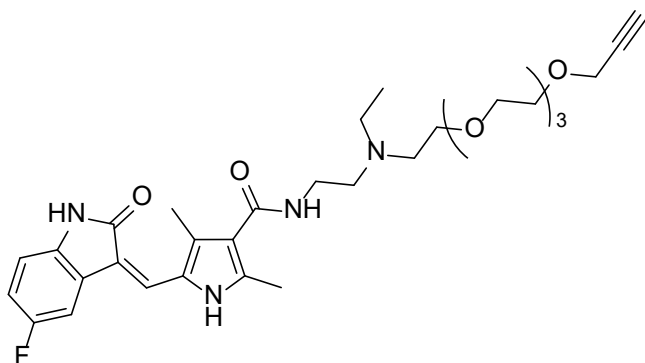
By using general procedure 18 with **52a** (48.9 mg, 0.16 mmol) to give the desired product (65.3 mg, 0.09 mmol, 64%). ^{1}H NMR (500 MHz, CDCl$_3$) δ 13.38 (s, 1H), 8.45 (s, 1H), 7.63 (t, J = 5.8 Hz, 1H), 7.25 (s, 1H), 7.12 (dd, J = 8.6, 2.3 Hz, 1H), 6.92–6.79 (m, 2H), 4.18 (d, J = 2.3 Hz, 2H), 3.93 (q, J = 4.3 Hz, 2H), 3.88–3.80 (m, 2H), 3.71–3.60 (m, 12H), 3.56–3.45 (m, 2H), 3.38 (t, J = 4.7 Hz, 2H), 3.35–3.32 (m, 2H), 2.52 (s, 3H), 2.46 (t, J = 2.3 Hz, 1H) 2.44 (s, 3H), 1.38 (t, J = 7.2 Hz, 3H). ^{13}C NMR (126 MHz, CDCl$_3$) δ 169.8, 166.7, 159.9 and 158.0 (d, $^1J_{C-F}$ = 238 Hz), 138.7, 133.3, 130.8, 127.2 and 127.1 (d, $^3J_{C-F}$ = 9 Hz), 126.2, 124.0, 118.4, 114.5 and 114.4 (d, $^4J_{C-F}$ = 3 Hz), 112.8 and 112.6 (d, $^2J_{C-F}$ = 24 Hz), 110.0 and 109.9 (d, $^3J_{C-F}$ = 8 Hz), 105.1 and 104.9 (d, $^2J_{C-F}$ = 25 Hz), 79.4, 74.6, 70.4, 70.4, 70.3, 70.2, 70.2, 69.0, 65.2, 58.3, 53.9, 52.8, 50.0, 35.4, 14.0, 11.0, 8.8.

(Z)-N-(3-ethyl-6,9,12,15,18,21-hexaoxa-3-azatetracos-23-yn-1-yl)-5-((5-fluoro-2-oxoindolin-3-ylidene)methyl)-2,4-dimethyl-1H-pyrrole-3-carboxamide (**54b**)
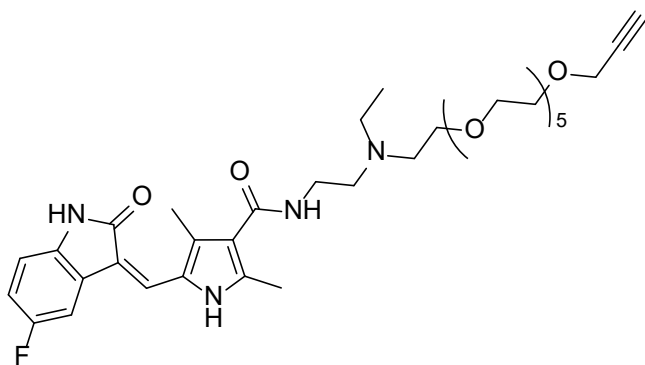
By using general procedure 18 with **52b** (54.7 mg, 0.18 mmol), and EDC (52.3 mg, 0.27 mmol) to give the desired product (63.0 mg, 0.09 mmol, 52%). ^{1}H NMR (700 MHz, CDCl$_3$) δ 13.40 (s, 1H), 8.25 (s, 1H), 7.66 (t, J = 5.7 Hz, 1H), 7.30 (s, 1H), 7.15 (dd, J = 8.6, 2.4 Hz, 1H), 6.89–6.80 (m, 2H), 4.19 (d, J = 2.4 Hz, 2H), 3.98–3.91 (m, 2H), 3.90–3.80 (m, 2H), 3.72–3.56 (m, 20H), 3.57–3.43 (m, 2H), 3.40–3.36 (m, 2H), 3.35–3.29 (m, 2H), 2.55 (s, 3H), 2.47 (s, 3H), 2.43 (t, J = 2.4 Hz, 1H), 1.39 (t, J = 7.2 Hz, 3H). ^{13}C NMR (176 MHz, CDCl$_3$) δ 169.8, 166.8, 159.7 and 158.4 (d, $^1J_{C-F}$ = 238 Hz), 138.9, 133.3, 131.0, 127.3 and 127.2 (d, $^3J_{C-F}$ = 9 Hz), 126.3, 124.2, 118.4, 114.5 and 114.5 (d, $^4J_{C-F}$ = 3 Hz), 112.8 and 112.7 (d, $^2J_{C-F}$ = 24 Hz), 110.1 and 110.0 (d, $^3J_{C-F}$ = 9 Hz), 105.2 and 105.1 (d, $^2J_{C-F}$ = 25 Hz), 79.6, 74.6, 70.5, 70.5, 70.5, 70.5 (3), 70.5, 70.3, 70.2, 69.1, 65.3, 58.4, 54.2, 53.0, 50.2, 35.6, 14.2, 11.2, 8.9.

Ethyl   5-((Z)-4-((14-(4-(5-ethyl-1-(5-(((Z)-5-fluoro-2-oxoindolin-3-ylidene)methyl)-2,4-dimethyl-1H-pyrrol-3-yl)-1-oxo-8,11,14,17-tetraoxa-2,5-diazaoctadecan-18-yl)-1H-1,2,3-triazol-1-yl)-4-oxo-6,9,12-trioxa-3-azatetradecyl)oxy)-3-hydroxybenzylidene)-4-oxo-2-(phenylamino)-4,5-dihydrothiophene-3-carboxylate (**55a**)
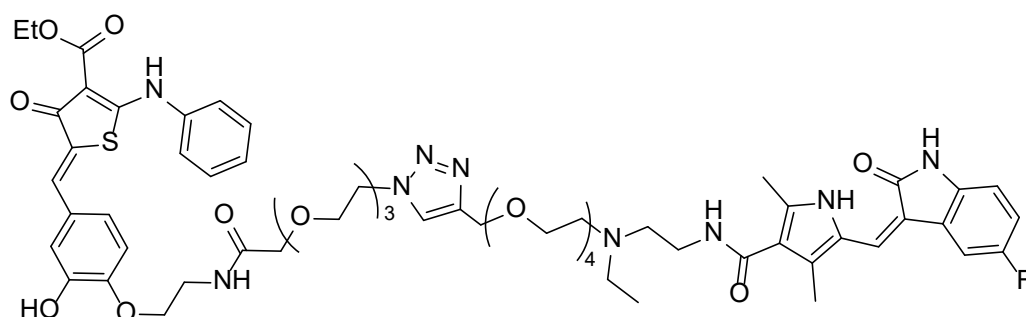
55a was synthesized according to general procedure 14 with the assistance of ligand, tris[(1-benzyl-1*H*-1,2,3-triazol-4-yl)methyl]amine. **45c** (52.2 mg, 0.08 mmol), **54a** (43.3 mg, 0.07 mmol), CuSO$_4$ • 5H$_2$O (20.3 mg, 0.08 mmol), sodium ascorbate (29.3 mg, 0.15 mmol), and tris[(1-benzyl-1H-1,2,3-triazol-4-yl)methyl]amine (78.5 mg, 0.15 mmol) in THF (2 mL) were reacted to give the desired product (39.4 mg, 30 µmol mmol, 40%). ^{1}H NMR (500 MHz, DMSO-d_6) δ 13.75 (s, 1H), 11.23 (s, 1H), 9.32 (s, 1H), 9.25 (s, 1H), 8.01 (s, 1H), 7.92 (t, J = 6.0 Hz, 1H), 7.78 (t, J = 5.7 Hz, 1H), 7.75 (dd, J = 9.4, 2.6 Hz, 1H), 7.72 (s, 1H), 7.56–7.48 (m, 5H), 7.45–7.39 (m, 1H), 7.03–6.90 (m, 4H), 6.84 (dd, J = 8.5, 4.5 Hz, 1H), 4.54–4.44 (m, 4H), 4.27 (q, J = 7.1 Hz, 2H), 3.99 (t, J = 5.7 Hz, 2H), 3.89 (s, 2H), 3.77 (t, J = 5.3 Hz, 4H), 3.62–3.43 (m, 24H), 3.41–3.36 (m, 2H), 3.33–3.25 (m, 4H), 2.46 (s, 3H), 2.44 (s, 3H), 1.28 (t, J = 7.0 Hz, 3H), 1.23 (t, J = 7.1 Hz, 3H). ^{13}C NMR (126 MHz, DMSO-d_6) δ 180.4, 174.8, 169.1, 169.0, 165.3, 164.3, 158.7 and 156.8 (d, $^1J_{C-F}$ = 235 Hz), 147.8, 146.4, 143.2, 137.0, 136.5, 134.1, 129.7, 129.5, 129.1 (2), 127.7, 126.6 and 126.5 (d, $^3J_{C-F}$ = 10 Hz), 126.1, 125.4, 125.1 (2), 124.3, 123.7, 122.4, 118.8, 115.3, 114.7 and 114.7 (d, $^4J_{C-F}$ = 3 Hz), 113.9 and 113.6 (d, $^2J_{C-F}$ = 33 Hz), 112.9, 109.6 and 109.5 (d, $^3J_{C-F}$ = 12 Hz), 105.7 and 105.4 (d, $^2J_{C-F}$ = 28 Hz), 96.4, 69.6, 69.5, 69.3, 69.2, 69.2, 69.0, 69.0, 69.0 (4), 68.4, 68.1, 66.7, 63.8, 62.9, 59.0, 51.1, 50.9, 48.8, 47.6, 37.0, 33.7, 13.9, 13.0, 10.2, 8.0. HRMS-ESI (m/z): [M+H]$^+$ calculated for C$_{61}$H$_{77}$O$_{15}$N$_9$FS, 1226.5238; found, 1226.5245.

Ethyl 5-((Z)-4-((23-(4-(5-ethyl-1-(5-(((Z)-5-fluoro-2-oxoindolin-3-ylidene)methyl)-2,4-di methyl-1H-pyrrol-3-yl)-1-oxo-8,11,14,17,20,23-hexaoxa-2,5-diazatetracosan-24-yl)-1H-1,2,3 -triazol-1-yl)-4-oxo-6,9,12,15,18,21-hexaoxa-3-azatricosyl)oxy)-3-hydroxybenzylidene)-4- oxo-2-(phenylamino)-4,5-dihydrothiophene-3-carboxylate (**55b**)
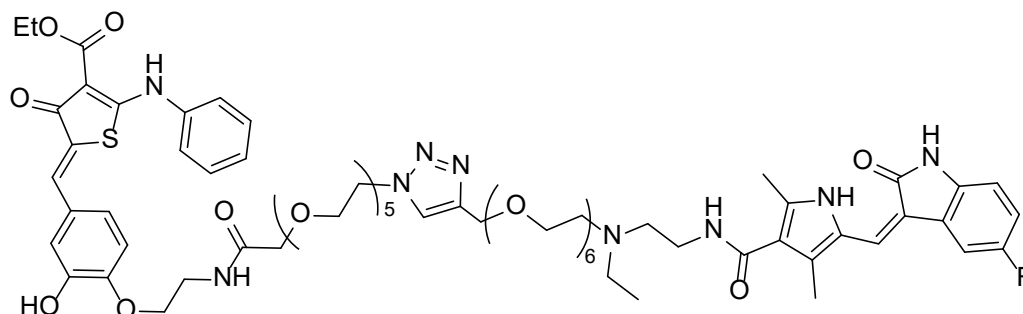
55b was synthesized according to general procedure 14 with the assistance of ligand, tris[(1-benzyl-1*H*-1,2,3-triazol-4-yl)methyl]amine. **45d** (51.1 mg, 0.07 mmol), **54b** (47.2 mg, 0.06 mmol), CuSO₄ • 5H₂O (16.5 mg, 0.07 mmol), sodium ascorbate (23.7 mg, 0.12 mmol), and tris[(1-benzyl-1H-1,2,3-triazol-4-yl)methyl]amine (63.7 mg, 0.12 mmol) in THF (1.5 mL) were reacted to give the desired product (51.4 mg, 30 µmol, 55%). ^{1}H NMR (600 MHz, CDCl₃) δ 13.46 (s, 1H), 11.50 (s, 1H), 8.53 (s, 1H), 8.09 (t, *J* = 6.2 Hz, 1H), 7.73 (s, 1H), 7.72 (s, 1H), 7.69 (t, *J* = 6.0 Hz, 1H), 7.51–7.46 (m, 2H), 7.40–7.36 (m, 3H), 7.31 (s, 1H), 7.15 (d, *J* = 8.4 Hz, 1H), 7.06 (d, *J* = 2.2 Hz, 1H), 7.01 (dd, *J* = 8.44, 2.2 Hz, 1H), 6.85–6.81 (m, 3H), 5.53 (s, 1H), 4.64 (s, 2H), 4.49 (t, *J* = 5.1 Hz, 2H), 4.40 (q, *J* = 7.1 Hz, 2H), 4.13 (t, *J* = 5.1 Hz, 2H), 3.98 (s, 2H), 3.96–3.91 (m, 2H), 3.86 (s, 1H), 3.81 (t, *J* = 5.2 Hz, 2H), 3.74–3.53 (m, 50H), 3.46–3.41 (m, 1H), 3.39–3.36 (m, 2H), 3.33–3.30 (m, 2H), 2.55 (s, 3H), 2.48 (s, 3H), 1.42 (t, *J* = 7.1 Hz, 3H), 1.39 (t, *J* = 7.1 Hz, 3H). ^{13}C NMR (151 MHz, CDCl₃) δ 182.3, 176.2, 171.1, 169.8, 166.9, 166.8, 160.9, 160.7, 160.4, 160.2, 159.8 and 158.2 (d, $^1J_{C\text{-}F}$ = 238 Hz), 147.8, 146.5, 144.5, 138.9, 137.1, 133.5, 131.8, 131.0, 129.9 (2), 129.1, 127.8, 127.6, 127.2 and 127.1 (d, $^3J_{C\text{-}F}$ = 9 Hz), 126.3, 125.3, 124.1, 124.0, 124.0 (2), 123.4, 118.3, 116.6, 116.3, 114.7, 114.6 and 114.6 (d, $^4J_{C\text{-}F}$ = 3 Hz), 112.8 and 112.7 (d, $^2J_{C\text{-}F}$ = 24 Hz), 112.2, 110.1 and 110.1 (d, $^3J_{C\text{-}F}$ = 8 Hz), 105.2 and 105.0 (d, $^2J_{C\text{-}F}$ = 25 Hz), 98.0, 70.7, 70.4, 70.4, 70.4 (4), 70.4, 70.3, 70.3, 70.2, 70.2, 70.0, 69.6, 69.3, 67.9, 65.2, 64.2, 60.6, 54.3, 52.9, 50.2, 50.2, 38.4, 35.5, 14.4, 14.2, 11.2, 8.9. HRMS-ESI (m/z): [M+H]$^+$ calculated for C₇₁H₉₇O₂₀N₉FS, 1446.6549; found, 1446.6588.

5.1.2.6 ENPP1 PROTAC

*Diethyl (E)-(2-(1-benzylpiperidin-4-yl)vinyl)phosphonate (**62**)*
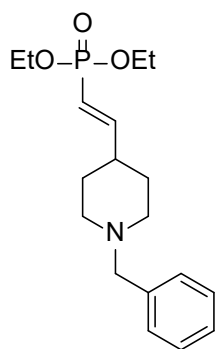
The compound was synthesized according to the previously reported method.[143] Tetraethyl methylenediphosphonate (2.5 mL, 10.0 mmol) is carefully added dropwise to a stirred solution of NaH (434.0 mg, 11.0 mmol) in toluene (20 mL) at room temperature. The reaction mixture is then placed under Ar and a solution of 1-benzylpiperidine-4-carbaldehyde (2.0 mL, 10.0 mmol) in toluene (10 mL) was slowly added, keeping the temperature below 40 °C. The resulting mixture is left to stir at room temperature overnight and then quenched by the addition of an aqueous saturated NH₄Cl solution. The organic phase was separated, washed with brine, dried over MgSO₄, and evaporated to dryness. Chromatography (EtOAc in Hexanes) provides diethyl (E)-(2-(1-benzylpiperidin-4-yl)vinyl)phosphonates as a colorless oil (1.5 g, 4.6 mmol, 46%). ^{1}H NMR (700 MHz, CDCl₃) δ 7.39–7.20 (m, 5H), 6.74 (ddd, J = 21.3, 17.3, 6.1 Hz, 1H), 5.61 (ddd, J = 21.3, 17.3, 1.5 Hz, 1H), 4.10–4.02 (m, 4H), 3.52 (s, 2H), 2.95–2.89 (m, 2H), 2.17–2.09 (m, 1H), 2.05–1.98 (m, 2H), 1.79–1.69 (m, 2H), 1.56–1.49 (m, 2H), 1.31 (t, J = 7.1 Hz, 6H).

*Diethyl (2-(piperidin-4-yl)ethyl)phosphonate (**63**)*
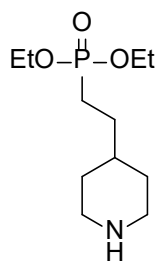
The compound was synthesized according to the previously reported method.[143] To a mixture of diethyl (E)-(2-(1-benzylpiperidin-4-yl)vinyl)phosphonate (506.1 mg, 1.5 mmol) in ethanol (8 mL) is added catalytic Pd/C (10%, 50.000 mg, 47 μmol). The mixture is placed under an atmosphere of hydrogen and stirred at room temperature for 12 h, filtered through packed celite, and evaporated to dryness under reduced pressure to give the diethyl (2-(piperidin-4-yl)ethyl)phosphonates as colorless oils.

*2-Amino-5-hydroxy-4-methoxybenzoic acid (**56**)*
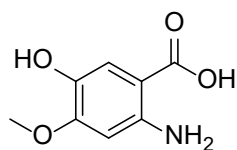
The compound was synthesized according to the previously reported method.[168] To 5-hydroxy-4-methoxy-2-nitrobenzoic acid (2.0 g, 9.4 mmol) and 10% Pd/C (200.0 mg, 0.19 mmol) under H₂ (1 atm) was added MeOH (60 mL). The reaction was stirred at room temperature overnight. The solution was filtered

169

through Celite and the filtrate was evaporated to afford 2-amino-5-hydroxy-4-methoxybenzoic acid. The crude was immediately used in the further reaction without purification (1.6 g, 8.7 mmol, 93%). ^{1}H NMR (700 MHz, DMSO-d_6) δ 8.20 (s, 2H), 7.07 (s, 1H), 6.27 (s, 1H), 3.72 (s, 3H).

6-Hydroxy-7-methoxyquinazolin-4(1H)-one (**57**)
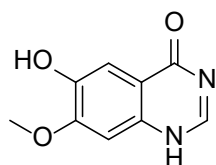
The compound was synthesized according to the previously reported method.[169] **56** (1.0 g, 5.5 mmol) was added in excess of formamide (4.35 mL, 109.2 mmol). The reaction mixture was then heated at 140 °C for 4–6 h. The reaction was monitored with TLC and upon completion; ice water was added to the reaction mixture. The resultant solid was filtered, washed with water, dissolved in ethyl acetate, dried over MgSO$_4$, and concentrated to obtain the pure desired product. When the product did not precipitate on the addition of ice, the reaction mixture was extracted with ethyl acetate, dried over MgSO$_4$, and concentrated to obtain the desired product (486.9 mg, 2.5 mmol, 46%). ^{1}H NMR (600 MHz, DMSO-d_6) δ 11.92 (s, 1H), 9.80 (s, 1H), 7.90 (s, 1H), 7.37 (s, 1H), 7.08 (s, 1H), 3.89 (s, 3H).

7-Methoxy-4-oxo-1,4-dihydroquinazolin-6-yl acetate (**58**)
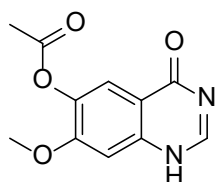
The compound was synthesized according to the previously reported method.[170] Pyridine (0.8 mL, 9.9 mmol) was added dropwise to the solution of **57** (380.0 mg, 2.0 mmol) in acetic anhydrate (4.0 mL). The reaction mixture was heated at 100 °C for 2 h and then cooled to room temperature. After the mixture was poured into ice water, a white solid was precipitated. The precipitate was collected, washed, and dried to give the desired product as a white solid (432.0 mg, 1.8 mmol, 93%). ^{1}H NMR (400 MHz, DMSO-d_6) δ 12.17 (s, 1H), 8.07 (s, 1H), 7.74 (s, 1H), 7.27 (s, 1H), 3.91 (s, 3H), 2.29 (s, 3H).

4-Chloro-7-methoxyquinazolin-6-yl acetate (**59**)
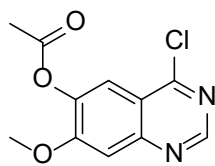
The compound was synthesized according to the previously reported method.[170] **58** (2.0g, 8.5 mmol) was dissolved in $SOCl_2$ (17.5 mL). The mixture was stirred at 80 °C for 2.5 h and then concentrated under vacuum, providing the desired compound (2.2 g, 7.7 mmol, 90%), which could be used in the next step without further purification. ^{1}H NMR (400 MHz, DMSO-d_6) δ 9.01 (s, 1H), 8.01 (s, 1H), 7.63 (s, 1H), 4.02 (s, 3H), 2.35 (s, 3H).

4-Chloro-7-methoxyquinazolin-6-ol (**60**)
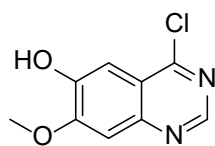
The compound was synthesized according to the previously reported method.[170] **59** (231.0 mg, 0.9 mmol) was dissolved in 3.2 mL of NH_3 (7 N in MeOH) and the mixture was stirred for 1.5 h at room temperature. The solvent was removed under vacuum and titration with Et_2O afforded the desired product as a beige solid (193.6 g, 0.9 mmol, 100%). ^{1}H NMR (700 MHz, DMSO-d_6) δ 10.80 (s, 1H), 8.80 (s, 1H), 7.42 (s, 1H), 7.41 (s, 1H), 4.01 (s, 3H).

Tert-butyl (2-((4-chloro-7-methoxyquinazolin-6-yl)oxy)ethyl)carbamate (**61**)
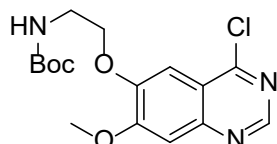
The synthetic procedure was modified from the reported method.[171] **60** (1.47 g, 7.0 mmol) and K_2CO_3 (1.55 g, 11.2 mmol) were mixed with 35 mL of dry DMF under Ar. Tert-Butyl N-(2-bromoethyl)carbamate (1.88 g, 8.4 mmol) was added and the solution was stirred for 5 h at 60 °C. H_2O was added and the aqueous layer was extracted with DCM. The organic layer was dried over $MgSO_4$ and the solvent was removed under a vacuum. The product was purified by flash column chromatography (PE/EA) to afford the desired product as a white solid (1.27 g, 3.6 mmol, 51%). ^{1}H NMR (700 MHz, DMSO-d_6) δ 8.87 (s, 1H), 7.45 (s, 1H), 7.42 (s, 1H), 7.04 (t, J = 5.6 Hz, 1H), 4.20 (t, J = 5.8 Hz, 2H), 4.01 (s, 3H), 3.39 (q, J = 5.8 Hz, 2H), 1.38 (s, 9H). ^{13}C NMR (176 MHz, DMSO-d_6) δ 157.6, 156.5, 155.3, 151.9, 150.1, 148.2, 118.2, 106.7, 102.9, 77.5, 67.2, 56.2, 38.7, 27.8 (3).

Tert-butyl (2-((4-(4-(2-(diethoxyphosphoryl)ethyl)piperidin-1-yl)-7-methoxyquinazolin-6-yl)oxy)ethyl)carbamate (**64**)
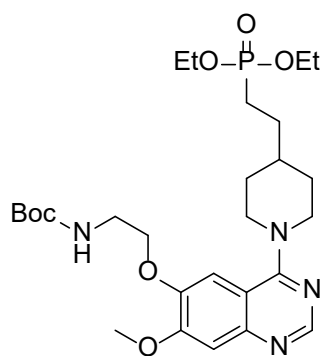
The synthetic procedure was adapted from the reported method.[143] DIPEA (348.4 µL, 2.0 mmol) was added to a mixture of **63** (324.1 mg, 1.3 mmol) and **61** (353.8 mg, 1.0 mmol) in isopropyl alcohol (4.5 mL). After stirring at 90°C for 3 h, the reaction mixture was cooled and evaporated to dryness. Purification of silica gel (MeOH/DCM) provided the desired product (485 mg, 0.9 mmol, 86%) as oil. ^{1}H NMR (700 MHz, CDCl$_3$) δ 8.63 (s, 1H), 7.38 (s, 1H), 7.26 (s, 1H), 7.11 (s, 1H), 4.23–4.05 (m, 8H), 3.99 (s, 3H), 3.64 (q, J = 5.3 Hz, 2H), 3.04 (t, J = 12.7 Hz, 2H), 1.85–1.63 (m, 9H), 1.45 (s, 9H), 1.34 (t, J = 7.1 Hz, 3H), 1.31 (t, J = 7.1 Hz, 3H). ^{13}C NMR (176 MHz, CDCl$_3$) δ 164.1, 155.9, 154.7, 153.2, 149.1, 147.3, 111.4, 107.6, 105.5, 79.6, 61.5 and 61.5 (d, $^2J_{C-P}$ = 7 Hz) (2), 56.1, 53.5 (2), 50.1, 39.9, 36.9 and 36.8 (d, $^3J_{C-P}$ = 16 Hz), 31.8 (2), 29.0 and 28.9 (d, $^2J_{C-P}$ = 5 Hz), 28.4 (3), 23.4 and 22.6 (d, $^1J_{C-P}$ = 142 Hz), 16.5 and 16.5 (d, $^3J_{C-P}$ = 6 Hz) (2).

Diethyl (2-(1-(6-(2-aminoethoxy)-7-methoxyquinazolin-4-yl)piperidin-4-yl)ethyl)phosphonate (**65**)
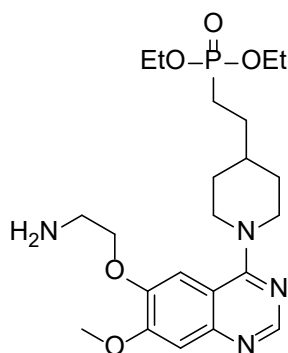
To a solution of **43** (213.9 mg, 0.4 mmol) in 12 mL of dichloromethane was added 4 M HCl in 1,4-dioxane (3 mL, 12.0 mmol). The mixture was stirred at room temperature for 30 min, followed by evaporation of the solvent to give a product as a colorless oil with quantitative yield.

2-(2,6-Dioxopiperidin-3-yl)-4-fluoroisoindoline-1,3-dione (**66**)
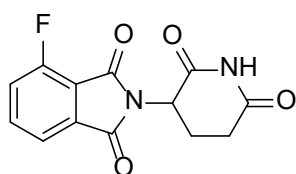
The compound was synthesized according to the previously reported method.[172] A solution of 3-fluoroisobenzofuran-1,3-dione (1.0 g, 6.0 mmol), 2,6-dioxopiperidine-3-ammonium chloride (1.0 mg, 6.0 mmol), and NaOAc (0.6 g, 7.2 mmol) in AcOH (40 mL) was refluxed overnight. The reaction mixture was poured into H$_2$O and extracted with EA. The organic phases were combined, dried with anhydrous sodium sulfate, and concentrated under reduced pressure (1.4 g, 5.2 mmol, 87%). The crude product was used in further steps without

purification. ^{1}H NMR (500 MHz, DMSO-d_6) δ 11.15 (s, 1H), 7.98–7.91 (m, 1H), 7.78 (d, J = 7.3 Hz, 1H), 7.73 (t, J = 9.1 Hz, 1H), 5.15 (dd, J = 12.9, 5.4 Hz, 1H), 2.97–2.58 (m, 2H), 2.54–2.50 (m, 2H).

General procedure 19

The compound was synthesized according to the previously reported method.[173] To a solution of **66** (552.4 mg, 2.0 mmol) and tert-butyl glycinate or tert-butyl 4-aminobutanoate (262.3 mg, 2.0 mmol) in anhydrous DMSO (20 mL) was added DIPEA (0.7 mL, 4.0 mmol). The reaction mixture was stirred under 90 °C for 1 day, then cooled down. The mixture was diluted with ethyl acetate, washed with H$_2$O and brine, dried with MgSO$_4$, then filtered and concentrated, and purified by column chromatography (PE/EA) to yield the desired products.

Tert-butyl (2-(2,6-dioxopiperidin-3-yl)-1,3-dioxoisoindolin-4-yl)glycinate (**67a**)
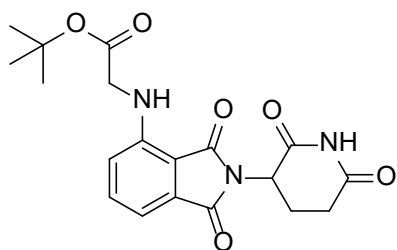
By using general procedure 19 with **66** (552.4 mg, 2.0 mmol), tert-butyl glycinate (262.3 mg, 2.0 mmol) to give the desired product (348.4 mg, 0.9 mmol, 45%). ^{1}H NMR (600 MHz, DMSO-d_6) δ 11.10 (s, 1H), 7.58 (dd, J = 8.5, 7.1 Hz, 1H), 7.07 (d, J = 7.0 Hz, 1H), 6.97 (d, J = 8.5 Hz, 1H), 6.84 (t, J = 6.1 Hz, 1H), 5.07 (dd, J = 12.8, 5.5 Hz, 1H), 4.09 (d, J = 6.0 Hz, 2H), 2.95–2.83 (m, 2H), 2.64–2.53 (m, 2H), 2.51–2.02 (m, 22H), 1.43 (s, 9H).

Tert-butyl 4-((2-(2,6-dioxopiperidin-3-yl)-1,3-dioxoisoindolin-4-yl)amino)butanoate (**67b**)
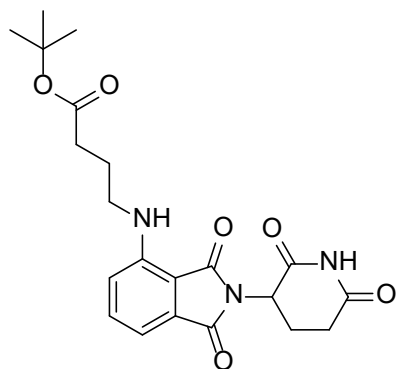
By using general procedure 19 with **66** (331.5 mg, 1.2 mmol), tert-butyl 4-aminobutanoate (248.4 mg, 1.6 mmol), and DIPEA (627.1 μL, 3.6 mmol) in DMSO (10 mL) to give the desired product (265.1 mg, 0.64 mmol, 53%). ^{1}H NMR (600 MHz, DMSO-d_6) δ 11.08 (s, 1H), 7.58 (dd, J = 8.6, 7.0 Hz, 1H), 7.11 (d, J = 8.6 Hz, 1H), 7.02 (d, J = 7.0 Hz, 1H), 6.64 (t, J = 6.2 Hz, 1H), 5.04 (dd, J = 12.9, 5.4 Hz, 1H), 3.31 (q, J = 6.7 Hz, 2H), 2.28 (t, J = 7.2 Hz, 2H), 1.77 (p, J = 7.2 Hz, 2H), 1.38 (s, 9H).

2-(2,6-Dioxopiperidin-3-yl)-4-(prop-2-yn-1-ylamino)isoindoline-1,3-dione (**73**)
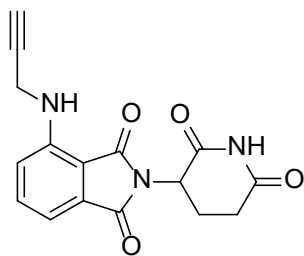
The compound was synthesized according to the previously reported method.[174] A mixture of propargylamine hydrochloride (192.1 μL, 3.0 mmol), **66** (828.6 mg, 3.0 mmol), and DIPEA (1.6 mL, 9.0 mmol) in dry *N,N*-dimethylformamide (12 mL) was stirred at 90 °C for 12 h. The mixture was cooled to room temperature, poured into water, and extracted with ethyl acetate. The combined organic phases were washed with water and brine, dried over MgSO$_4$, and concentrated under reduced pressure. The crude residue was purified by silica gel flash column chromatography (PE/EA) to afford the title compound as a yellow oil. 1H NMR (700 MHz, DMSO-d6) δ 11.14 (s, 1H), 7.64 – 7.59 (m, 1H), 7.27 – 7.21 (m, 1H), 7.13 – 7.10 (m, 1H), 6.92 (t, *J* = 6.2 Hz, 1H), 5.15 (dd, J = 13.0, 5.5 Hz, 1H), 4.06 – 3.97 (m, 2H), 3.03 (s, 1H), 2.94 – 2.82 (m, 2H), 2.63 – 2.52 (m, 2H).

General procedure 20

The respective carboxylic acid-functionalized thalidomides were prepared from responsible Boc-protected carboxylates by stirring in TFA/DCM (1:2 v/v) solution for 1 h at room temperature to give **68a** and **68b**. After a solution of carboxylic acid-functionalized linker or thalidomide (0.20 mmol, 1 equiv.), PyBOP (0.24 mmol, 1.2 equiv.), and DIPEA (0.60 mmol, 3 equiv.) in DMF (0.2 M) was stirred for 10 min, and **65** (0.24 mmol, 1.2 equiv.) was added. The mixture was stirred at room temperature for 1 h. The reaction solvent was removed under reduced pressure with help of toluene. The crude was diluted with H$_2$O/ACN and purified by preparative chromatography.

The deprotection of **69a** to give **70** and **71** was synthesized in the following conditions with different TMSBr amounts, reaction temperature, and reaction time. TMSBr was added to a cooled solution of **69a** (0.01 mmol) in anhydrous DCM (0.01 M) that was cooled by an ice bath under Ar blow. The reaction mixture was allowed to warm to the respective temperature. After reaction completion, the reaction was quenched by the addition of methanol (0.01 M). The mixture was evaporated to dryness and purified by preparative chromatography.

Diethyl (2-(1-(6-(2-(2-(2-azidoethoxy)acetamido)ethoxy)-7-methoxyquinazolin-4-yl)piperidin-4-yl)ethyl)phosphonate (**72a**)
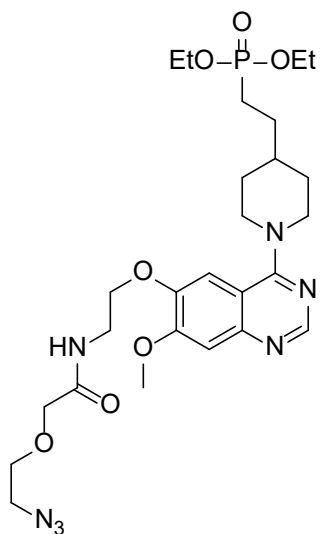
By using general procedure 20 with **40a** (29.0 mg, 0.2 mmol) to give the desired product (63.0 mg, 0.11 mmol, 53%). ^{1}H NMR (600 MHz, DMSO-d_6) δ 8.73 (s, 1H), 7.92 (t, J = 5.8 Hz, 1H), 7.38 (s, 1H), 7.22 (s, 1H), 4.68–4.59 (m, 2H), 4.20 (t, J = 5.8 Hz, 2H), 4.02–3.93 (m, 9H), 3.64 (t, J = 5.3 Hz, 2H), 3.55 (q, J = 5.8 Hz, 2H), 3.47 (t, J = 5.3 Hz, 2H), 3.44–3.40 (m, 2H), 1.93–1.87 (m, 2H), 1.82–1.71 (m, 3H), 1.50–1.41 (m, 2H), 1.35–1.26 (m, 2H), 1.22 (t, J = 7.0 Hz, 6H). ^{13}C NMR (151 MHz, DMSO-d_6) δ 168.9, 160.4, 155.6, 146.8, 146.7, 137.1, 107.2, 105.5, 99.5, 69.3, 69.2, 66.8, 60.4 and 60.4 (d, $^2J_{C-P}$ = 6 Hz) (2), 56.0, 49.5, 48.8 (2), 37.0, 34.8 and 34.7 (d, $^3J_{C-P}$ = 16 Hz), 30.9 (2), 27.8 and 27.7 (d, $^2J_{C-P}$ = 5 Hz), 21.9 and 21.0 (d, $^1J_{C-P}$ = 139 Hz), 15.9 and 15.9 (d, $^3J_{C-P}$ = 6 Hz) (2).

Diethyl (2-(1-(6-(2-(2-(2-(2-azidoethoxy)ethoxy)acetamido)ethoxy)-7-methoxyquinazolin-4-yl) piperidin-4-yl)ethyl)phosphonate (**72b**)
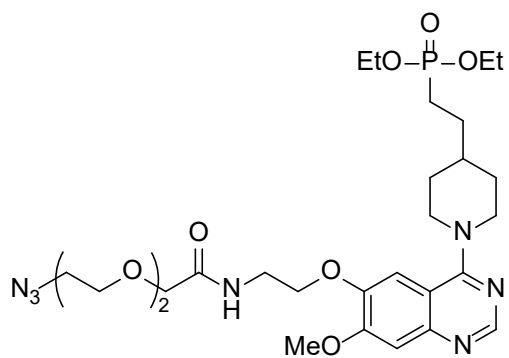
By using general procedure 20 with **40b** (37.8 mg, 0.2 mmol) to give the desired product (71.4 mg, 0.11 mmol, 56%). ^{1}H NMR (600 MHz, DMSO-d_6) δ 8.73 (s, 1H), 7.87 (t, J = 5.8 Hz, 1H), 7.38 (s, 1H), 7.24 (s, 1H), 4.69–4.60 (m, 2H), 4.20 (t, J = 5.9 Hz, 2H), 4.01–3.95 (m, 7H), 3.92 (s, 2H), 3.74–3.64 (m, 2H), 3.62–3.59 (m, 4H), 3.55 (q, J = 5.9 Hz, 2H), 3.50–3.42 (m, 2H), 3.42–3.38 (m, 2H), 1.94–1.86 (m, 2H), 1.83–1.71 (m, 3H), 1.51–1.40 (m, 2H), 1.36–1.26 (m, 2H), 1.22 (t, J = 7.0 Hz, 6H). 13C NMR (151 MHz, DMSO) δ 169.2, 160.4, 155.6, 146.8, 146.8, 137.3, 107.2, 105.6, 99.6, 69.8, 69.5, 69.0, 68.8, 66.9, 60.5 and 60.4 (d, $^2J_{C-P}$ = 6 Hz) (2), 56.0, 49.5, 48.8 (2), 37.0, 34.9 and 34.7 (d, $^3J_{C-P}$ = 16 Hz), 30.9 (2), 27.8 and 27.8 (d, $^2J_{C-P}$ = 5 Hz), 21.9 and 21.0 (d, $^1J_{C-P}$ = 139 Hz), 15.9 and 15.9 (d, $^3J_{C-P}$ = 6 Hz) (2).

Diethyl (2-(1-(6-(2-(2-((2-(2,6-dioxopiperidin-3-yl)-1,3-dioxoisoindolin-4-yl)amino)acet amido)ethoxy)-7-methoxyquinazolin-4-yl)piperidin-4-yl)ethyl)phosphonate (**69a**)
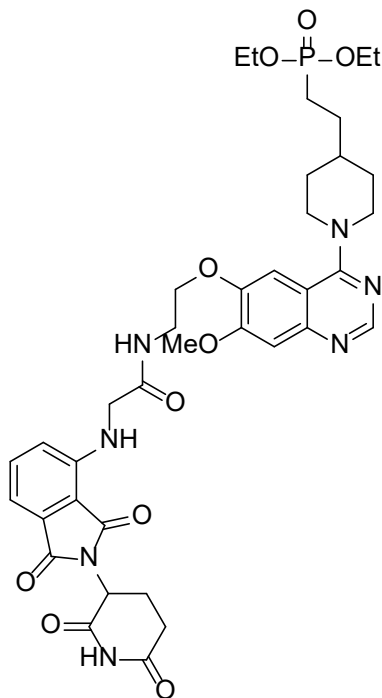
By using general procedure 20 with **68a** (0.2 mmol) prepared from **67a** to give the desired product (62.9 mg, 0.08 mmol, 33%). ^{1}H NMR (600 MHz, DMSO-d_6) δ 11.10 (s, 1H), 8.73 (s, 1H), 8.42 (t, J = 5.7 Hz, 1H), 7.51 (dd, J = 8.5, 7.1 Hz, 1H), 7.38 (s, 1H), 7.22 (s, 1H), 7.04 (d, J = 7.1 Hz, 1H), 6.97 (t, J = 5.7 Hz, 1H), 6.85 (d, J = 8.5 Hz, 1H), 5.07 (dd, J = 12.8, 5.4 Hz, 1H), 4.63 (d, J = 12.9 Hz, 2H), 4.19 (t, J = 5.7 Hz, 2H), 3.97 (d, J = 17.8 Hz, 4H), 3.54 (q, J = 5.7 Hz, 2H), 3.44 (t, J = 12.9 Hz, 2H), 2.97–2.85 (m, 1H), 2.66–2.52 (m, 5H), 2.03 (t, J = 10.4 Hz, 3H), 1.89 (d, J = 11.5 Hz, 3H), 1.75 (t, J = 17.3 Hz, 2H), 1.46 (d, J = 16.6 Hz, 1H), 1.36–1.26 (m, 2H), 1.21 (t, J = 7.1 Hz, 6H). ^{13}C NMR (151 MHz, DMSO-d_6) δ 172.4, 169.6, 168.7, 168.3, 166.9, 160.4, 155.6, 146.8, 146.7, 145.4, 137.1, 135.7, 131.6, 117.0, 110.6, 109.5, 107.1, 105.5, 99.5, 66.9, 60.5 and 60.4 (d, $^2J_{C-P}$ = 6 Hz) (2), 56.0, 48.9 (2), 48.2, 44.8, 37.5, 34.8 and 34.7 (d, $^3J_{C-P}$ = 35 Hz), 30.9 (2), 30.6, 27.8 and 27.7 (d, $^2J_{C-P}$ = 5 Hz), 21.9 and 21.0 ((d, $^1J_{C-P}$ = 139 Hz), 21.8 15.9 and 15.9 (d, $^3J_{C-P}$ = 6 Hz) (2). ^{31}P NMR (243 MHz, DMSO-d_6) δ 32.0 (s, 1P). HRMS-ESI (m/z): [M+H]$^+$ calculated for $C_{37}H_{47}O_{10}N_7P$, 780.3117; found, 780.3109.

(2-(1-(6-(2-(2-((2-(2,6-Dioxopiperidin-3-yl)-1,3-dioxoisoindolin-4-yl)amino)acetamido)
ethoxy)-7-methoxyquinazolin-4-yl)piperidin-4-yl)ethyl)phosphonic acid (**70**)
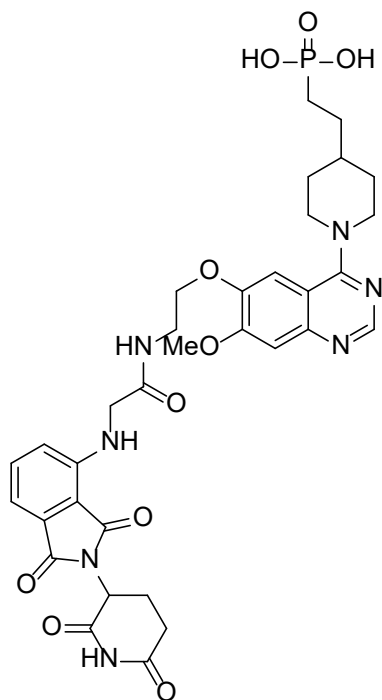
By using TMSBr (1 mL) in DCM (2 mL) at 60 °C overnight. ^{1}H NMR (700 MHz, DMSO-d_6) δ 14.10 (s, 2H), 11.04 (s, 1H), 8.66 (s, 1H), 8.34 (t, J = 5.7 Hz, 1H), 7.45 (t, J = 7.8 Hz, 1H), 7.32 (s, 1H), 7.15 (s, 1H), 6.98 (d, J = 7.8 Hz, 1H), 6.90 (t, J = 5.7 Hz, 1H), 6.79 (d, J = 7.8 Hz, 1H), 5.01 (dd, J = 12.9, 5.5 Hz, 1H), 4.57 (d, J = 12.9 Hz, 2H), 4.13 (t, J = 5.7 Hz, 2H), 3.97–3.80 (m, 5H), 3.48 (q, J = 5.7 Hz, 2H), 3.43–3.29 (m, 2H), 2.88–2.76 (m, 1H), 2.60–2.44 (m, 2H), 2.00–1.92 (m, 1H), 1.82 (d, J = 12.9 Hz, 2H), 1.71–1.62 (m, 1H), 1.62–1.52 (m, 1H), 1.46 (s, 1H), 1.43–1.36 (m, 2H), 1.27–1.18 (m, 2H). 13C NMR (176 MHz, DMSO) δ 172.4, 169.7, 168.7, 168.4, 166.9, 160.4, 155.6, 146.8, 146.8, 145.4, 137.1, 135.8, 131.7, 117.1, 110.7, 109.5, 107.2, 105.6, 99.5, 67.0, 56.1, 49.0 (2), 48.2, 44.8, 37.6, 35.0 and 34.9 (d, $^3J_{C-P}$ = 16 Hz), 31.0 (2), 30.6, 28.3 and 28.2 (d, $^2J_{C-P}$ = 4 Hz), 23.1 and 22.3 (d, $^1J_{C-P}$ = 138 Hz), 21.8. HRMS-ESI (m/z): [M+H]$^+$ calculated for $C_{33}H_{39}O_{10}N_7P$, 724.2491; found, 724.2481.

Ethyl hydrogen (2-(1-(6-(2-(2-((2-(2,6-dioxopiperidin-3-yl)-1,3-dioxoisoindolin-4-yl) amino)acetamido)ethoxy)-7-methoxyquinazolin-4-yl)piperidin-4-yl)ethyl)phosphonate (**71**)
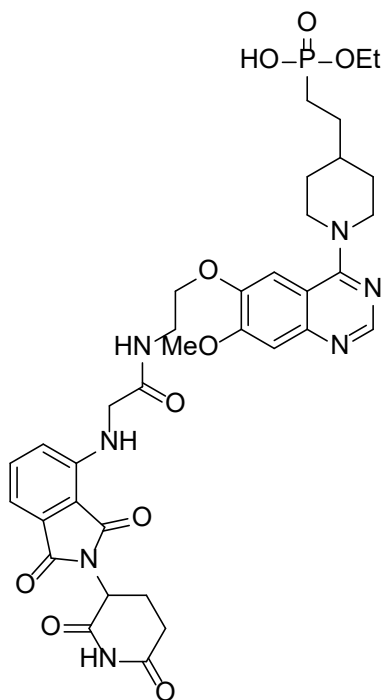
By using TMSBr (0.2 mL) in DCM (2 mL) at room temperature for 1 h. ^{1}H NMR (600 MHz, DMSO-d_6) δ 14.21 (s, 1H), 11.10 (s, 1H), 8.73 (s, 1H), 8.42 (t, J = 5.7 Hz, 1H), 7.51 (dd, J = 8.5, 7.1 Hz, 1H), 7.38 (s, 1H), 7.23 (s, 1H), 7.04 (d, J = 7.1 Hz, 1H), 6.97 (t, J = 5.7 Hz, 1H), 6.85 (d, J = 8.5 Hz, 1H), 5.07 (dd, J = 12.9, 5.5 Hz, 1H), 4.63 (d, J = 12.9 Hz, 2H), 4.19 (t, J = 5.7 Hz, 2H), 4.03–3.91 (m, 7H), 3.54 (q, J = 5.7 Hz, 2H), 3.45 (d, J = 12.0 Hz, 2H), 2.97–2.83 (m, 1H), 2.64–2.50 (m, 2H), 2.06–1.99 (m, 1H), 1.93–1.84 (m, 2H), 1.79–1.69 (m, 3H), 1.50–1.39 (m, 2H), 1.34–1.24 (m, 2H), 1.21 (t, J = 7.0 Hz, 3H). ^{13}C NMR (151 MHz, DMSO-d_6) δ 172.4, 169.6, 168.7, 168.3, 166.9, 160.4, 155.5, 146.8, 146.7, 145.4, 137.1, 135.7, 131.6, 117.0, 110.6, 109.5, 107.1, 105.5, 99.5, 66.9, 59.4 and 59.4 (d, $^2J_{\text{C-P}}$ = 6 Hz), 56.0, 48.9 (2), 48.2, 44.8, 37.5, 34.8 and 34.7 (d, $^3J_{\text{C-P}}$ = 16 Hz), 30.9 (2), 30.6, 28.2 and 28.2 (d, $^2J_{\text{C-P}}$ = 4 Hz), 23.1 and 22.2 (d, $^1J_{\text{C-P}}$ = 138 Hz), 21.8, 16.0 and 16.0 (d, $^3J_{\text{C-P}}$ = 6 Hz). ^{31}P NMR (243 MHz, DMSO-d_6) δ 29.0 (s, 1P). HRMS-ESI (m/z): [M+H]$^+$ calculated for $C_{35}H_{43}O_{10}N_7P$, 752.2804; found, 752.2826.

Diethyl (2-(1-(6-(2-(4-((2-(2,6-dioxopiperidin-3-yl)-1,3-dioxoisoindolin-4-yl)amino)butan amido)ethoxy)-7-methoxyquinazolin-4-yl)piperidin-4-yl)ethyl)phosphonate (**69b**)
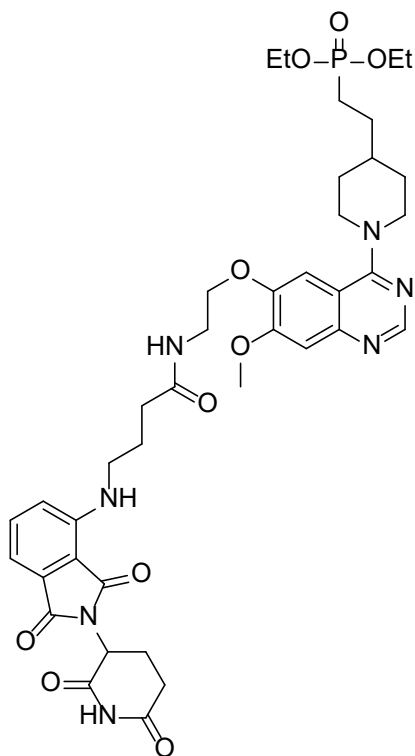
By using general procedure 20 with **68b** (0.14 mmol) prepared from **67b** to give the desired product (28.4 mg, 0.04 mmol, 25%). ^{1}H NMR (600 MHz, DMSO-d_6) δ 11.08 (s, 1H), 8.72 (s, 1H), 8.20 (t, J = 5.6 Hz, 1H), 7.52 (dd, J = 8.6, 7.0 Hz, 1H), 7.37 (s, 1H), 7.21 (s, 1H), 7.06 (d, J = 8.6 Hz, 1H), 6.99 (d, J = 7.0 Hz, 1H), 6.61 (t, J = 5.7 Hz, 1H), 5.03 (dd, J = 12.9, 5.5 Hz, 1H), 4.63 (d, J = 12.9 Hz, 2H), 4.17 (t, J = 5.7 Hz, 2H), 4.04–3.91 (m, 8H), 3.53–3.40 (m, 4H), 3.28 (q, J = 6.6 Hz, 2H), 2.91–2.82 (m, 1H), 2.63–2.51 (m, 1H), 2.19 (t, J = 7.2 Hz, 2H), 2.03–1.97 (m, 1H), 1.91–1.86 (m, 2H), 1.82–1.68 (m, 5H), 1.49–1.41 (m, 2H), 1.35–1.25 (m, 2H), 1.21 (t, J = 7.0 Hz, 6H). ^{13}C NMR (151 MHz, DMSO-d_6) δ 172.4, 171.8, 169.7, 168.4, 166.9, 160.3, 155.6, 146.9, 146.6, 145.9, 137.0, 135.8, 131.8, 116.7, 110.0, 108.6, 107.0, 105.5, 99.4, 67.0, 60.5 and 60.4 (d, $^2J_{C-P}$ = 6 Hz) (2), 56.0, 48.8 (2), 48.1, 41.0, 37.4, 34.8 and 34.7 (d, $^3J_{C-P}$ = 16 Hz), 32.0, 30.9 (2), 30.6, 27.8 and 27.7 (d, $^2J_{C-P}$ = 5 Hz), 24.2, 21.9 and 21.0 (d, $^1J_{C-P}$ = 139 Hz), 21.7, 15.9 and 15.9 (d, $^3J_{C-P}$ = 6 Hz) (2). ^{31}P NMR (243 MHz, DMSO-d_6) δ 32.0 (s, 1P). HRMS-ESI (m/z): [M+H]$^+$ calculated for $C_{39}H_{51}O_{10}N_7P$, 808.3430; found, 808.3420.

Diethyl (2-(1-(6-(2-(2-(2-(4-(((2-(2,6-dioxopiperidin-3-yl)-1,3-dioxoisoindolin-4-yl)amino) methyl)-1H-1,2,3-triazol-1-yl)ethoxy)acetamido)ethoxy)-7-methoxyquinazolin-4-yl)piperidin-4-yl)ethyl)phosphonate (**74a**)
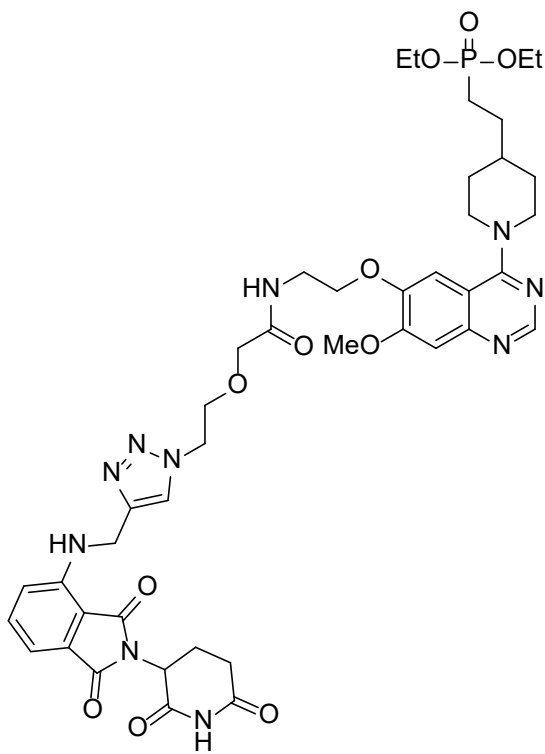
By using general procedure 14, **72a** (53.0 mg, 0.09 mmol), **73** (33.4 mg, 0.11 mmol), CuSO$_4$ • 5H$_2$O (24.5 mg, 0.10 mmol), and sodium ascorbate (35.4 mg, 0.18 mmol) in 2 mL of THF to give the title compound (12.6 mg, 10 μmol, 16%). ^{1}H NMR (600 MHz, DMSO-d_6) δ 11.09 (s, 1H), 8.72 (s, 1H), 8.06 (s, 1H), 7.91 (t, J = 5.8 Hz, 1H), 7.53 (dd, J = 8.5, 6.9 Hz, 1H), 7.36 (s, 1H), 7.20 (s, 1H), 7.13 (d, J = 8.5 Hz, 1H), 7.03 (s, 1H), 7.01 (d, J = 6.9 Hz, 1H), 5.04 (dd, J = 12.9, 5.4 Hz, 1H), 4.63 (d, J = 12.9 Hz, 2H), 4.55 (t, J = 5.0 Hz, 4H), 4.17 (t, J = 6.0 Hz, 2H), 4.00–3.93 (m, 8H), 3.89 (s, 2H), 3.84 (t, J = 5.2 Hz, 2H), 3.51 (q, J = 5.8 Hz, 2H), 3.48–3.41 (m, 2H), 2.91–2.83 (m, 1H), 2.61–2.54 (m, 1H), 2.05–1.98 (m, 1H), 1.93–1.84 (m, 2H), 1.79–1.70 (m, 3H), 1.49–1.41 (m, 2H), 1.33–1.25 (m, 2H), 1.21 (t, J = 7.0 Hz, 6H). ^{13}C NMR (151 MHz, DMSO-d_6) δ 172.4, 169.6, 168.8, 168.4, 166.8, 160.4, 155.6, 146.7, 145.4, 144.0, 137.1, 135.7, 131.6, 123.0, 117.1, 115.2, 110.5, 109.2, 107.2, 105.5, 99.5, 69.2, 68.8, 66.7, 60.5 and 60.4 (d, $^2J_{C-P}$ = 6 Hz) (2), 56.0, 48.8 (2), 48.8, 48.1, 37.2, 37.0, 34.8 and 34.7 (d, $^3J_{C-P}$ = 17 Hz), 30.9 (2), 30.6, 27.8 and 27.7 (d, $^2J_{C-P}$ = 5 Hz), 21.9 and 21.0 (d, $^1J_{C-P}$ = 139 Hz), 21.7, 15.9 and 15.9 (d, $^3J_{C-P}$ = 6 Hz) (2). ^{31}P NMR (243 MHz, DMSO-d_6) δ 32.0 (s, 1P). HRMS-ESI (m/z): [M+H]$^+$ calculated for C$_{42}$H$_{54}$O$_{11}$N$_{10}$P, 905.3706; found, 905.3727.

*Diethyl (2-(1-(6-(2-(2-(2-(2-(4-(((2-(2,6-dioxopiperidin-3-yl)-1,3-dioxoisoindolin-4-yl)amino)
methyl)-1H-1,2,3-triazol-1-yl)ethoxy)ethoxy)acetamido)ethoxy)-7-methoxyquinazolin-4-
yl)piperidin-4-yl)ethyl)phosphonate* (**74b**)
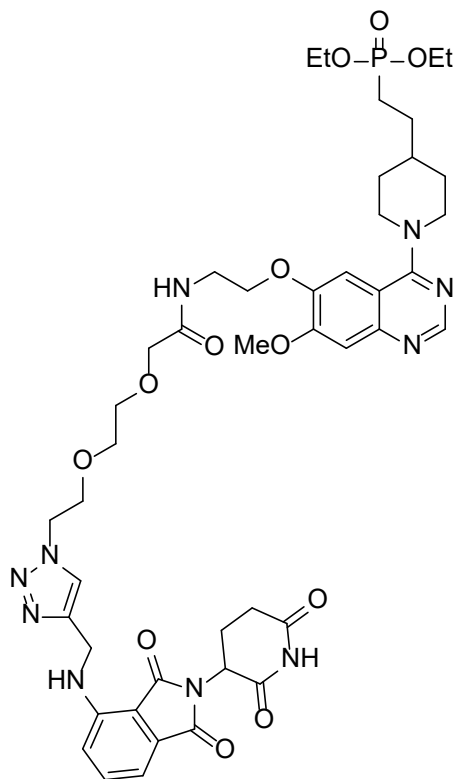
By using general procedure 14, **72b** (61.4 mg, 0.10 mmol), **73** (36.0 mg, 0.12 mmol), CuSO$_4$ • 5H$_2$O (26.4 mg, 0.11 mmol), and sodium ascorbate (38.2 mg, 0.19 mmol) in 2 mL of THF to give the title compound (10.4 mg, 10 μmol, 11%). ^{1}H NMR (600 MHz, DMSO-d_6) δ 11.09 (s, 1H), 8.72 (s, 1H), 8.01 (s, 1H), 7.84 (t, J = 5.9 Hz, 1H), 7.53 (dd, J = 8.6, 7.1 Hz, 1H), 7.35 (s, 1H), 7.20 (s, 1H), 7.13 (d, J = 8.6 Hz, 1H), 7.03 (t, J = 6.1 Hz, 1H), 7.01 (d, J = 7.1 Hz, 1H), 5.04 (dd, J = 12.9, 5.4 Hz, 1H), 4.62 (d, J = 12.9 Hz, 2H), 4.55 (d, J = 5.6 Hz, 2H), 4.49 (t, J = 5.4 Hz, 2H), 4.18 (t, J = 5.9 Hz, 2H), 4.03–3.89 (m, 10H), 3.85 (s, 2H), 3.81–3.74 (m, 2H), 3.58–3.50 (m, 4H), 3.48–3.38 (m, 2H), 2.91–2.81 (m, 1H), 2.64–2.53 (m, 1H), 2.04–1.98 (m, 1H), 1.91–1.85 (m, 2H), 1.79–1.68 (m, 3H), 1.50–1.41 (m, 2H), 1.29 (d, J = 29.4 Hz, 2H), 1.21 (t, J = 7.0 Hz, 6H). ^{13}C NMR (151 MHz, DMSO-d_6) δ 172.4, 169.6, 169.2, 168.3, 166.8, 160.3, 155.5, 146.8, 146.7, 145.4, 143.9, 137.1, 135.7, 131.6, 122.8, 117.1, 110.5, 109.2, 107.1, 105.5, 99.5, 69.6, 69.4, 68.9, 68.3, 66.8, 60.5 and 60.4 (d, $^2J_{C-P}$ = 6 Hz) (2), 56.0, 48.9, 48.8 (2), 48.1, 37.2, 36.9, 34.8 and 34.7 (d, $^3J_{C-P}$ = 17 Hz), 30.9 (2), 30.6, 27.8 and 27.7 (d, $^2J_{C-P}$ = 5 Hz), 21.9 and 21.0 (d, $^1J_{C-P}$ = 139 Hz), 21.7, 15.9 and 15.9 (d, $^3J_{C-P}$ = 6 Hz) (2). ^{31}P NMR (243 MHz, DMSO-d_6) δ 32.0 (s, 1P). HRMS-ESI (m/z): [M+H]$^+$ calculated for C$_{44}$H$_{58}$O$_{12}$N$_{10}$P, 949.3968; found, 949.3993.

5.1.3 Molecular docking

Computational docking of 2-((pyrrol-2-yl)methylene)thiophen-4-one to ATP-binding site and 2-5A binding site of RNase L (PDB code: 4OAU, 1WDY) was done by Schrödinger Maestro 13.1. The 3-dimensional structures of 2-((pyrrol-2-yl)methylene)thiophen-4-ones were prepared after calculating energy minimization by MM2 at Chem3D 18.2 and the chemical states were generated by the ligand preparation module. The conformation of RNase L was prepared according to the protein preparation module, including hydrogen addition, water molecule removal, and energy minimization. The binding site was generated by the grid generation module and using ATP as the ligand. The glide dock was performed by the glide dock module and evaluated according to the docking score, small molecule orientation, solvent exposure, and interactions between small molecules and RNase L. The interactions were visualized by using PyMOL

5.2 Biological evaluation

5.2.1 Protein expression and purification

His$_6$-TEV-RNase L was subcloned to the pFastBacHT vector and expressed in High Five™ insect cells according to the supplier manuals. The cells were grown to 2×10^6 cells/mL in 500 mL serum-free Sf-900™ II medium (Gibco®) transfected with an MOI of 5, followed by incubation at 27 °C and 110 rpm for 72 h. Cells were harvested at 4 °C and 600 × g for 15 min and the pellet was resuspended in lysis buffer (25 mM Tris, pH 7.4, 50 mM KCl, 5 mM MgCl$_2$, 10% glycerol, 0.1 mM PMSF, SIGMAFAST™ Protease Inhibitor Cocktail (EDTA-free, Sigma Aldrich), DNase I Grade II (Sigma Aldrich)), homogenized and disrupted using the Sonic Dismembrator FB-705 (fisherbrand) on ice. The lysate was centrifuged at 65,000 g at 4 °C for 1 h. The supernatant was applied to an immobilized nickel affinity chromatography column (HisTrap™ HP, GE Healthcare) equilibrated with buffer A (25 mM Tris, pH 7.4, 50 mM KCl, 5 mM MgCl$_2$, 10% glycerol). Elution was performed by adding Buffer B (25 mM Tris, pH 7.4, 50 mM KCl, 5 mM MgCl$_2$, 10% glycerol, 0.5 M imidazole) in a gradient from 5% to 100%. The His-tag was cleaved using TEV protease overnight while dialyzing against buffer A with 1 mM DTT (MWCO 3.5 kDa). The protein was loaded onto a nickel column equilibrated with buffer A and the flow-through was collected. Elution was performed with buffer B. The protein was further purified using a High Load Superdex 75 pg 16/600 column equilibrated with gel filtration buffer (25 mM Tris, pH 7.4, 50 mM KCl, 5 mM MgCl$_2$, 10% glycerol, 7 mM β-mercaptoethanol). The purified protein was concentrated and stored at -80 °C. The concentration of purified protein was determined using the Pierce™ Coomassie (Bradford) Protein-Assay-Kit (Thermo Scientific) with BSA as a standard according to the manufacturer's descriptions.

5.2.2 *in vitro* assays

5.2.2.1 FRET-based RNA cleavage assay

Purified human full length RNase L (5 nM) was incubated with 0.5 nM 2-5A for 5 min on ice in FRET RNA cleavage buffer (25 mM Tris, pH 7.4, 100 mM KCl, 10 mM MgCl$_2$, 2 mM glutathione, 0.1% (v/v) NP-40), followed by incubation with various concentrations of the compound in FRET RNA cleavage buffer containing 50 μM ATP (25 mM Tris, pH 7.4, 100 mM KCl, 10 mM MgCl$_2$, 2 mM glutathione, 50 μM ATP, 0.1% (v/v) NP-40) for 30 min on ice.

50 nM RNA probe (5' FAM-UUA UCA AAU UCU UAU UUG CCC CAU UUU UUU GGU-BHQ -1 3' or 5' Alexa647-UUA UCA AAU UCU UAU UUG CCC CAU UUU UUU GGU-IBQ 3' or 5' Alexa647-CCAUUUUUUUGG-IBQ 3' or) was added and the mixture was further incubated for 120 min at room temperature. Fluorescence intensity (F) was measured using a TECAN Spark plate reader. The inhibition rate (IR) was calculated as follows.

$$IR = \frac{1 - (F(compound) - F(DMSO)}{F(2' - 5'A) - F(DMSO)} \cdot 100\%$$

The half maximal inhibitory concentration (IC_{50}) was determined by fitting the following function in Graph Pad Prism8:

$$Y = \frac{Bottom + (Top - Bottom)}{1 + ((IC_{50}/X)^{HillSlope}}$$

and the following rules were inserted: $Bottom = 1 \cdot Y_{min}$, $Top = 1 \cdot Y_{max}$, $IC_{50} = 1 \cdot (Value\ of\ X\ at\ Y_{mid})$ and $HillSlope = 1 \cdot \text{sgn}(Y\ at\ X_{max} - Y\ at\ X_{min})$.

5.2.2.2 Gel-based RNA cleavage assay.

Purified RNase L (60 nM) was incubated in RNA gel electrophoresis cleavage buffer (25 mM Tris, pH 7.4, 100 mM KCl, 10 mM $MgCl_2$, 7 mM β-mercaptoethanol, 50 μM ATP) with 2 nM 2-5A for 5 min, followed by incubation with compound for 30 min. The mixture was further incubated with an RNA probe (5' Cy3 CCCACCCACCUUCCCACCCACCCACCCCACCC 3') in the dark for 30 min. After incubation, the sample was mixed with 6×TBE loading buffer (45% (v/v) H_2O, 40% (v/v) glycerol, 15% (v/v) 10×TBE) and denatured at 80 °C. 5 μL of the sample were loaded on a 15% (v/v) acrylamide/8 M urea gel. The gel was run for 25 min in 60 °C prewarmed 1×TBE buffer. Cy3 fluorescence was detected with a ChemiDoc MP (Bio-Rad) with an exposure time of 2 min.

5.2.2.3 Thermal shift assay

NanoDSF was performed using NanoTemper Prometheus NT.48. Samples contained 3 μM RNase L and 60 μM compound, 3% DMSO or 1.75 μM 2-5A in buffer (25 mM Hepes, pH 7.4, 100 mM KCl, 10 mM $MgCl_2$, 2.5 μM ATP) and were incubated for 50 min. The samples were heated at a rate of 1 °C per minute from 20 °C to 90 °C. The mean ΔT_m (°C) value was

calculated from three independent tests.

5.2.2.4 Biolayer interferometry (BLI).

Direct binding was evaluated by Biolayer interferometry using an Octet Red384 (Pall ForteBio) instrument using 384 well plate format and a sample volume of 50 µL. Protein was biotinylated with EZ-Link Sulfo NHS-LC-LC-Biotin (Thermo Scientific) aiming for one biotin per protein molecule according to the manufacturers' protocol. The protein was immobilized on Streptavidin (SA) Biosensors equilibrated in assay buffer containing 20 mM HEPES (pH 7.5), 150 mM NaCl, 1 mM $MgCl_2$, 0.05% Tween-20, 1% DMSO and 0.3 mg/mL BSA. A baseline was recorded for 300 seconds followed by an association step with a dilution series of 100 µM to 0 µM compound and a dissociation step in a buffer for 400 seconds each. Data was analyzed by double referencing to sensors loaded with 10 µg/mL biocytin instead of protein and to sensors immersed in a buffer instead of compound.

5.2.3 Cellular assays

5.2.3.1 Antiproliferation MTT assay in cancer cells

Cancer cells (obtained from DSMZ, German Collection of Microorganisms and Cell Cultures, Braunschweig, Germany) were seeded in 96-well plates with 3000-5000 cells/well and were incubated for 8-24 h. The old medium was discarded and the media with compounds were added to the 96-well plates. Data were normalized to the medium with 1% DMSO. The cells were then incubated for 72 h or in time-dependent tests at 3, 6, 12, 24, 48, and 72 h. MTT solution (5 mg/mL, 20 µL) was added per well in dark and incubated for 4 h. Then the old medium with MTT solution was removed and 150 µL DMSO was added per well. The absorbance of the well was measured at 492 nm by a TECAN plate reader.

5.2.3.2 Cell colony formation analysis

JAR and K562 cells were cultured in RPMI 1640 Medium (Thermo Fisher Scientific) containing 10% (v/v) fetal bovine serum (Gibco), and 1% (v/v) penicillin/streptomycin. A549, HeLa, and MCF7 were cultured in Dulbecco's Modified Eagle Medium (Thermo Fisher

Scientific) containing 10% (v/v) fetal bovine serum (Gibco), 1% (v/v) penicillin/streptomycin. The cells in the exponential growth stage were made into cell suspension by the conventional digestion and passage method. The cells were counted and the cell concentration was adjusted with a culture medium. Cell suspension (2 mL) was inoculated into a 6-well plate culture dish according to the concentration of 200 cells in each dish, and the culture dish was gently shaken in the cross direction to disperse the cells evenly. Placed the 6-well plate in the incubator for 10 days. When there was a visible colony in the 6-well plate, the culture was terminated, the culture medium was discarded, and the colony was carefully soaked in PBS solution twice and dried in the air. The cells were fixed with methanol for 15 min, discarded methanol, dyed with Giemsa dye solution for 10 minutes, washed off the dye solution slowly with running water, and then dried in the air. Colony numbers and types were assessed manually under a microscope.

5.2.3.3 Cell migration assay

The back of a 6-well plate was marked with at least five horizontal, uniform, and parallel lines. 5–$10*10^5$ cells were inoculated per well depending on the cell type. On the next day, a sterile toothpick was used to scratch across the line. Then, cells were washed 2-3 times with PBS and a low serum medium (<2%) was added. After 0, 24, 48, and 72 h, pictures were taken with a microscope. In total 6-8 horizontal lines were randomly drawn and the average distance between the cells was calculated with Image J.

5.2.3.4 Apoptosis assay and Western blot.

JAR cells were seeded in 10 cm dishes for 2.5×10^6 per dish. After 24 h, cells were treated with either 10 μM of compounds or different concentrations of compound **4l** (0, 1.25, 2.5, 5, and 10 μM) for 24 h. Cells and supernatant were then collected for measuring PARP cleavage by Western Blotting. Whole-cell proteins of JAR cells were extracted with RIPA lysis buffer, containing 10 mM Tris-Cl pH 7.4, 150 mM NaCl, 10 mM KCl, 1 mM EDTA, 0.5% deoxycholic acid, 1% IGEPAL, 0.1% SDS and protease inhibitor mixture (Roche). After cooling the cell suspension on ice for 15 minutes, the cell debris was precipitated and removed through 13,000 rpm centrifugation at 4° C. The concentration of proteins in the supernatant was measured by a DC protein assay (Bio-Rad). Then 30 μg of total proteins from each sample was loaded on a 10% SDS-PAGE gel. The electrophoretically separated proteins on an SDS-PAGE gel were

transferred to a PVDF membrane. Anti-GAPDH (Sigma-Aldrich Cat#G8795) and Anti-PARP (Cell Signaling Cat#9542S) antibodies were used to probe the membranes to measure cleaved PARP relative to GAPDH and control. The quantification analysis was performed using the Image J software.

5.2.3.5 Flow cytometry

Cells were seeded in 6-well plates and treated with the indicated concentrations of compounds for 24 hours. Cells were harvested and washed in PBS. FITC Annexin V Apoptosis Detection Kit (BioLegend BV, Article no: 640914) was used according to instructed protocol. After several washing steps, cells were analyzed by a SONY Cell Sorter SH800S.

5.2.3.6 Ribosomal RNA cleavage assay.

HeLa cells were seeded in 6-well plates and cultured in DMEM containing 10% FBS and antibiotic antimycotic solution at 37 °C and 5% CO_2. Cells were treated with 0.5% DMSO or compound for four hours followed by transfection of 2 μg / mL poly I:C or mock transfection using Lipofectamine 2000. Four hours after transfection, the medium was removed and total RNA was extracted using RNeasy Mini Kit (Qiagen). The concentration was determined using a NanoDrop 2000c (Thermo Fisher Scientific) and equal concentrations of RNA were separated by denaturing glyoxal agarose gel electrophoresis. RNA was visualized using ethidium bromide which was added to the RNA during glyoxylation and the gel was imaged on a ChemiDoc MP (Bio-Rad Laboratories).

6. Supporting information
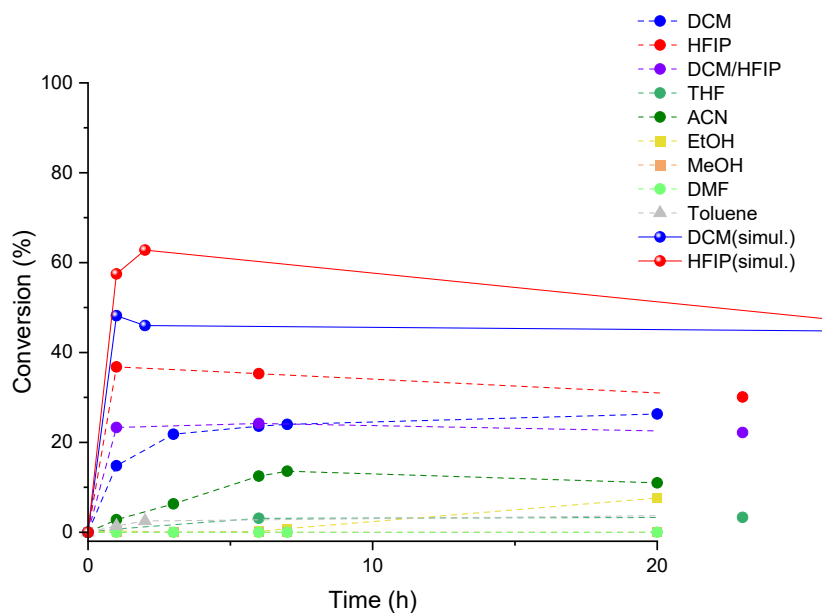
Figure S1. The reaction screening of Petasis reaction over reaction time.
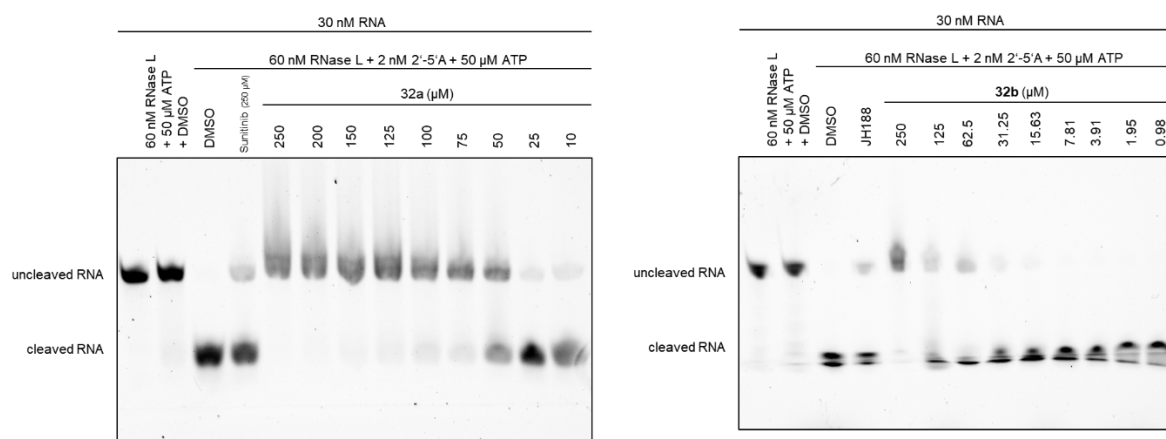
Figure S2. Dose-dependent response of RNase L inhibitor **32a** and **32b** in gel-based RNA cleavage assay.
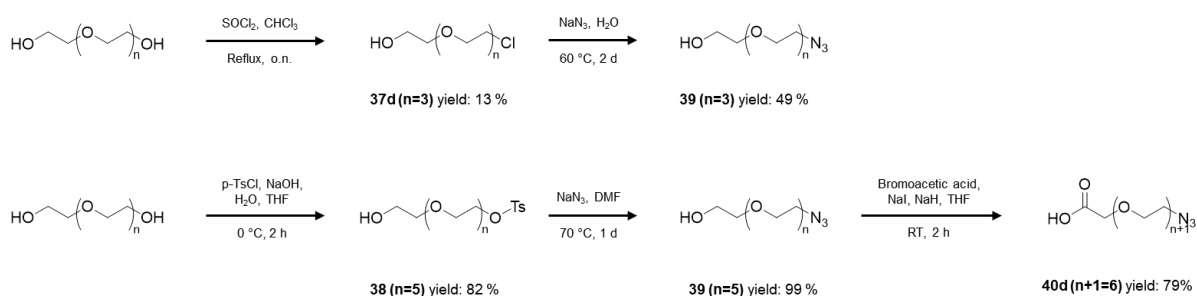
Figure S3. The synthesis of COOH- and azide-tagged PEG linker with two synthetic routes.
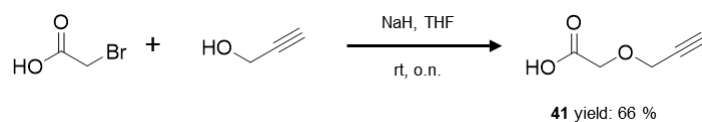
Figure S4. Synthetic route to obtain COOH- and alkyne-tagged linker **41**.
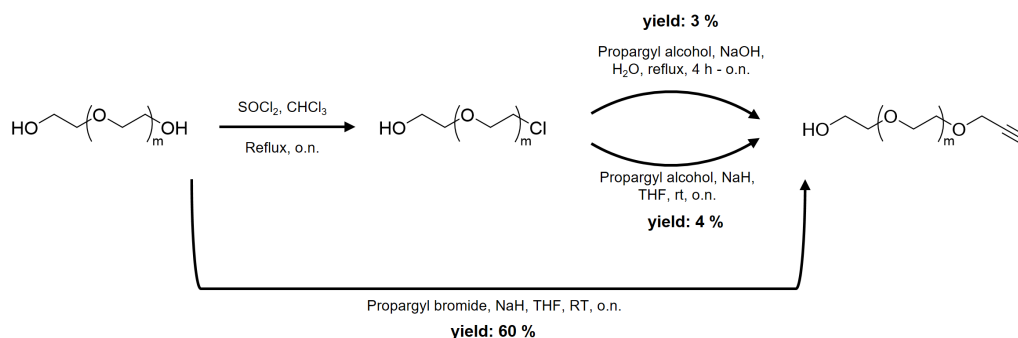
Figure S5. Synthetic route for alkyne-tagged PEG linker.
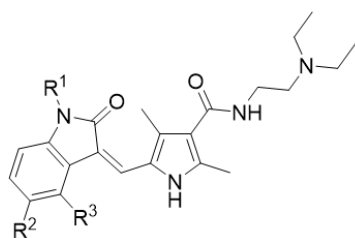
Cpd	R¹	R²	R³	Yield (%)	Inhibition (%)
Sunitinib	H	F	H	21	77
75a	H	Cl	H	52	88
75b	H	H	H	74	50
75c	H	F	F	86	49
75d	Me	H	H	65	90

Figure S6. Sunitinib derivatives and the RNase L inhibition measured in FRET-based RNA cleavage assay.

Table S1. Reagent amount screening to conjugate **40a** and **44** yielding **45a** in DMF.

PyBOP	DIPEA	Reaction condition	Conversion[a]
1 equiv.	3 equiv.	rt, o.n.	26%
1.2 equiv.	1.5 equiv.	rt, o.n.	>95%
1.5 equiv.	4 equiv.	rt, 3 h	67%
3 equiv.	6 equiv.	rt, o.n.	43%

[a]monitored by LC-MS

7. References

1.   Woolhouse, M.; Scott, F.; Hudson, Z.; Howey, R.; Chase-Topping, M., Human viruses: discovery and emergence. *Philos. Trans. R. Soc. B-Biol. Sci.* **2012,** *367* (1604), 2864-2871.

2.   Fontana, L. M.; Villamagna, A. H.; Sikka, M. K.; McGregor, J. C., Understanding viral shedding of severe acute respiratory coronavirus virus 2 (SP Rs-CoV-2): Review of current literature. *Infect. Control Hosp. Epidemiol.* **2021,** *42* (6), 659-668.

3.   Samuel, C. E., Antiviral actions of interferons. *Clin. Microbiol. Rev.* **2001,** *14* (4), 778-809.

4.   Sadler, A. J.; Williams, B. R. G., Interferon-inducible antiviral effectors. *Nat. Rev. Immunol.* **2008,** *8* (7), 559-568.

5.   Garcia-Sastre, A.; Biron, C. A., Type 1 interferons and the virus-host relationship: A lesson in detente. *Science* **2006,** *312* (5775), 879-882.

6.   Garcia, M. A.; Gil, J.; Ventoso, I.; Guerra, S.; Domingo, E.; Rivas, C.; Esteban, M., Impact of protein kinase PKR in cell biology: from antiviral to antiproliferative action. *Microbiol. Mol. Biol. Rev.* **2006,** *70* (4), 1032-1060.

7.   Samuel, C. E., ADARs: viruses and innate immunity. In *Adenosine Deaminases Acting on RNA*; **2012,** *353*, 163-195.

8.   Malathi, K.; Dong, B. H.; Gale, M.; Silverman, R. H., Small self-RNA generated by RNase L amplifies antiviral innate immunity. *Nature* **2007,** *448* (7155), 816-U9.

9.   Silverman, R. H., Viral encounters with 2 ',5 '-oligoadenylate synthetase and RNase L during the interferon antiviral response. *J. Virol.* **2007,** *81* (23), 12720-12729.

10.   Lipinski, C. A.; Lombardo, F.; Dominy, B. W.; Feeney, P. J., Experimental and computational approaches to estimate solubility and permeability in drug discovery and development settings. *Adv. Drug Del. Rev.* **2012,** *64*, 4-17.

11.   Ramirez-Moya, J.; Baker, A. R.; Slack, F. J.; Santisteban, P., ADAR1-mediated RNA editing is a novel oncogenic process in thyroid cancer and regulates miR-200 activity. *Oncogene* **2020,** *39* (18), 3738-3753.

12.   Jha, B. K.; Polyakova, I.; Kessler, P.; Dong, B. H.; Dickerman, B.; Sen, G. C.; Silverman, R. H., Inhibition of RNase L and RNA-dependent protein kinase (PKR) by sunitinib impairs antiviral innate immunity. *J. Biol. Chem.* **2011,** *286* (30), 26319-26326.

13.   Sen, G. C.; Lebleu, B.; Brown, G. E.; Kawakita, M.; Slattery, E.; Lengyel, P., Interferon, double-stranded RNA and mRNA degradation. *Nature* **1976,** *264* (5584), 370-373.

14.   Lebleu, B.; Sen, G. C.; Shaila, S.; Cabrer, B.; Lengyel, P., Interferon, double-stranded RNA, and protein phosphorylation. *Proc. Natl. Acad. Sci. U. S. A.* **1976,** *73* (9), 3107-3111.

15.   Roberts, W. K.; Hovanessian, A.; Brown, R. E.; Clemens, M. J.; Kerr, I. M., Interferon-mediated protein kinase and low-molecular-weight inhibitor of protein synthesis. *Nature* **1976,** *264* (5585), 477-480.

16.   Hovanessian, A. G.; Brown, R. E.; Kerr, I. M., Synthesis of low molecular weight

inhibitor of protein synthesis with enzyme from interferon-treated cells. *Nature* **1977,** *268* (5620), 537-540.

17. Kerr, I. M.; Brown, R. E., pppA2'p5'A2'p5'A: an inhibitor of protein synthesis synthesized with an enzyme fraction from interferon-treated cells. *Proc. Natl. Acad. Sci. U. S. A.* **1978,** *75* (1), 256-260.

18. Baglioni, C.; Minks, M. A.; Maroney, P. A., Interferon action may be mediated by activation of a nuclease by pppA2′p5′A2′p5′A. *Nature* **1978,** *273* (5664), 684-687.

19. Bisbal, C.; Silverman, R. H., Diverse functions of RNase L and implications in pathology. *Biochimie* **2007,** *89* (6-7), 789-798.

20. Silverman, R. H., A scientific journey through the 2-5A/RNase L system. *Cytokine Growth Factor Rev.* **2007,** *18* (5-6), 381-388.

21. Chakrabarti, A.; Jha, B. K.; Silverman, R. H., New insights into the role of RNase L in innate immunity. *J. Interferon Cytokine Res.* **2011,** *31* (1), 49-57.

22. Han, Y. C.; Donovan, J.; Rath, S.; Whitney, G.; Chitrakar, A.; Korennykh, A., Structure of human RNase L reveals the basis for regulated RNA decay in the IFN response. *Science* **2014,** *343* (6176), 1244-1248.

23. Huang, H.; Zeqiraj, E.; Dong, B. H.; Jha, B. K.; Duffy, N. M.; Orlicky, S.; Thevakumaran, N.; Talukdar, M.; Pillon, M. C.; Ceccarelli, D. F.; Wan, L. C. K.; Juang, Y. C.; Mao, D. Y. L.; Gaughan, C.; Brinton, M. A.; Perelygin, A. A.; Kourinov, I.; Guarne, A.; Silverman, R. H.; Sicheri, F., Dimeric Structure of Pseudokinase RNase L Bound to 2-5A Reveals a Basis for Interferon-Induced Antiviral Activity. *Mol. Cell* **2014,** *53* (2), 221-234.

24. Baglioni, C., Interferon-induced enzymatic activities and their role in the antiviral state. *Cell* **1979,** *17* (2), 255-264.

25. Kristiansen, H.; Gad, H. H.; Eskildsen-Larsen, S.; Despres, P.; Hartmann, R., The oligoadenylate synthetase family: an ancient protein family with multiple antiviral activities. *J. Interferon Cytokine Res.* **2011,** *31* (1), 41-47.

26. Diaz-Guerra, M.; Rivas, C.; Esteban, M., Full activation of RNaseL in animal cells requires binding of 2-5A within ankyrin repeats 6 to 9 of this interferon-inducible enzyme. *J. Interferon Cytokine Res.* **1999,** *19* (2), 113-119.

27. Dong, B. H.; Silverman, R. H., 2-5A-dependent RNase Molecules Dimerize during Activation by 2-5A (∗). *J. Biol. Chem.* **1995,** *270* (8), 4133-4137.

28. Drappier, M.; Michiels, T., Inhibition of the OAS/RNase L pathway by viruses. *Curr. Opin. Virol.* **2015,** *15*, 19-26.

29. Chang, H. W.; Watson, J. C.; Jacobs, B. L., The E3L gene of vaccinia virus encodes an inhibitor of the interferon-induced, double-stranded RNA-dependent protein kinase. *Proc. Natl. Acad. Sci. U. S. A.* **1992,** *89* (11), 4825-4829.

30. Beattie, E.; Denzler, K. L.; Tartaglia, J.; Perkus, M. E.; Paoletti, E.; Jacobs, B. L., Reversal of the interferon-sensitive phenotype of a vaccinia virus lacking E3L by expression of the reovirus S4 gene. *J. Virol.* **1995,** *69* (1), 499-505.

31. Rivas, C.; Gil, J.; Melkova, Z.; Esteban, M.; Diaz-Guerra, M., Vaccinia virus E3L protein

is an inhibitor of the interferon (IFN)-induced 2-5A synthetase enzyme. *Virology* **1998,** *243* (2), 406-414.

32. Xiang, Y.; Condit, R. C.; Vijaysri, S.; Jacobs, B.; Williams, B. R. G.; Silverman, R. H., Blockade of interferon induction and action by the E3L double-stranded RNA binding proteins of vaccinia virus. *J. Virol.* **2002,** *76* (10), 5251-5259.

33. Min, J. Y.; Krug, R. M., The primary function of RNA binding by the influenza A virus NS1 protein in infected cells: Inhibiting the 2 '-5 ' oligo (A) synthetase/RNase L pathway. *Proc. Natl. Acad. Sci. U. S. A.* **2006,** *103* (18), 7100-7105.

34. Engel, D. A., The influenza virus NS1 protein as a therapeutic target. *Antiviral Res.* **2013,** *99* (3), 409-416.

35. Krug, R. M., Functions of the influenza A virus NS1 protein in antiviral defense. *Curr. Opin. Virol.* **2015,** *12*, 1-6.

36. Huismans, H.; Joklik, W. K., Reovirus-coded polypeptides in infected cells: isolation of two native monomeric polypeptides with affinity for single-stranded and double-stranded RNA. *Virology* **1976,** *70* (2), 411-424.

37. Denzler, K. L.; Jacobs, B. L., Site-directed mutagenic analysis of reovirus σ3 protein binding to dsRNA. *Virology* **1994,** *204* (1), 190-199.

38. Olland, A. M.; Jane-Valbuena, J.; Schiff, L. A.; Nibert, M. L.; Harrison, S. C., Structure of the reovirus outer capsid and dsRNA-binding protein sigma 3 at 1.8 angstrom resolution. *EMBO J.* **2001,** *20* (5), 979-989.

39. Kubota, K.; Nakahara, K.; Ohtsuka, T.; Yoshida, S.; Kawaguchi, J.; Fujita, Y.; Ozeki, Y.; Hara, A.; Yoshimura, C.; Furukawa, H.; Haruyama, H.; Ichikawa, K.; Yamashita, M.; Matsuoka, T.; Iijima, Y., Identification of 2 '-phosphodiesterase, which plays a role in the 2-5A system regulated by interferon. *J. Biol. Chem.* **2004,** *279* (36), 37832-37841.

40. Silverman, R. H.; Weiss, S. R., Viral phosphodiesterases that antagonize double-stranded RNA signaling to RNase L by degrading 2-5A. *J. Interferon Cytokine Res.* **2014,** *34* (6), 455-463.

41. Zhao, L.; Jha, B. K.; Wu, A.; Elliott, R.; Ziebuhr, J.; Gorbalenya, A. E.; Silverman, R. H.; Weiss, S. R., Antagonism of the interferon-induced OAS-RNase L pathway by murine coronavirus ns2 protein is required for virus replication and liver pathology. *Cell Host Microbe* **2012,** *11* (6), 607-616.

42. Gusho, E.; Baskar, D.; Banerjee, S., New advances in our understanding of the "unique" RNase L in host pathogen interaction and immune signaling. *Cytokine* **2020,** *133*.

43. Malathi, K.; Paranjape, J. M.; Ganapathi, R.; Silverman, R. H., HPC1/RNASEL mediates apoptosis of prostate cancer cells treated with 2 ',5 '-oligoadenylates, topoisomerase I inhibitors, and tumor necrosis factor-related apoptosis-inducing ligand. *Cancer Res.* **2004,** *64* (24), 9144-9151.

44. Bisbal, C.; Martinand, C.; Silhol, M.; Lebleu, B.; Salehzada, T., Cloning and Characterization of a RNase L Inhibitor. A new component of the interferon-regulated 2-5A pathway*. *J. Biol. Chem.* **1995,** *270* (22), 13308-13317.

45. Martinand, C.; Salehzada, T.; Silhol, M.; Lebleu, B.; Bisbal, C., RNase L inhibitor (RLI)

antisense constructions block partially the down regulation of the 2-5A/RNase L pathway in encephalomyocarditis-virus-(EMCV)-infected cells. *Eur. J. Biochem.* **1998,** *254* (2), 248-255.

46. van Eyll, O.; Michiels, T., Influence of the Theiler's virus L* protein on macrophage infection, viral persistence, and neurovirulence. *J. Virol.* **2000,** *74* (19), 9071-9077.

47. Nilsen, T. W.; Maroney, P. A.; Robertson, H. D.; Baglioni, C., Heterogeneous nuclear RNA promotes synthesis of (2', 5') oligoadenylate and is cleaved by the (2', 5') oligoadenylate-activated endoribonuclease. *Mol. Cell. Biol.* **1982,** *2* (2), 154-160.

48. Cayley, P. J.; Davies, J. A.; McCullagh, K. G.; Kerr, I. M., Activation of the ppp(A2′p)$_n$A system in interferon-treated, Herpes simplex virus-infected cells and evidence for novel inhibitors of the ppp(A2′p)$_n$A-dependent RNase. *Eur. J. Biochem.* **1984,** *143* (1), 165-174.

49. Hersh, C. L.; Brown, R. E.; Roberts, W. K.; Swyryd, E. A.; Kerr, I. M.; Stark, G. R., Simian virus 40-infected, interferon-treated cells contain 2',5'-oligoadenylates which do not activate cleavage of RNA. *J. Biol. Chem.* **1984,** *259* (3), 1731-1737.

50. Han, J. Q.; Barton, D. J., Activation and evasion of the antiviral 2 '-5 ' oligoadenylate synthetase/ribonuclease L pathway by hepatitis C virus mRNA. *RNA* **2002,** *8* (4), 512-525.

51. Townsend, H. L.; Jha, B. K.; Han, J. Q.; Maluf, N. K.; Silverman, R. H.; Barton, D. J., A viral RNA competitively inhibits the antiviral endoribonuclease domain of RNase L. *RNA* **2008,** *14* (6), 1026-1036.

52. Keel, A. Y.; Jha, B. K.; Kieft, J. S., Structural architecture of an RNA that competitively inhibits RNase L. *RNA* **2012,** *18* (1), 88-99.

53. Farrell, P. J.; Sen, G. C.; Dubois, M. F.; Ratner, L.; Slattery, E.; Lengyel, P., Interferon action: two distinct pathways for inhibition of protein synthesis by double-stranded RNA. *Proc. Natl. Acad. Sci. U. S. A.* **1978,** *75* (12), 5893-5897.

54. Zilberstein, A.; Kimchi, A.; Schmidt, A.; Revel, M., Isolation of two interferon-induced translational inhibitors: a protein kinase and an oligo-isoadenylate synthetase. *Proc. Natl. Acad. Sci. U. S. A.* **1978,** *75* (10), 4734-4738.

55. Floydsmith, G.; Yoshie, O.; Lengyel, P., Interferon action. Covalent linkage of (2'-5')pppApApA(32P)pCp to (2'-5')(A)n-dependent ribonucleases in cell extracts by ultraviolet irradiation. *J. Biol. Chem.* **1982,** *257* (15), 8584-8587.

56. Silverman, R. H.; Jung, D. D.; Nolansorden, N. L.; Dieffenbach, C. W.; Kedar, V. P.; Sengupta, D. N., Purification and analysis of murine 2-5A-dependent RNase. *J. Biol. Chem.* **1988,** *263* (15), 7336-7341.

57. Zhou, A. M.; Hassel, B. A.; Silverman, R. H., Expression cloning of 2-5A-dependent RNAase: a uniquely regulated mediator of interferon action. *Cell* **1993,** *72* (5), 753-765.

58. Carroll, S. S.; Cole, J. L.; Viscount, T.; Geib, J.; Gehman, J.; Kuo, L. C., Activation of RNase L by 2',5'-oligoadenylates - Kinetic characterization. *J. Biol. Chem.* **1997,** *272* (31), 19193-19198.

59. Tanaka, N.; Nakanishi, M.; Kusakabe, Y.; Goto, Y.; Kitade, Y.; Nakamura, K. T., Structural basis for recognition of 2 ',5 '-linked oligoadenylates by human ribonuclease

L. *EMBO J.* **2004,** *23* (20), 3929-3938.

60. Rebouillat, D.; Hovanessian, A. G., The human 2 ',5 '-oligoadenylate synthetase family: Interferon-induced proteins with unique enzymatic properties. *J. Interferon Cytokine Res.* **1999,** *19* (4), 295-308.

61. Dong, B. H.; Silverman, R. H., Alternative function of a protein kinase homology domain in 2 ',5 '-oligoadenylate dependent RNase L. *Nucleic Acids Res.* **1999,** *27* (2), 439-445.

62. Andersen, J. B.; Mazan-Mamczarz, K.; Zhan, M.; Gorospe, M.; Hassel, B. A., Ribosomal protein mRNAs are primary targets of regulation in RNase-L-induced senescence. *RNA Biol.* **2009,** *6* (3), 305-315.

63. Rath, S.; Donovan, J.; Whitney, G.; Chitrakar, A.; Wang, W.; Korennykh, A., Human RNase L tunes gene expression by selectively destabilizing the microRNA-regulated transcriptome. *Proc. Natl. Acad. Sci. U. S. A.* **2015,** *112* (52), 15916-15921.

64. Cooper, D. A.; Jha, B. K.; Silverman, R. H.; Hesselberth, J. R.; Barton, D. J., Ribonuclease L and metal-ion-independent endoribonuclease cleavage sites in host and viral RNAs. *Nucleic Acids Res.* **2014,** *42* (8), 5202-5216.

65. Cooper, D. A.; Banerjee, S.; Chakrabarti, A.; Garcia-Sastre, A.; Hesselberth, J. R.; Silverman, R. H.; Barton, D. J., RNase L targets distinct sites in influenza A virus RNAs. *J. Virol.* **2015,** *89* (5), 2764-2776.

66. Hassel, B. A.; Zhou, A.; Sotomayor, C.; Maran, A.; Silverman, R. H., A dominant negative mutant of 2-5A-dependent RNase suppresses antiproliferative and antiviral effects of interferon. *EMBO J.* **1993,** *12* (8), 3297-3304.

67. Zhou, A. M.; Paranjape, J.; Brown, T. L.; Nie, H. Q.; Naik, S.; Dong, B. H.; Chang, A. S.; Trapp, B.; Fairchild, R.; Colmenares, C.; Silverman, R. H., Interferon action and apoptosis are defective in mice devoid of 2',5'-oligoadenylate-dependent RNase L. *EMBO J.* **1997,** *16* (21), 6355-6363.

68. Liang, S. L.; Quirk, D.; Zhou, A. M., RNase L: Its biological roles and regulation. *IUBMB Life* **2006,** *58* (9), 508-514.

69. Rasmussen, S. B.; Jensen, S. B.; Nielsen, C.; Quartin, E.; Kato, H.; Chen, Z. J.; Silverman, R. H.; Akira, S.; Paludan, S. R., Herpes simplex virus infection is sensed by both Toll-like receptors and retinoic acid-inducible gene-like receptors, which synergize to induce type I interferon production. *J. Gen. Virol.* **2009,** *90*, 74-78.

70. Li, G. Q.; Xiang, Y.; Sabapathy, K.; Silverman, R. H., An apoptotic signaling pathway in the interferon antiviral response mediated by RNase L and c-Jun NH2-terminal kinase. *J. Biol. Chem.* **2004,** *279* (2), 1123-1131.

71. Silverman, R. H., Implications for RNase L in prostate cancer biology. *Biochemistry* **2003,** *42* (7), 1805-1812.

72. Chakrabarti, A.; Banerjee, S.; Franchi, L.; Loo, Y. M.; Gale, M.; Nunez, G.; Silverman, R. H., RNase L activates the NLRP3 inflammasome during viral infections. *Cell Host Microbe* **2015,** *17* (4), 466-477.

73. Campbell, I. L.; Kay, T. W. H.; Oxbrow, L.; Harrison, L. C., Essential role for interferon-gamma and interleukin-6 in autoimmune insulin-dependent diabetes in NOD/Wehi mice.

J. Clin. Invest. **1991,** *87* (2), 739-742.

74. Huang, X. J.; Hultgren, B.; Dybdal, N.; Stewart, T. A., Islet expression of interferon-α precedes diabetes in both the BB rat and streptozotocin-treated mice. *Immunity* **1994,** *1* (6), 469-478.

75. Zeng, C.; Yi, X.; Zipris, D.; Liu, H. L.; Zhang, L.; Zheng, Q. Y.; Malathi, K.; Jin, G.; Zhou, A. M., RNase L contributes to experimentally induced type 1 diabetes onset in mice. *J. Endocrinol.* **2014,** *223* (3), 277-287.

76. Wang, L. M.; Zhou, A. M.; Vasavada, S.; Dong, B. H.; Nie, H. Q.; Church, J. M.; Williams, B. R. G.; Banerjee, S.; Silverman, R. H., Elevated levels of 2',5'-linked oligoadenylate-dependent ribonuclease L occur as an early event in colorectal tumorigenesis. *Clin. Cancer Res.* **1995,** *1* (11), 1421-1428.

77. Doetsch, P.; Wu, J. M.; Sawada, Y.; Suhadolnik, R. J., Synthesis and characterization of (2′-5′)ppp3′dA(p3′dA)$_n$, an analogue of (2′-5′)pppA(pA)$_n$. *Nature* **1981,** *291* (5813), 355-358.

78. Eppstein, D. A.; Vanderpas, M. A.; Schryver, B. B.; Sawai, H.; Lesiak, K.; Imai, J.; Torrence, P. F., Cordycepin analogs of ppp5'A2 'p5'A2 'p5'A (2-5A) inhibit protein synthesis through activation of the 2-5A-dependent endonuclease. *J. Biol. Chem.* **1985,** *260* (6), 3666-3671.

79. Torrence, P. F.; Brozda, D.; Alster, D.; Charubala, R.; Pfleiderer, W., Only one 3'-hydroxyl group of ppp5'A2'p5'A2'p5'A (2-5A) is required for activation of the 2-5A-dependent endonuclease. *J. Biol. Chem.* **1988,** *263* (3), 1131-1139.

80. Kovacs, T.; Pabuccuoglu, A.; Lesiak, K.; Torrence, P. F., Fluorodeoxy Sugar Analogues of 2′, 5′-Oligoadenylates as Probes of Hydrogen Bonding in Enzymes of the 2-5A System. *Bioorg. Chem.* **1993,** *21* (2), 192-208.

81. Ueno, Y.; Ishihara, S.; Ito, Y.; Kitade, Y., Synthesis of 2 ',5 '-oligoadenylate analogs containing an adenine acyclonucleoside and their ability to activate human RNase L. *Bioorg. Med. Chem. Lett.* **2004,** *14* (17), 4431-4434.

82. Sawai, H.; Lesiak, K.; Imai, J.; Torrence, P. F., Replacement of the ribofuranose oxygen of 2-5A derivatives by methylene: synthesis of an aristeromycin analog of 2-5A core 5'-monophosphate (5'-O-phosphoryladenylyl)(2'-5') adenylyl (2'-5') adenosine 5'-monophosphate. *J. Med. Chem.* **1985,** *28* (9), 1376-1380.

83. Kariko, K.; Li, S. W.; Sobol, R. W.; Suhadolnik, R. J.; Charubala, R.; Pfleiderer, W., Phosphorothioate analogs of 2', 5'-oligoadenylate. Activation of 2', 5'-oligoadenylate-dependent endoribonuclease by 2', 5'-phosphorothioate cores and 5'-monophosphates. *Biochemistry* **1987,** *26* (22), 7136-7142.

84. Kariko, K.; Sobol, R. W.; Suhadolnik, L.; Li, S. W.; Reichenbach, N. L.; Suhadolnik, R. J.; Charubala, R.; Pfleiderer, W., Phosphorothioate analogs of 2', 5'-oligoadenylate. Activation of 2', 5'-oligoadenylate-dependent endoribonuclease by 2', 5'-phosphorothioate cores and 5'-monophosphates. *Biochemistry* **1987,** *26* (22), 7127-7135.

85. Beigelman, L.; Matulicadamic, J.; Haeberli, P.; Usman, N.; Dong, B. H.; Silverman, R. H.; Khamnei, S.; Torrence, P. F., Synthesis and biological activities of a

phosphorodithioate analog of 2′, 5′-oligoadenylate. *Nucleic Acids Res.* **1995,** *23* (19), 3989-3994.

86. Pav, O.; Protivinska, E.; Pressova, M.; Collinsova, M.; Jiracek, J.; Snasel, J.; Masojidkova, M.; Budesinsky, M.; Rosenberg, I., Activation of murine RNase L by isopolar 2 '-phosphonate analogues of 2 ',5 ' oligoadenylates. *J. Med. Chem.* **2006,** *49* (13), 3955-3962.

87. Lesiak, K.; Torrence, P. F., Synthesis and biological activities of oligo (8-bromoadenylates) as analogs of 5'-O-triphosphoadenylyl (2'-5') adenylyl (2'-5') adenosine. *J. Med. Chem.* **1986,** *29* (6), 1015-1022.

88. Kitade, Y.; Nakata, Y.; Hirota, K.; Maki, Y.; Pabuccuoglu, A.; Torrence, P. F., 8-Methyladenosine-substituted analogs of 2-5A: synthesis and properties. *Nucleic Acids Res.* **1991,** *19* (15), 4103-4108.

89. Torrence, P. F.; Brozda, D.; Alster, D. K.; Pabuccuoglu, A.; Lesiak, K., A new and potent 2-5A analogue which does not require a 5′-polyphosphate to activate mouse L-cell RNase L. *Antiviral Res.* **1992,** *18* (3-4), 275-289.

90. Kitade, Y.; Wakana, M.; Terai, S.; Tsuboi, T.; Nakanishi, M.; Yatome, C.; Dong, B. H.; Silverman, R. H.; Torrence, P. F., 2-bromoadenosine-substituted 2 ',5 '-oligoadenylates modulate binding and activation abilities of human recombinant RNase 1. *Nucleosides Nucleotides* **1998,** *17* (12), 2323-2333.

91. Kitade, Y.; Wakana, M.; Tsuboi, T.; Yatome, C.; Bayly, S. F.; Player, M. R.; Torrence, P. F., 2-methyladenosine-substituted 2 ',5 '-oligoadenylates: Conformations, 2-5A binding and catalytic activities with human ribonuclease L. *Bioorg. Med. Chem. Lett.* **2000,** *10* (4), 329-331.

92. Kanou, M.; Ohomori, H.; Takaku, H.; Yokoyama, S.; Kawai, G.; Suhadolnik, R. J.; Sobol, R., Chemical synthesis and biological activities of analogues of 2', 5'-oligoadenylates containing 8-substituted adenosine derivatives. *Nucleic Acids Res.* **1990,** *18* (15), 4439-4446.

93. Kanou, M.; Ohomori, H.; Nagai, K.; Yokoyama, S.; Suhadolnik, R. J.; Sobol, R.; Takaku, H., Purine 8-substitution modulates the ribonuclease L binding and activation abilities of 2′, 5′-oligoadenylates. *Biochem. Biophys. Res. Commun.* **1991,** *176* (2), 769-774.

94. Nagai, K.; Kanbara, K.; Nakashima, H.; Yamamoto, N.; Torrence, P. F.; Suhadolnik, R. J.; Takaku, H., Characterization and biological activity of 8-substituted analogues of 2′, 5′-oligoadenylates. *Biochim. Biophys. Acta* **1993,** *1156* (3), 321-326.

95. Sawai, H.; Hirano, A.; Mori, H.; Shinozuka, K.; Dong, B. H.; Silverman, R. H., Synthesis, characterization, and biological properties of 8-azido- and 8-amino-substituted 2 ',5 '-oligoadenylates. *J. Med. Chem.* **2003,** *46* (23), 4926-4932.

96. Player, M. R.; Kalinichenko, E. N.; Podkopaeva, T. L.; Mikhailopulo, I. A.; Seela, F.; Torrence, P. F., Dissection of the roles of adenine ring nitrogen (N-1) and exocyclic amino (N-6) moieties in the interaction of 2-5A with RNase L. *Biochem. Biophys. Res. Commun.* **1998,** *245* (2), 430-434.

97. Kalinichenko, E. N.; Podkopaeva, T. L.; Budko, E. V.; Seela, F.; Dong, B. H.; Silverman,

R.; Vepsalainen, J.; Torrence, P. F.; Mikhailopulo, I. A., 3-deazaadenosine analogues of p5´A2´p5´A2´p5´A: synthesis, stereochemistry, and the roles of adenine ring nitrogen-3 in the interaction with RNase L. *Biorg. Med. Chem.* **2004,** *12* (13), 3637-3647.

98. Jamoulle, J. C.; Imai, J.; Lesiak, K.; Torrence, P. F., Synthesis and biological activity of tubercidin analogs of ppp5'A2'p(5'A2'p)$_n$5'A. *Biochemistry* **1984,** *23* (13), 3063-3069.

99. Imai, J.; Lesiak, K.; Torrence, P. F., Respective role of each of the purine N-6 amino groups of 5'-O-triphosphoryladenylyl(2'-5')adenylyl(2-5')adenosine in binding to and activation of RNase L. *J. Biol. Chem.* **1985,** *260* (3), 1390-1393.

100. Kitade, Y.; Alster, D. K.; Pabuccuoglu, A.; Torrence, P. F., Uridine analogs of 2′, 5′-oligoadenylates: on the biological role of the middle base of 2-5A trimer. *Bioorg. Chem.* **1991,** *19* (3), 283-299.

101. Kitamura, Y.; Kito, S.; Nakashima, R.; Tanaka, K.; Nagaoka, K.; Kitade, Y., Doxifluridine-conjugated 2-5A analog shows strong RNase L activation ability and tumor suppressive effect. *Biorg. Med. Chem.* **2016,** *24* (16), 3870-3874.

102. Verheijen, J. C.; van der Marel, G. A.; van Boom, J. H.; Bayly, S. F.; Player, M. R.; Torrence, P. F., 2 ',5 '-oligoadenylate-peptide nucleic acids (2-5A-PNAs) activate RNase L. *Biorg. Med. Chem.* **1999,** *7* (3), 449-455.

103. Costales, M. G.; Matsumoto, Y.; Velagapudi, S. P.; Disney, M. D., Small molecule targeted recruitment of a nuclease to RNA. *J. Am. Chem. Soc.* **2018,** *140* (22), 6741-6744.

104. Thakur, C. S.; Jha, B. K.; Dong, B. H.; Das Gupta, J.; Silverman, K. M.; Mao, H. X.; Sawai, H.; Nakamura, A. O.; Banerjee, A. K.; Gudkov, A.; Silverman, R. H., Small-molecule activators of RNase L with broad-spectrum antiviral activity. *Proc. Natl. Acad. Sci. U. S. A.* **2007,** *104* (23), 9585-9590.

105. Costales, M. G.; Aikawa, H.; Li, Y.; Childs-Disney, J. L.; Abegg, D.; Hoch, D. G.; Velagapudi, S. P.; Nakai, Y.; Khan, T.; Wang, K. W.; Yildirim, I.; Adibekian, A.; Wang, E. T.; Disney, M. D., Small-molecule targeted recruitment of a nuclease to cleave an oncogenic RNA in a mouse model of metastatic cancer. *Proc. Natl. Acad. Sci. U. S. A.* **2020,** *117* (5), 2406-2411.

106. Meyer, S. M.; Tanaka, T.; Zanon, P. R. A.; Baisden, J. T.; Abegg, D.; Yang, X. Y.; Akahori, Y.; Alshakarchi, Z.; Cameron, M. D.; Adibekian, A.; Disney, M. D., DNA-encoded library screening to inform design of a ribonuclease targeting chimera (RiboTAC). *J. Am. Chem. Soc.* **2022,** *144* (46), 21096-21102.

107. Tang, J. L.; Wang, Y. J.; Zhou, H.; Ye, Y. X.; Talukdar, M.; Fu, Z. Y.; Liu, Z. H.; Li, J. H.; Neculai, D.; Gao, J. L.; Huang, H., Sunitinib inhibits RNase L by destabilizing its active dimer conformation. *Biochem. J.* **2020,** *477* (17), 3387-3399.

108. Daou, S.; Talukdar, M.; Tang, J. L.; Dong, B. H.; Banerjee, S.; Li, Y. Z.; Duffy, N. M.; Ogunjimi, A. A.; Gaughan, C.; Jha, B. K.; Gish, G.; Tavernier, N.; Mao, D.; Weiss, S. R.; Huang, H.; Silverman, R. H.; Sicheri, F., A phenolic small molecule inhibitor of RNase L prevents cell death from ADAR1 deficiency. *Proc. Natl. Acad. Sci. U. S. A.* **2020,** *117* (40), 24802-24812.

109. Tang, J. L.; Dong, B. H.; Liu, M.; Liu, S. Y.; Niu, X. G.; Gaughan, C.; Asthana, A.; Zhou,

H.; Xu, Z. S.; Zhang, G. L.; Silverman, R. H.; Huang, H., Identification of small molecule inhibitors of RNase L by fragment-based drug discovery. *J. Med. Chem.* **2022,** *65* (2), 1445-1457.

110. Sun, L.; Liang, C.; Shirazian, S.; Zhou, Y.; Miller, T.; Cui, J.; Fukuda, J. Y.; Chu, J. Y.; Nematalla, A.; Wang, X. Y.; Chen, H.; Sistla, A.; Luu, T. C.; Tang, F.; Wei, J.; Tang, C., Discovery of 5- 5-Fluoro-2-oxo-1,2-dihydroindol-(3Z)-ylidenemethyl -2,4-dimethyl-1H-p yrrole-3-carboxylic acid (2-diethylaminoethyl)amide, a novel tyrosine kinase inhibitor targeting vascular endothelial and platelet-derived growth factor receptor tyrosine kinase. *J. Med. Chem.* **2003,** *46* (7), 1116-1119.

111. Pietras, K.; Sjoblom, T.; Rubin, K.; Heldin, C. H.; Ostman, A., PDGF receptors as cancer drug targets. *Cancer Cell* **2003,** *3* (5), 439-443.

112. Mendel, D. B.; Laird, A. D.; Xin, X. H.; Louie, S. G.; Christensen, J. G.; Li, G. M.; Schreck, R. E.; Abrams, T. J.; Ngai, T. J.; Lee, L. B.; Murray, L. J.; Carver, J.; Chan, E.; Moss, K. G.; Haznedar, J. O.; Sukbuntherng, J.; Blake, R. A.; Sun, L.; Tang, C.; Miller, T.; Shirazian, S.; McMahon, G.; Cherrington, J. M., In vivo antitumor activity of SU11248, a novel tyrosine kinase inhibitor targeting vascular endothelial growth factor and platelet-derived growth factor receptors: Determination of a pharmacokinetic/pharmacodynamic relationship. *Clin. Cancer Res.* **2003,** *9* (1), 327-337.

113. Alfei, S.; Turrini, F.; Catena, S.; Zunin, P.; Grilli, M.; Pittaluga, A. M.; Boggia, R., Ellagic acid a multi-target bioactive compound for drug discovery in CNS? A narrative review. *Eur. J. Med. Chem.* **2019,** *183*.

114. Song, X. M. T.; Tan, L.; Wang, M.; Ren, C. X.; Guo, C. J.; Yang, B.; Ren, Y. L.; Cao, Z. X.; Li, Y. Z.; Pei, J., Myricetin: A review of the most recent research. *Biomed. Pharmacother.* **2021,** *134*.

115. Hwang, J. M.; Borgelt, L.; Wu, P., Multicomponent petasis reaction for the synthesis of functionalized 2-aminothiophenes and thienodiazepines. *ACS Comb. Sci.* **2020,** *22* (10), 495-499.

116. Callaghan, J. T.; Bergstrom, R. F.; Ptak, L. R.; Beasley, C. M., Olanzapine - Pharmacokinetic and pharmacodynamic profile. *Clin. Pharmacokinet.* **1999,** *37* (3), 177-193.

117. Filippakopoulos, P.; Qi, J.; Picaud, S.; Shen, Y.; Smith, W. B.; Fedorov, O.; Morse, E. M.; Keates, T.; Hickman, T. T.; Felletar, I.; Philpott, M.; Munro, S.; McKeown, M. R.; Wang, Y. C.; Christie, A. L.; West, N.; Cameron, M. J.; Schwartz, B.; Heightman, T. D.; La Thangue, N.; French, C. A.; Wiest, O.; Kung, A. L.; Knapp, S.; Bradner, J. E., Selective inhibition of BET bromodomains. *Nature* **2010,** *468* (7327), 1067-1073.

118. Wang, K.; Kim, D. B.; Domling, A., Cyanoacetamide MCR (III): Three-component Gewald reactions revisited. *J. Comb. Chem.* **2010,** *12* (1), 111-118.

119. Domling, A.; Wang, W.; Wang, K., Chemistry and biology of multicomponent reactions. *Chem. Rev.* **2012,** *112* (6), 3083-3135.

120. Wu, P.; Givskov, M.; Nielsen, T. E., Reactivity and synthetic applications of multicomponent Petasis reactions. *Chem. Rev.* **2019,** *119* (20), 11245-11290.

121. Candeias, N. R.; Montalbano, F.; Cal, P.; Gois, P. M. P., Boronic acids and esters in the Petasis-borono Mannich multicomponent reaction. *Chem. Rev.* **2010,** *110* (10), 6169-6193.

122. Ricardo, M. G.; Llanes, D.; Wessjohann, L. A.; Rivera, D. G., Introducing the petasis reaction for late-stage multicomponent diversification, labeling, and stapling of peptides. *Angew. Chem.-Int. Edit.* **2019,** *58* (9), 2700-2704.

123. Potowski, M.; Esken, R.; Brunschweiger, A., Translation of the copper/bipyridine-promoted Petasis reaction to solid phase-coupled DNA for encoded library synthesis. *Biorg. Med. Chem.* **2020,** *28* (9).

124. Hwang, J.; Qiu, X. Q.; Borgelt, L.; Haacke, N.; Kanis, L.; Petroulia, S.; Gasper, R.; Schiller, D.; Lampe, P.; Sievers, S.; Imig, J.; Wu, P., Synthesis and evaluation of RNase L-binding 2-aminothiophenes as anticancer agents. *Biorg. Med. Chem.* **2022,** *58*.

125. Faull, A. W.; Hull, R., Some reactions of ethyl 2-anilino-4-oxo-4, 5-dihydrothiophen-3-carboxylate. *J. Chem. Soc.-Perkin Trans. 1* **1981,** (4), 1078-1082.

126. Li Petri, G.; Spano, V.; Spatola, R.; Holl, R.; Raimondi, M. V.; Barraja, P.; Montalbano, A., Bioactive pyrrole-based compounds with target selectivity. *Eur. J. Med. Chem.* **2020,** *208*.

127. Bhardwaj, V.; Gumber, D.; Abbot, V.; Dhiman, S.; Sharma, P., Pyrrole: a resourceful small molecule in key medicinal hetero-aromatics. *RSC Adv.* **2015,** *5* (20), 15233-15266.

128. Carpten, J.; Nupponen, N.; Isaacs, S.; Sood, R.; Robbins, C.; Xu, J.; Faruque, M.; Moses, T.; Ewing, C.; Gillanders, E.; Hu, P.; Buinovszky, P.; Makalowska, I.; Baffoe-Bonnie, A.; Faith, D.; Smith, J.; Stephan, D.; Wiley, K.; Brownstein, M.; Gildea, D.; Kelly, B.; Jenkins, R.; Hostetter, G.; Matikainen, M.; Schleutker, J.; Klinger, K.; Connors, T.; Xiang, Y.; Wang, Z.; De Marzo, A.; Papadopoulos, N.; Kallioniemi, O. P.; Burk, R.; Meyers, D.; Gronberg, H.; Meltzer, P.; Silverman, R.; Bailey-Wilson, J.; Walsh, P.; Isaacs, W.; Trent, J., Germline mutations in the ribonuclease L gene in families showing linkage with HPC1. *Nature Genet.* **2002,** *30* (2), 181-184.

129. Xiang, Y.; Wang, Z. F.; Murakami, J.; Plummer, S.; Klein, E. A.; Carpten, J. D.; Trent, J. M.; Isaacs, W. B.; Casey, G.; Silverman, R. H., Effects of RNase L mutations associated with prostate cancer on apoptosis induced by 2 ',5 '-oligoadenylates. *Cancer Res.* **2003,** *63* (20), 6795-6801.

130. Malathi, K.; Paranjape, J. M.; Ganapathi, R.; Silverman, R. H., HPC1/RNASEL mediates apoptosis of prostate cancer cells treated with 2 ',5 '-oligoadenylates, topoisomerase I inhibitors, and tumor necrosis factor-related apoptosis-inducing ligand. *Cancer Res.* **2004,** *64* (24), 9144-9151.

131. Ferri, E.; Le Thomas, A.; Wallweber, H. A.; Day, E. S.; Walters, B. T.; Kaufman, S. E.; Braun, M. G.; Clark, K. R.; Beresini, M. H.; Mortara, K.; Chen, Y. C. A.; Canter, B.; Phung, W.; Liu, P. S.; Lammens, A.; Ashkenazi, A.; Rudolph, J.; Wang, W. R., Activation of the IRE1 RNase through remodeling of the kinase front pocket by ATP-competitive ligands. *Nat. Commun.* **2020,** *11* (1).

132. Gerry, C. J.; Schreiber, S. L., Unifying principles of bifunctional, proximity-inducing

small molecules. *Nat. Chem. Biol.* **2020,** *16* (4), 369-378.

133. Corson, T. W.; Aberle, N.; Crews, C. M., Design and applications of bifunctional small molecules: why two heads are better than one. *ACS Chem. Biol.* **2008,** *3* (11), 677-692.

134. Lee, S.; Kim, J.; Jo, J.; Chang, J. W.; Sim, J.; Yun, H., Recent advances in development of hetero-bivalent kinase inhibitors. *Eur. J. Med. Chem.* **2021,** *216*.

135. Henning, N. J.; Boike, L.; Spradlin, J. N.; Ward, C. C.; Liu, G.; Zhang, E.; Belcher, B. P.; Brittain, S. M.; Hesse, M. J.; Dovala, D.; McGregor, L. M.; Misiolek, R. V.; Plasschaert, L. W.; Rowlands, D. J.; Wang, F.; Frank, A. O.; Fuller, D.; Estes, A. R.; Randal, K. L.; Panidapu, A.; McKenna, J. M.; Tallarico, J. A.; Schirle, M.; Nomura, D. K., Deubiquitinase-targeting chimeras for targeted protein stabilization. *Nat. Chem. Biol.* **2022,** *18* (4), 412-+.

136. Conway, S. J., Bifunctional molecules beyond PROTACs. *J. Med. Chem.* **2020,** *63* (6), 2802-2806.

137. Maniaci, C.; Ciulli, A., Bifunctional chemical probes inducing protein–protein interactions. *Curr. Opin. Chem. Biol.* **2019,** *52*, 145-156.

138. Mullard, A., Targeted protein degraders crowd into the clinic. *Nat. Rev. Drug Discov.* **2021,** *20* (4), 247-250.

139. Kopytek, S. J.; Standaert, R. F.; Dyer, J. C. D.; Hu, J. C., Chemically induced dimerization of dihydrofolate reductase by a homobifunctional dimer of methotrexate. *Chem. Biol.* **2000,** *7* (5), 313-321.

140. Sartori, A.; Portioli, E.; Battistini, L.; Calorini, L.; Pupi, A.; Vacondio, F.; Arosio, D.; Bianchini, F.; Zanardi, F., Synthesis of novel c (AmpRGD)–sunitinib dual conjugates as molecular tools targeting the αvβ3 integrin/VEGFR2 couple and impairing tumor-associated angiogenesis. *J. Med. Chem.* **2017,** *60* (1), 248-262.

141. Bischoff, E.; Tranthi, T. A.; Decker, K. F. A., Nucleotide pyrophosphatase of rat liver: a comparative study on the enzymes solubilized and purified from plasma membrane and endoplasmic reticulum. *Eur. J. Biochem.* **1975,** *51* (2), 353-361.

142. Onyedibe, K. I.; Wang, M. D.; Sintim, H. O., ENPP1, an old enzyme with new functions, and small molecule inhibitors—a STING in the tale of ENPP1. *Molecules* **2019,** *24* (22).

143. Carozza, J. A.; Brown, J. A.; Bohnert, V.; Fernandez, D.; AlSaif, Y.; Mardjuki, R. E.; Smith, M.; Li, L. Y., Structure-aided development of small-molecule inhibitors of ENPP1, the extracellular phosphodiesterase of the immunotransmitter cGAMP. *Cell Chem. Biol.* **2020,** *27* (11), 1347-1358.

144. Pradere, U.; Garnier-Amblard, E. C.; Coats, S. J.; Amblard, F.; Schinazi, R. F., Synthesis of nucleoside phosphate and phosphonate prodrugs. *Chem. Rev.* **2014,** *114* (18), 9154-9218.

145. Heidel, K. M.; Dowd, C. S., Phosphonate prodrugs: an overview and recent advances. *Future Med. Chem.* **2019,** *11* (13), 1625-1643.

146. Nemec, V.; Schwalm, M. P.; Muller, S.; Knapp, S., PROTAC degraders as chemical probes for studying target biology and target validation. *Chem. Soc. Rev.* **2022,** *51* (18), 7971-7993.

147. Yamamoto, J.; Ito, T.; Yamaguchi, Y.; Handa, H., Discovery of CRBN as a target of thalidomide: a breakthrough for progress in the development of protein degraders. *Chem. Soc. Rev.* **2022,** *51* (15), 6234-6250.

148. Guo, W. H.; Qi, X. L.; Yu, X.; Liu, Y.; Chung, C. I.; Bai, F.; Lin, X. C.; Lu, D.; Wang, L. F.; Chen, J. W.; Su, L. H.; Nomie, K. J.; Li, F.; Wang, M. C.; Shu, X. K.; Onuchic, J. N.; Woyach, J. A.; Wang, M. L.; Wang, J., Enhancing intracellular accumulation and target engagement of PROTACs with reversible covalent chemistry. *Nat. Commun.* **2020,** *11* (1).

149. Bekes, M.; Langley, D. R.; Crews, C. M., PROTAC targeted protein degraders: the past is prologue. *Nat. Rev. Drug Discov.* **2022,** *21* (3), 181-200.

150. Bricelj, A.; Steinebach, C.; Kuchta, R.; Gutschow, M.; Sosic, I., E3 ligase ligands in successful PROTACs: an overview of syntheses and linker attachment points. *Front. Chem.* **2021,** *9*.

151. Kuhnert, M.; Koster, H.; Bartholomaus, R.; Park, A. Y.; Shahim, A.; Heine, A.; Steuber, H.; Klebe, G.; Diederich, W. E., Tracing binding modes in hit-to-lead optimization: chameleon-like poses of aspartic protease inhibitors. *Angew. Chem.-Int. Edit.* **2015,** *54* (9), 2849-2853.

152. Saravanan, J.; Mohan, S.; Roy, J. J., Synthesis of some 3-substituted amino-4,5-tetramethylene thieno 2,3-d 1,2,3 -triazin-4(3(H)under-bar)-ones as potential antimicrobial agents. *Eur. J. Med. Chem.* **2010,** *45* (9), 4365-4369.

153. Ouyang, L.; Zhang, L.; Liu, J.; Fu, L. L.; Yao, D. H.; Zhao, Y. Q.; Zhang, S. Y.; Wang, G.; He, G.; Liu, B., Discovery of a small-molecule bromodomain-containing protein 4 (BRD4) inhibitor that induces AMP-activated protein kinase-modulated autophagy-associated cell death in breast cancer. *J. Med. Chem.* **2017,** *60* (24), 9990-10012.

154. Masaoka, T.; Chung, S.; Caboni, P.; Rausch, J. W.; Wilson, J. A.; Taskent-Sezgin, H.; Beutler, J. A.; Tocco, G.; Le Grice, S. F. J., Exploiting drug-resistant enzymes as tools to identify thienopyrimidinone inhibitors of human immunodeficiency virus reverse transcriptase-associated ribonuclease H. *J. Med. Chem.* **2013,** *56* (13), 5436-5445.

155. De Vita, E.; Schuler, P.; Lovell, S.; Lohbeck, J.; Kullmann, S.; Rabinovich, E.; Sananes, A.; Hessling, B.; Hamon, V.; Papo, N.; Hess, J.; Tate, E. W.; Gunkel, N.; Miller, A. K., Depsipeptides featuring a neutral P1 are potent inhibitors of kallikrein-related peptidase 6 with on-target cellular activity. *J. Med. Chem.* **2018,** *61* (19), 8859-8874.

156. Rahm, F.; Viklund, J.; Tresaugues, L.; Ellermann, M.; Giese, A.; Ericsson, U.; Forsblom, R.; Ginman, T.; Gunther, J.; Hallberg, K.; Lindstrom, J.; Persson, L. B.; Silvander, C.; Talagas, A.; Diaz-Saez, L.; Fedorov, O.; Huber, K. V. M.; Panagakou, I.; Siejka, P.; Gorjanacz, M.; Bauser, M.; Andersson, M., Creation of a novel class of potent and selective MutT homologue 1 (MTH1) inhibitors using fragment-based screening and structure-based drug design. *J. Med. Chem.* **2018,** *61* (6), 2533-2551.

157. Dethe, D. H.; Erande, R. D.; Ranjan, A., Biomimetic total syntheses of flinderoles B and C. *J. Am. Chem. Soc.* **2011,** *133* (9), 2864-2867.

158. Xu, M. H.; Zhu, J. S.; Diao, Y. Y.; Zhou, H. C.; Ren, X. L.; Sun, D. H.; Huang, J.; Han, D. M.; Zhao, Z. J.; Zhu, L. L.; Xu, Y. F.; Li, H. L., Novel selective and potent inhibitors

of malaria parasite dihydroorotate dehydrogenase: discovery and optimization of dihydrothiophenone derivatives. *J. Med. Chem.* **2013,** *56* (20), 7911-7924.

159. Irie, T.; Asami, T.; Sawa, A.; Uno, Y.; Hanada, M.; Taniyama, C.; Funakoshi, Y.; Masai, H.; Sawa, M., Discovery of novel furanone derivatives as potent Cdc7 kinase inhibitors. *Eur. J. Med. Chem.* **2017,** *130*, 406-418.

160. Zhang, B.; Braun, B. M.; Skelly, J. D.; Ayers, D. C.; Song, J., Significant Suppression of Staphylococcus aureus Colonization on Intramedullary Ti6Al4V Implants Surface-Grafted with Vancomycin-Bearing Polymer Brushes. *ACS Appl. Mater. Interfaces* **2019,** *11* (32), 28641-28647.

161. Sato, R.; Kozuka, J.; Ueda, M.; Mishima, R.; Kumagai, Y.; Yoshimura, A.; Minoshima, M.; Mizukami, S.; Kikuchi, K., Intracellular protein-labeling probes for multicolor single-molecule imaging of immune receptor–adaptor molecular dynamics. *J. Am. Chem. Soc.* **2017,** *139* (48), 17397-17404.

162. Ma, L.; Tu, C. L.; Le, P.; Chitoor, S.; Lim, S. J.; Zahid, M. U.; Teng, K. W.; Ge, P. H.; Selvin, P. R.; Smith, A. M., Multidentate polymer coatings for compact and homogeneous quantum dots with efficient bioconjugation. *J. Am. Chem. Soc.* **2016,** *138* (10), 3382-3394.

163. Assali, M.; Cid, J. J.; Pernia-Leal, M.; Munoz-Bravo, M.; Fernandez, I.; Wellinger, R. E.; Khiar, N., Glyconanosomes: Disk-shaped nanomaterials for the water solubilization and delivery of hydrophobic molecules. *ACS Nano* **2013,** *7* (3), 2145-2153.

164. Jezowska, M.; Honcharenko, D.; Ghidini, A.; Stromberg, R.; Honcharenko, M., Enabling multiple conjugation to oligonucleotides using "click cycles". *Bioconjugate Chemistry* **2016,** *27* (11), 2620-2628.

165. Wurz, R. P.; Dellamaggiore, K.; Dou, H.; Javier, N.; Lo, M. C.; McCarter, J. D.; Mohl, D.; Sastri, C.; Lipford, J. R.; Ceet, V. J., A "click chemistry platform" for the rapid synthesis of bispecific molecules for inducing protein degradation. *J. Med. Chem.* **2018,** *61* (2), 453-461.

166. Komiya, C.; Aihara, K.; Morishita, K.; Ding, H.; Inokuma, T.; Shigenaga, A.; Otaka, A., Development of an intein-inspired amide cleavage chemical device. *J. Org. Chem.* **2016,** *81* (2), 699-707.

167. Matheson, C. J.; Casalvieri, K. A.; Backos, D. S.; Minhajuddin, M.; Jordan, C. T.; Reigan, P., Substituted oxindol-3-ylidenes as AMP-activated protein kinase (AMPK) inhibitors. *Eur. J. Med. Chem.* **2020,** *197*.

168. Wangsahardja, J.; Marcolin, G. M.; Lizarme, Y.; Morris, J. C.; Hunter, L., Concise synthesis of dictyoquinazol A via a dimerisation–cyclocondensation sequence. *Synlett* **2016,** *27* (8), 1237-1240.

169. Kraege, S.; Stefan, K.; Juvale, K.; Ross, T.; Willmes, T.; Wiese, M., The combination of quinazoline and chalcone moieties leads to novel potent heterodimeric modulators of breast cancer resistance protein (BCRP/ABCG2). *Eur. J. Med. Chem.* **2016,** *117*, 212-229.

170. Li, Z.; Huang, Y. Y.; Wu, Y. N.; Chen, J. Y.; Wu, D. Y.; Zhan, C. G.; Luo, H. B., Absolute binding free energy calculation and design of a subnanomolar inhibitor of

phosphodiesterase-10. *J. Med. Chem.* **2019,** *62* (4), 2099-2111.

171. Forcellini, E.; Boutin, S.; Lefebvre, C. A.; Shayhidin, E. E.; Boulanger, M. C.; Rheaume, G.; Barbeau, X.; Lague, P.; Mathieu, P.; Paquin, J. F., Synthesis and biological evaluation of novel quinazoline-4-piperidinesulfamide derivatives as inhibitors of NPP1. *Eur. J. Med. Chem.* **2018,** *147*, 130-149.

172. Cheng, J. F.; Li, Y.; Wang, X.; Dong, G. Q.; Sheng, C. Q., Discovery of novel PDEδ degraders for the treatment of KRAS mutant colorectal cancer. *J. Med. Chem.* **2020,** *63* (14), 7892-7905.

173. Powell, C. E.; Gao, Y.; Tan, L.; Donovan, K. A.; Nowak, R. P.; Loehr, A.; Bahcall, M.; Fischer, E. S.; Janne, P. A.; George, R. E.; Gray, N. S., Depsipeptides featuring a neutral P1 are potent inhibitors of kallikrein-related peptidase 6 with on-target cellular activity. *J. Med. Chem.* **2018,** *61* (9), 4249-4255.

174. Xiao, Z. P.; Song, S. S.; Chen, D.; van Merkerk, R.; van der Wouden, P. E.; Cool, R. H.; Quax, W. J.; Poelarends, G. J.; Melgert, B. N.; Dekker, F. J., Proteolysis targeting chimera (PROTAC) for macrophage migration inhibitory factor (MIF) has anti-proliferative activity in lung cancer cells. *Angew. Chem.-Int. Edit.* **2021,** *60* (32), 17514-17521.

8. Abbreviations

2-5A	$2',5'$-oligoadenylate
ABCE1	ATP-binding cassette sub-family E member 1
ACN	acetonitrile
AcOH	acetic acid
ADAR	RNA-specific adenosine deaminase
AKR	ankyrin repeat
ATP	adenosine triphosphate
ATPC	2-aminothiophenone-3-carboxylate
BB	biobreeding
BLI	biolayer interferometry
Boc	tert-butyloxycarbonyl
Boc2O	di-tert-butyl dicarbonate
cGAMP	cyclic guanosine monophosphate–adenosine monophosphate
ciRNA	competitive inhibitor RNA
COMU	(1-cyano-2-ethoxy-2-oxoethylideneaminooxy)dimethylamino-morpholino-carbenium hexafluorophosphate
CuAAC	copper(I)-catalyzed alkyne-azide cycloaddition
Cy3	cyanine 3®
DCC	*N,N'*-dicyclohexylcarbodiimide
DCM	dichloromethane
DIPEA	*N,N*-diisopropylethylamine
DMAP	4-dimethylaminopyridine
DMEM	Dulbecco's modified eagle medium
DMF	dimethylformamide
DMSO	dimethyl sulfoxide
DNA	deoxyribonucleic acid
dsRNA	double-stranded RNA
DUBTAC	deubiquitinase-targeting chimera
E3 ligase	E3 ubiquitin ligase
EA	ethyl acetate
E-C15	ENPP1 inhibitor compound 15
EDC	1-ethyl-3-(3-dimethylaminopropyl)carbodiimide
EDTA	ethylenediaminetetraacetic acid

eIF2α	eukaryotic translation initiation factor 2 subunit 1
EMCV	encephalomyocarditis virus
ENPP1	ectonucleotide pyrophosphatase/phosphodiesterase 1
ER	endoplasmic reticulum
ESI	electron spray ionization
Et2O	diethyl ether
EtOH	ethanol
FAM	6-carboxyfluorescein
FDA	food and drug administration
FITC	fluorescein isothiocyanate
FRET	Förster resonance energy transfer
GMP	guanosine monophosphate
HATU	hexafluorophosphate azabenzotriazole tetramethyl uronium
HCV	hepatitis C virus
HEPES	4-(2-hydroxyethyl)-1-piperazineethanesulfonic acid
HFIP	hexafluoroisopropanol,
HOAt	1-hydroxy-7-azabenzotriazol
HOBt	1-hydroxybenzotriazol
HRMS	high resolution mass spectrometry
HTS	high throguhput screen
IBQ	IowaBlack
IC50	half maximal inhibitory concentration
IFN	interferon
IPA	isopropanol
IRE1	inositol-requiring enzyme 1
ISG	IFN-stimulated gene
JAK	Janus kinase
JNK	c-Jun N-terminal kinases
LC-MS	liquid chromatography−mass spectrometry
LDA	lithium diisopropylamide
MCR	multicomponent reaction
MeOH	methanol
MHV	mouse hepatitis virus
MPLC	medium-pressure liquid chromatography

mRNA	messenger RNA
MTT	3-(4,5-dimethylthiazol-2-yl)-2,5-diphenyltetrazolium bromide
NADPH	nicotinamide adenine dinucleotide phosphate
nanoDSF	nano differential scanning fluorimetry
NLRP	NLR family pyrin domain
NMR	nuclear magnetic resonance
NOE	nuclear Overhauser effect
o.n.	overnight
OAS	2′, 5′-oligoadenylate synthetase
PAGE	polyacrylamide gel electrophoresis
PARP	poly (ADP-ribose) polymerase
PBS	phosphate-buffered saline
PDB	protein data bank
PDE	phosphodiesterase
PDGFR	platelet-derived growth factor receptor
PE	Petroleum benzine
PEG	polyethylene glycol
Petasis	Petasis borono-Mannich
PI	propidium iodide
PK	pseudo-kinase
PKR	RNA-dependent protein kinase
PNA	peptide nucleic acid
poly I:C	polyinosinic:polycytidylic acid
PROTAC	proteolysis targeting chimera
p-TsCl	*p*-toluenesulfonyl chloride
PVDF	polyvinylidene fluoride
PyBOP	benzotriazol-1-yloxytripyrrolidinophosphonium hexafluorophosphate
RIBOTAC	ribonuclease targeting chimera
RIPA	radio-immunoprecipitation assay
RLI	RNase L inhibitor
RNA	ribonucleic acid
RNase	ribonuclease
RNase L	ribonuclease L, latent ribonuclease
rRNA	ribosomal RNA

rt	room temperature
RTK	receptor tyrosine kinase
SAR	structure-activity relationship
SDS	sodium dodecyl sulfate
siRNA	small interfering RNA
ssRNA	single-stranded RNA
STAT	transducer and activator of transcription
STZ	streptozotocin
SV40	simian virus 40
TBE	Tris/Borate/EDTA
TEA	triethylamine
TFA	trifluoroacetic acid
THF	tetrahydrofuran
TLC	thin layer chromatography
Tm	melting temperature
TMEV	Theiler′s murine encephalomyelitis virus
TMSBr	bromotrimethylsilane
UV	ultraviolet
VEGFR	vascular endothelial growth factor receptor